A study of tectonic elements of the western continental margin of India and adjoining ocean basins to understand the early opening of the Arabian Sea

Thesis submitted to

Goa University

For the Degree of

DOCTOR OF PHILOSOPHY

in

Earth Science

by

Yatheesh Vadakkeyakath

M.Sc. (Tech.)

DEPARTMENT OF EARTH SCIENCE
GOA UNIVERSITY, GOA

2007

Dedicated to

My Father

STATEMENT

As required by the University Ordinance 0.19.8 (ii), I state that the present thesis entitled "***A study of tectonic elements of the western continental margin of India and adjoining ocean basins to understand the early opening of the Arabian Sea***" is my original contribution and same has not been submitted on any previous occasion for any other degree or Diploma of this University or any other University/Institute. To the best of my knowledge, the present study is the first comprehensive work of its kind from the area mentioned. The literature related to the problem investigated has been cited. Due acknowledgements have been made wherever facilities and suggestions have been availed of.

Place: Goa University
Date: 25-01-2007

(Yatheesh Vadakkeyakath)
Candidate

CERTIFICATE

As required by the University Ordinance 0.19.8 (vi), this is to certify that the thesis entitled ***"A study of tectonic elements of the western continental margin of India and adjoining ocean basins to understand the early opening of the Arabian Sea"*** submitted by **Mr. Yatheesh Vadakkeyakath** for the award of the degree of Doctor of Philosophy in Earth Science is based on the original and independent work carried out by him during the period of study under our supervision.

The thesis or any part thereof has not been previously submitted for any other Degree or Diploma in any University or Institute. The material obtained from other sources has been duly acknowledged.

Dr. K. Mahender
Reader,
Dept. of Earth Sciences,
Goa University,
Taleigao Plateau – 403 206,
Goa

Place: Goa University
Date:

G. C. Bhattacharya 25/1/07

Shri G.C. Bhattacharya
Scientist F
Geological Oceanography Division
National Institute of Oceanography
Dona Paula - 403 004, Goa

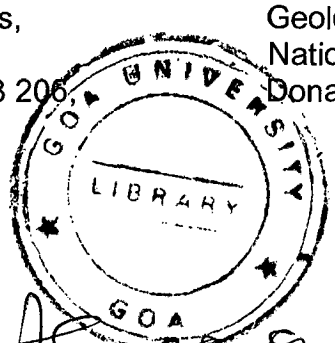

22/2/08

(Prof. A. C. NARAYANA)

ACKNOWLEDGEMENTS

It is my pleasure and privilege to place on record my sincere gratitude to my research guides, ***Shri. G.C. Bhattacharya,*** *Scientist 'F', National Institute of Oceanography (NIO), Goa, and* ***Dr. K. Mahender,*** *Reader, Goa University, Goa for their guidance, advices, help and invaluable encouragement.*

I express my sincere thanks to ***Dr. S.R. Shetye,*** *Director, National Institute of Oceanography (NIO), Goa, and* ***Shri. Rasik Ravindra,*** *Director, National Centre for Antarctic & Ocean Research (NCAOR), Goa, for their permission, facilities and encouragement extended to carry out this work.*

I am extremely grateful to ***Dr. Ehrlich Desa,*** *former Director, NIO, for awarding me Junior Research Fellowship of NIO and his constant inspiration and support to carryout this work.*

The financial support received from ***Council of Scientific and Industrial Research*** *(CSIR), New Delhi, in the form of Senior Research Fellowship is gratefully acknowledged.*

I am thankful to ***Dr. S. Rajan,*** *PD-CLCS, NCAOR, and* ***Shri. T.M. Mahadevan,*** *former Director, AMD, for their constant support and encouragement.*

My sincere thanks are due to ***Dr. J.S. Collier,*** *Imperial College, London, and* ***Ms. Chris Lane,*** *Southampton Oceanography Centre, UK, for providing the end co-ordinates of their seismic reflection profile in the Offshore Indus Basin.*

I am also thankful to ***Dr. K. Srinivas*** *and* ***Shri. T. Ramprasad,*** *for extending their help and wholehearted support at various stages of this work. The encouragement received from* ***Dr. M.V. Ramana, Dr. S.W.A. Naqvi, Dr. A.K. Chaubey, Dr. Rajiv Nigam, Dr. V. Purnachandra Rao*** *and* ***Ms. Maria Desa*** *is gratefully acknowledged.*

I sincerely thank ***Dr. M. Tapaswi*** *and all the staff of Library, for their timely help as and when it was required.*

My thanks are due to ***Dr. J.S. Sarupriya, Dr. P.D. Kunte*** *and* ***Ms. Lasitha,*** *Data and Information Division, NIO, for their help while accessing Indian and International database.*

The support received from ***Prof. A.G.Desai,*** *Professor and Head, Department of Earth Sciences, Goa University and the timely help received from Mr. Gauns and the other Administrative Staff are gratefully acknowledged.*

I take this opportunity to thank Dr. Thamban, Dr. John Kurian, Dr. Sudheer, Dr. Balakrishnan, and Dr. Anilkumar, for their support and encouragement while carrying out this study.

My special thanks are due to all my friends at NIO and NCAOR, especially, Anil, Rajani, Ramesh, Nuncio, Sreekumar, Sudheesh, Krishnan, Sree, Asha, Swapna, Sreejith, Shoby, Sumesh, Ananth, Simi, Radhika, Ajay, Anoop, Syam, Sreejith Kattumadam, Laju, Nisha, Sindhu, Sini, Shetkar, Laluraj, Vineesh and Sijin for making my stay at NIO and NCAOR memorable.

My many special thanks are due to my wife, Mrs. Aparna Sudhan and my son, Nadan Dev, for their patience, co-operation and moral support.

CONTENTS

List of Figures

List of Tables

List of Annexure

PREFACE

The arrangement of continents, continental fragments and ocean basins of the Indian Ocean area was formed by fragmentation and dispersal of the continental assemblage of Gondwanaland. The studies carried out so far have provided a broader understanding of the evolution of this region. However, studies, which are required to trace this history in detail, particularly for the early stages of drifting, still lack in most of the areas. Paucity of detailed geoscientific investigations of the continental margins bordering the Indian Ocean appear to be one of the reasons for this knowledge gap, the geological complexity may be the other reason. The present study focuses on one such areas of knowledge gap, which is believed to be related to the early opening of the Arabian Sea.

In the Arabian Sea region, the Arabian Basin and its conjugate Eastern Somali Basin are believed to have been formed by seafloor spreading process along Carlsberg Ridge since early Tertiary time. According to this model, the Laxmi and Laccadive ridges broadly mark the landward boundary of this early Tertiary oceanic crust. However, there exists substantial swath of deep offshore region, between Laxmi-Laccadive ridges and the continental shelves of western India and southern Pakistan, whose genesis and evolution remains to be confidently established. The present study deals with these deep offshore regions, which mainly contain the Laxmi and Offshore Indus basins and aims to reconstruct the early drift stage dispositions of various continental fragments and other regional tectonic elements of these areas, in the framework of plate tectonic evolution.

The main data used for the present study are sea-surface magnetic, gravity and bathymetric profiles, satellite derived free-air gravity anomalies, GEBCO bathymetry contours, published regional scale tectonic element identifications and available finite rotation parameters of relative motion among India, Seychelles, Madagascar and Laxmi Ridge. The contents of the study are presented in seven chapters in the following manner:

Chapter 1 presents the broad tectonic framework and evolutionary history of the Indian Ocean in general and Arabian Sea region in particular. Further, in

this chapter, the geographical entity of the study area is introduced along with the objectives and scope of the present study.

Chapter 2 presents a review of pertinent previous publications over and adjacent to the areas considered in this study and synthesizes the available knowledge about the structure, tectonics and overall geological framework of those areas. Further, this chapter also presents a brief account of the current understanding of the process of continental break-up and ocean basin formation.

Chapter 3 presents a description of the various data used for the present study and methodologies adopted for their interpretation. The description of methodology specifically includes the method of paleogeographic reconstruction, the tool that has been extensively used in the present work.

Chapter 4 deals with the analysis of various geophysical signatures of the Laxmi and Offshore Indus basin areas and establishing the similarity of geophysical signatures and thereby a similar nature of the crust (i.e. oceanic) underlying these two basins. Subsequently, the chapter describes interpretation of the observed magnetic anomalies of these areas in terms of two-limbed seafloor spreading type lineations.

Chapter 5 deals with the evaluation and improvement of the paleogeographic reconstruction models pertaining to the early drift and pre-drift juxtaposition of India, Seychelles and Madagascar continental blocks. The existing models have been evaluated and improved primarily in light of the conjugate tectonic elements inferred in the present study and the finite rotation parameters estimated based on these magnetic lineations, which describe the relative motion between India-Pakistan and Laxmi Ridge.

Chapter 6 presents the stage-by-stage paleogeographic reconstructions of the study area. These reconstructions provide a new view about the dispositions of India, Seychelles and Madagascar during the early drift stages wherein the Laxmi Ridge and Laccadive Plateau could be accommodated as intervening microcontinental slivers.

Chapter 7 presents a summary of the study and highlights the important results obtained. This chapter also includes some suggestions for further studies.

Finally a detailed list of references cited in the text has been provided. The references quoted are arranged in alphabetical order and is included at the end of the thesis.

A section of the thesis, which proposes a new model of India-Madagascar juxtaposition have been recently published in the international journal of Gondwana Research. A reprint of that paper has been annexed at the end of this volume.

CHAPTER 1

Chapter - 1

GENERAL BACKGROUND

1.1 Introduction

The Indian Ocean (Fig. 1.1), which borders the Indian mainland in the east, south and west, is the third largest ocean of the world after the Pacific and Atlantic oceans. The Bay of Bengal and Arabian Sea are part of this Indian Ocean. As far as systematic marine geoscience is concerned, this Indian Ocean area still remains less studied as compared to the Pacific and Atlantic oceans. The geographic limits of the Indian Ocean are Iran, Pakistan, India and Bangladesh in the north; Burma, Thailand, Malaysian Peninsula, Sunda subduction zone and Australia in the east; Antarctic continent in the south and Africa and Arabia in the west. In the plate tectonic perspective, Indian Ocean (Fig. 1.2) comprises major parts of the Indo-Australian plate, the Arabian Plate, the African plate and the Antarctic plate. Most of the major tectonic features of this area have been identified based on various geoscientific studies carried out during the International Indian Ocean Expedition (IIOE) in 1960s. Incidentally, this was also the period when the hypothesis of seafloor spreading was getting metamorphosed into the theory of plate tectonics. This new concept, therefore, provided an excellent framework for several researchers to propose first order models for the broad evolutionary history of the Indian Ocean (McKenzie and Sclater, 1971; Norton and Sclater, 1979). According to those models, the Western Indian Ocean as a whole have evolved by rifting and drifting of India, Seychelles, Madagascar and Africa from each other, while its Arabian Sea region have evolved mainly by drifting among India, Madagascar and Seychelles. The major knowledge gaps in this understanding are the juxtaposition of India, Madagascar and Seychelles in their pre-drift configuration, the timings of initiation of their drift and their early drift evolution till about 62.5 Ma (chron 28ny). In the present work, an attempt is made to provide several important clues for bridging this knowledge gap.

In this chapter, firstly, the geographical entity of the study area has been introduced. Since the study area falls in the Western Indian Ocean, therefore to view the study area in the regional perspective, a brief description have been

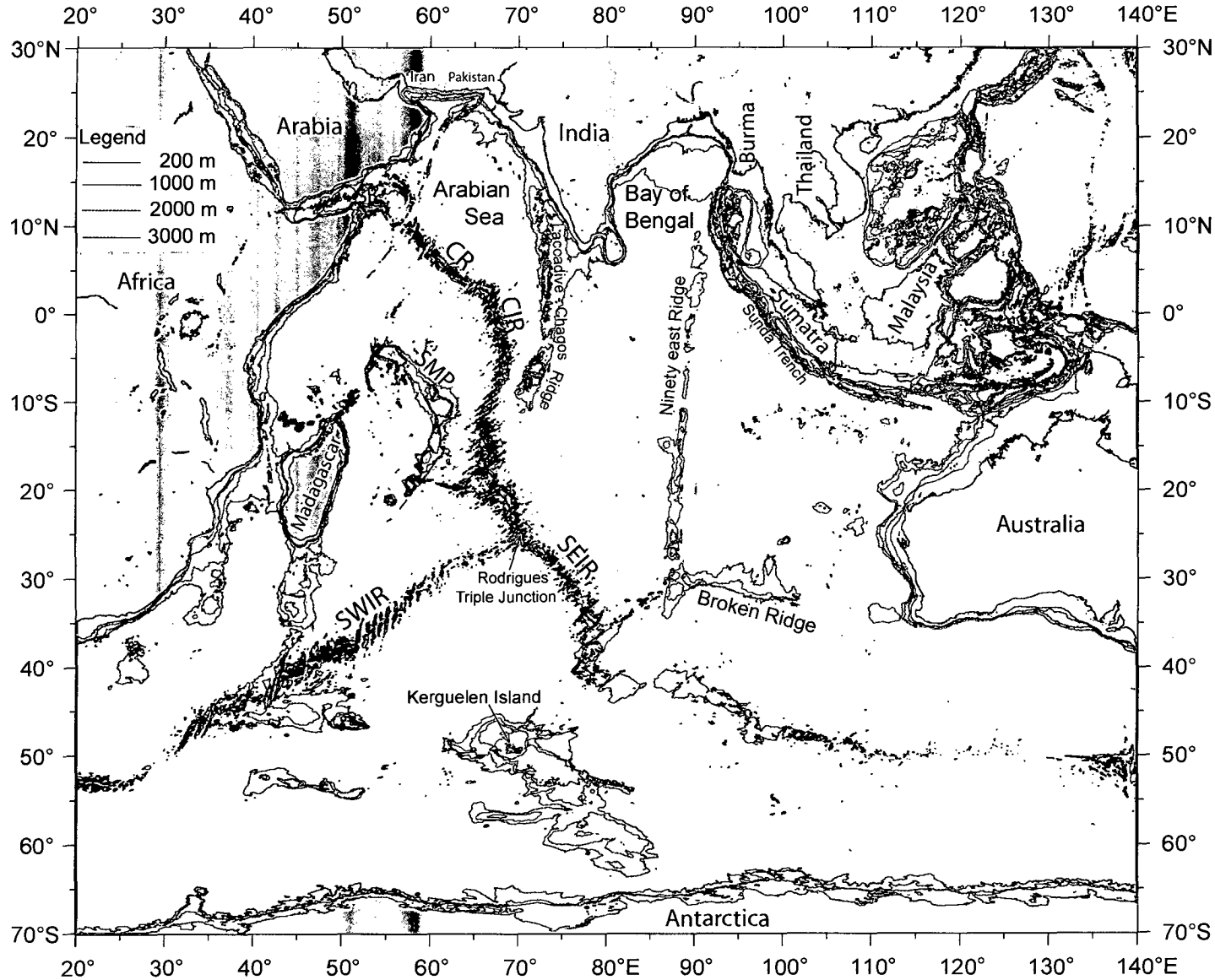

Fig. 1.1. Generalized physiography of the Indian Ocean along with selected (200 m, 1000 m, 2000 m, and 3000 m) bathymetric contours.

CR: Carlsberg Ridge; CIR: Central Indian Ridge; SEIR: Southeast Indian Ridge; SWIR: Southwest Indian Ridge; SR: Sheba Ridge; SMP: Seychelles-Mascarene Plateau

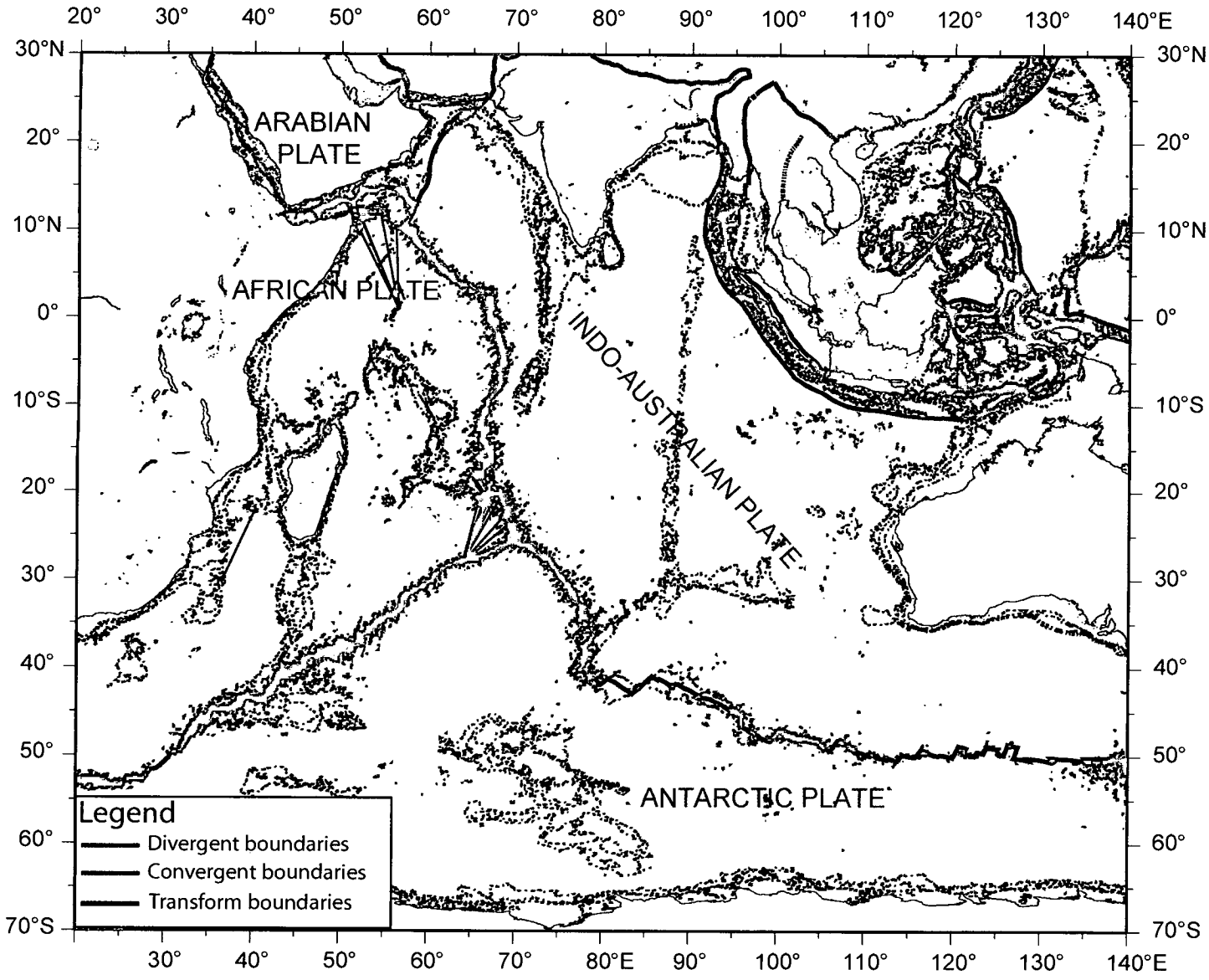

Fig. 1.2. Lithospheric plates in the Indian Ocean described by the divergent, convergent and transform boundaries.

provided about the main physiographic and structural features of the Western Indian Ocean and its generally accepted broad plate tectonic evolutionary model. At the end of this chapter, the objectives and scope of the study have been introduced.

1.2 Study area

The study area (Fig. 1.3) mainly covers the western continental margin of India and adjoining deep-sea basins. However, for understanding the plate tectonic evolution of the study area, some features of the conjugate areas, such as Seychelles, eastern continental margin of Madagascar and the ocean basins adjoining these regions have also been considered in this study.

1.3 Main features of the Western Indian Ocean

The Western Indian Ocean is defined (Bhattacharya and Chaubey, 2001) as that part of the Indian Ocean, which broadly lies west of 80°E and north of 40°S (Fig. 1.4). The Western Indian Ocean contains mid-oceanic ridges, continental fragments, submarine plateaus, deep-sea basins and one of the world's largest deep sea fans. A detailed account of these physiographic and tectonic features has been summarized in two earlier works (Laughton et al., 1970; Schlich, 1982) and later updated (Bhattacharya and Chaubey, 2001).

Study of various publications indicated that same offshore areas or features have been referred in different studies by different names. Bhattacharya and Chaubey (2001) attempted to reduce this confusion by designating various geological domains in the Western Indian Ocean with their most widely used names. For further discussion in this study, the nomenclature used by Bhattacharya and Chaubey (2001) have been followed.

1.3.1 *Mid-oceanic ridge system*

The Western Indian Ocean area contains (Fig. 1.4) three branches of active mid-oceanic ridges (spreading centres), which converge at a ridge-ridge-ridge junction (25.5°S, 70°E), referred as Rodrigues Triple Junction (RTJ). The northern branch of this system is comprised of three segments known as the Central Indian Ridge, the Carlsberg Ridge and the Sheba Ridge. The segment of

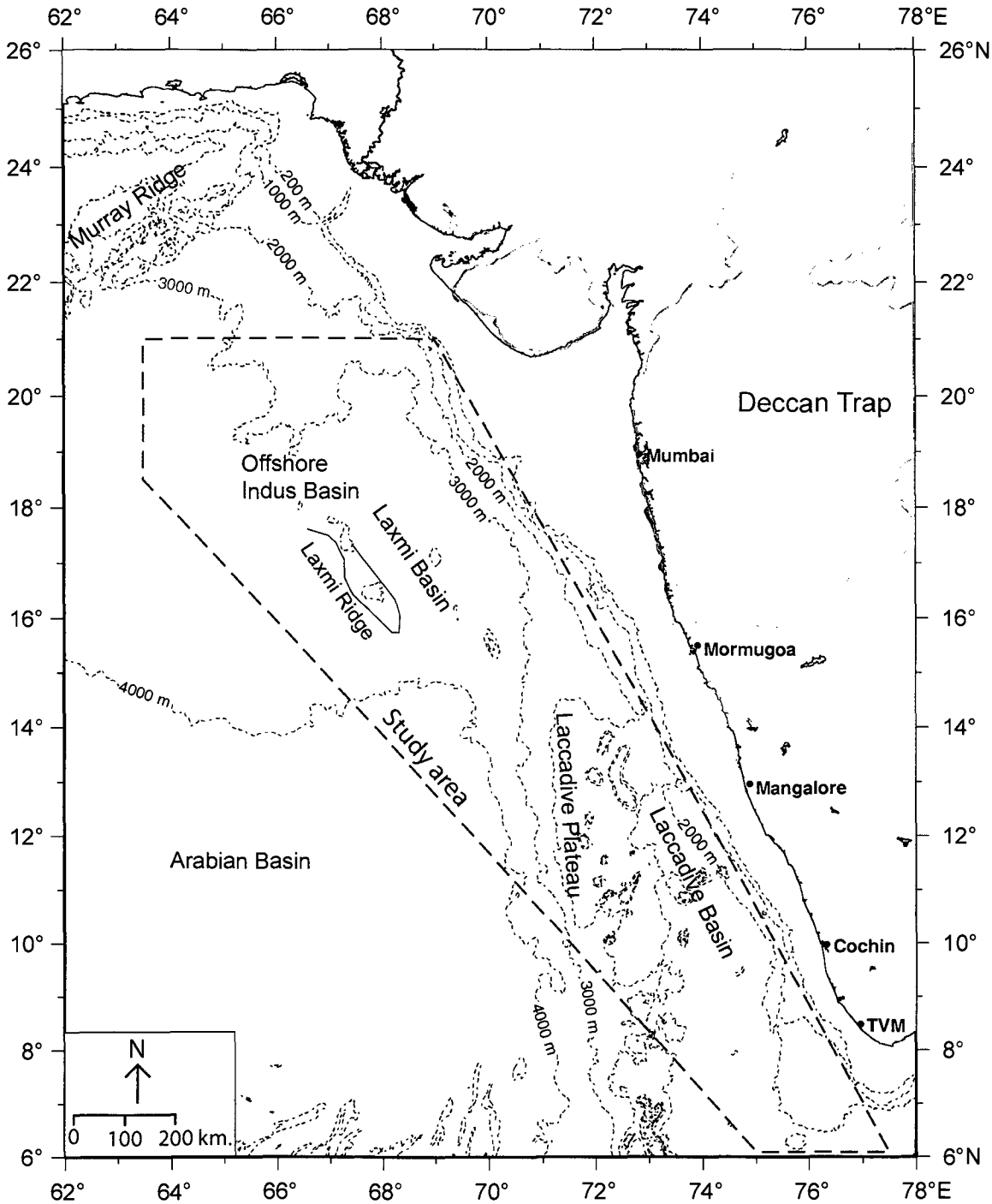

Fig. 1.3. Generalized map of the western continental margin of India and adjoining deep-sea basins. Outline of the study area is marked by red dashed lines. TVM: Trivandrum.

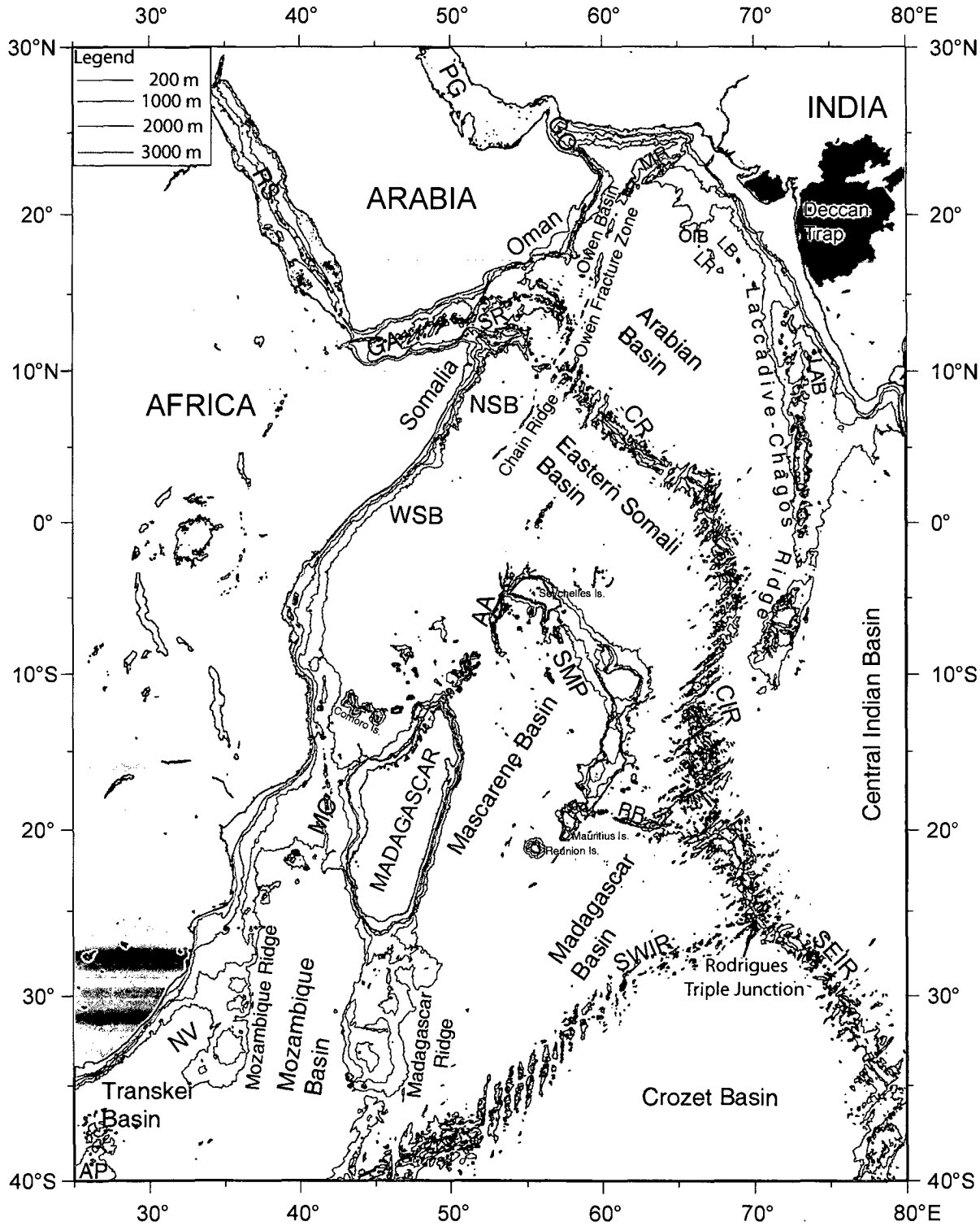

Fig. 1.4. Locations of major ocean basins and other physiographic features of the Western Indian Ocean along with selected bathymetric contours. AP: Agulhas Plateau; NV: Natal Valley; MC: Mozambique Channel; WSB: Western Somali Basin; NSB: Northern Somali Basin; RS: Red Sea; GA: Gulf of Aden; PG: Persian Gulf; GO: Gulf of Oman; MR: Murray Ridge; OIB: Offshore Indus Basin; LB: Laxmi Basin; LR: Laxmi Ridge; LAB:Laccadive Basin; AA: Amirante Arc; SMP: Seychelles-Mascarene Plateau; RR: Rodrigues Ridge; SR: Sheba Ridge; CR:Carlsberg Ridge; CIR: Central Indian Ridge; SEIR: Southeast Indian Ridge; SWIR: Southwest Indian Ridge.

this northern branch, which lies between Rodrigues Triple Junction and the equator, is known as the Central Indian Ridge (CIR). The CIR is a north-south lineation, comprising of *enechelon* displacement of the NW-SE trending ridge axis by numerous NE-SW trending fracture zones. Further north from CIR, the northwest-southeast trending ridge segment, which lies between the equator and Owen Fracture Zone (OFZ) is referred as the Carlsberg Ridge (CR). The nearly E-W trending Sheba Ridge (SR) is an extension of Carlsberg Ridge in the Gulf of Aden and the Owen Fracture Zone defines the major right lateral offset between the Carlsberg Ridge and the Sheba Ridge.

The other two branches of this mid-Indian Ocean Ridge system are Southwest Indian Ridge (SWIR) and Southeast Indian Ridge (SEIR). Southwest Indian Ridge starts from Rodrigues Triple Junction and joins the southern part of the mid-Atlantic Ocean Ridge system at the Bouvet Triple Junction near 55°S and 1°W. The Southeast Indian Ridge is a NW-SE trending feature, which start from the Rodrigues Triple Junction and extend southeastwards to join the Pacific-Antarctic mid-oceanic ridge system south of Australia.

1.3.2 *Submarine plateaus and aseismic ridges*

The Western Indian Ocean (Fig. 1.4) contains a number of prominent topographic features, which protrude high above the ocean floor. Most of these features morphologically show considerable elongation and are wholly submarine, but few rise above sea level and emerge as islands. The main features of this type are the Agulhas Plateau, the Madagascar Ridge, the Mozambique Ridge, the Laxmi Ridge and the Laccadive-Chagos Ridge.

The Agulhas Plateau lies about 500 km southeast of the Cape of Good Hope. The Madagascar Ridge is a N-S elongated feature located south of Madagascar between 26°S and 36°S. The Mozambique Ridge is an elongated feature lying roughly parallel to the coast of southeast Africa. The Laxmi Ridge is an aseismic basement high feature, located approximately 700 km west of Mumbai. The Laccadive-Chagos Ridge is a slightly arcuate, elongated aseismic ridge, which extends for about 3000 km off the southwest coast of India approximately along 73°E between 14°N and 9°S. The Seychelles-Mascarene Plateau Complex is a 2600 km long arcuate system of wide, partially isolated

shallow banks and small islands, and is located in the areas between Madagascar Island and the Central Indian-Carlsberg Ridge segments. The Rodrigues Ridge is a narrow, linear 450 km long volcanic ridge that intersects the Mascarene Plateau perpendicularly about 200 km north of Mauritius.

1.3.3 *Seamounts*

The geological and geophysical atlas of the Indian Ocean (Udintsev et al., 1975) and several later publications indicated the presence of number of seamounts in the Western Indian Ocean. However, very few of them have been systematically studied and only meager published information is available. Prominent among these seamounts are the Error seamount, Sagar Kanya seamount and a chain of seamounts located in the Laxmi Basin. The Error seamount (Matthews, 1966; Ramana et al., 1987) is located approximately at the northwestern boundary of the Carlsberg Ridge and appears to be part of the system of features, which constitute the Owen Fracture Zone. The Sagar Kanya seamount (Bhattacharya and Subrahmanyam, 1991) is a 2464 m high edifice located about 200 km west of the Laccadive Plateau. The Laxmi Basin seamount chain consisting of Raman seamount, Panikkar Seamount and Wadia guyot is about 250 km in length and is located approximately along the axial part of the Laxmi Basin (Bhattacharya et al., 1994a).

1.3.4 *Deep sea basins*

The Western Indian Ocean consists of several deep sea basins (Fig. 1.4), some of which were created by the present system of mid-ocean ridges and some others were formed by paleo-spreading regimes or remnants of the continental break-up stage tectonics. Prominent among these basins are the Natal Valley, the Transkei Basin, the Mozambique Basin, the Mozambique Channel, the Western Somali Basin, the Northern Somali Basin, the Owen Basin, the Gulf of Oman, the Gulf of Aden, the Madagascar Basin, the Mascarene Basin, the Eastern Somali Basin, the Arabian Basin, the Offshore Indus Basin, the Laxmi Basin, the Laccadive Basin, the Central Indian Basin and the Crozet Basin.

The Mozambique Basin is located between the N-S trending Madagascar and Mozambique ridges. The NNE-SSW trending Mozambique Channel extends

from 12°S to 25°S and separates the Madagascar Island and the African mainland. The Western Somali Basin is bound to the west and northwest by the east coast of Africa and its northern boundary is defined by a broad bathymetric high at 4°N, which extends from the African continental margin to the southern end of the Chain Ridge. The small ocean basin located approximately north of 4°N between the African continental margin and the Chain Ridge is referred to as the Northern Somali Basin. The Owen Basin is bounded to the east by the Owen Fracture Zone, to the west by the Oman continental margin, to the south by the Sheba Ridge and to the north it opens into the Gulf of Oman. The Persian Gulf and Gulf of Oman is a convergent region at the northern margin of the Arabian plate. The Gulf of Oman is bounded by the Makran Ranges in the north and Oman Mountains in the southwest. The Persian Gulf is an elongate depression located between the Zagros Mountains to the northeast and the Arabian Peninsula to the west, south and southeast.

The Madagascar Basin is bounded on the southeast by the rough topography of the southwest Indian Ridge, and to the southwest by the gentle upward slope of the Madagascar Ridge. The Mascarene Basin lies between Madagascar Island and the Seychelles-Mascarene Plateau and corresponds to the northwestern extension of the Madagascar Basin. To the south, the basin abuts the complex northeastern flank of the Madagascar Ridge and to the north, the basin is limited by an irregular boundary passing through the Seychelles Bank, the Amirante Arc and the northern tip of Madagascar Island. The Eastern Somali Basin is bounded to the north by the Carlsberg Ridge; to the south by the northern part of the Seychelles-Mascarene Plateau; to the east by the Central Indian Ridge and to the west by the Chain Ridge. The Arabian Basin is bounded to the west by Owen Fracture Zone, to the south by Carlsberg Ridge, and most of the northern and eastern sides by the aseismic Laxmi Ridge and the Laccadive Plateau. The Offshore Indus Basin is bounded by the E-W trending buried Laxmi Ridge segment in the south, the Murray Ridge and the Owen Fracture zone in the northwest, and the continental slope of India and Pakistan in the northeast. The Laxmi Basin is located between the Laxmi Ridge and the western continental slope of India. The northern boundary of this basin is considered (Bhattacharya et al., 1994b) to be limited approximately along 21°N where the bathymetric

contours of the adjacent continental slope of western India abruptly change westerly. Towards south, this basin abuts the northern extremity of the Laccadive Plateau. The Laccadive Basin is a narrow and triangular shaped basin, which is located between the Laccadive Plateau in the west and the southwestern continental slope of India in the east. The northern boundary of the basin lies approximately near 16°N where the northern extremity of the Laccadive Plateau apparently meets the adjacent continental slope of western India. Towards south, this basin opens to the Central Indian Basin. The Central Indian Basin is bounded in the west by the southern part of the Central Indian Ridge, the Chagos Bank and the Maldive Ridge; in the east by the Ninety East Ridge; and in the south by the Southeast Indian Ridge. The Crozet Basin is bounded in the northwest by the Southwest Indian Ridge, in the northeast by the Southeast Indian Ridge and in the south by the Ob, Lena and Marion Dufresne seamount chain.

1.4 Broad plate tectonic evolutionary history of the Western Indian Ocean

The evolution of the Western Indian Ocean is a part of the evolution of the Indian Ocean. Various paleogeographic reconstruction models have been proposed to depict the evolutionary history of the Indian Ocean. These models were proposed based on the identification of seafloor spreading type magnetic anomalies, fracture zone traces from magnetic, bathymetric and satellite altimetry data, and the paleomagnetic studies of the continental rocks (McKenzie and Sclater, 1971; Norton and Sclater, 1979; Besse and Courtillot, 1988; Scotese et al., 1988; Royer et al., 1992; Reeves and Leven, 2001). Following is a broad synthesis of the views of various authors regarding the evolution of the Indian Ocean with focus on Western Indian Ocean.

It is generally believed that the present day configuration of continents, continental fragments and oceans was created by fragmentation and dispersal of a super continent named the Pangea. The Pangea super continent consisting of almost all the continental landmasses was surrounded by the universal ocean "Panthalassa" (the ancestral Pacific) and eastern shores of Pangea were indented by a triangular sea called "Paleo-Tethys". During Triassic, a strip continent (known as Cimmerian strip continent) which comprised parts of present day Turkey, Iran, Afghanistan, Tibet, China and Indo-China rifted from southern

Paleo-Tethyan margin and drifted towards north. This Cimmerian movement caused the closing of Paleo-Tethys and opening of a "Neo-Tethys" sea in its wake.

About 200 Ma the Pangean super continent began to split, first into a northern part (Laurasia) and a southern part (Gondwanaland). It is considered that the break-up of Gondwanaland also coincided with the commencement of closure of Neo-Tethys Sea by subduction under the Eurasian margin. This subduction gave rise to the development of an island arc system, named the Kohistan-Ladakh Island arc, which as will be described later was the zone of first contact between the Indian and Eurasian plates. The unified Gondwanaland in the southern hemisphere was comprised of present day South America, Africa, Arabia, Madagascar, Sri Lanka, India, Australia, and New Zealand. The origin of Indian Ocean is related to the fragmentation and dispersal of Gondwanaland. Main episodes of fragmentation and dispersal of Gondwanaland are summarized below:

Stage 1:

Break-up of the Gondwanaland started by a rifting episode, which was initiated earlier than 152 Ma (Late Jurassic). By about 152 Ma, commencement of seafloor spreading along short E-W trending spreading segments offset by long N-S trending transform faults divided the Gondwanaland into west Gondwanaland (Fig. 1.5a) consisting of Africa, Arabia and South America and the east Gondwanaland consisting of Antarctica, Australia, New Zealand, Madagascar, Seychelles, India and Sri Lanka. This was the stage during which the Mozambique, the Western Somali and probably the Northern Somali basins began to form and mark opening of the Indian Ocean. After this break up, east Gondwanaland moved south in comparison to west Gondwanaland.

Stage 2:

Further break up of east Gondwanaland began in Cretaceous. At about 133 Ma (Early Cretaceous) the conjoined Antarctica-Australia rifted and drifted away from Madagascar-Seychelles-India continental block (Fig. 1.5b).

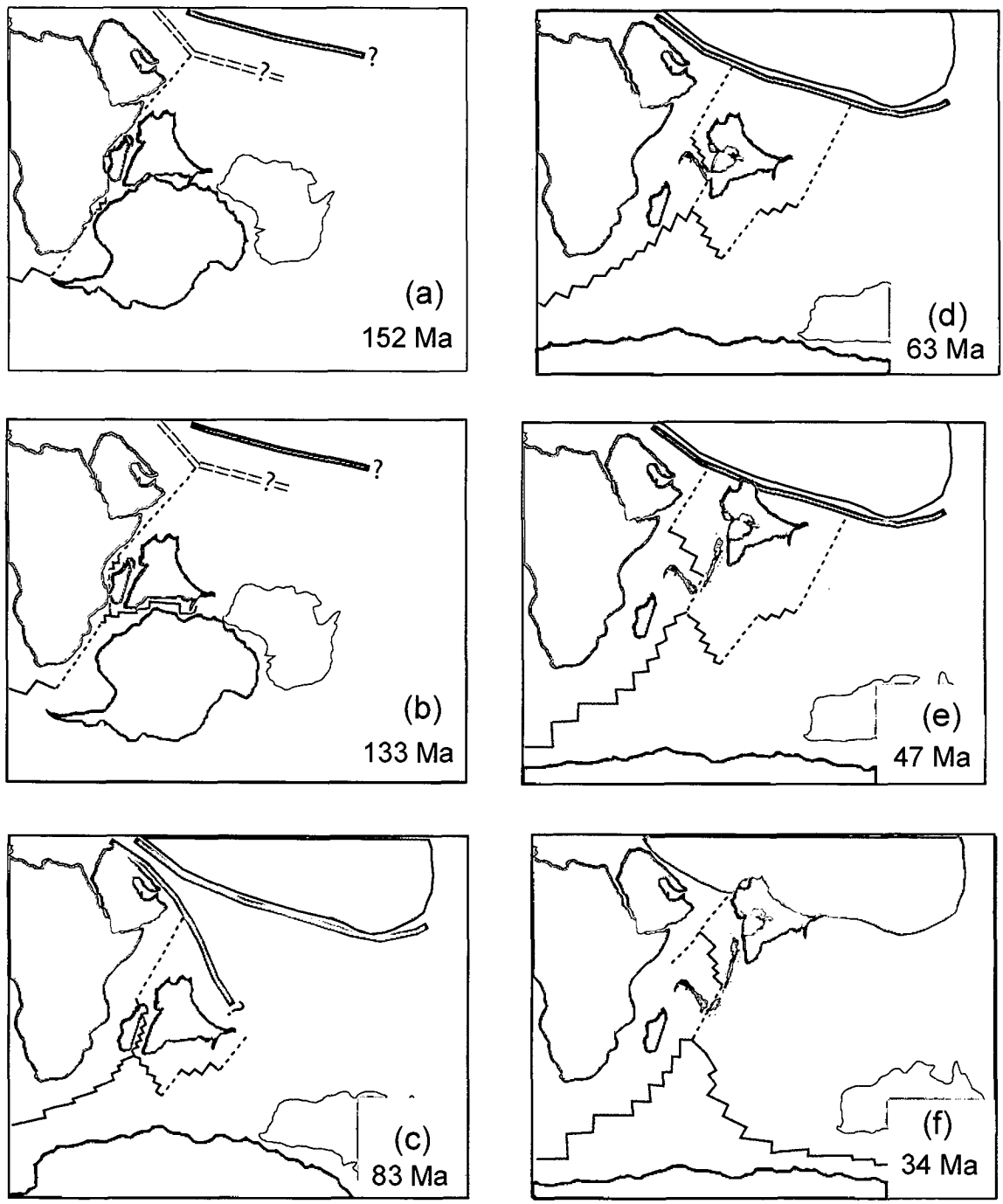

Fig.1.5. Cartoons depicting snapshots of broadly agreed evolution of Western Indian Ocean from 152 Ma to 34 Ma. (a) Late Jurassic (152 Ma), (b) Early Cretaceous (133 Ma), (c) Late Cretaceous (83 Ma); (d) Late Paleocene (63 Ma); (e) Middle Eocene (47 Ma); and (f) Early Oligocene (34 Ma).

Stage 3:

Following separation of Madagascar-Seychelles-India block from Antarctica-Australia block, the spreading of seafloor continued in a uniform fashion for about 15 my. Later, the spreading between Africa-Arabia and Madagascar-Seychelles-India blocks experienced a change. The Madagascar-Seychelles-India-block possibly came over the location of the Marion Hotspot around 88 Ma. Due to the influence of this hotspot, rifting was initiated and around 83 Ma (chron 34ny) due to seafloor spreading, the Madagascar separated from Seychelles-India block and got welded to the African Plate (Fig. 1.5c). This separation resulted in opening of the Mascarene and Madagascar basins and establishment of a three-plate system with a triple junction in the Western Indian Ocean. Most importantly, this event probably marked the beginning of the tectonic events, which resulted in shaping the present day deep offshore regions off the west coast of India. After separation, Seychelles-India block continued its northward drift and at the same time experienced a gradual anti-clockwise rotation.

Stage 4:

While drifting northward, around 69-65 Ma (Late Cretaceous), wide spread volcanism took place over the Indian landmass and created the Deccan Trap continental flood basalt province which is considered to be related to the onset of the Reunion hotspot activity. As India continued to move northward, the adjacent offshore areas came under the influence of the Reunion hotspot. This resulted in commencement of formation of the Laccadive-Chagos Ridge and reorganization of the nearby spreading centres. Around 63 Ma (Late Paleocene), spreading in the Mascarene Basin gradually ceased and jumped north of Seychelles, carving the Laxmi Ridge out of the Seychelles (Fig. 1.5d) to form a new spreading centre – the Paleo-Carlsberg Ridge. The spreading along this Paleo-Carlsberg Ridge caused the opening of the conjugate Arabian and Eastern Somali basins and welding of the Seychelles to the African Plate.

Stage 5:

As the rapid northward movement of India continued, the Arabian and Eastern Somali basins continued to grow and simultaneously the Neo-Tethys

continued to be subducted. Finally around 50 Ma (Middle Eocene), the continental India came into contact with the Kohistan-Ladakh Island arc system (Fig. 1.5e) and gradually closed the Neo-Tethys along the Indus-Tzangpo suture zone. This event is termed as "soft collision" or the first contact between India and Asia. This resulted in slowing down of the spreading rates at the Carlsberg, Central Indian and Southeast Indian ridges. In response to the continued collision of India and Asia, the plate boundaries in the Indian Ocean area started re-organization. Along the Paleo-Carlsberg Ridge spreading slowed down to imperceptible level from chron 21n (~47 Ma) onwards and probably by about 40 Ma the plate boundaries in the Indian Ocean began to assume the present day configuration.

Stage 6:

The latest episode of spreading along the Carlsberg Ridge (Fig. 1.5f) commenced around 34 Ma (Late Oligocene). Following this Late Oligocene re-organization, a new phase of accelerated spreading commenced in the Western Indian Ocean. During Late Miocene, shortly before chron 5 (~11 Ma), the Carlsberg Ridge spreading centre propagated westward as the Sheba Ridge and opened the Gulf of Aden. The accelerated spreading caused subduction of entire oceanic crust north of Indian Plate and brought continental crust of Indian and Eurasian plates into contact. This contact or the "hard collision" as it is known might probably have occurred during Middle Miocene (~16–11 Ma) and as a result the Himalayas emerged as a highland. The rapid rise of the Himalayas continued and by Late Miocene (~11–7.5 Ma), the Himalayas became a lofty mountain range. Consequent accelerated erosion of the Himalayas brought large volume of sediments in the Indus and Bengal fan area. At present the Carlsberg Ridge is active and continue to accrete the Arabian and eastern Somali basins at a rate of about 1.2 cm/year.

1.5 Objectives and scope of the study

As discussed in the previous section, the evolutionary history of the Arabian Sea region could be described in two stages. The first stage around 83 Ma (chron 34ny) was the rifting and subsequent drifting of the Seychelles-India block from Madagascar, which resulted in creation of oceanic crust in the

Mascarene and Madagascar basins; and the second stage around 62.5 Ma (chron 28ny) was the rifting and drifting of India from Seychelles, which resulted in creation of oceanic crust in the conjugate Arabian and Eastern Somali basins. The evolution of the Arabian Sea region for the period younger to 62.5 Ma (chron 28ny) was broadly described in the pioneering studies of Norton and Sclater (1979) and Besse and Courtillot (1988). Several later studies (Bhattacharya et al. 1992; Miles and Roest, 1993; Chaubey et al., 1998; Dyment, 1998; Miles et al., 1998; Royer et al., 2002; Chaubey et al., 2002a) have further refined understanding of this post-62.5 Ma evolution. However, the evolution of the Arabian Sea region for the period prior to 62.5 Ma has not yet been well constrained. The present study in general aims to understand the plate tectonic evolution of the Arabian Sea region, during its early opening period, i.e., between ~62.5 Ma and the time of initiation of the India-Madagascar separation. In specific this study aims to arrive at improved models of the relative positions of India, Madagascar and Seychelles in their pre-drift configuration, the timing of initiation of their drift and their subsequent early drift evolution till about 62.5 Ma (chron 28ny).

For achieving the objectives, the study utilized various data, such as; sea-surface magnetic, gravity and bathymetric profiles, satellite derived free-air gravity anomalies, GEBCO bathymetry contours, published regional scale tectonic element identifications and available finite rotation parameters of relative motions among India, Seychelles, Madagascar and Laxmi Ridge. The paleogeographic reconstruction technique has been extensively used in this study to evaluate the various published paleogeographic reconstruction models as well to provide a revised model describing the early opening history of the Arabian Sea.

CHAPTER 2

Chapter - 2

GEOLOGICAL FRAMEWORK

2.1 Introduction

The continental margins off west coast of India, Seychelles and east coast of Madagascar are believed to have been evolved by rifting and successive drifting of India, Seychelles and Madagascar. The present day geological scenario of the deep offshore regions around these continental margins is a consequence of this rift, drift and subsequent tectonic and sedimentary evolution. Various studies carried out so far have revealed the existing regional structural and sedimentary features of these areas and allowed proposing broad models of their evolution. In order to view the results of the present study in the background of these existing geological knowledge, relevant available information about structure and tectonics of various features of the areas in the deep offshore regions adjacent to west coast of India as well its conjugate Madagascar and Seychelles, have been collated in this chapter. Further, as the western continental margin of India was classified as a passive continental margin (Biswas, 1982, 1987), therefore in order to appreciate the passive continental margin setting, a brief account of the concept of continental margin in general and evolution of the passive continental margin in particular have also been presented in this chapter.

2.2 Tectonic elements of the western continental margin of India and the adjoining land and oceanic areas

Marine geoscientific investigations on the continental shelf, slope and deep offshore regions off west coast of India have so far revealed the existence of several physiographic, sedimentary and basement features. Many parts of the continental shelf have been investigated in detail in connection with hydrocarbon exploration but most of these results are not available in public domain, whereas, not many studies were carried out in the deep offshore regions. In following paragraphs the information about the regional features of this area have been presented.

2.2.1 *Features on the western part of the Indian mainland*

The Indian subcontinent is made up of three major physiographic provinces (Fig. 2.1), the Himalayas, the Indo-Gangetic Plain and the Peninsular Shield, all of which are characterized by distinctive geomorphological, structural, stratigraphic and deep crustal features (Mahadevan, 1994). The Peninsular Shield comprises of Precambrian terrains of South India and the Deccan Trap volcanic province. The Precambrian terrains in South India are further divided into Southern Granulite Terrain (SGT), Eastern Ghat Mobile Belt (EGMB), Western Dharwar Craton (WDC) and Eastern Dharwar Craton (EDC). Since the study area is adjacent to the western part of India, emphasis for description is given to the Southern Granulite Terrain, Western Dharwar Craton and Deccan Trap, which form a major part of the western Indian mainland.

The Southern Granulite Terrain (SGT) of India (Fig. 2.1) is one of the few terrains in the world that has preserved Archean crust with extensive granulites, believed to be of lower-crustal origin (Anand and Rajaram, 2003). The SGT primarily consists of several granulite blocks, which are dissected by a number of shear zones. The most prominent shear zones are the Achankovil Shear Zone, the Palghat-Cauvery Shear Zone and the Moyar Shear Zone (Kroner and Brown, 2005). The Achankovil Shear Zone is a 10-20 km wide and 100 km long NW-SE trending dextral shear zone bounding the Madurai Block in the north and Kerala-Khondalite Belt (KKB) in the south. Some authors considered that the Palghat-Cauvery Shear Zone and Moyar Shear Zone together form a 100-150 km wide shear zone system of which the Palghat-Cauvery Shear Zone is the southern one. These shear zones are important in the context of India-Madagascar pre-drift juxtaposition, as they are often considered to be conjugate of several comparable shear zones in the Madagascar. The Western Dharwar Craton (WDC), which is composed of Dharwar type schist belt, is bounded (Fig. 2.1) to the south by the Southern Granulite Terrain (SGT), to the east by the Eastern Dharwar Craton (EDC) and to the northwest by the Deccan Trap flows. The most characteristic feature of the Archean cover sequence of the Dharwar craton is their arcuate NS trend with convexity towards east. A major portion of the deeper geology of western India lies hidden under the Deccan Traps (Fig. 2.1), which is one of the largest known continental flood basalt (CFB) provinces on the Earth.

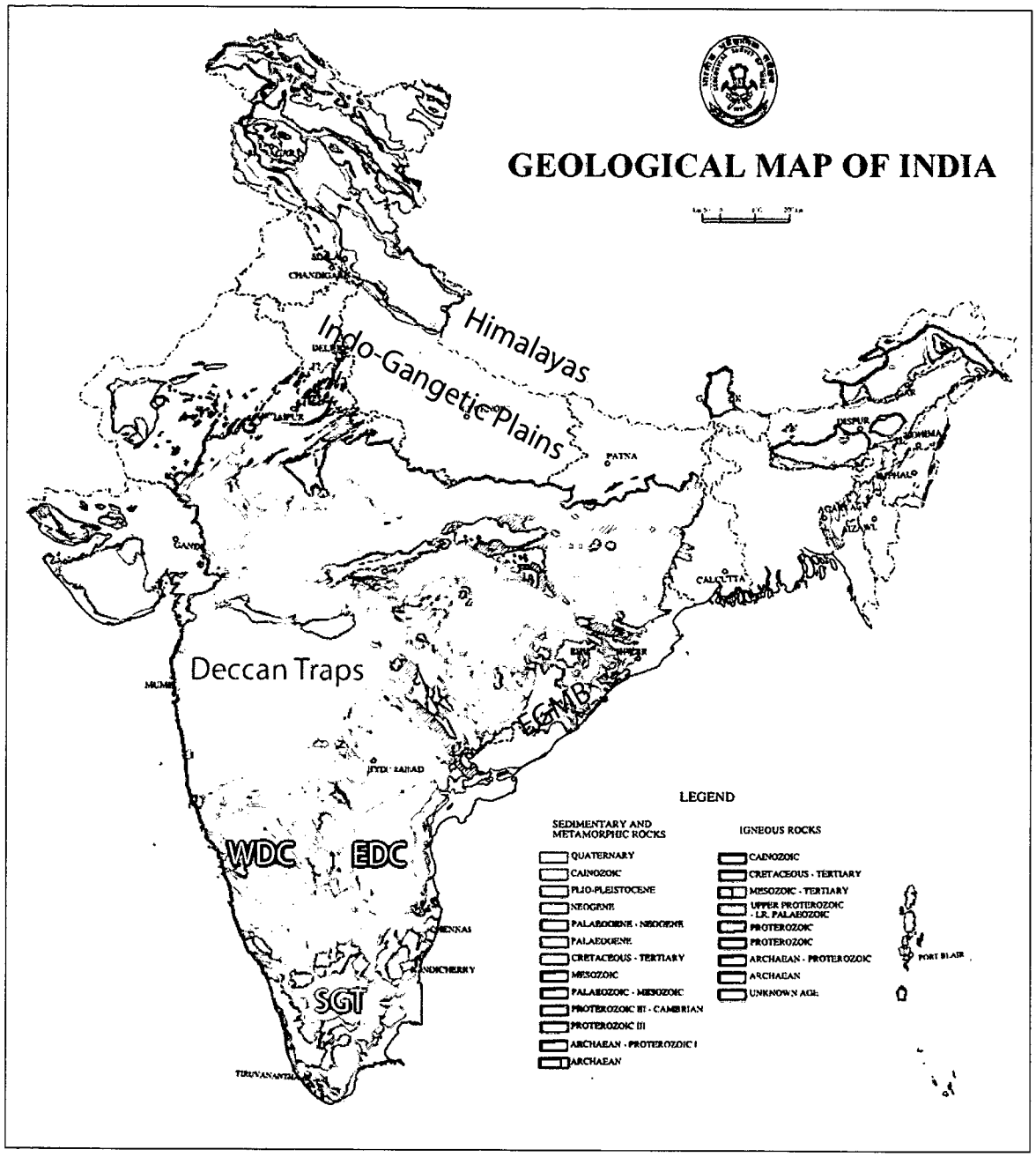

Fig. 2.1 Detailed geological map of India (modified after GSI, 1999 as reproduced in Naqvi, 2005). SGT: Southern Granulite Terrain; EGMB: Eastern Ghat Mobile Belt; WDC: Western Dharwar Craton; EDC: Eastern Dharwar Craton.

The Deccan Trap CFB extend over nearly 500,000 sq. km. and lie flat as horizontal sheets and are believed to have erupted sub-aerially through fissures in the Earth's crust (Kumar, 1986). A large thermal anomaly, generated by a deep mantle plume (Reunion Hotspot) is commonly postulated to explain the genesis of the Deccan Trap CFB event (Morgan, 1972, 1981; Courtillot et al., 1986; White and McKenzie, 1989; Duncan, 1990; Baksi and Farrar, 1991; Basu et al., 1993). The timing and duration of this volcanic event over the Indian peninsula have been a subject of considerable debate (Alvarez et al., 1980; Baksi, 1988, 1994; Courtillot et al., 1988; Duncan and Pyle, 1988; Rampino and Stothers, 1988; Acton and Gordon, 1989; Vandamme et al., 1991; Negi et al., 1993; Basu et al., 1993) and various postulated ages of their emplacement range between 62-72 Ma. However, views appear to converge on a short duration (1my) peak volcanism around 65 Ma (Courtillot et al., 1986; Vandamme et al., 1991; Hofmann et al., 2000).

Three orogenic trends predominate the Precambrian basement grains of the western part of the Indian peninsula. These are the Dharwar trend, the Delhi-Aravalli fold trend and the Satpura trend (Fig. 2.2). The generally NNW oriented Dharwar trend is the dominant basement grain in the western peninsular India (Biswas, 1982). It is expected that Dharwar trend continue below much of the area now covered by Deccan Trap CFB (Das and Ray, 1976; Krishnan, 1968; Biswas, 1982; Gombos et al., 1995). The Aravalli Delhi Fold trend is a major segment of the NW Indian shield and consists of intensely folded, deformed and metamorphosed rocks of Proterozoic period that are intruded by various granites, basic and ultra-basic rocks (Tewari and Rao, 2003). This NE-SW oriented trend bifurcates into two branches at its southward end; the Delhi trend swings E-W into the Kutch region and NE-SW trending Aravalli trend continues across the Cambay graben into the Kathiawar Peninsula. The ENE-WSW Satpura trend along the Narmada Rift is the other dominant structural fabric of the western India (Biswas, 1982). These three major trends, resulting from orogenesis dating back more than 2000 Ma, were the zones of deformed and weakened crust along which later Phanerozoic rifting was facilitated (Biswas, 1982, 1987; Gombos et al., 1995). Kutch, Cambay and Narmada (Fig. 2.2) are three pericontinental rift basins on the western margin of India, which evolved during different phases of

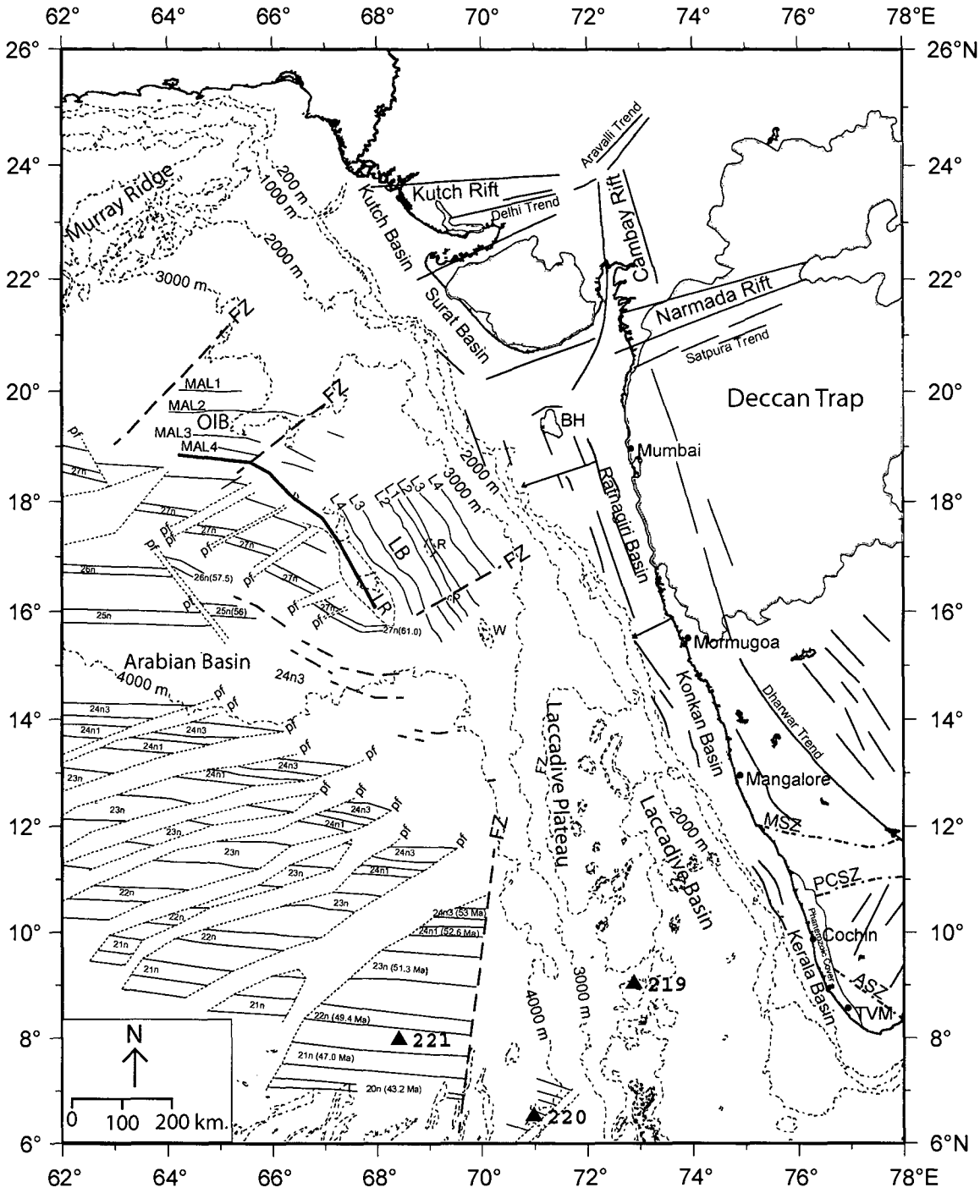

Fig. 2.2. Major structural and tectonic trends within the study area and adjacent regions. Thin dotted lines are selected bathymetry contours (in metres). Solid annotated triangles are DSDP drill sites with site numbers. Inferred magnetic lineations: L1-L4 in the Laxmi Basin and MAL1-MAL4 in the offshore Indus Basin. Identified magnetic isochrons are labelled with anomaly number and corresponding age in Ma [eg. 24n3 (53.12)]. FZ: Fracture Zone; pf: pseudofaults; R: Raman Seamount; P: Panikkar Seamount; W: Wadia Guyot; BH: Bombay High; LB: Laxmi Basin; LR: Laxmi Ridge; OIB: Offshore Indus Basin; ASZ: Achankovil Shear Zone; PCSZ: Palghat - Cauvery Shear Zone; MSZ: Moyar Shear Zone. Compiled from Biswas (1982), Singh and Lal (1993), Bhattacharya and Chaubey (2001), Bhattacharya et al. (1994a, b), Malod et al. (1997), Chaubey et al. (2002a) and Meissner et al. (2002).

India's geotectonic history during its break-up from Gondwanaland, its northward drift and final collision with Eurasia (Biswas, 1982). These basins were formed by rifting along Precambrian tectonic trends. Interplay of three major Precambrian tectonic trends of western India, Dharwar (NNW-SSE), Aravalli-Delhi (NE-SW) and Satpura (ENE-WSW) controlled the tectonic style of these basins. The geological history of the basins indicates that these basins were formed by sequential reactivation of primordial faults. The Kutch Basin opened up first in the Early Jurassic (rifting was initiated in Late Triassic) along the Delhi trend followed by the Cambay basin in the Early Cretaceous along the Dharwar trend and the Narmada Basin in Late Cretaceous time along the Satpura trend.

One of the major geomorphic features in the western peninsular India adjacent to the study area is the Western Ghats escarpment, which forms the western edge of the mountainous Sahyadri Range. This spectacular Western Ghat escarpment has more than 700 m drop at places (Valdiya, 2001). This feature appears to be interesting in connection with the evolution of the western continental margin because some researchers (Widdowson, 1997; Widdowson and Gunnell, 1999) believe that this feature was formed at the time of rifting of Seychelles from India (~65 Ma) and subsequently retreated by about 120-180 km.

2.2.2 *Western continental shelf of India*

The western continental shelf of India (Fig.2.2) is considered to be limited by 200 m isobath. Towards north this shelf is relatively wider, being more than 300 km in the areas north off Mumbai coast, whereas towards south this width gradually narrows down to about 50 km off Trivandrum. In contrast to this, the continental slope is narrow in the north but widens towards south (Biswas, 1989).

A series of narrow regional and local horsts and graben structures formed by longitudinal extension faults characterizes the basement trends of the shelf area. The style of faulting is controlled by three major orogenic trends of western part of the Indian mainland. From Kerala offshore to Bombay offshore, the Dharwarian trend (NNW-SSE) predominates, to the north, in the Gulf of Cambay region – the Satpura trend (ENE-WSW) dominates the structural style while

further north in Kutch–Saurashtra region the Aravalli–Delhi trend (NE-SW) is predominant (Biswas, 1989).

The western continental shelf sedimentary basins appear to have been divided into several sub-basins delimited by transverse basement arches or fault bounded highs (Ramaswamy and Rao, 1980; Biswas and Singh, 1988; Biswas, 1989; Nair et al., 1992; Singh and Lal, 1993; Raju et al., 1999). These basins (Fig. 2.2) are Kutch Basin, Surat Basin, Ratnagiri Basin, Konkan Basin and Kerala Basin. The southwesterly plunging Saurashtra Arch separates the Kutch Basin from the Surat Basin. West plunging Bombay Arch occurs between the Surat and Ratnagiri basins. The Konkan Basin is separated from the Ratnagiri Basin by the southwesterly plunging Vengurla Arch and from the southernmost Kerala Basin by southwesterly plunging Tellicherry Arch. The southern extension of the NNW-SSE trending Cambay graben in the offshore area together with a series of parallel horst-graben features cut across the Bombay Arch isolating the Bombay High.

2.2.3 *Laxmi Ridge*

Laxmi Ridge (Fig. 2.2) is a prominent physiographic feature located in the deep offshore region off west coast of India. This physiographic feature was first observed and named by Naini and Talwani (1977), and subsequently studied by various researchers (Naini and Talwani, 1982; Kolla and Coumes, 1990; Droz and Bellaiche, 1991; Shaynurov and Terekhov, 1991, Miles and Roest, 1993; Pandey et al., 1995; Malod et al., 1997; Chaubey et al., 1998; Miles et al., 1998; Talwani and Reif, 1998, Singh, 1999, 2002; Lane et al., 2003, 2005; Collier et al., 2004a, b, Mishra et al., 2004; Bansal et al., 2005; Krishna et al., 2006). This is an aseismic basement high feature, mostly buried under sediment cover. The average water depth over the ridge is about 2.8 km and has a basement relief of about 2 km (Naini and Talwani, 1982; Droz and Bellaiche, 1991). Even though a positive basement feature, this ridge is associated with a characteristic broad negative free-air gravity anomaly (~50 mgal). It is expressed as NW–SE trending topographic high in the southerly end, while its topographic expression is not discernible northward beyond 18°30'N. However, based on associated characteristic gravity low and the adjacent magnetic anomalies, it was deduced that around 65°30'E this ridge turns WNW-ENE and extends westwards at least

up to 63°40'E (Miles and Roest, 1993). The southward extension of the physiographic expression of the NW-SE trending most prominent segment of the Laxmi Ridge appears to terminate abruptly against an oceanic crust containing east-west trending magnetic lineations (Bhattacharya and Chaubey, 2001).

In absence of direct evidences like drill well information, various authors have inferred nature of the basement of the Laxmi Ridge based on geophysical data. Some researchers (Naini and Talwani, 1982; Kolla and Coumes, 1990; Miles and Roest, 1993) considered this physiographic feature as a continental sliver, forming the boundary between rifted transitional type of crust lying landward (north and east) and the oceanic crust of the Arabian Basin in the south and west. On the other hand consideration of some other studies (Bhattacharya et al., 1994b; Malod et al., 1997) appear to suggest this ridge is flanked on both sides by oceanic crust. Based on the gravity modeling and plate tectonic reconstructions, Todal and Eldholm (1998) opined that the Laxmi Ridge is a marginal high complex, comprising both continental and oceanic crust, where inner part of the ridge is underlain by faulted continental blocks. Talwani and Reif (1998) have modeled the Laxmi Ridge as a continental fragment lying between the oceanic crust of Arabian Basin in the west and the oceanic crust of the Laxmi Basin in the east. Based on the modeling of velocity structure of the Laxmi Ridge using the recently acquired seismic reflection and refraction data, Collier et al. (2004a, b) observed that the Laxmi Ridge is associated with bright reflectivity similar to the confirmed continental crust in the continental rise region off Pakistan. Using the same data, Lane et al. (2005) inferred that the Laxmi Ridge is underlain by magmatic underplating. Bansal et al. (2005), based on their admittance analysis of gravity data, interpreted the Laxmi Ridge as a fragment of continental crust.

2.2.4 *Laxmi Basin*

Naini and Talwani (1982) divided the deep offshore regions off western continental margin of India into two provinces viz., the Eastern Basin and the Western Basin. The dividing line between these two provinces was considered to coincide approximately along the western limit of the Laxmi Ridge and the Laccadive Plateau. Bhattacharya et al. (1994b) considered a part of this Eastern Basin as a distinct entity and named that part as the "Laxmi Basin". The Laxmi

Basin (Fig. 2.2) was considered to be bounded in the west by the Laxmi Ridge, in the south by the northern extremity of the Laccadive Plateau, and in the east by the continental slope of India respectively. The northern limit of the basin is considered to be limited approximately along 21°N, where the bathymetric contours of the adjacent slope region abruptly change to westerly trend. It may be noted that the deep-sea basin region eastward of the Laxmi Ridge and the Laccadive Plateau was referred by Biswas and Singh (1988) as the "Laxmi-Laccadive depression." In this context the Laxmi Basin represents a part of the Laxmi-Laccadive depression. Approximately along the axial part of this basin, a NNW-SSE trending seamount chain is present (Bhattacharya et al., 1994a). Apart from these seamounts, the water depths in the Laxmi Basin area range between 3000 and 3750 m and seafloor gently dips southwestward (Bhattacharya et al., 1994a). In this region, the sediment thickness is minimum over the seamounts and the adjacent Laxmi Ridge, whereas in rest of the basin, it attains a maximum thickness of about 2.0 km (Naini, 1980).

The seismic refraction and gravity studies (Naini, 1980; Naini and Talwani, 1982) in this region suggest that; i) the crustal thickness is about 17 km, which implies that the underlying crust is thicker than normal oceanic crust and nearly half that of a standard continental crust and ii) the basin is characterized by a low amplitude (~20 mgal) short wavelength (~60 km) free-air gravity low superimposed on a long wavelength (~350 km) gravity high. Based on a study of closely spaced magnetic and gravity profiles, Bhattacharya et al. (1994b) mapped the existence of well-correlatable NNW-SSE trending linear magnetic anomalies in this basin. These linear magnetic anomalies were reported to be symmetric about a central negative magnetic anomaly and the axis of symmetry coincides with a characteristic short-wavelength free-air gravity low. The magnetic lineations are contiguous and parallel to the adjacent segment of the Laxmi Ridge in the west and the continental shelf in the east. It was inferred (Bhattacharya et al., 1994b) that the Laxmi Basin magnetic lineations (Fig.2.2) record a two-limbed seafloor spreading anomaly sequence, probably representing anomalies 33n (~79 Ma, Late Cretaceous) through 28n (~62 Ma, Late Paleocene). In the axial part of the Laxmi Basin, a well-defined basement peak was observed by Naini (1980) in one of the seismic profiles. This feature is about 30 km wide and rises

by about 3.0 sec TWT above the adjacent basement. Basement rises were also observed (Naini, 1980) in the neighbouring seismic profiles, but they are much subdued and sub-surface. Together these features were considered (Naini, 1980) to represent an axial basement high zone in the Laxmi Basin. Based on analysis of additional seismic profiles in the nearby areas, Rao et al. (1992) inferred that this basement high zone represents a 360 km long linear feature and named it as the Panikkar Ridge. This basement high zone approximately coincides with the reported axis of symmetry of two-limbed seafloor spreading magnetic anomalies, which Bhattacharya et al. (1994b) inferred to represent an extinct spreading centre.

Difference of opinion exists regarding the nature of the crust underlying the Laxmi Basin. Based on semi-continental crustal thickness and lack of identifiable seafloor spreading type magnetic anomalies, Naini and Talwani (1982) believed that the crust underlying this region is transitional in nature. Based on identification of hyperbolic reflection pattern, typical of an oceanic crust, in the multichannel seismic reflection data from deep offshore regions off Ratnagiri coast, Biswas (1989) and Biswas and Singh (1988) favoured an oceanic nature of the basement in this area. Based on observation of structural and tectonic grains parallel to the ancient Precambrian structural grain of the adjacent western part of the Indian subcontinent, Kolla and Coumes (1990) inferred that the Laxmi Basin area represents rifted transitional crust. As mentioned earlier, based on identification of seafloor spreading type magnetic anomalies, Bhattacharya et al. (1994b) opined that the Laxmi Basin is underlain by oceanic crust formed as a result of a now extinct two-limbed seafloor spreading. Based on interpretation of gravity data it was opined that this area is an underplated normal oceanic crust (Pandey et al., 1995; Singh, 1999). Studying ship-borne and satellite gravity and magnetic data, Miles et al. (1998) concluded that the crust in the Laxmi Basin is rifted and underplated continental crust. It may be mentioned here, that areas north and northwest of the Laxmi Basin, i.e. in the areas northward of Laxmi Ridge, Malod et al. (1997) inferred the existence of oceanic type of crust, which evolved during chrons 29r-29n (about 66-64 Ma, early Paleocene). Mainly based on gravity and magnetic data and paleogeographic reconstructions, Todal and Eldholm (1998) opined that the crust underlying the Laxmi Basin is of continental

in nature. Talwani and Reif (1998) on the other hand favoured oceanic nature of the crust underlying the Laxmi Basin. Studies of Bernard and Munschy (2000) for understanding the structural scheme and evolution of Mascarene Basin, suggested that the Laxmi Basin need to be underlain by an oceanic crust matching in width with the missing oceanic crust in the northwest Mascarene Basin. Based on the gravity and magnetic modeling, Krishna et al. (2006) opined that the Laxmi Basin is underlain by continental crust, which subsequently got modified by extensive stretching and volcanic outpourings of the Reunion hotspot. According to them, the magnetic anomalies in the Laxmi Basin, that Bhattacharya et al. (1994b) interpreted as seafloor spreading magnetic anomalies, could best be explained as volcanic intrusives within the stretched continental crust.

2.2.5 *Offshore Indus Basin*

The Offshore Indus Basin (Fig. 2.2) is located in the upper Indus Fan region (Miles et al., 1998) and is bounded by the east-west trending buried Laxmi Ridge to the south, the Murray Ridge and the Owen Fracture zone in the northwest and the continental slope of India and Pakistan in the northeast. Some researchers (Malod et al., 1997; Collier et al., 2004a, b) used the nomenclature of 'Gop Rift' for the Offshore Indus Basin region. The southern boundary of the basin lies approximately along 3000 m isobath, where the basin merges with the northern boundary of the Laxmi Basin. The water depths in the basin range from 1400-1600 m at the foot of the continental slope to ~3400 m near the E-W trending buried segment of the Laxmi Ridge (Bhattacharya and Chaubey, 2001). The maximum sediment thickness in the basin is about 6 sec two-way travel time (TWT), of which the fan type sediments may exceed 3 sec TWT. These sediments are interpreted to have been deposited since the Cretaceous period, but the fan type sequences were probably deposited since Middle Oligocene to Early Miocene (Kolla and Coumes, 1987). The tectonic structure of the basement comprised of E-W trending horst and graben with several NE-SW basement fault. Malod et al. (1997) reported the presence of a basement high feature, called Palitana Ridge, in the axial part of the Offshore Indus Basin. The genesis of this feature has been attributed by Malod et al. (1997) to the uplifting during the

Miocene reactivation. This feature has been well demarcated in the most recent available seismic reflection section of Collier et al. (2004a, b).

As in the case of the Laxmi Basin, difference in opinion exists about the nature of the crust in the Offshore Indus Basin also. Naini and Talwani (1982) had observed some of the linear magnetic anomalies in this region; however, they were not successful to model these anomalies in terms of seafloor spreading. Malod et al. (1997) interpreted the Offshore Indus Basin to have been underlain by oceanic crust formed as a result of two-limbed seafloor spreading between the Laxmi Ridge and the adjacent continental slope of Pakistan. They identified these magnetic lineations as 29r-29n (~66-64 Ma, Early Paleocene), and made attempt to correlate this result with the inferred seafloor spreading magnetic anomalies in the Laxmi Basin. Based on the gravity and magnetic modeling exercises, Miles et al. (1998) interpreted that the Offshore Indus Basin is underlain by underplated and thinned continental crust, where the magnetic anomalies can be explained in terms of intrusives within the thinned continental crust instead of seafloor spreading type magnetic anomalies. Krishna et al. (2006) negated the possibility of an oceanic crust underlying the Laxmi Basin region; however, they supported the views that the Offshore Indus Basin region is underlain by oceanic crust.

2.2.6 *Laccadive Basin*

The Laccadive Basin – a narrow triangular shaped basin – is located between the Laccadive Plateau in the west and the southwestern continental slope of India in the east (Fig.2.2). The northern boundary of the basin lies approximately near 16°N where the northern extremity of the Laccadive Plateau apparently meets the adjacent continental slope of western India. In the south, this basin opens into the Central Indian Basin. The water depth in this basin varies from ~2000 m in the north to ~2800 m in the south (Bhattacharya and Chaubey, 2001). Based on limited magnetic and seismic reflection data Rao and Bhattacharya (1975) inferred that the underlying basement in this area is block-faulted. The seismic reflection studies (Ramaswamy and Rao, 1980; Naini and Talwani, 1982; Rao and Srivastava, 1984) suggest that the sediment thickness in this basin is about 2.5 sec (TWT) in the southern part, which gradually increases to about 3.5 sec (TWT) towards the northern part of the basin. The underlying

basement widens and deepens towards south and is characterized by several basement high features, which form an approximately NNW-SSE trending lineament which was named by Naini and Talwani (1982) as the 'Prathap Ridge'.

The Laccadive Basin is reported to be associated with broad low to subdued magnetic anomaly, and generally low free-air gravity anomaly (Rao and Bhattacharya 1977; Naini and Talwani, 1982; Rao et al., 1987; Subrahmanyam et al., 1995). However, these geophysical signatures are locally modified due to the presence of Prathap Ridge, which is associated with relative free-air gravity high. Based on gravity studies, Subrahmanyam et al. (1995) opined that the Prathap Ridge is offset along pre-exiting ENE-WSW trending Precambrian fault trends extending from adjacent Indian mainland and was formed during the separation of India from Madagascar. The Prathap Ridge is mostly buried below sediments and divides the basin in two parts. Based on widely spaced seismic reflection profiles, Rao et al. (1987) inferred that the ridge is depicted as a single peak basement high in the north, and multiple peaks in the south. Based on the magnetic data and seismic reflection studies Krishna et al., (1992) interpreted that, the Prathap Ridge consists of basement having variable magnetic signatures, and formed due to Reunion Hotspot activity. By identifying rotated fault blocks representing half-grabens, which are equidistant from a central basement high (Prathap Ridge) in the Laccadive Basin, Chaubey et al. (2002b) suggest that the basin is formed as a result of failed rift and volcanism of the stretched continental regime.

2.2.7 *Laccadive – Chagos Ridge*

The Laccadive-Chagos Ridge is one of the most prominent physiographic and aseismic features of the Indian Ocean (Fig. 1.1). This slightly arcuate major elongated tectonic feature is considered to extend for about 2500 km between 12°S and 14°N. A considerable length of the crest of this ridge is composed of shoals, banks, and coral reefs at depths less than 1500 m. This ridge can be divided into three main segments by breaches in its topographic continuity due to several relatively deep saddle like features (Bhattacharya and Chaubey, 2001). Following Bhattacharya and Chaubey (2001) these three segments of Laccadive-Chagos Ridge are being referred from north to south as the Laccadive Plateau, the Maldive Ridge and the Chagos Bank.

Gravity data in the Laccadive Plateau region indicates that the Free-air gravity anomaly, in general, is negative and subdued. However, a belt of relative positive anomalies was observed approximately over the crestal region (Talwani and Kahle, 1975; Avraham and Bunce, 1977; Naini, 1980; Naini and Talwani, 1982). The magnetic anomalies over the eastern half of the Laccadive Plateau are reported (Naini and Talwani, 1982; Rao et al., 1987) to be subdued, whereas its western half in contrast, appears to be associated with several prominent high amplitude anomalies. Seismic reflection studies suggest that the basement in general is in the form of a broad bulge, over which at places sharp peaks are present. These peaks are devoid of sediment cover and some of them reach very close to the sea surface. In the areas north of 12°N, the basement appears to consist of smaller blocks that drop in a step-like fashion to the west (Naini, 1980; Naini and Talwani, 1982; Reddy et al., 1988).

A number of workers have postulated that the Laccadive-Chagos Ridge is an inactive and subsided part of a linear volcanic feature formed during the northward motion of the Indian plate over the Reunion Hotspot. The linearity of this ridge and the north-south age progression of the volcanic rocks along the trace of the ridge are considered as strong evidences for such a hotspot model (Francis and Shor, 1966; Dietz and Holden, 1970; Whitmarsh, 1974; Morgan, 1981; Duncan, 1981; Duncan and Hargraves, 1990; Verzhbitsky, 2003). However, a number of alternate models were also forwarded to explain the origin of this ridge. Particularly, it appears that many observations and inferences do favour a non–hotspot model of origin for the Laccadive Plateau region. For example, based on seismic refraction studies Babenko et al. (1981) inferred that the Moho in this region lies at a depth of about 18-19 km, which suggests that the thickness of the crust in the Laccadive Plateau region is higher than the normal oceanic crust. Higher than normal oceanic crust thickness was also inferred by Naini and Talwani (1982) from analysis of seismic refraction data and by Chaubey et al. (2002b) from two-dimensional modeling of gravity and magnetic data. Based on identification of several rotated fault blocks from multichannel seismic reflection data, Murty et al. (1999) inferred existence of continental ribbon (or continental fragment) structure over the Laccadive Plateau region. The lack of appreciable magnetic anomalies led Rao et al. (1987) to infer continental origin

for the Laccadive Plateau region. Based on two-dimensional modeling of magnetic data, Satyanarayana et al. (1997) inferred that the basement of the Laccadive Plateau region is volcanic in nature. Narain et al. (1968), based on seismic refraction results of Francis and Shor (1966), have opined that the Laccadive Plateau region forms a transition between oceanic crust to the west and continental crust to the east. Fisher et al. (1971) have suggested that the Laccadive-Chagos Ridge was built up over an old transform fault during India's northward movement. By considering the refraction velocities over Laccadive-Chagos Ridge (Francis and Shor, 1966) and plate reconstruction models, McKenzie and Sclater (1971) opined that the Laccadive-Chagos Ridge was formed due to volcanism since Upper Cretaceous. Avraham and Bunce (1977) suggested that the Laccadive-Chagos Ridge is composed of structural elements of multiple origin. They suggested that the ridge consists in part of several north-south fracture zones and in parts of volcanic features formed either by leaky transform faults or by the passage of Indian plate over a hotspot.

2.3 Tectonic elements of the areas conjugate to the western continental margin of India and adjoining areas

As described in the previous sections, the western continental margin of India and the adjoining deep offshore regions were formed due to the rifting and successive drifting of India, Seychelles and Madagascar. In this framework, some of the tectonic elements off west coast of India appear to be related to separation of India and Seychelles while few others appear to be related to India–Madagascar separation. Therefore, a brief account of those tectonic elements from the conjugate areas of Seychelles and Madagascar that appears genetically related to the study area has been presented in this section.

2.3.1 *Features on the eastern part of Madagascar mainland*

About two-third part of Madagascar is occupied by Precambrian rocks (Boast and Nairn, 1982), which are overlain and intruded by Mesozoic and Cenozoic rocks related to the separation of Madagascar from Africa and India during the break up of Gondwanaland. The Precambrian of Madagascar can be subdivided into southern and central-northern sectors, separated by Ranotsara Shear Zone (Fig. 2.3). The southern Madagascar is divided into six tectonic units

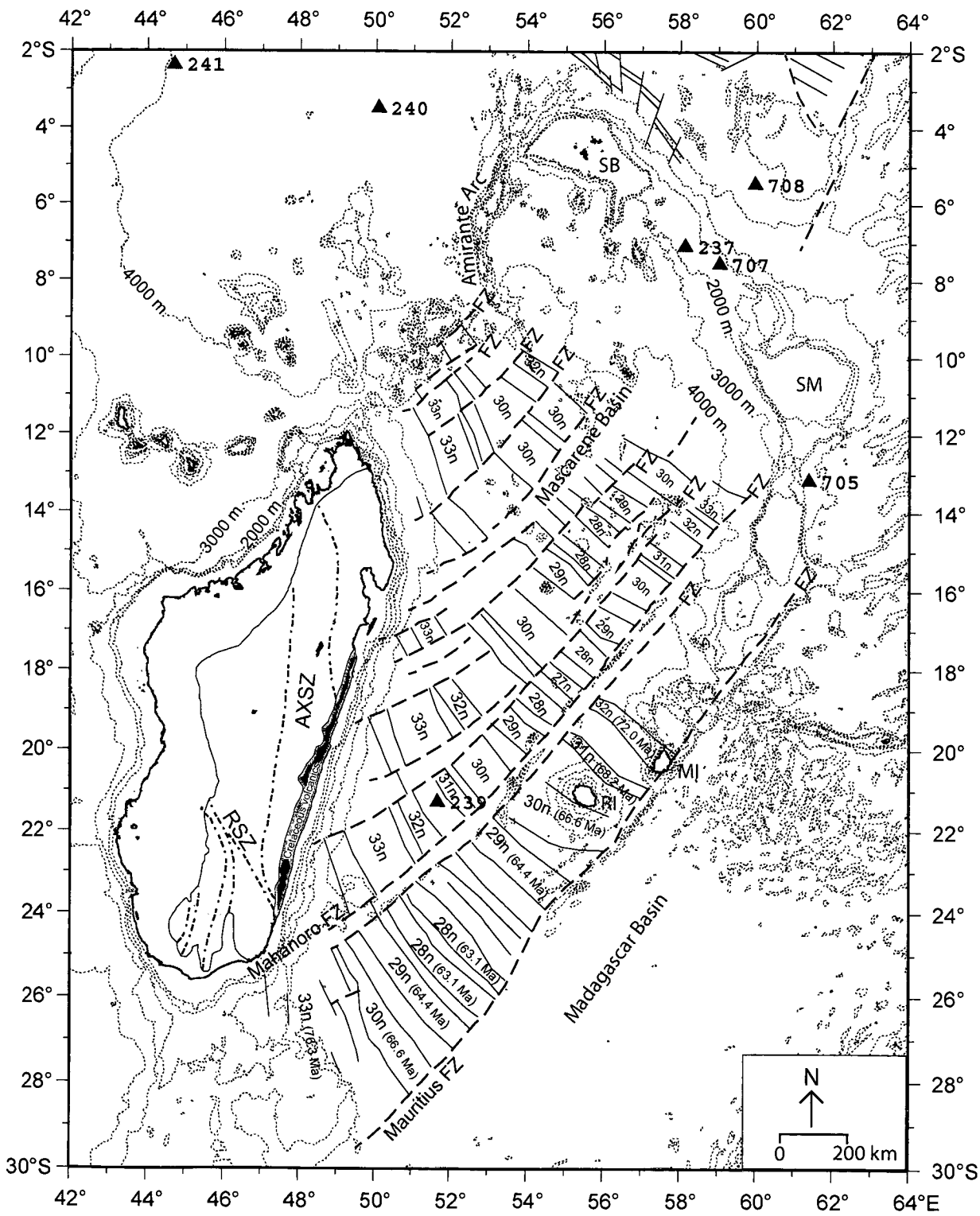

Fig. 2.3. Major structural and tectonic trends within the Mascarene Basin and adjacent Madagascar and Seychelles regions. RSZ: Ranotsara Shear Zone; AXSZ: Axial Shear Zone; SB: Seychelles Bank; SM: Saya de Malha Bank; MI: Mauritius Island; RI: Reunion Island. Compiled from Windley et al. (1994), Bernard and Munschy (2000), and Chaubey et al. (2002a). Other details are as in Fig. 2.2.

(Windley et al., 1994) and the central-northern Madagascar is divided into five tectonic units (Collins et al., 2000a, b; Collins and Windley, 2002), which are separated from each other by a regionally significant unconformity or by shear zones. In the southern Madagascar, from west to east, these tectonic units are Vohibory belt, Ampanihy belt, Bekily belt, Betroka belt, Tranomaro belt and Dauphin–Anosyan belt. The tectonic units in the north-central Madagascar, subdivided by Collins and Windley (2002) are the Antongil Block, Antananarivo Block, Itremo Sheet, Tsaratanana Sheet and the Bemarivi Belt. The Axial Shear Zone is a high-grade zone which forms a central N-S axis to the north-central region of Madagascar. It is dominated by granulite and high amphibolite facies gneisses that commonly contain graphite.

The Ranotsara Shear Zone and the Axial Shear Zone have been considered by several authors (Katz and Premoli, 1979; Windley et al., 1994; Sacks et al., 1997) to provide the qualitative models to depict the India-Madagascar juxtaposition in Gondwanaland perspective. Windley et al. (1994) considered the sinistral Ranotsara Shear Zone and the dextral Axial Shear Zone as the continuation of Achankovil Shear Zone and Palghat-Cauvery Shear Zone in India respectively. However, based on the detailed field studies in the Achankovil shear zone area, Sacks et al. (1997) reported that the Achankovil shear zone is dextral in nature and therefore, the proposition put forward by Windley et al. (1994) cannot be accepted.

The additional geological information available from the Madagascar in context of the present study is the presence of volcanics throughout the east coast of Madagascar. Storey et al. (1995) made an attempt to obtain the age for these volcanic rocks based on the $^{40}Ar/^{39}Ar$ method, and they provided a mean age of ~88 Ma for this volcanic province. This Cretaceous volcanic province in the east coast of Madagascar is considered to have been formed by the influence of Marion hotspot.

2.3.2 *Eastern continental margin of Madagascar*

The continental shelf of Madagascar (Fig. 2.3) is generally narrow, averaging about 25 km in width. At some places, all along the northeast coast, no shelf is present (Pepper and Everhart, 1963). The straight east coast is bordered

by a narrow shelf whose edge is a fault scarp to extend from Fort Dauphin to the Bay of Antongil. The scarp dips steeply to 1800 m, and the continental slope to this depth lies along the fault plane. The Bay of Antongil, which is bordered on each side by a fault trending northwestward along its shore, is probably a down-faulted block trending at an acute angle to the main coastal fault (Pepper and Everhart, 1963). This straight edge has been interpreted by several authors (Barron, 1987; Lawver et al., 1999) as an evidence of transform motion between India and Madagascar that is believed to have been taken place between 160 and 105 Ma.

2.3.3 *Seychelles–Mascarene Plateau*

Seychelles, a Precambrian continental fragment in the Western Indian Ocean, is located approximately between 4°S and 6°S and between 54°E and 57°E (Figure 2.3). This oval shaped Seychelles Bank, of an area of about 80000 sq. km, has an almost flat top lying at an average water depth of 50 m. The edge of the bank is well defined by steep slopes, which drops to depths exceeding 3000 m in all directions, except for the southwest and the southeast. The Seychelles Bank is connected by a 2000 m deep saddle to the Amirante Arc in the southwest, whereas to the southeast, it is separated from the remainder of Mascarene Plateau by a 1500 m deep saddle (Mart, 1988).

Although situated in an oceanic environment, the continental character of the Seychelles Bank has been confirmed by seismic refraction profiling (Francis et al., 1966) and by the determination of Precambrian ages of around 700 Ma of the granitic rocks, which make up most of the Islands. The numerous islands that protrude from the Seychelles Bank are founded on igneous rocks, which outcrop prominently on the three largest islands, Mahe, Praslin and Silhouette. The Precambrian basement of the Mahe and adjacent island groups show that the granites in these islands are commonly hornblende granite, as well as porphyritic granite and aplite, with dioritic and gabbroic xenoliths in places (Baker, 1963 quoted by Mart, 1988). The granites of Mahe and its adjoining islands (except Silhouette and North Island, which are Paleocene) are Late Precambrian and are the type usually found on major continental landmasses (Khanna and Walton, 1992). The sedimentary sequence observed on the Seychelles Bank consists of Quaternary sediments. However a thick sedimentary sequence was encountered

in several exploratory bore holes, which were drilled at the western edge of the bank. The Mesozoic series drilled in these boreholes consists of about 300 m of clastic Triassic sediments overlain by about 2000 m of Jurassic rocks. The Jurassic series is covered by 400-900 m of Cretaceous rocks, the upper part of which consists of volcanic rocks. The volcanics, in turn, are overlain by a Tertiary sedimentary sequence, which consists of approximately 1500 m of carbonates, with clastics in places (Kamen-Kaye, 1985 quoted by Mart, 1988). Seismic refraction measurements show that the Seychelles Bank has a crustal thickness of more than 30 km, and the continental crust is characterized by three layers that show seismic compressional velocities of 5.7, 6.3 and 6.8 km/sec. The region southeast of Seychelles represents a normal passive continental margin (Matthews and Davies, 1966).

The Mascarene Plateau (Fig. 2.3) is a major physiographic feature located in the area between Madagascar and the Central Indian-Carlsberg Ridge segments. This feature is connected with the Seychelles continental block through a broad 1500 m deep saddle in the north, and to the Mauritius Island, through a 2500 m deep channel in the south (Mart, 1988). This arcuate aseismic ridge consists of the Saya de Malha Bank, the Nazareth Bank, the Cargados Carajos Bank and Mauritius Island. Among these, the Saya de Malha, the Nazareth and the Cargados Carajos banks are submerged at water depths of approximately 50 m. These banks are bounded by steep scarps that drop down to depths greater than 2000 m. The Saya de Malha Bank, which is the largest among the three banks, has a 350 km wide southward dipping summit surface (Kara and Sivukha, 1990 quoted by Bhattacharya and Chaubey, 2001). The radiometric dating of the basalts of Saya de Malha Bank provided an age of 45 Ma, where as Nazareth bank basalts provided an age of 31 Ma. The Mauritius Island is an eroded volcanic island built perhaps by three eruptive episodes.

2.3.4 *Madagascar Ridge*

Madagascar Ridge (Fig. 1.3) is a major physiographic feature, which extends south of the Madagascar Island. This N-S striking elongated feature extends between latitudes between 26°S and 36°S, with a maximum width of 750 km at 32°S latitude. This aseismic ridge separates Madagascar Basin from Mozambique Basin in such a ways that it acts as the western boundary of the

Madagascar Basin and Eastern Boundary of the Mozambique Basin. To the south, this ridge abuts at the Southwest Indian Ridge.

The bathymetric map compiled by Goslin et al. (1980) provided detailed information on the topography of the Madagascar Ridge. Based on the detailed analysis of the bathymetry and seismic data, Goslin et al. (1980) suggested that the Madagascar Ridge could be separated into two distinct domains – northern domain and southern domain, which are separated by a broad saddle deeper than 2000 m. The northern area, between latitude 31°S and the continental shelf of the Madagascar, shows complex seafloor and basement topography and is associated with short wave length magnetic anomalies (Schlich, 1982). The crust underlying this northern domain is considered to be anomalous, as it has neither purely continent nor oceanic affinity (Bhattacharya and Chaubey, 2001). The southern area, between latitudes 32°S and 35°S, is generally flattish at depths of less than 1500 m. This part of the ridge corresponds to a subdued topography, where the Moho is inferred to lie about 14 km below sea level. The velocity-depth distribution of the southern domain is closely related to that of mean oceanic crust (Recq et al., 1979 quoted by Schlich, 1982; Goslin et al., 1981). Gravity studies also suggested a contrast in the isostatic compensation of the two domains. The northern domain appears to have achieved local isostatic equilibrium by crustal thickening, where as the southern domain is isostatically unbalanced with respect to the northern domain and the adjacent ocean basins (Goslin et al., 1981; Bhattacharya and Chaubey, 2001).

The western flank of the Madagascar Ridge, facing the Mozambique Basin, is steep and approximately rectilinear in its southern and central part. The eastern flank shows obvious differences in topography north and south of 31°S/32°S. To the north, the eastern flank has many small-scale topographic features on its slope. To the south, a smooth slope separates the ridge from the adjacent Madagascar Basin (Goslin et al., 1980). It is suggested (Schlich, 1982) that the southern domain of the Madagascar Ridge had probably been created simultaneously during an episode of anomalous volcanism on the flanks of the Southwest Indian Ridge approximately at the time of anomaly 31n or 29n (~68-64 Ma).

2.3.5 *Mascarene Basin*

The Mascarene Basin (Fig. 2.3) is bordered on the west by the steep, linear and presumably faulted eastern margin of the Madagascar Precambrian massif and to the east by the Mascarene Plateau (Schlich, 1974). This basin corresponds to the northwestern extension of the Madagascar Basin where the limit is marked by the Mauritius Fracture Zone, which offsets the magnetic pattern right laterally by about 700 km. To the south, the Mascarene Basin abuts the complex northeastern flank of the Madagascar Ridge and to the north; the basin extends towards the Farquhar Group, the Amirante arc, Seychelles Bank and the northern tip of the Madagascar Island (Schlich, 1982; Bhattacharya and Chaubey, 2001).

Deep sea drilling at site 239 in the Mascarene Basin suggested a Late Cretaceous age for this basin (Schlich et al., 1974). Based on the analysis of bathymetric, magnetic and seismic data, the structural scheme of the Mascarene Basin was proposed first by Schlich and Fondeur (1974) and Schlich (1974) and later updated by Schlich (1982). These studies mapped three fracture zones between the Madagascar margin and the western scarp of the Mascarene Plateau running almost parallel to the Madagascar Basin fracture zone system, and identified two complete sequences of early Paleocene and late Cretaceous magnetic anomalies in the southern Mascarene Basin. Since the youngest magnetic anomaly identified in Mascarene Basin is the anomaly 28n, Schlich (1982) suggested that spreading in the Mascarene Basin ceased just prior to time of anomaly 27n. The extinct spreading centre corresponds to a clearly identifiable topographic high, which could be observed on several bathymetric profiles. To the south, the Late Cretaceous magnetic anomalies 32n to 34n have been easily recognized which lie at the foot of the northern Madagascar Ridge. But, these studies could not identify the magnetic lineations in the northern part of the Mascarene Basin and its age was doubtful (Masson, 1984). However, geophysical studies by Masson (1984) inferred three transform faults in the northern part of the Mascarene Basin.

Subsequent studies by Dyment (1991, 1996) and Sahabi (1993) provided revised magnetic anomaly identifications in the southern Mascarene Basin, but the kinematic evolution of the northern part of the Mascarene Basin remained

unknown. Recently, based on the bathymetric, seismic and magnetic data, Bernard and Munschy (2000) proposed a new structural scheme for the whole Mascarene Basin, including the northern part of the Mascarene Basin. They identified five new compartments and numerous fracture zones in the northern part of the Mascarene Basin (Fig. 2.3). Their interpretation suggests a southward progressive extinction of the Mascarene spreading centre.

According to the presence of anomaly 34n (83 Ma) off the Madagascar margin in the Mascarene Basin, it is believed that the seafloor spreading in the Mascarene Basin commenced during mid-Cretaceous time (Norton and Sclater, 1979; Besse and Courtillot, 1988). Since this time falls under the Cretaceous long normal superchron, the precise age of the rift-drift transition cannot be determined from the magnetic lineations.

2.3.6 *Madagascar Basin*

The Madagascar Basin is bound on the southeast by the rough topography of the Southwest Indian Ridge, and to the southwest by the gentle upward slope of the Madagascar Ridge. To the northwest, the Madagascar Basin is considered to have been separated from the Mascarene Basin by a clearly defined approximately NE-SW trending Mauritius Fracture Zone. To the northeast, the Madagascar Basin is limited by the rugged topography of the southern section of the Central Indian Ridge. Two major fracture zones, nearly parallel to the trend of Southwest Indian Ridge, have been traced throughout the Madagascar Basin (Schlich, 1974; Schlich, 1975 quoted by Bhattacharya and Chaubey, 2001). The basin contains the entire sequence of anomalies 20n to 30n (~43 to 66 Ma). The oldest anomaly, 30n (~66 Ma), was found in the southern Madagascar Basin close to the Madagascar Ridge, where as the youngest anomaly, 20n (~43 Ma) was observed in the area south of the Mauritius Islands. The DSDP site 245 in the southern Madagascar Basin was located south of and immediately next to anomaly 29n (~64 Ma). The oldest sediments recovered from this site are of Early Paleocene (~63.6 – 66.4 Ma). The Madagascar Basin is inferred to have been created by spreading from the Central Indian Ridge and its conjugate northern basin is considered to lie just east of the Laccadive-Chagos Ridge and forms part of the Central Indian Basin.

2.4 Dated volcanism in the areas related to the study

The ages of various volcanic formations in and around Indian mainland, Seychelles Bank and Madagascar mainland have been estimated by various researchers (Fisher et al., 1968; Shipboard Scientific Party, 1972; Duncan and Hargrave, 1990; Valsangkar et al., 1981; Dickin et al., 1987; Storey et al., 1995; Rathore et al., 1997; Radhakrishna et al., 1990, 1994, 1999; Hofmann et al., 2000; Torsvik et al., 2000; Widdowson et al., 2000; Anil Kumar et al., 2001; Pande et al., 2001; Kothari et al., 2001). In Table 2.1, available estimated ages of volcanic formations in and around Indian mainland (Fig. 2.4) have been compiled and presented. This age estimates are of volcanic samples recovered from drill wells over the continental shelf area, volcanic rocks exposed in the coastal belt, and volcanic rock recovered from a drill hole over the Laccadive Plateau. The compiled data shows occurrence of volcanic rocks of broadly three age groups. The rocks of around 65 Ma age, were related to Deccan Trap basalts (Rathore et al., 1997; Hofmann et al., 2000). The rocks older than 85 Ma perhaps represent India-Madagascar separation related volcanism or even older events. The volcanic rocks younger than 65 Ma, perhaps represents those formed by passage of India over Reunion Hotspot. The evidence of two episodes of volcanism over Laccadive Plateau (Padua Bank) and the estimated ages of 102 Ma and 60 Ma for these events (Kothari et al., 2001) appears interesting. The 60 Ma age corresponds well with the ages along the predicted track of Reunion Hotspot, so it could be related to the hotspot volcanism. However, the 102 Ma age volcanism appears to be surprising due to the fact that the Laccadive Plateau is considered by many authors as a trail of Reunion Hotspot implying that all volcanism over the Laccadive Plateau should be same or younger than 65 Ma. May be the presence of 102 Ma age volcanic rocks over the Laccadive Plateau indicates that this plateau region is a continental fragment which was in existence even before the India-Madagascar separation.

The available estimated ages of volcanic formations in and around Madagascar is compiled in Table 2.2. This age estimates are of volcanic samples recovered from the Cretaceous volcanic and dyke rocks from Madagascar mainland (Fig. 2.5). From this compilation, it is observed that the Cretaceous volcanic and intrusive rocks of Madagascar crop out semi-continuously along the

Table 2.1 Estimated ages of volcanic rocks from selected locations over the western part of the Indian mainland and offshore region as compiled from various publications. Where the position locations are not given in the publication, they were digitized from respective figures.

ID	Latitude (°N)	Longitude (°E)	Rock type and sample locale	Age (Ma)	Dating Method	Reference
A	19° 00'	71° 33'	Basalts, continental shelf off Bombay	65	K-Ar	Rathore et al. (1997)
B	17° 55'	73° 38'	Deccan Trap basalts, Mahabaleswar	65	$^{40}Ar/^{39}Ar$	Hofmann et al. (2000)
C	15° 30'	73° 44'	Basaltic dykes, Goa coast	63	$^{40}Ar/^{39}Ar$	Widdowson et al. (2000)
D	13° 27'	72° 32'	Basalts, Padua Bank, Laccadive Plateau	102+	K-Ar	Kothari et al. (2001)
E	13° 21'	74° 39	Felsic volcanic rocks, St. Mary Islands, northwest off Mangalore	93##	K-Ar	Valsangkar et al. (1981)
F	12° 48'	77° 10'	Mafic dykes, Huliyardurga, Karnataka	89	$^{40}Ar/^{39}Ar$	Anil Kumar et al. (1988, 2001)
G	12° 22'	75° 16'	Dolerite dykes, North Kerala	129	K-Ar	Radhakrishna et al. (1999)
H	11° 56'	75° 28'	Dolerite dykes, North Kerala	99	K-Ar	Radhakrishna et al. (1999)
I	11° 56'	75° 30'	Dolerite dykes, North Kerala	54	$^{40}Ar/^{39}Ar$	Radhakrishna et al. (1999)
J	11° 53'	75° 45'	Dolerite dykes, North Kerala	112	K-Ar	Radhakrishna et al. (1999)
K	11° 27'	75° 47'	Dolerite dykes, North Kerala	61	$^{40}Ar/^{39}Ar$	Radhakrishna et al. (1999)
L	11° 18'	75° 53'	Felsic dykes, North Kerala	82	K-Ar	Radhakrishna et al. (1999)
M	11° 07'	76° 45'	Dolerite Dykes, Agali-Anaikatti, Karnataka	106	K-Ar	Radhakrishna et al. (1999)
N	9° 45'	76° 40'	Leucogabbro dykes, Central Kerala	85	$^{40}Ar/^{39}Ar$	Radhakrishna et al. (1994)
O	9° 20'	77° 10'	Mafic dykes, South Kerala	144	K-Ar	Radhakrishna et al. (1990)

K–Ar : Potassium – Argon $^{40}Ar/^{39}Ar$: ^{40}Argon – ^{39}Argon
ID : Identification of the locations as given in Fig. 2.4.
+ : In this area, age of basalts in different flows range between 60 and 102 Ma
##: In this area Torsvik et al. (2000) dated some rocks at ~91 Ma, using U-Pb method and Pande et al. (2001) at ~85 Ma using $^{40}Ar/^{39}Ar$ Method.

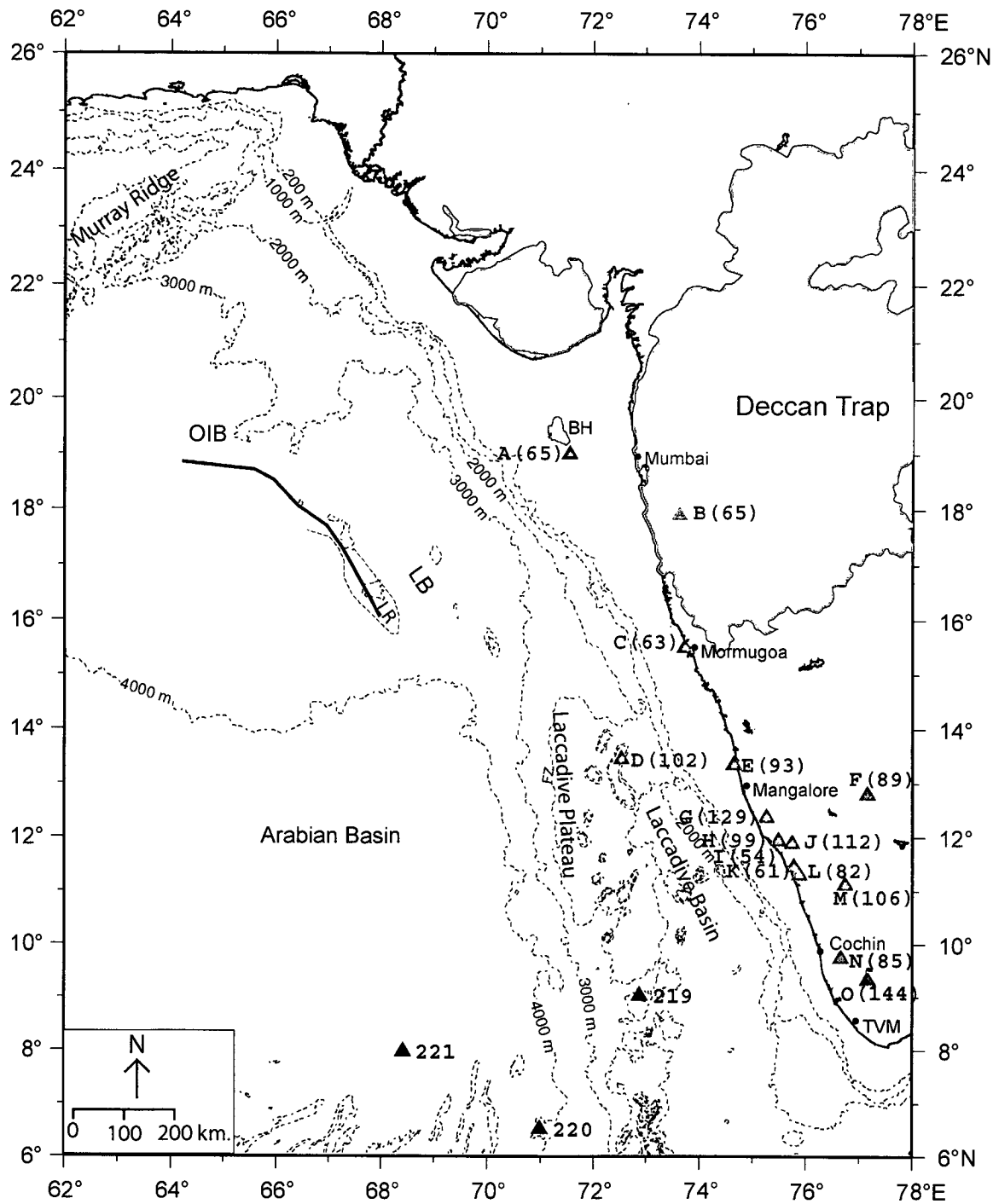

Fig. 2.4. Locations of selected volcanic formations in the west coast of India and the adjacent offshore regions with their estimated ages of emplacement. Red solid triangles are locations where volcanic formations were dated and ages (in Ma) of formations at locations are given within parenthesis. Details of age compilation are presented in Table 2.1. Other details are as in Fig. 2.2.

Table 2.2 Estimated ages of volcanic rocks from selected locations over the eastern part of the Madagascar mainland, Seychelles and the adjoining areas as compiled from various publications. Where the position locations are not given in the publication, they were digitized from respective figures.

ID	Latitude (°S)	Longitude (°E)	Rock type and sample locale	Age (Ma)	Dating Method	Reference
A	24° 34'	46° 11'	Rhyolite, Volcan de L'Androy	87	$^{40}Ar/^{39}Ar$	Storey et al. (1995)
B	24° 24'	46° 05'	Rhyolite, Volcan de L'Androy	85	$^{40}Ar/^{39}Ar$	Storey et al. (1995)
C	23° 09'	47° 35'	Basalt, Eastern Madagascar	89	$^{40}Ar/^{39}Ar$	Storey et al. (1995)
D	22° 42'	47° 40'	Basalt, Eastern Madagascar	89	$^{40}Ar/^{39}Ar$	Storey et al. (1995)
F	21° 17'	48° 05'	Basalt, Manajary, Eastern Madagascar	87	$^{40}Ar/^{39}Ar$	Storey et al. (1995)
G	20° 55'	48° 14'	Basalt, Manajary, Eastern Madagascar	85	$^{40}Ar/^{39}Ar$	Storey et al. (1995)
H	20° 42'	48° 17'	Basalt, Manajary, Eastern Madagascar	84	$^{40}Ar/^{39}Ar$	Storey et al. (1995)
I	19° 24'	48° 38'	Rhyolite, between Manajary and Tamatave, Eastern Madagascar	88	$^{40}Ar/^{39}Ar$	Storey et al. (1995)
J	17° 14'	49° 16'	Basalt, north of Tamatave, Eastern Madagascar	86	$^{40}Ar/^{39}Ar$	Storey et al. (1995)
K	14° 50'	50° 14'	Basalt, south of Sambava, Eastern Madagascar	91	$^{40}Ar/^{39}Ar$	Storey et al. (1995)
L	13° 29'	50° 02'	Basalt, south of Vohemar, Eastern Madagascar	90	$^{40}Ar/^{39}Ar$	Storey et al. (1995)
M	13° 16'	50° 01'	Basalt, Analalava Pluton, northeastern Madagascar	92	U-Pb	Torsvik et al. (2000)
N	6° 40'	52° 35'	Tholeiitic basalts, Western flank of Amirante arc	82	K-Ar	Fisher et al. (1968)
O	4° 19'	55° 43'	Dolerite dykes, Praslin Island	73	K-Ar	Dickin et al. (1987)
P	4° 28'	55° 13'	Syenite, Silhouette Island	66	K-Ar	Dickin et al. (1987)
R	4° 39'	54° 01'	Basalts, Owen Bank	75	K-Ar	Davey et al. (1980) quoted by Plummer (1995)
S	4° 24'	54° 09'	Basalts, Reith Bank	78	K-Ar	Croxton et al. (1981) quoted by Plummer (1995)

K–Ar : Potassium – Argon $^{40}Ar/^{39}Ar$: ^{40}Argon – ^{39}Argon
ID : Identification of the locations as given in Fig. 2.5.

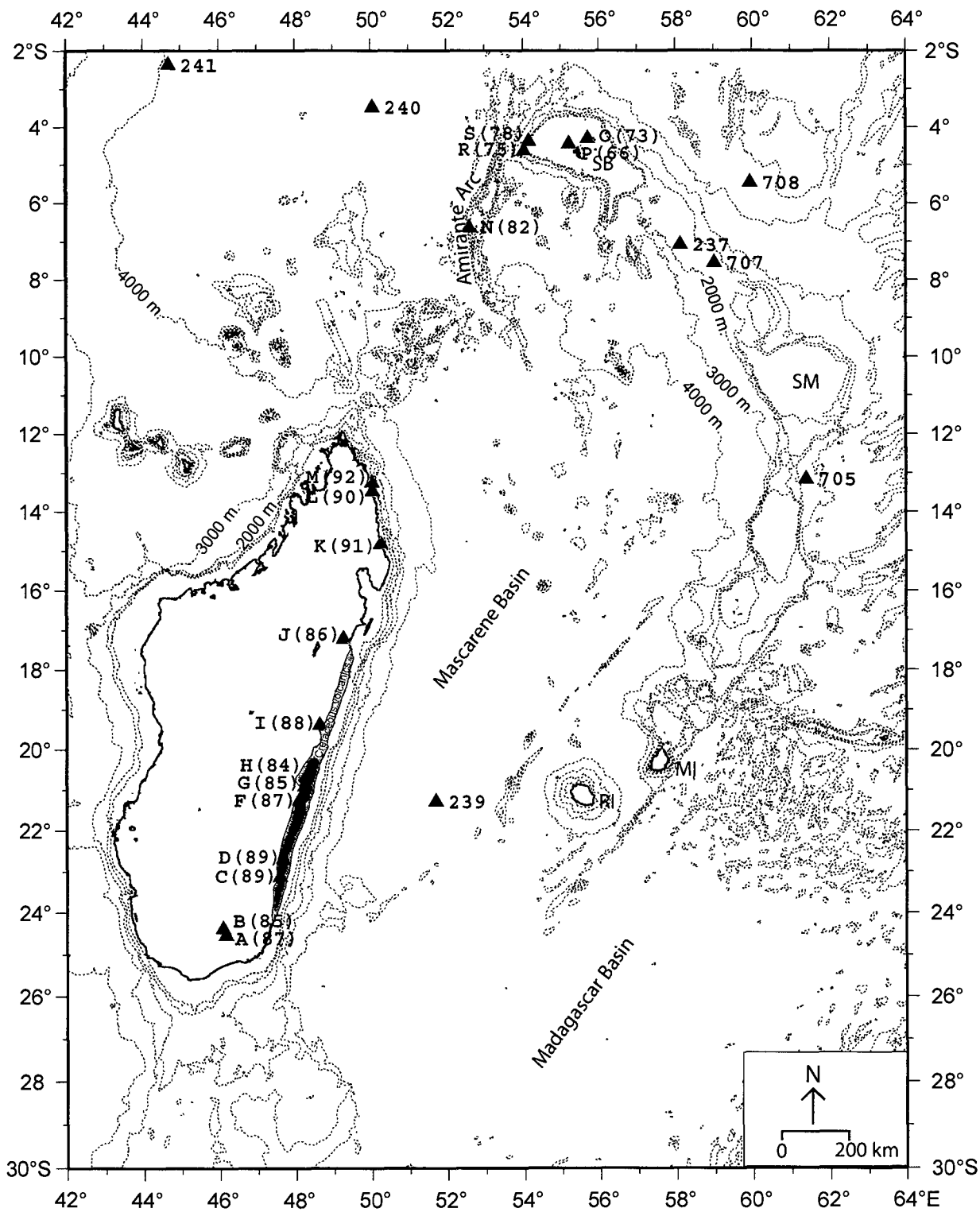

Fig. 2.5. Locations of selected volcanic formations in the east coast of Madagascar, Seychelles and the adjacent regions with their estimated ages of emplacement. Red solid triangles are locations where volcanic formations were dated and ages (in Ma) of formations at locations are given within parenthesis. Details of age compilation are presented in Table 2.2. Other details are as in Fig. 2.3.

~1500 km length of the east coast of Madagascar, which marks the rifted margin. The rocks include basalt flows, dykes and some rhyolitic flows. Along the rifted margin, the flows lie mainly on the Precambrian basement, whereas most of the dykes are parallel to the coast. The Volcan de L'Androy complex in southern Madagascar contains the thickest sequence of Cretaceous volcanic rocks exposed on the Island. The compiled age information in and around the Madagascar mainland and its offshore region indicate that these widespread Cretaceous flood basalts of Madagascar can be related to the track of the Marion hotspot.

The geochronological studies on igneous rocks from Seychelles indicated that the region has been subjected to, or influenced by, several phases of igneous activity. These major igneous rocks are initial granite emplacement (~650 Ma), Karoo Dolerite equivalents (~180 Ma), Lebombo-Movene volcanic equivalents (~140 Ma), Amirante volcanism (~75 Ma) and Deccan Trap equivalents (~63 Ma). However, the volcanics are yet to be recognized in Seychelles related to the rift between Seychelles and Madagascar, which is predicted to have occur at around 96-84 Ma (Plummer, 1995), before the initiation of the seafloor spreading in the Mascarene Basin at around 83 Ma. In Table 2.2 available estimated ages of volcanic formations in and around Seychelles is compiled. These age estimates are of volcanic samples recovered from Amirante Arc, Praslin Island, Silhouette Island and the basement sampled at ODP Site 707 in the saddle between Seychelles and Saya de Malha (Fig. 2.5).

2.5 Passive continental margins – types, formation and evolution

Geologically, continental margins represent a transition zone, where thick granitic continental crust changes to thin basaltic oceanic crust (Davis and Fitzgerald, 2004). Depending on their characteristics, the continental margins have been broadly categorized into two basic types; 1) Passive (or Atlantic type) continental margins and, 2) Active (or Pacific type) continental margins. The passive continental margins are usually characterized by a relatively wide continental shelf, an extensive continental rise and are devoid of significant seismic activity. The passive margins develop during the processes of continental break-up and subsequent ocean basin formation. They are located within the plate interior where the continent and adjacent ocean floor are part of the same

plate. On the other hand the active continental margins are seismically very active and are, instead of a continental rise, characterized by a trench at the foot of the continental slope. The active continental margins develop where an oceanic plate is consumed beneath a continental plate at a subduction zone. Therefore in case of active margins, the continent and adjacent ocean floor belongs to different plates (Seibold and Berger, 1993; Open University Course Team, 1995).

The western continental margin of India was considered as a passive continental margin (Biswas, 1982, 1987) and later a major portion of this margin was further categorized as volcanic passive (rifted) margin (Todal and Eldholm, 1998). Therefore, to appreciate the western continental margin of India in terms of a volcanic passive continental margin framework, the generalized concepts of formation of various types of passive continental margins in general and volcanic passive (rifted) margins in particular have been briefly described in the following paragraphs.

(a) Types of passive margins

Passive margins are broadly divisible into rifted and sheared (or transform) types. Rifted continental margins form where the initial plate separation is approximately perpendicular to the rupture. They show a gradational transition, and their morphology can be subdivided into continental shelf, continental slope and continental rise. Rifted margins comprise a group with two end members: non-volcanic rifted margins - that have evolved without extensive igneous activity, and volcanic rifted margins - those in which igneous processes played a major role in their formation. Since the lithosphere has wide range of responses to rifting at different mantle temperatures, so there is probably a continuum of margin structures between non-volcanic and volcanic (Jones, 1999).

Sheared (or transform) continental margins form when the initial split is along a transform fault and differ from rifted continental margins both in their structure and development. They are usually characterized by steep continental slopes that connect the ridge-trough complexes of the oceanic transform and the transition between the thick continental crust and thin oceanic crust is sharp, usually occurring over distances of less than ~30 km. The outer parts of a

transform margin usually are underlain by a basement ridge, which bounds on its landward side a deep sedimentary basin (Jones, 1999).

(b) Formation and evolution of passive margins

Generally agreed sequence of phases for the evolution (Fig. 2.6) of passive margins is:

i) rifting;

ii) onset of drifting, i.e., separation of continental crust as oceanic crust accretes in the gap between continental blocks; and

iii) post-rift evolution, dominated by massive subsidence of the rifted margins and shaping of those margins by sedimentary and secondary (mostly gravity) tectonics (National Research Council, 1979).

Continental rifting, a thermo-mechanical process, is the first stage of the process by which continents break-up. Crustal thinning, thermal anomalies (high heat flow) and uplift are clearly associated with rifting but regarding the mechanism of initiation of rifting, there exist two models, active rifting and passive rifting. In the passive model, lithospheric tension causes failure of the continental lithosphere and results extension. The two types of the tectonic extensional stresses, which have been suggested for the lithospheric tension, are convective drag on the base of the lithosphere caused by major cellular convection currents, and plate interior stress caused by plate boundary forces. In the active model, the anomalous upper mantle develops first by some form of convective upwelling and doming and consequently, volcanism and extension. The uplifted dome and its deep isostatic compensation give rise to local tension in the lithosphere. As the lithosphere thins by heating up, the stress becomes concentrated into the relatively thin strong layer near the surface, with consequent stretching and faulting. The passive model with its modifications explains the formation of passive margins segments away from hot spot regions. Whereas the active model explains volcanism, plateau uplift and rifting primarily as a consequence of the formation of anomalously hot and low density region in the underlying mantle – a hot spot (Bott, 1995). The end products of active and passive rifting are likely to be very similar and the difference between the two are not easy to recognize in the geological record (Fitton, 1983; Golombek et al., 1996). Geologic record

suggests that rifting process often localize along ancient orogenic belts and suture zones. By weakening the crust, these pre-existing crustal discontinuities play a major role in the localization and distribution of crustal strain (Corti et al., 2003).

(c) The sediment cover and deep crustal structure at rifted continental margins

(i) *Sediment cover*

Normally passive margins are characterized by thick piles of sediments, however, there are a few starved margins where sediments are thin or absent due to lack of supply of sediments during their development. In general, the sedimentary rocks found at passive margins had been formed during three successive stages. First, the continental basement may be overlain by the pre-rift sediments, i.e. the sediments deposited prior to rifting. Second, syn-rift sediments of the rifting stage of margin development may be deposited at the time of initial rifting and continental stretching. Third, post-rift sediments of the drifting stage are deposited subsequent to continental break-up and onset of seafloor spreading. They are separated from the underlain syn-rift sediments by the post-rift or break-up unconformity. The post-rift sediments are generally un-faulted (except for growth faults at the slope) indicating a quiet tectonic environment apart from slow but persistent subsidence at an exponentially decreasing rate. Syn-rift sediments are typically deposited in half-grabens formed by intense stretching and thinning of the continental crust and lithosphere (Bott, 1995).

(ii) *Deep crustal structure*

The crustal thinning and stretching eventually lead to the break-up of continents forming a new ocean basin with a pair of passive continental margins on both the sides (Fig. 2.6). The detailed information on the structure of passive continental margins has come from seismic experiments, which suggest that the continental basement thins towards the ocean and that the transition from thick continental to thin oceanic crust occurs over distances of a few tens of kilometers to over a hundred kilometers. Various criteria have been considered to define the position of the ocean-continent boundary. These criteria have been based on crustal thickness, vertical and lateral variations in seismic velocity, seismic mode

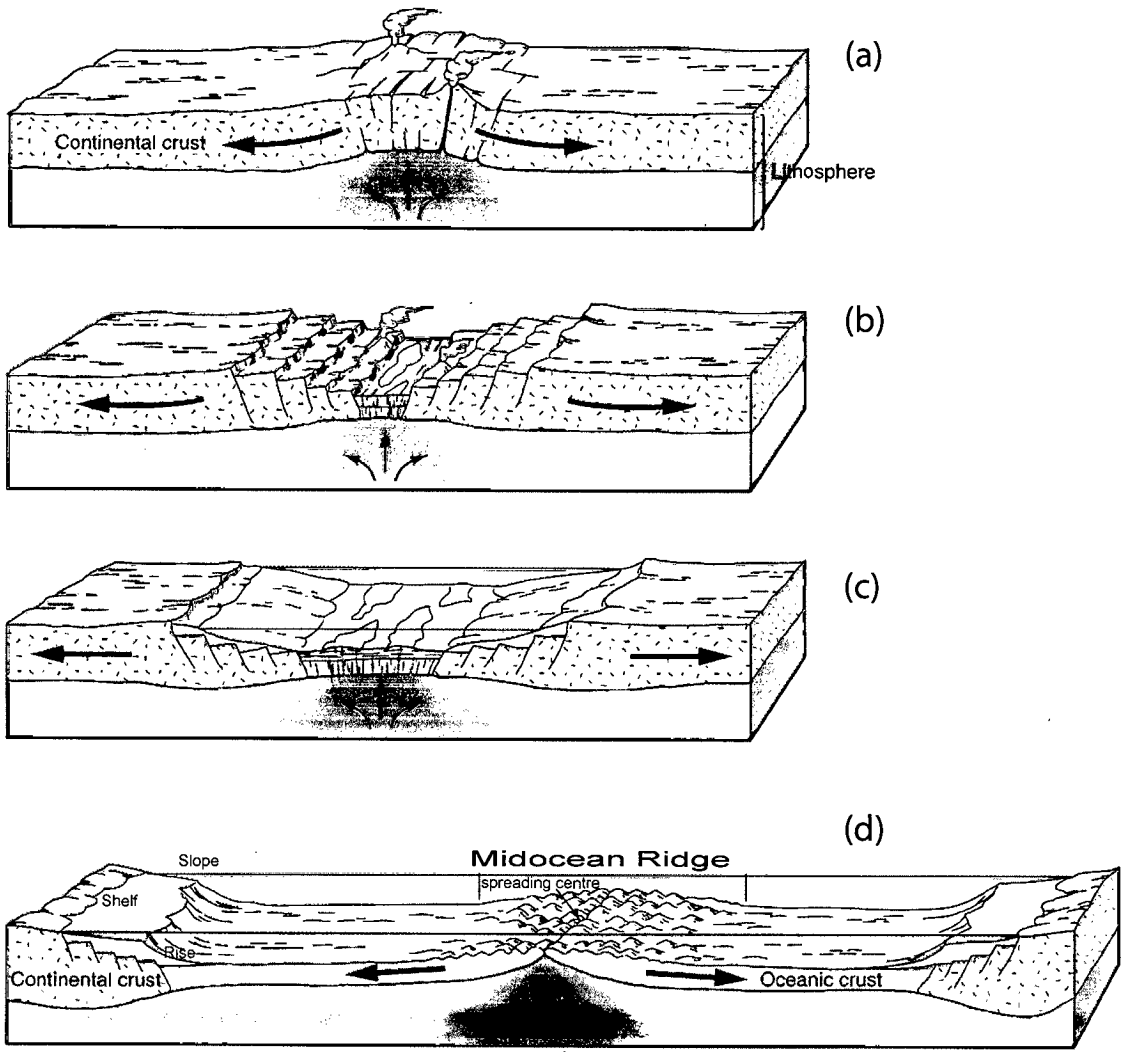

Fig. 2.6. Schematic representation of the concept of continental break-up and formation of a pair of passive margins at successive stages. Stage a: initiation of breaking of a continental mass along a week zone; Stage b: crustal thinning, rifting and initiation of seafloor spreading; Stage c: continents drift away as seafloor spreading continues and Stage d: subsiding continental land masses as they drift away under the load of sedimentation giving rise to shelf, slope and rise configuration. Modified after Trujillo and Turman (2005).

conversion, steep isostatic gravity gradients, the terminations of linear magnetic anomalies and the basement topography and composition. However, none of these criteria has been generally applicable because of the difficulty of distinguishing oceanic crust from continental crust modified by deformation and intrusion of basaltic material during the process of crustal attenuation (Jones, 1999).

The 'seaward-dipping-reflectors (SDRs)' first discovered by K. Hinz (1981) quoted by Talwani and Abreu (2000) and later studied extensively by many (eg. Mutter et al. 1982; White and McKenzie, 1989; Eldholm et al. 1995; Talwani and Abreu, 2000) appear to be a characteristic feature in most of the volcanic passive margins. These reflectors generally exhibit convex upward curvature with dips that increase in a seaward direction and a distinct geometry quite unlike the internal stratification of sedimentary accumulations. The SDR sequences lie adjacent to the oldest magnetic lineations in deeper water, indicating a close association with continental rifting and the onset of seafloor spreading (Jones, 1999). These SDRs are considered to represent enormous volumes of basaltic lavas, and this has been confirmed by deep drilling at places (Eldholm et al. 1995). The mechanism for producing such large amount of lava and the nature of the underlying crust is still a subject of much discussion, but it is generally agreed that eruptions took place in a sub-areal or shallow water setting from a source seaward of the present location of the reflectors and the dips arise from loading and subsidence (Jones, 1999). This sub-areal source is considered to be a sub-aerial spreading ridge along which the early opening of the ocean takes place. It is considered that during early stages of seafloor spreading, melt production rates are unusually high resulting in the development of a sub-areal spreading ridge (Jones, 1999). Some (Smythe, 1983 and Skogseid and Eldholm, 1987 quoted by Jones, 1999; White and McKenzie, 1989) believe that this SDR's were emplaced over an extended continental crust. Others (Talwani et al., 1995; Talwani and Abreu, 2000) consider that the SDRs provinces represent the initial stage of formation of oceanic crust when the spreading rate was high and called it the "*Initial Oceanic Crust*". They further inferred that the SDRs were emplaced symmetrically at both conjugate margins by a sub-areal spreading ridge and the SDRs constitute the extrusive part of the initial oceanic crust. This sub-areal

spreading produced lavas could flow large distances and gave rise to smooth oceanic basement. One of the view (Hinz, 1981 quoted by Talwani and Abreu, 2000) is that the subaerial extrusion of volcanics are onto a continental crust, while the other view (Mutter et al., 1982; Talwani and Abreu, 2000) is that the entire crustal material lying above Moho and underlying the SDRs wedge was emplaced after separation and the continental crust is present landward of this province. Formation of SDRs province stops when at later stage the spreading rate slows down, the ridge axis subsides below sea level and the lengths of lava flows became reduced due to rapid quenching giving rise to typical magnetic lineations and the rough basement surface.

(d) Ocean basins adjacent to passive margins

When the continental blocks move apart, the sudden upwelling of magma takes place, which solidifies, cools and get magnetized through Curie temperature in the direction of the Earth's magnetic field at that time. From the paleomagnetic results, it has been found that the Earth's dipole moment alternates between two anti-parallel polarity states, a normal state, in which the field at the Earth's surface is directed northward, and a reversed stage in which the field has the opposite direction. Therefore, the new crust formed as a result of seafloor spreading becomes magnetized in the prevalent direction of the magnetic field. When the field reverses, the oceanic crust generated at that time also becomes reversely magnetized. These two states result in formation of symmetrical stripes of normal and reverse magnetized blocks on either side of the spreading centre (Fig. 2.7). Hence, magnetic profiles across these magnetized blocks provide alternate positive and negative magnetic lineations of high amplitude with wavelengths of a few kilometers to several tens of kilometers. These oceanic magnetic lineations can be correlated with the geomagnetic polarity reversal timescales and thus the age of the ocean floor can be inferred. Usually the oldest oceanic magnetic lineations landward can constrain the time at which drifting (by seafloor spreading) began, but some continental slopes are bordered by a magnetically quiet zone, leaving the early history of seafloor spreading unclear (Jones, 1999).

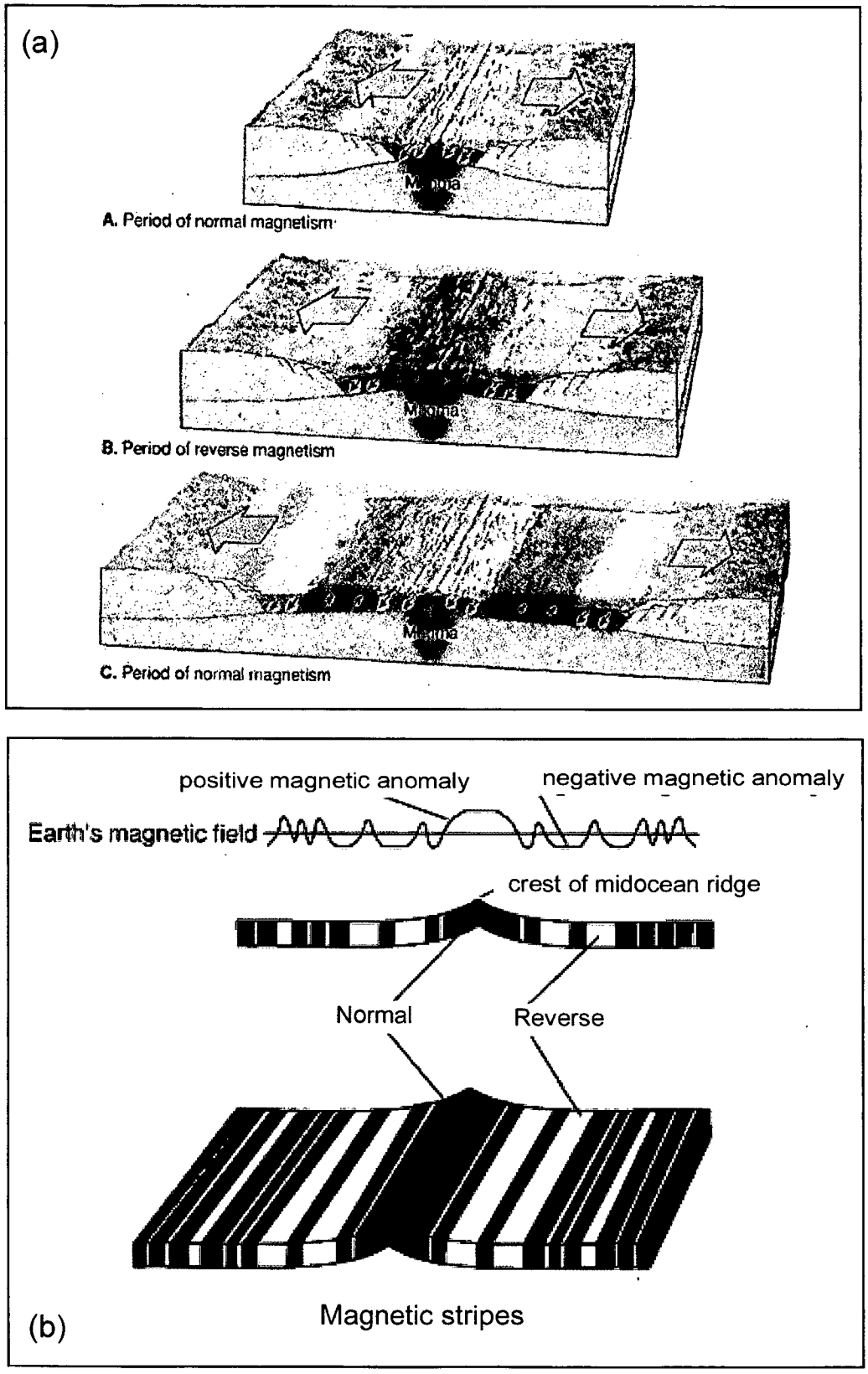

Fig. 2.7 Schematic representation of alternate normally and reversely magnetized oceanic crust and associated magnetic anomaly pattern. (a) Generation of alternate bands of magnetized crust by seafloor spreading; (b) The positive and negative magnetic anomalies along a profile across the normally and reversely magnetized blocks of the oceanic crust.

(e) Continental fragments off passive margins

Slivers of continents or continental fragments have been found to exist in the deep-sea areas adjacent to many of the continental margins. These continental fragments pose problems in fitting conjugate margins. Issues such as, why do continental fragments occur in some places, what is the nature of the crust between the fragments and the continent proper, are not clear in all cases. Some of these fragments seem to be located near areas where seafloor spreading changed direction and where initial rifting was propagating with time along the line between continental masses (National Research Council, 1979). In some cases an existing spreading ridge propagated or jumped onto a continental margin, severing a small segment of stretched crust from a large continent, while the existing mid-ocean ridge became extinct (Müller et al. 2001).

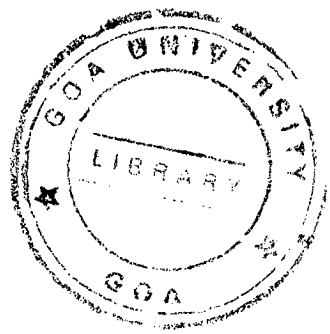

CHAPTER 3

Chapter - 3

DATA AND METHODOLOGY

3.1 Introduction

The main data utilized for the present study are; sea-surface gravity, magnetic and bathymetric profiles, satellite derived free-air gravity anomalies, GEBCO bathymetry contours, published regional scale tectonic element identifications and available finite rotation parameters of relative motions of the continental blocks bordering the study area. The methods of forward modeling of magnetic and gravity data, and paleogeographic reconstruction have been used as main tools for interpretation. In this chapter, the types and sources of these data and methodology adopted for interpretation have been described.

3.2 Types and sources of data

3.2.1 *Sea-surface magnetic and gravity profiles*

Several geoscientific studies carried out in the deep offshore regions west of India/Pakistan mainland attempted to infer about the nature of the crust underlying the Laxmi Basin and Offshore Indus Basin regions. Out of these studies, some (Bhattacharya et al., 1994b; Malod et al., 1997; Talwani and Reif, 1998) inferred the crust underlying both these basins as oceanic in nature, while some others (Miles et al., 1998; Todal and Eldholm, 1998) inferred both these basins to be underlain by thinned continental crust. A recent study carried out by Krishna et al. (2006) supports oceanic crust inference for the Offshore Indus Basin, but favours the inference of a thinned continental crust underlying the Laxmi Basin. In view of these divergent opinions, it is felt necessary to re-look into the available gravity and magnetic data of the study area and carry out reinterpretation.

The sea-surface gravity and magnetic data of the Laxmi Basin and Offshore Indus Basin regions, which are available in the public domain, were collected during various cruises of Indian and foreign research vessels. The Indian magnetic and gravity data were acquired during various cruises conducted by the National Institute of Oceanography, Goa, onboard ORV Sagar Kanya belonging to the Ministry of Earth Sciences, New Delhi. The additional magnetic and gravity data in and around the study area were extracted from the CD ROM

database entitled "Marine Geological and Geophysical data from NGDC", which was obtained from the National Geophysical Data Centre (NGDC), Boulder, Colorado, USA. The NGDC database is a compilation of data generated by various international organizations from time to time. The residual total field magnetic anomalies were calculated by removing the International Geomagnetic Reference Field (IGRF) of the appropriate epoch from the measured magnetic total field values. Similarly, residual gravity anomalies were obtained by applying normal and Eötvös corrections to the gravity measurements. The locations of these gravity and magnetic anomaly profiles used in the present study are shown in Fig. 3.1 and the summary of cruise identifications is presented in Table 3.1.

3.2.2 *Published seismic reflection and refraction information*

In this study, few published (Fig. 3.2) seismic data in the Laxmi Basin (Naini and Talwani, 1982; Krishna et al., 2006) and Offshore Indus Basin (Naini and Talwani, 1982; Malod et al., 1997; Collier et al., 2004a, b) have been used to examine the morphology of the basement of these regions as well as to provide seismic constraints while carrying out the gravity and magnetic modeling. The seismic reflection section (along C1707-04) in the Laxmi Basin presented in Naini and Talwani (1982) is a continuous seismic reflection profile, acquired onboard R/V Conrad using a single channel receiver and airgun sound sources. The velocity-depth information presented by them over several refraction stations in the study area are based on sonobuoy refraction experiments. The interpreted line drawing of a seismic reflection section (along RE-02) in the Laxmi Basin, which was presented in Krishna et al. (2006), is based on the reflection data acquired onboard M/V Anweshak, using a 48-channel streamer and Bolt-type airgun array with a total capacity of 10L. Since the publication of Krishna et al. (2006) did not present the time section over the full profile, so the interpreted line drawings presented by them for the full profile have been considered to get the estimate of depth to the basement while carrying out gravity and magnetic modeling. The seismic reflection section (MD51-01a) in the Offshore Indus Basin region presented in Malod et al. (1997) is based on single channel seismic reflection data acquired onboard R/V Marion Dufresne using a water gun sound source. The latest available multichannel seismic reflection section (CD144-01) in the Offshore Indus Basin presented in Collier et al. (2004a, b) is based on the

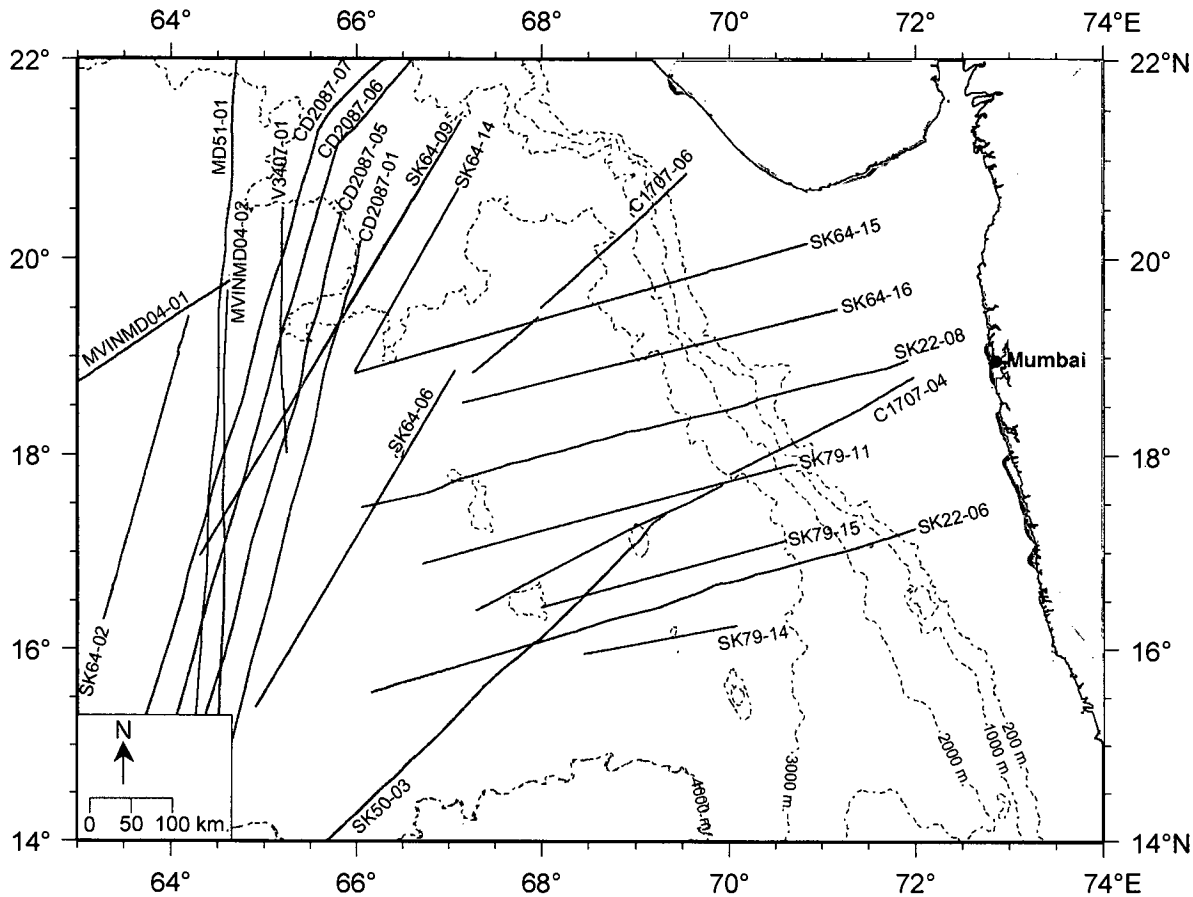

The data along these profiles were collected by National Institute of Oceanography, India.

The data along these profiles were extracted from the database of National Geophysical Data Centre, Boulder, Colorado.

The data along this profile has been obtained from Malod et al. (1997).

Deccan Trap

Fig. 3.1 The locations of the sea-surface gravity and magnetic profiles used in the present study. Annotations along the tracks are profile identifiers, the details of which are given in Table 3.1. Thin dotted lines are selected bathymetry contours (in metres).

Table 3.1 Cruise identification and types of data used in the present study. Wherever information is available, the method for obtaining primary position during data acquisition has been mentioned under the column 'Primary navigation'.

Cruise ID	Vessel	Year	Type of Data			Primary Navigation	Data Source
			G	M	S		
SK-22	ORV Sagar Kanya	1986	Y	Y	----	INS with TS	NIO Database
SK-50	ORV Sagar Kanya	1989	Y	Y	----	INS with TS	NIO Database
SK-64	ORV Sagar Kanya	1991	Y	Y	----	GPS	NIO Database
SK-79	ORV Sagar Kanya	1992	Y	Y	----	GPS	NIO Database
CD2087	RV Charles Darwin	1987	Y	Y	----	GPS, TS	NGDC Database
CD2787	RV Charles Darwin	1987	Y	Y	----	GPS, TS	NGDC Database
VE3407	RV Vema	1977	----	Y	----	TS	NGDC Database
C1707	RV Robert D. Conrad	1974	Y	Y	Y	GPS, TS	NGDC Database
MVINMD04	RV Melville	1977	----	Y	----	----	NGDC Database
MD51	RV Marion Dufresne	1986	----	Y	Y	GPS	Malod et al. (1997)
CD144	RV Charles Darwin	2003	Y	Y	Y	GPS	Collier et al. (2004a, b)
RE	MV Anweshak	----	----	----	Y	----	Krishna et al. (2006)

G: Gravity data; M: Magnetic data; S: Seismic data

INS: Integrated Navigation System; TS: Transit satellite; GPS: Global Positioning System

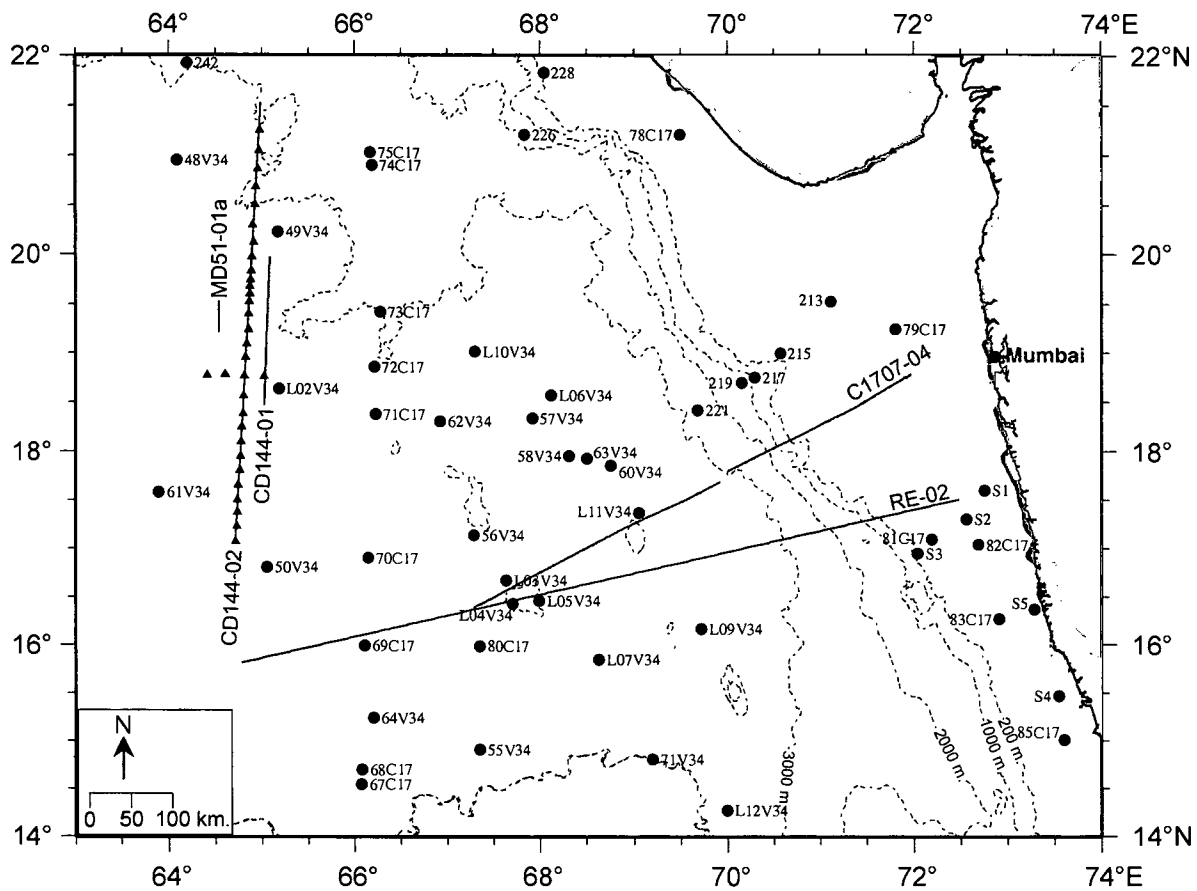

Published seismic reflection profiles after Naini and Talwani (1982), Malod et al. (1997), Collier et al. (2004a, b) and Krishna et al. (2006)

48V34 Locations of the published refraction stations along with the station identifications after Naini and Talwani (1982)

Locations of the published refraction stations after Collier et al. (2004a, b)

Deccan Trap

Fig. 3.2 The locations of the published seismic reflection profiles and the refraction stations in the deep offshore regions off India/Pakistan coast. Annotations along the tracks are profile identifiers, the details of which are given in Table 3.1. Thin dotted lines are bathymetry contours (in metres).

data acquired onboard R/V Charles Darwin using a 2.4 km, 96-channel streamer and a 3890 cubic inch airgun array fired every 30 seconds. The seismic refraction section CD144-02 presented by Collier et al. (2004a, b) is based on refraction data acquired using the Ocean Bottom Seismometers (OBS).

3.2.3 *Satellite derived free-air gravity anomalies*

In this study, the satellite derived free-air gravity anomalies (Fig. 3.3) have been mainly used to construct free-air gravity profiles in between sea-surface gravity transects in some areas of the Laxmi Basin and Offshore Indus Basin regions. The contour maps of satellite derived free-air gravity anomalies have been used to infer and/or refine the extents of some of the tectonic elements, which are not readily available. The satellite derived free-air gravity anomalies have been extracted from the binary gridded file of gravity anomalies (version 11.2) for the world (Sandwell and Smith, 1997, 2003), available from the ftp site ftp://topex.ucsd.edu/pub/global_grav_2min/, which is maintained by the Scripps Institution of Oceanography, USA. This gridded gravity anomaly is for 2 minutes spatial resolution and the stored anomaly values are in gravity units (10^{-6} m/sec^2). These values have been multiplied with 0.1 to convert them into mgal while generating shaded-relief image and profiles of anomalies. A comparison with shipboard gravity data shows that the accuracy of the satellite derived gravity anomaly is about 4-7 mgal for random ship tracks (Sandwell and Smith, 1997).

3.2.4 *Mapped seafloor spreading magnetic lineations*

The mapped seafloor spreading type magnetic lineations (Fig. 3.4) used in this study are those presented by Bhattacharya et al. (1994b) in the Laxmi Basin, Malod et al. (1997) in the Offshore Indus Basin and those from Mascarene Basin area presented by Schlich (1982), Dyment (1991, 1996) and Bernard and Munschy (2000).

The magnetic lineations in the Laxmi Basin have been interpreted by Bhattacharya et al. (1994b) as a two-limbed seafloor spreading sequence corresponding to anomalies 33n (66.5 Ma) to 28n (63.0 Ma). In a similar way, the magnetic lineations in the Offshore Indus Basin have been interpreted by Malod et al. (1997) as a two-limbed seafloor spreading sequence corresponding to anomalies 29r-29n (65.58 – 63.98 Ma). India is believed (Norton and Sclater, 1979; Besse and Courtillot, 1988) to have been juxtaposed with Madagascar and

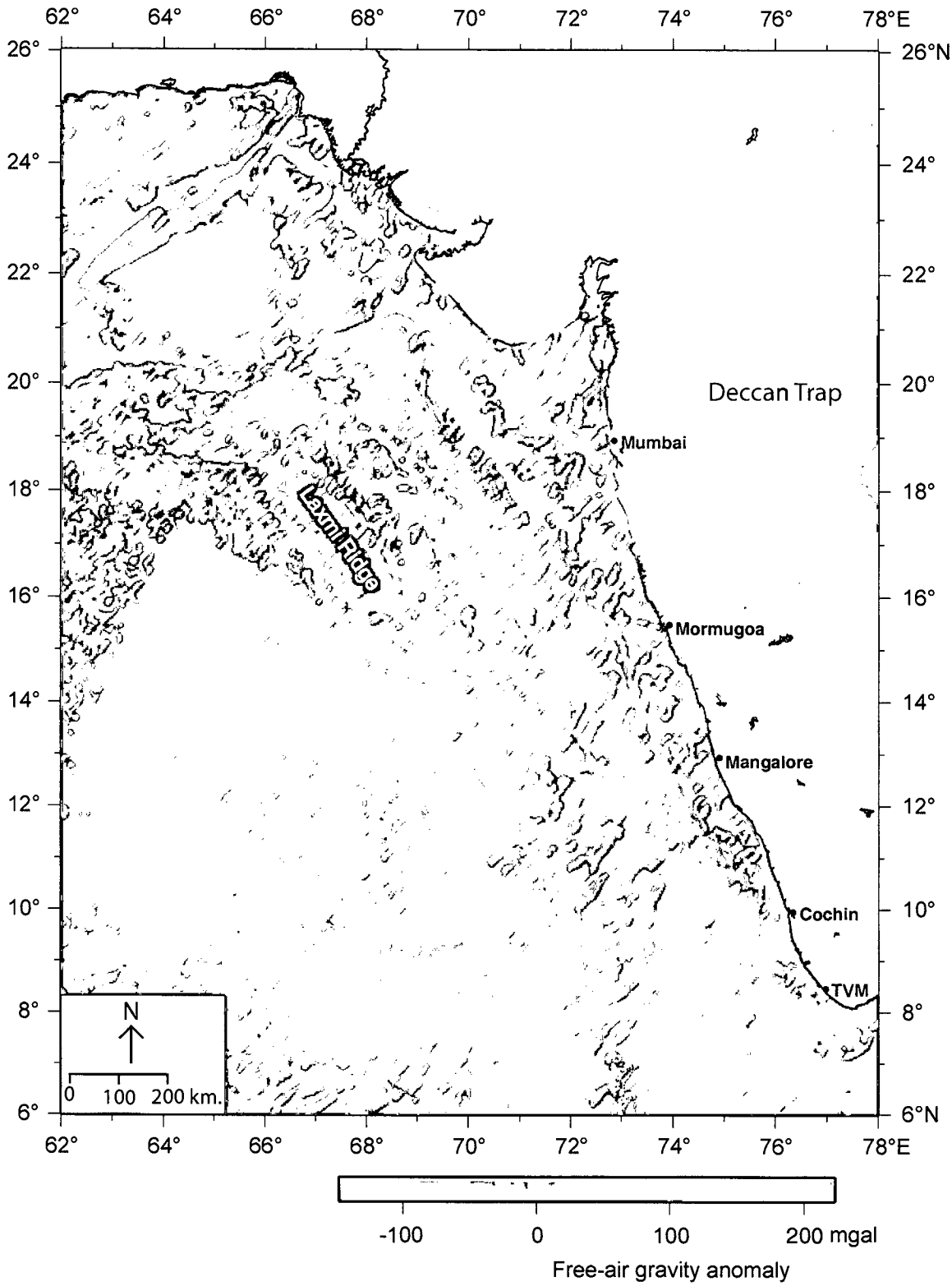

Fig. 3.3 Colour shaded-relief image of the satellite derived free-air gravity anomalies (Sandwell and Smith 1997, 2003) of the deep offshore regions off west coast of India.

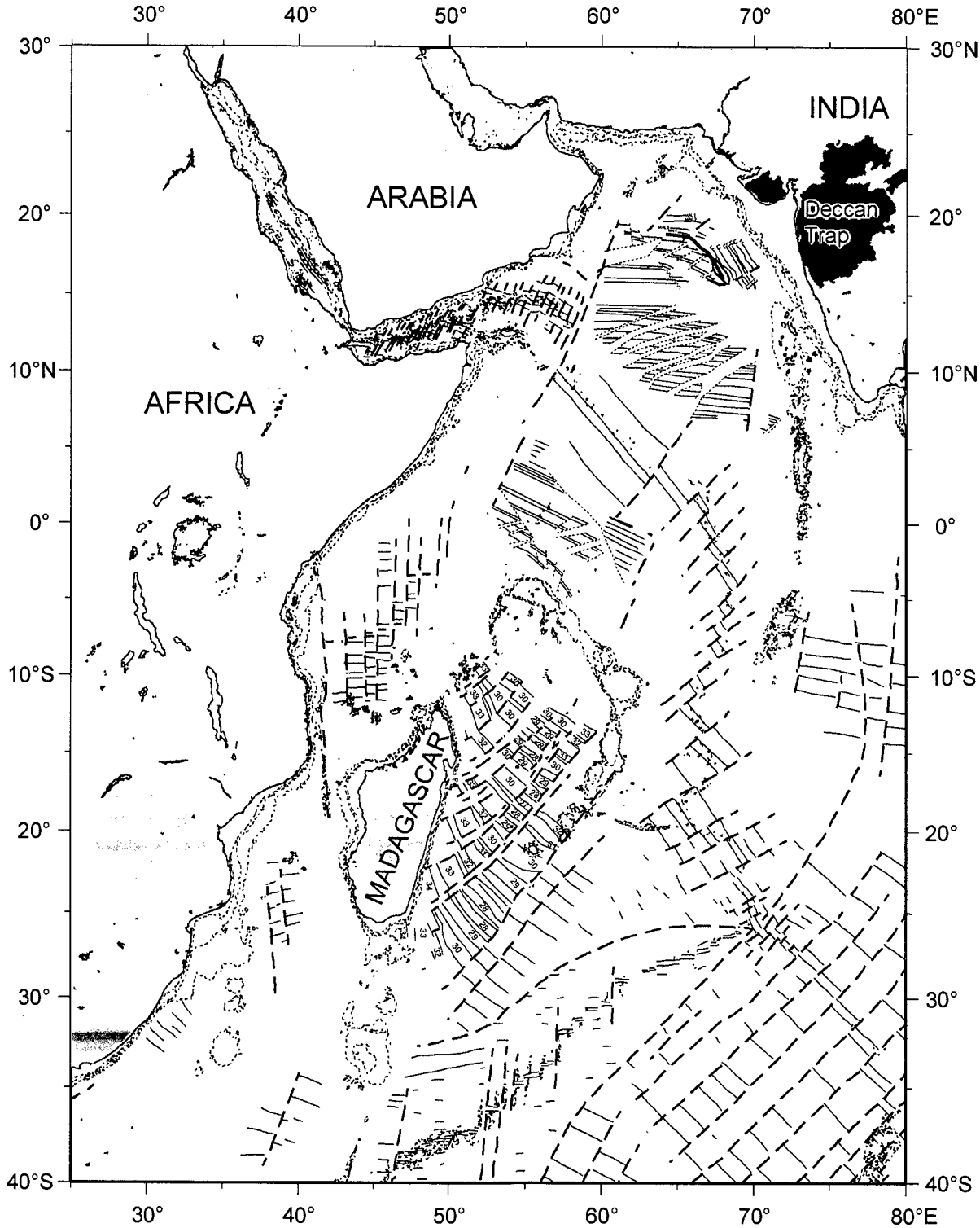

Fig. 3.4 Generalized map of the Western Indian Ocean showing locations of the mapped seafloor spreading magnetic lineations. The lineations used in the present study are given as thin red lines with numbers. The other magnetic lineations are shown as thin grey lines. Magnetic lineation identifications used in the present study have been compiled from Malod et al. (1997), Bhattacharya et al. (1994b) and Bernard and Munschy (2000). The other magnetic lineations of the Arabian Sea and remaining part of the Western Indian Ocean are from Chaubey et al., 2002a; Royer et al., 2002; and NGDC database. The thick dashed lines orthogonal to magnetic lineations represent fracture zones.

magnetic lineations in the Mascarene Basin is considered to record the episode of seafloor spreading which was related with the separation of India and Madagascar. It is observed that the oldest magnetic lineations mapped (Fig. 3.4) in the Mascarene Basin area are anomaly 34n (83.0 Ma), which are located along the east coast of Madagascar and its conjugate in the southwestern part of Seychelles-Mascarene Plateau. In the southern part of Mascarene Basin, conjugate magnetic isochron sequence 34ny (83.0 Ma) – 27ny (60.920 Ma), which are offset by NE-SW trending right lateral fracture zones, are present. No continuous sequences of conjugate magnetic isochrons were mapped in the northern part of the Mascarene Basin, although anomalies 32n-30n, 34n-30n, 34n-32n are reported (Dyment, 1996) to exist at few locales. The magnetic anomalies in the Mascarene Basin show an increasing age of fossil ridge axis from south (anomaly 27n) to the north (anomaly 30n) possibly suggesting a southward progressive extinction of the Mascarene Basin spreading centre.

3.2.5 *GEBCO bathymetry contours*

In this work, bathymetry contours (Fig. 1.3) have been used to define the boundaries of some of the offshore tectonic elements, such as the terrace like feature off Trivandrum, Laccadive Plateau, Seychelles Bank and northern Madagascar Ridge. These bathymetric contours were extracted from the CD ROM database entitled "The Centenary Edition of the GEBCO Digital Atlas (GDA)", which was prepared by the General Bathymetric Charts of the Oceans (GEBCO) functioning under the auspices of the Intergovernmental Oceanographic Commission (IOC) and the International Hydrographic Organization (IHO). The bathymetry contours in this database are in ASCII format and are available as isobaths of 200 m, 500 m, and at 500 m contour intervals thereafter.

The bathymetric contours published in the GEBCO Digital Atlas are based on the bathymetry data acquired, as discrete soundings and continuous recording along ship tracks, by hydrographic and oceanographic ships during surveys and on passage between survey areas and ports. This Centenary Edition of the GEBCO digital Atlas, published in 2003 (Intergovernmental Oceanographic Commission et al., 2003), contains the most recent and completely updated bathymetry contours for the Indian Ocean region. For the present study required bathymetry contours, of 200 m, 1000 m and all other contours of greater depth

values at 1000 m interval, have been extracted and stored as separate ASCII data files.

3.2.6 *Available finite rotation parameters*

Finite rotation parameters are a set of values used to describe the relative motion of two lithospheric plates over a sphere in a fixed reference frame. It consists of an Euler pole, about which two plates move over a sphere, and an Euler angle, which is the amount of angle to be rotated about the Euler pole. Angle is positive when the motion of the moving plate is counter clockwise with respect to the fixed plate when viewed from outside the Earth (Duncan, 1981). In plate tectonic reconstructions, using a set of finite rotation parameters one brings pairs of conjugate isochrons of same age from two plates into coincidence. Therefore, the finite rotations for the entire period of relative motion between two plates are usually presented as a table consisting sets of finite rotation parameters along with their corresponding isochron ages and anomaly numbers (anomaly identifications) for corresponding magnetic lineations (isochrons) if available. The present study involves understanding and improvement of the relative motion of India, Laxmi Ridge, Seychelles and Madagascar since the time of their early drifting. However, it was observed that different sets of finite rotation parameters defining the relative motions of these continental blocks were suggested in various publications. All these different sets of finite rotation parameters were therefore compiled (Table 3.2) for evaluation and selecting the most suitable set, which can be used for developing reconstruction models for this study. Further, as it was observed that in earlier studies different authors have used different geomagnetic timescales while giving the finite rotation parameters, therefore, while compiling these rotation parameters, the ages corresponding to each isochrons have been re-assigned using the common geomagnetic polarity timescale of Cande and Kent (1995). Following Cox and Hart (1986), the symbol $_{FIX}ROT_{MOB}$ is used to mean the finite rotation of plate MOB (the mobile plate) with respect to plate FIX (the fixed plate). For example, finite rotation of India with respect to Madagascar in fixed Madagascar reference frame can be represented as $_{MAD}ROT_{IND}$. This convention of symbols has been followed in this study while presenting the tables of finite rotation parameters.

Table 3.2 Finite rotation parameters describing relative motions between various plates used in the present study. The given rotation angles are those required to reconstruct the plate positions backwards in time. Angle is positive when the motion of the moving plate is counter clockwise with respect to the fixed plate when viewed from outside the earth. Ages are after Cande and Kent (1995).

(a) Between Laxmi Ridge (LAX) and Seychelles (SEY) in fixed Seychelles reference frame ($_{SEY}ROT_{LAX}$), after Royer et al. (2002).

Chron	Age (Ma)	Finite rotation parameters		
		Lat. (deg.)	Long. (deg.)	Angle (deg.)
21ny	46.264	18.64	43.37	-22.559
22ny	49.037	18.94	39.62	-23.195
23n1y	50.778	18.55	38.73	-26.157
24n1y	52.364	19.17	34.18	-26.232
25ny	55.904	19.41	29.02	-30.111
26ny	57.554	19.61	25.62	-30.729
27ny	60.920	18.83	24.86	-35.411

(b) Between India (IND) and Africa (AFR) in fixed Africa reference frame ($_{AFR}ROT_{IND}$), after Norton and Sclater (1979).

Chron	Age (Ma)	Finite rotation parameters		
		Lat. (deg.)	Long. (deg.)	Angle (deg.)
16n	35.842	13.3	54.1	-20.8
22n	49.376	12.9	45.3	-30.1
28n	63.067	18.8	26.2	-38.4
34n	83.000	18.7	25.8	-56.0
M1	115.00	24.5	33.5	-59.0
Fit	Jurassic	29.6	36.1	-56.8

(c) Between India (IND) and Africa (AFR) in fixed Africa reference frame ($_{AFR}ROT_{IND}$), after Besse and Courtillot (1988)

Chron	Age (Ma)	Finite rotation parameters		
		Lat. (deg.)	Long. (deg.)	Angle (deg.)
6n	21.583	16.2	44.2	-11.9
21n	47.085	12.6	48.3	-28.3
24n	52.855	15.9	38.6	-31.1
25n	56.148	17.6	33.9	-32.7
28n	63.067	15.3	31.0	-40.5
29n	64.360	14.1	30.2	-44.7
34n	83.000	16.8	21.2	-55.0
M02	123.500	18.6	27.0	-54.8
M15	141.500	20.4	33.6	-56.2

(d) Between hotspot (HS) and India (IND) in fixed hotspot reference frame ($_{HS}ROT_{IND}$), after Morgan (1981)

Chron	Age (Ma)	Finite rotation parameters		
		Lat. (deg.)	Long. (deg.)	Angle (deg.)
---	15.000	-31.6	219.7	10.8
---	21.000	-30.6	223.5	12.8
---	45.000	-42.5	206.8	12.9
28n	63.067	-28.3	194.5	40.5
34n	83.000	-22.6	186.3	60.3
---	125.000	-16.7	180.9	73.8
---	140.000	-15.6	181.6	69.5
---	160.000	-12.2	188.1	77.1
---	200.000	-9.1	191.6	66.1

(e) Between hotspot (HS) and Africa (AFR) in fixed hotspot reference frame ($_{HS}ROT_{AFR}$), after Morgan (1981)

Chron	Age (Ma)	Finite rotation parameters		
		Lat. (deg.)	Long. (deg.)	Angle (deg.)
---	15.000	---	---	---
---	21.000	-65.0	150.0	3.0
---	45.000	-52.0	109.1	6.5
28n	63.067	-47.0	118.8	11.4
34n	83.000	-33.6	109.9	19.5
---	125.000	-26.5	132.7	32.7
---	200.000	6.2	100.7	22.4

(f) Between hotspot (HS) and India (IND) in fixed hotspot reference frame ($_{HS}ROT_{IND}$), after Müller et al. (1993)

Chron	Age (Ma)	Finite rotation parameters		
		Lat. (deg.)	Long. (deg.)	Angle (deg.)
5	10.435	36.1	21.9	-5.81
6	21.583	40.6	4.3	-10.71
13	33.302	30.9	17.4	-19.33
18	39.278	31.3	16.9	-23.00
21	47.085	27.9	11.1	-29.06
25	56.148	24.7	6.2	-37.29
31	68.236	19.1	3.4	-53.37
33y	73.619	18.7	2.5	-58.12
33o	79.075	18.1	1.8	-63.00
34	83.000	17.1	2.3	-65.48
---	90.000	16.3	5.0	-67.29
---	100.000	14.5	10.3	-70.31
---	110.000	13.7	10.1	-71.68
M0	118.700	14.2	10.3	-72.09
M10	130.000	13.3	15.5	-75.34

(g) Between hotspot (HS) and Africa (AFR) in fixed hotspot reference frame ($_{HS}ROT_{AFR}$), after Müller et al. (1993)

Chron	Age (Ma)	Finite rotation parameters		
		Lat. (deg.)	Long. (deg.)	Angle (deg.)
5	10.435	59.3	-31.6	-1.89
6	21.583	50.9	-44.5	-4.36
13	33.302	40.3	-43.0	-7.91
18	39.278	37.7	-41.2	-9.65
21	47.085	32.8	-40.8	-12.09
25	56.148	30.1	-41.7	-13.89
31	68.236	26.4	-40.9	-16.23
33y	73.619	22.3	-39.6	-17.80
33o	79.075	18.0	-38.9	-19.98
34	83.000	19.0	-40.9	-21.53
---	90.000	19.4	-41.9	-23.31
---	100.000	18.9	-41.4	-25.35
---	110.000	17.7	-39.5	-26.71
M0	118.700	18.7	-39.7	-27.37
M10	130.000	16.7	-37.5	-28.52

3.2.7 *Other onshore and offshore tectonic elements*

(a) Onshore tectonic elements

The onshore tectonic elements (Fig. 3.5 and Fig. 3.6) considered in this study are; (i) the Precambrian lineaments which have been used in earlier studies to constrain the juxtaposition of India-Seychelles-Madagascar, (ii) the Narmada-Son lineament representing a failed continental rift (Narmada Rift) system of India which orthogonally cuts the west coast of India, and (iii) the locations of volcanics on the conjugate shores, which are between 90 Ma and 65 Ma in age and are considered to be related to those rifting which initiated separation of the continental blocks under consideration of this study. The Precambrian lineaments of India and Madagascar, which have been considered for the above purpose in various earlier studies, are Achankovil Shear Zone (ASZ), Moyar Shear Zone (MSZ) and Palghat-Cauvery Shear Zone (PCSZ) of India (Fig. 3.5) and the Ranotsara Shear Zone (RSZ) and Axial Shear Zone (AXSZ) of Madagascar. The geographical extents of these Precambrian lineaments have been digitized from figures presented in Meissner et al. (2002), Windley et al. (1994) and Biswas (1982).

The location of India-Madagascar rifting related volcanics, which were considered in various earlier studies are:

A) on Indian side;

(i) St. Mary Islands (SMI) located off Mangalore (Valsangkar et al., 1981; Torsvik et al., 2000; Pande et al., 2001),

(ii) North Kerala Dykes (Radhakrishna et al., 1999)

(iii) Cretaceous dykes of Karnataka (Anil Kumar et al., 2001).

B) on Madagascar side;

(i) Cretaceous dyke rocks of Madagascar (Storey et al., 1995)

(ii) Analalava Gabbro Pluton located in northeastern part of Madagascar (Torsvik et al., 2000).

In a similar way, the locations of volcanics of age ~65.0 Ma, which have been reported in conjugate sides of India (Rathore et al., 1997; Hofmann et al., 2000; Widdowson et al., 2000) and Seychelles (Dickin et al., 1987) have also been

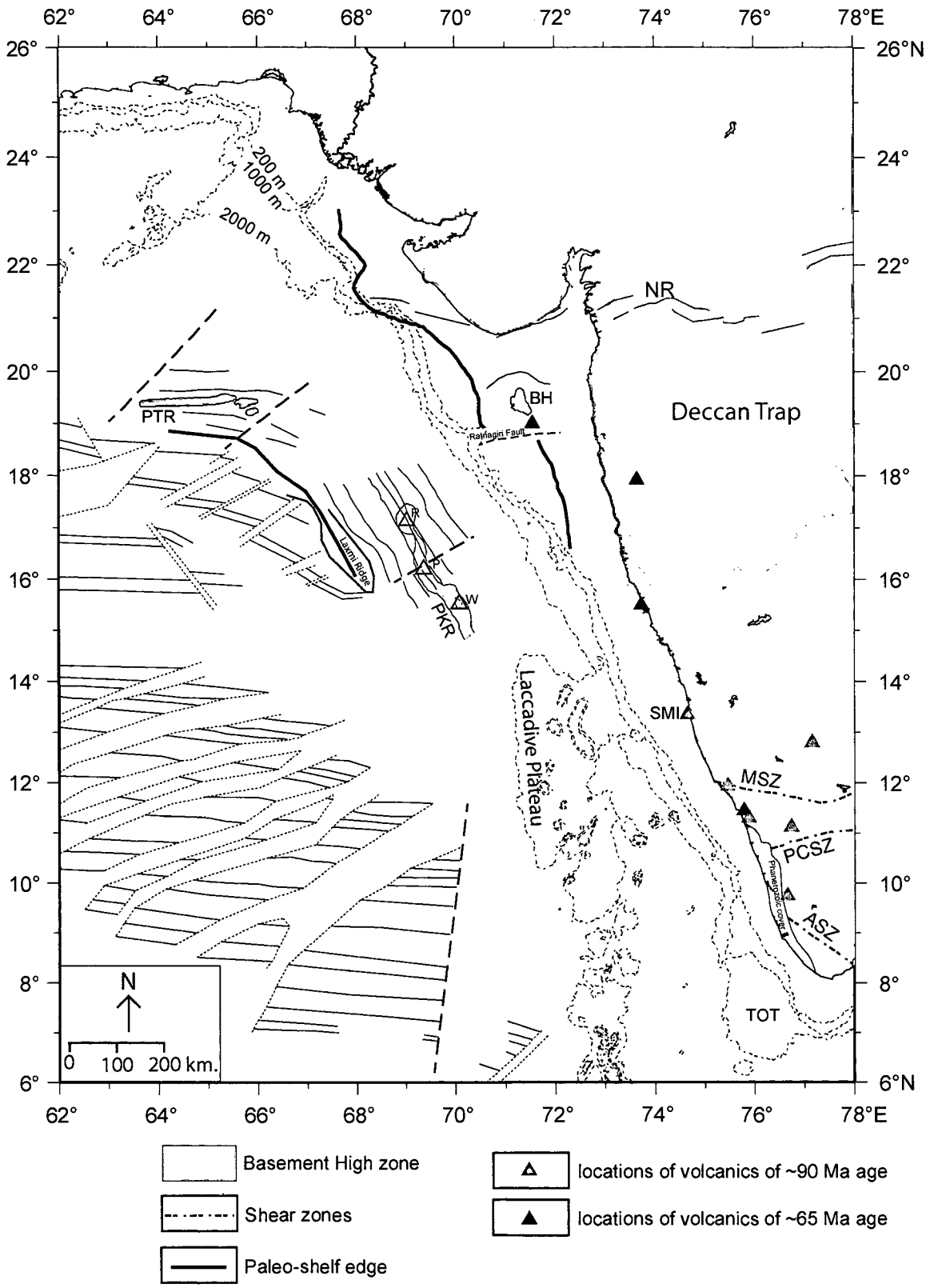

Fig. 3.5 Onshore and offshore tectonic elements in the west coast of India and the adjoining deep offshore regions. Locations of onshore shear zones simplified after Meissner et al. (2002). The axial basement high in the Laxmi Basin is modified after Srinivas (2004) and that in Offshore Indus Basin is after Malod et al. (1997). TOT: Terrace off Trivandrum; BH: Bombay High; R: Raman Seamount; P: Panikkar Seamount; W: Wadia Guyot; PTR: Palitana Ridge; PKR: Panikkar Ridge; ASZ: Achankovil Shear Zone; PCSZ: Palghat-Cauvery Shear Zone; MSZ: Moyar Shear Zone; NR: Narmada Rift; SMI: St. Mary Islands. Other details are as in Fig. 2.2.

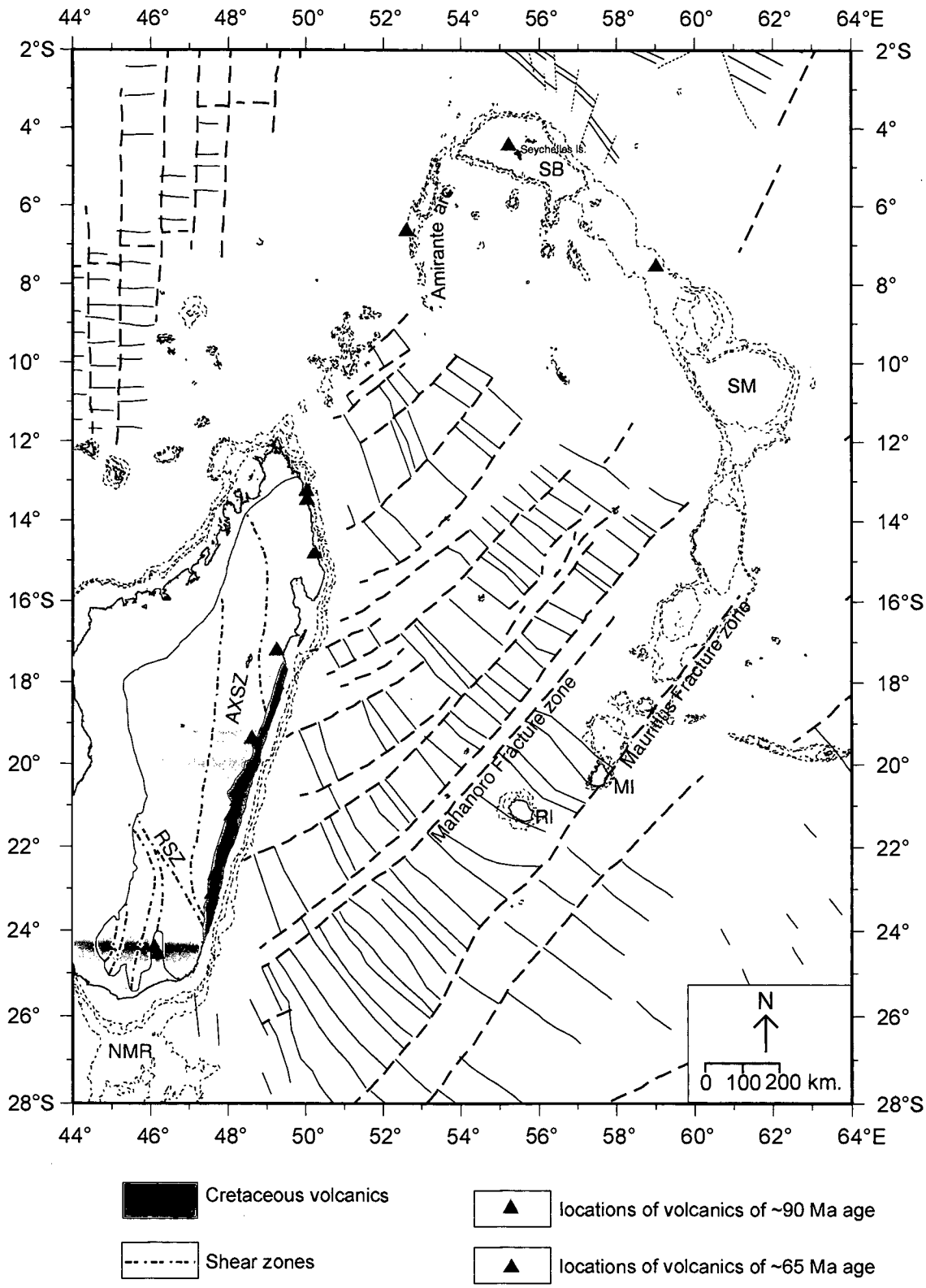

Fig. 3.6 Onshore and offshore tectonic elements in Madagascar, Seychelles and the adjoining deep offshore regions. Locations of onshore shear zones after Windley et al. (1994). NMR: Northern Madagascar Ridge; RSZ: Ranotsara Shear Zone; AXSZ: Axial Shear Zone; SB: Seychelles Bank; SM: Saya de Malha Bank; MI: Mauritius Island; RI: Reunion Island. Other details are as in Fig. 2.3.

compiled. The locations of these volcanics have been obtained by digitization from figures of the respective publications.

(b) Offshore tectonic elements

The major offshore tectonic elements (Fig. 3.5 and Fig. 3.6) of the study area and the adjoining regions are a terrace like feature located off Trivandrum, the Laxmi Ridge, the axial basement high zone (Panikkar Ridge) of the Laxmi Basin, the axial basement high zone (Palitana Ridge) of the Offshore Indus Basin, the Raman-Panikkar-Wadia seamount chain of the Laxmi Basin, the inferred offshore extension of Narmada Rift, the Bombay High, the paleo-shelf edge off west coast of India, the Laccadive-Chagos Ridge, the Seychelles Bank, the Mascarene Plateau and the northern Madagascar Ridge. Some of these features were digitized from figures of respective publications, such as; offshore extension of Narmada Rift from Bhattacharya and Subrahmanyam (1986), Bombay High from Biswas (1982), Panikkar Ridge from Srinivas (2004), Palitana Ridge from Malod et al. (1997), Raman-Panikkar-Wadia seamount chain from Bhattacharya et al. (1994a) and paleo–self edge from Rao and Srivastava (1981). The boundaries, which define the extent of other tectonic elements, have been inferred based on either GEBCO bathymetry contours or the satellite derived free-air gravity anomaly contours.

3.3 Methodology adopted

Several techniques have been used in this study to analyze the geophysical data from the complex deep offshore areas adjoining the west coast of India/ Pakistan. In these deep offshore regions, attempt has been made to understand nature of the crust underlying the Offshore Indus and Laxmi basins, based on the forward modeling technique of gravity (Talwani et al., 1959) and magnetic (Talwani and Heirtzler, 1964) data. As these regions are inferred to be underlain by oceanic crust formed as a result of two-limbed seafloor spreading, therefore further attempt has been made for the identification of those magnetic anomalies with reference to geomagnetic polarity reversal time scale and delineation of the boundaries of the magnetized blocks (isochrons). The boundaries of the magnetized blocks have been demarcated by following the conventional method of inter-profile correlation and comparison with synthetic anomaly profiles computed for model of juxtaposed normally and reversely

magnetized blocks of oceanic crust. After delineation of conjugate magnetic isochrons, the finite rotation parameters are estimated to describe the relative motion between India/Pakistan and Laxmi Ridge. Followed by these exercises, the paleogeographic reconstruction technique has been used to evaluate the existing plate tectonic evolutionary models for Western Indian Ocean and to provide improved models pertaining to the early drift and pre-drift juxtaposition of India, Seychelles and Madagascar continental blocks. In this section, tools and methods used in the present study have been briefly discussed.

3.3.1 *Computation of gravity anomalies over 2-D bodies*

Most of the submarine features can be approximated as two-dimensional bodies (Jones, 1999). The method proposed by Talwani et al. (1959) has been widely accepted for computation of gravitational attraction of a two-dimensional mass of constant density. In the present work, the gravity modeling has been carried out using the commercially available interactive GM-SYS software, a product of Northwest Geophysical Associates, Inc, where the gravity response for the given body is computed based on the method of Talwani et al. (1959). In this section, firstly a brief description of this method is given and then the steps for gravity modeling followed in this study are described.

a) Method of Talwani et al. (1959) for computation of gravitational attraction of a two-dimensional mass

The two-dimensional mass is a polygon (Fig. 3.7) lying in the x-z plane and extending to infinity in the y-direction. The vertical component of gravitational attraction, Δg, at the origin P(0,0) is

$$\Delta g = 2G\rho \oint z d\theta$$

where $\oint z d\theta$ is a line integral given by Hubbert (1948) quoted by Jones (1999).

$$\oint z d\theta = \int_A^B z d\theta + \int_B^C z d\theta + \int_C^D z d\theta + \ldots \int_F^A z d\theta$$

For a point Q on the side BC,

$$PS = a_i \text{ and } z = (x - a_i) \tan \gamma_i$$

Thus,

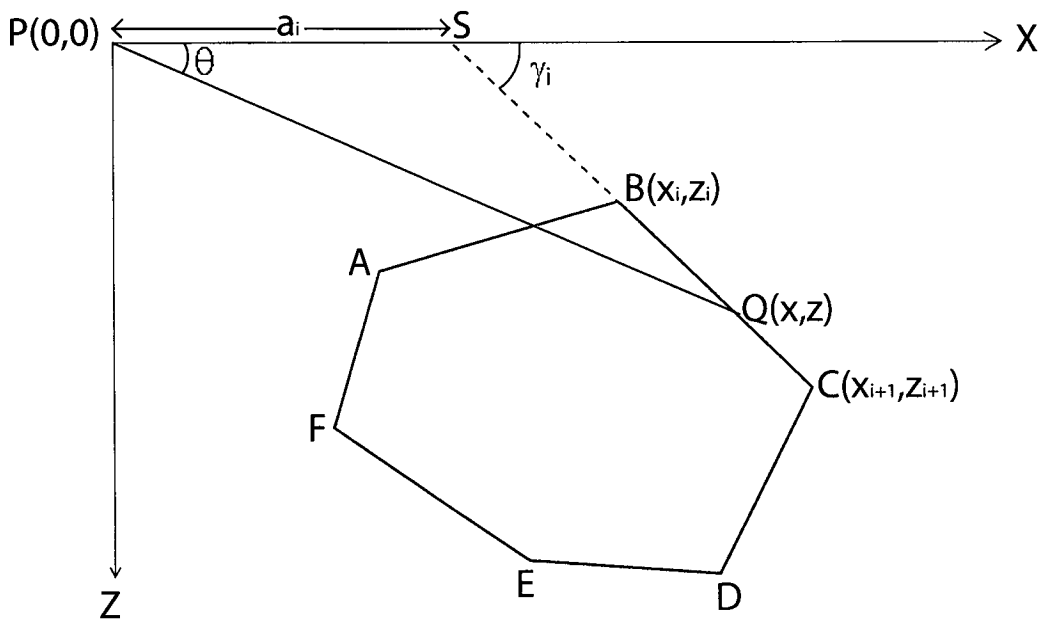

Fig. 3.7 Geometry of a two-dimensional polygon ABCDEF, lying in the x-z plane and extending to infinity in the y-direction (Redrawn from Jones, 1999) as used to compute gravitational attraction of two-dimensional bodies of arbitrary shape by the method of Talwani et al. (1959).

$$z = \frac{a_i \tan\gamma_i \tan\theta}{\tan\gamma_i - \tan\theta} \text{ and}$$

$$\int_{BC} z d\theta = a_i \sin\gamma_i \cos\gamma_i \left\{ (\theta_i - \theta_{i+1}) + \tan\gamma_i \ln\left[\frac{\cos\theta_i (\tan\theta_i - \tan\gamma_i)}{\cos\theta_{i+1} (\tan\theta_{i+1} - \tan\gamma_i)} \right] \right\}$$

By making the substitution,

$$a_i = x_{i+1} - z_{i+1} \left(\frac{x_{i+1} - x_i}{z_{i+1} - z_i} \right)$$

The depth at Q is

$$z = \frac{x_{i+1}(z_{i+1} - z_i) - z_{i+1}(x_{i+1} - x_i)}{(z_{i+1} - z_i)\cot\theta - (x_{i+1} - x_i)}$$

The gravitational attraction around the whole polygon is therefore,

$$\Delta g = 2G\rho \sum_{i=1}^{6} \left\{ \frac{x_i z_{i+1} - z_i x_{i+1}}{(x_{i+1} - x_i)^2 + (z_{i+1} - z_i)^2} \right\} \cdot \left\{ x_{i+1} - x_i)(\theta_i - \theta_{i+1}) + (z_{i+1} - z_i) \ln(\frac{r_{i+1}}{r_i}) \right\}$$

where,

$$r_i = \sqrt{x_i^{\,2} + z_i^{\,2}}$$

The expression for Δg is then readily transformed into computer code.

(b) Steps for gravity modeling followed in this study

The objective for gravity modeling in this study is to obtain a plausible crustal structure section, which is compatible with the observed gravity anomaly and known geological constraints. The broad steps followed for this purpose is given below:

(i) A crustal section is constructed by integrating all available bathymetric, seismic reflection and refraction results.

(ii) The main crustal units in this model are identified and the average interval velocities of these crustal units are calculated, wherever available or assigned from other geological considerations.

(iii) The layer densities for these crustal units are estimated according to the velocity-density relationship of Ludwig et al. (1970).

(iv) Considering each of these crustal units as separate body, defined by a co-ordinated bounding polygon surface and a density, the gravity anomaly for the crustal section is computed as a sum of anomalies for all separate bodies comprising the crustal section.

(v) The initial crustal model is refined by trial and error, to obtain a plausible model which gives good fit between the observed and computed gravity anomalies and satisfies other constraints.

3.3.2 *Computation of magnetic anomalies over 2-D bodies*

The magnetic anomalies observed in the study area are linear in nature and have good correlation from profile to profile. The sources of magnetic anomalies can be approximated by two-dimensional polygons extending to infinity in the direction of the magnetic anomaly (Jones, 1999). The most common method of computing the magnetic field over such bodies is to use the algorithms developed by Talwani and Heirtzler (1964). In this section, firstly a brief description of this method is given and then the steps for magnetic modeling followed in this study are described.

(a) Method of Talwani and Heirtzler (1964) for computation of magnetic anomalies caused by two-dimensional structures of arbitrary shape

According to the approach of Talwani and Heirtzler (1964), the total field magnetic anomaly at a point (0,0) due to a polygon stretching to infinity in the y-direction of the co-ordinate system (Fig 3.8a-d) can be calculated by first considering a volume element $\Delta x\Delta y\Delta z$ of an infinitely long magnetized rod (Fig. 3.8a) with a cross section ABCD. Let J be the intensity of magnetization, where J_x, J_y, and J_z are the components of this in the x, y, and z directions.

The magnetic moment $\vec{m}$, on the element volume $\Delta x\Delta y\Delta z$ is given by

$$\vec{m} = \vec{J}\Delta x\Delta y\Delta z$$

and its magnetic potential at the origin is

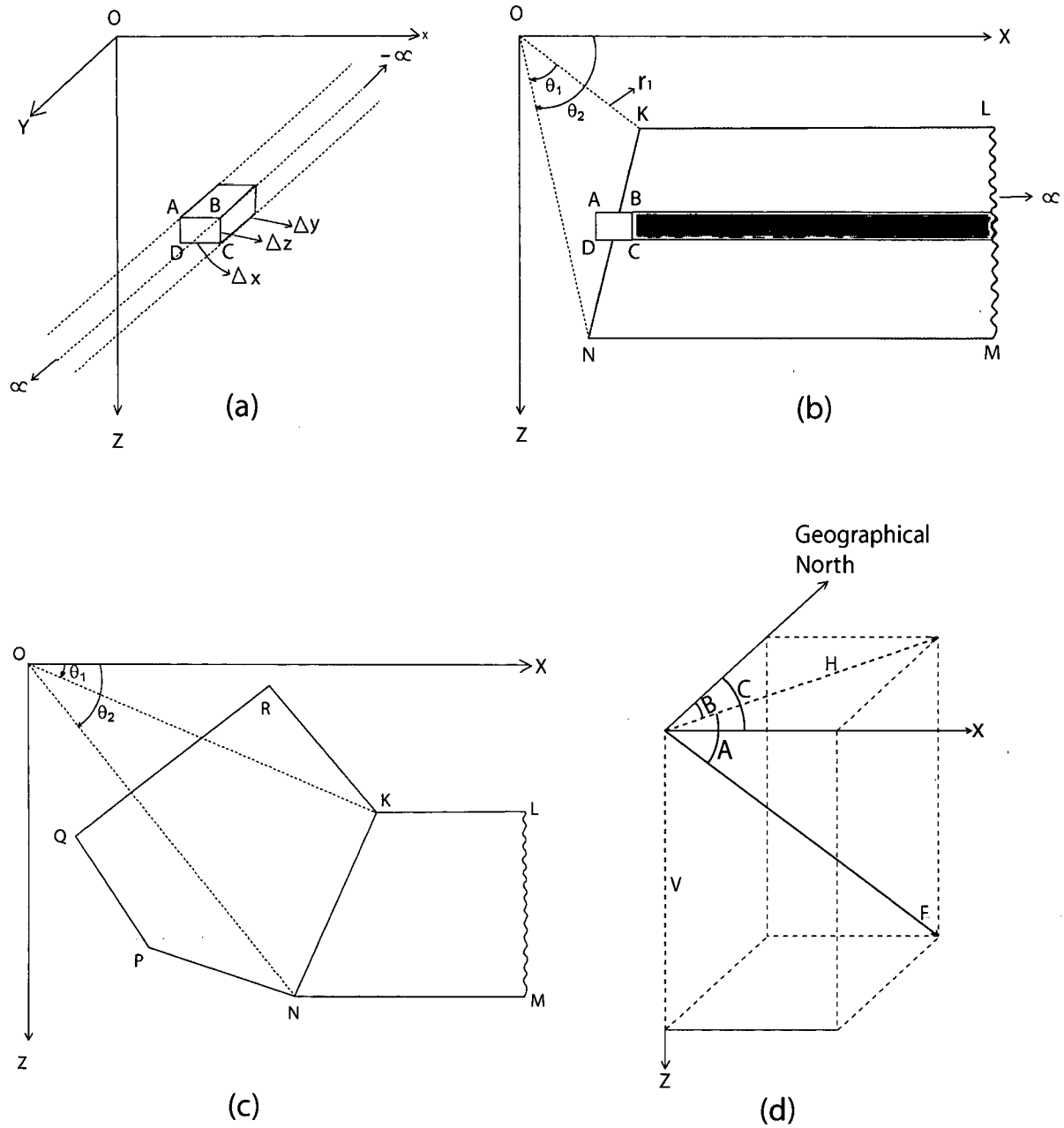

Fig. 3.8 Diagrams related to derivation of formulae for computation of the total field magnetic anomaly over two-dimensional polygon of infinite extent as used in the method of Talwani and Heirtzler (1964). Geometry of infinite rod (a) and lamina (b) Geometry of the polygon discussed in the text is shown in (c). The relation between the components of magnetization is illustrated in (d). (after Talwani and Heirtzler, 1964).

$$\Omega = \frac{\vec{m}.\vec{R}}{R^3} = \frac{J_x x + J_y y + J_z z}{(x^2 + y^2 + z^2)^{3/2}} \Delta x \Delta y \Delta z$$

The magnetic potential of the infinite rod of cross section ABCD is then given by

$$\Omega = \Delta x \Delta z \int_{-\infty}^{\infty} \frac{J_x x + J_y y + J_z z}{(x^2 + y^2 + z^2)^{3/2}} dy = 2\Delta x \Delta z \frac{J_x x + J_z z}{x^2 + z^2}$$

The vertical magnetic field strength (V) is then

$$V = -\frac{\partial \Omega}{\partial z} = 2\Delta x \Delta z \frac{2xzJ_x - J_z(x^2 - z^2)}{(x^2 + z^2)^2} \tag{3.1}$$

The horizontal magnetic field (H) in the x direction is given by

$$H = -\frac{\partial \Omega}{\partial x} = 2\Delta x \Delta z \frac{J_x(x^2 - z^2) + 2xzJ_z}{(x^2 + z^2)^2} \tag{3.2}$$

The values of V and H for the lamina shown shaded in Fig. 3.8b are obtained by integrating the equations 3.1 and 3.2 with respect to x, between the limits x and ∞. Thus,

$$V = 2\Delta z \frac{J_x z - J_z x}{x^2 + z^2} \tag{3.3}$$

$$H = 2\Delta z \frac{J_x x - J_z z}{x^2 + z^2} \tag{3.4}$$

To derive the field due to the prism KLMN, equations 3.3 and 3.4 are integrated with respect to z along KN between the depth limits Z_1 and Z_2

$$V = 2 \int_{z_1}^{z_2} \frac{J_x z - J_z x}{x^2 + z^2} dx$$

For any point on KN, $x = (x_1 + z_1 \cot \phi) - z \cot \phi$

$$V = 2 \sin \phi \left\{ J_x \left[(\theta_2 - \theta_1) \cos \phi + \sin \phi \log \frac{r_2}{r_1} \right] - J_z \left[(\theta_2 - \theta_1) \sin \phi - \cos \phi \log \frac{r_2}{r_1} \right] \right\}$$

$$H = 2 \sin \phi \left\{ J_x \left[(\theta_2 - \theta_1) \sin \phi - \cos \phi \log \frac{r_2}{r_1} \right] + J_z \left[(\theta_2 - \theta_1) \cos \phi + \sin \phi \log \frac{r_2}{r_1} \right] \right\}$$

The above equations can be rewritten as

$$V = 2(J_x.Q - J_z.P)$$
$$H = 2(J_x.P + J_z.Q)$$

where

$$P = \frac{z_{21}^{\ 2}}{z_{21}^{\ 2} + x_{12}^{\ 2}}(\theta_1 - \theta_2) + \frac{z_{21}x_{12}}{z_{21}^{\ 2} + x_{12}^{\ 2}}\log\frac{r_2}{r_1}$$

$$Q = \frac{z_{21}x_{12}}{z_{21}^{\ 2} + x_{12}^{\ 2}}(\theta_1 - \theta_2) + \frac{z_{21}^{\ 2}}{z_{21}^{\ 2} + x_{12}^{\ 2}}\log\frac{r_2}{r_1}$$

using the notation

$$x_{12} = x_1 - x_2$$
$$z_{21} = z_2 - z_1$$
$$r_1 = (x_1^{\ 2} + z_1^{\ 2})^{1/2}$$
$$r_2 = (x_2^{\ 2} + z_2^{\ 2})^{1/2}$$

The values for P and Q are calculated from the co-ordinates in Fig. 3.8c. The relations between J, J_x and J_z can be seen by referring to Fig. 3.8d, where J is defined with respect to the co-ordinate system and geographic north. The inclination of J is denoted as A (measured positive downwards) and the angle between the horizontal projection of J and geographic north is B. The angle in the x-y plane between the positive x-axis and geographic north is C, both B and C being measured in a clockwise direction from geographic north. The components of the magnetization J_x and J_z are then given by

$$J_x = J\cos A\cos(C - B)$$
$$J_z = J\sin A$$

If the polygon is magnetized by induction in the earth's field, then J=kF, A is the field Inclination (I) and B is the declination (D).

To obtain the field over the bounded polygonal section KNPQR the anomalies due to prisms such as KLMN that extend to infinity in the +x direction are calculated. Systematic addition of field values on moving around the polygon will give the total anomaly at (0,0) if due regard is made to the sign of the contributions of each prism as indicated by an increase or decrease in θ. For the anomalies small with respect to the total filed F, the total intensity anomaly, T is

the sum of the projections of H and V along the direction of F., i.e.,

$$T = V \sin I + H \cos I \cos(C - D)$$

Talwani and Heirtzler (1964) have provided a FORTRAN program, which can be used to calculate the synthetic magnetic anomaly of a two-dimensional body based on their method. Macnab (1966) developed an algorithm as an adaptation to Talwani and Heirtzler (1964) program to compute the magnetic anomaly caused by multiple bodies along a profile in a direction perpendicular to the strike direction of 2-D bodies. For the present work, an available (Bhattacharya, personal communication) software developed based on Macnab (1966) have been used to compute magnetic anomalies of models.

(b) Steps for magnetic modeling followed in this study

The study area contains magnetic lineations of alternate positive and negative magnetic anomalies. To interpret these magnetic anomalies, an initial model of juxtaposed magnetized blocks is considered as magnetic source. The magnetic polarity of these blocks is considered alternately normal and reverse. Given the boundaries of the blocks, their intensity of magnetization, the orientation of the regional field, the magnetic anomaly of the model can be calculated following the Talwani and Heirtzler (1964) method. During modeling, the boundaries of the blocks have been adjusted until an acceptable fit is obtained to the observed profile.

3.3.3 *Paleogeographic reconstruction*

The paleogeographic reconstruction, which is the process of restoring lithospheric plates back to the relative positions they occupied in the geological past, have been widely used to understand the evolution of ocean basins and the adjoining continents. Several researchers (McKenzie and Sclater, 1971; Norton and Sclater, 1979; Besse and Courtillot, 1988; Scotese et al., 1988; Royer et al., 1992; Royer et al., 2002) applied this technique to understand the evolution of the Indian Ocean region. Since paleogeographic reconstruction technique has been extensively used in the present study, therefore based on Cox and Hart (1986), some concepts and conventions related to usage of this technique, have been briefly described in this section.

(a) Great circles and small circles on a sphere

On a plane, straight lines were generally used to describe plate boundaries and directions of plate movement. Geometrically, the closest analog of a line on a sphere is a circle. It turns out that most of the elements of plate tectonics described by lines on the plane are described by circles on the globe. Plate tectonic geometry on a sphere turns out to be mainly a matter of relationships between circles. The centre of the circle drawn on a sphere is called the 'pole' of that circle. The angular length (δ) is the angle of an arc drawn on the surface of the sphere from the centre to some point on the circle. The equator is a circle centred at the North Pole or South Pole with an angular radius of $\delta = 90°$. The circles can also be made on a sphere by cutting the sphere with a plane. If the plane passes through the centre of the sphere, the intersection of the plane with the surface of the sphere will be a 'great circle' ($\delta = 90°$). Otherwise the intersection will be a 'small circle' ($\delta < 90°$). So, all longitudinal meridians are great circles, but not all latitudes. The only great circle in the latitude is the equator. All other latitude meridians are small circles. The great circle passing through longitude of zero degree is referred as the 'Index Meridian'.

(b) Frames of reference

Rotation of a point over a sphere can be executed only with reference to a fixed reference frame. For example, an ordinary reference globe consists of two parts. The first part is a sphere on which is printed a set of the latitude and longitude circles and the outlines of continents. The second one is a rigid metal or wooden framework that stands on the floor and supports the globe at the points by two pivot points, the globe being free to rotate within the rigid framework. This rigid frame is considered as the fixed reference frame. This can be considered as a physical three-dimensional object like fixed framework around the geographic globe and as a fixed set of points and curves on a piece of paper. The fixed reference frame consists of three perpendicular great circles drawn on a sphere (Fig. 3.9). The circles intersect at six points. Imagine six vectors originating at the centre of the sphere and ending at the six points of intersection of the circles. These compose a set of mutually perpendicular axes or unit vectors that can be referred as ± 1, ± 2, ± 3. The great circles that contain vectors 3 and 1 are

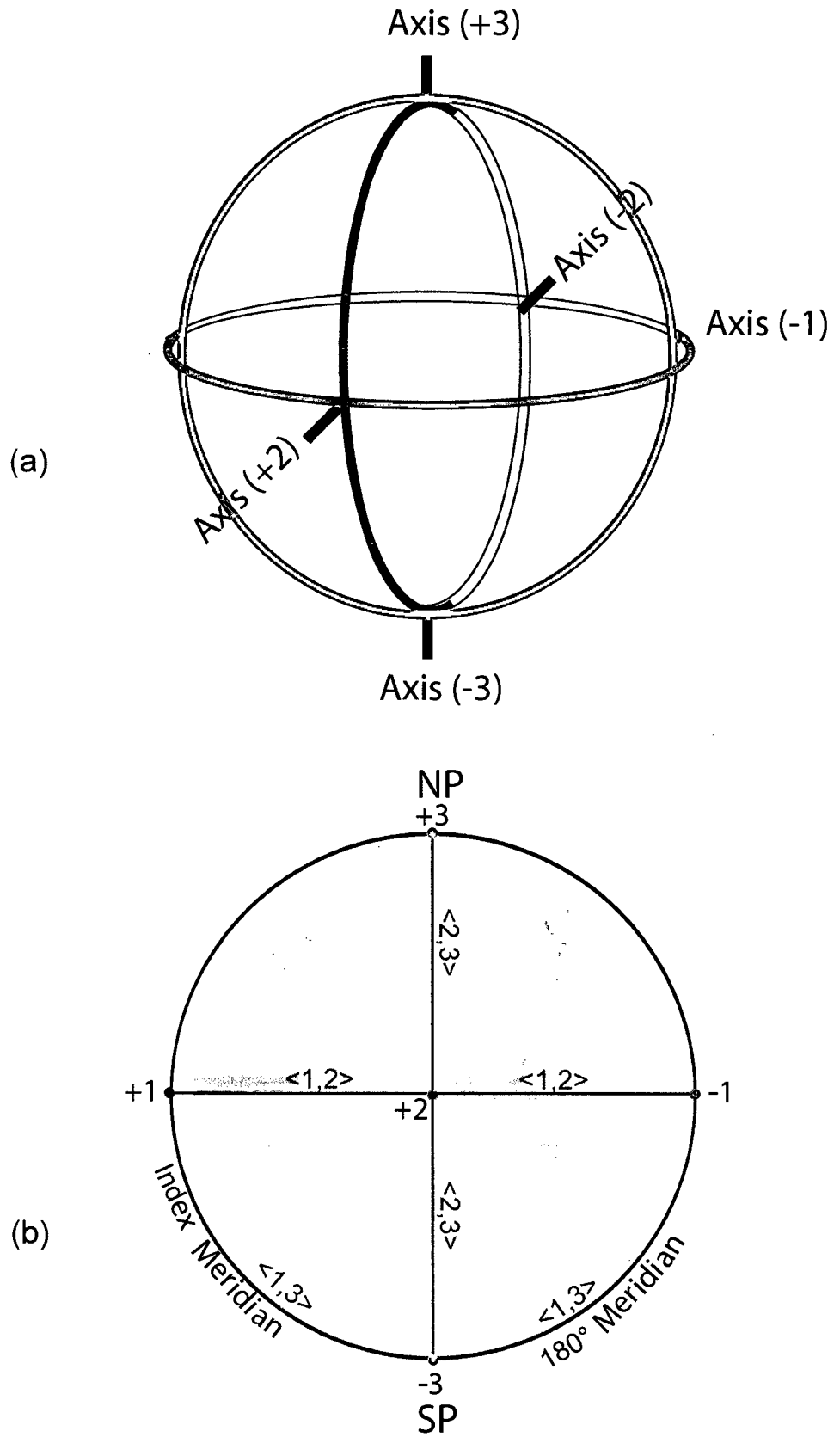

Fig. 3.9 Physical three-dimensional object like fixed framework around the geographic globe (a) Fixed reference frame consisting of three perpendicular great circles. The globe within the frame can rotate about either axis 2 or axis 3. (b) Globe representing the earth placed inside fixed reference frame, shown in an equal area projection (modified after Cox and Hart, 1986).

denoted by the symbol <3,1>. The three axes and the three reference circles <1,2>, <2,3> and <3,1> compose the principal elements of the fixed reference frame (Cox and Hart, 1986).

(c) Euler rotation parameters

Euler rotation parameters play an important role in the geometry of plate tectonics. They are named for the 18th century mathematician Leonhard Euler pronounced *'oiler'*. Euler's theorem is that *any motion of a rigid piece of a sphere over the surface of the sphere can be described as a rotation about some axis through the centre of the sphere*. The intersections of the axis with the surface are called Euler poles and the angle of rotation is called Euler angle. Euler latitude is analogous to a geographic line of latitude relative to the Earth's geographic North Pole. Euler pole is the pivot point about which two plates rotate relative to each other (Fig. 3.10a). It is like the hinge of a pair of scissors, and a transform fault is like the arc swept only by the point of one of the blades. The Euler pole is the only point that does not move relative to either plate. The motion of the plates over a sphere can be explained using the 'Euler rotation parameters'. These parameters are the key quantitative elements in plate tectonics. Since all transforms are segments of circles on a sphere, all plate motions on a sphere can be described efficiently and compactly using Euler rotation parameters. The transforms are segments of circles centred on the Euler pole (Fig. 3.10a, b).

(d) Determination of Euler pole using the trend of transform

To calculate the location of an Euler pole, three types of data are used. The first is the observed trend of transforms, as determined from their topography and geology. The second is the direction in which a block on one side of a fault slips past the block on the other side during an earthquake along a fault boundary, as determined by analyzing earthquake waves. The azimuth of this "slip vector" gives the direction of relative plate motion and thus is analogous to the trend of a transform. The third type of data is the velocity of spreading across ridges, as determined from the spacing of magnetic isochrons. In this study, the method of determining Euler pole from transform trends has been used. The other two methods could not be used because no data regarding slip vector is

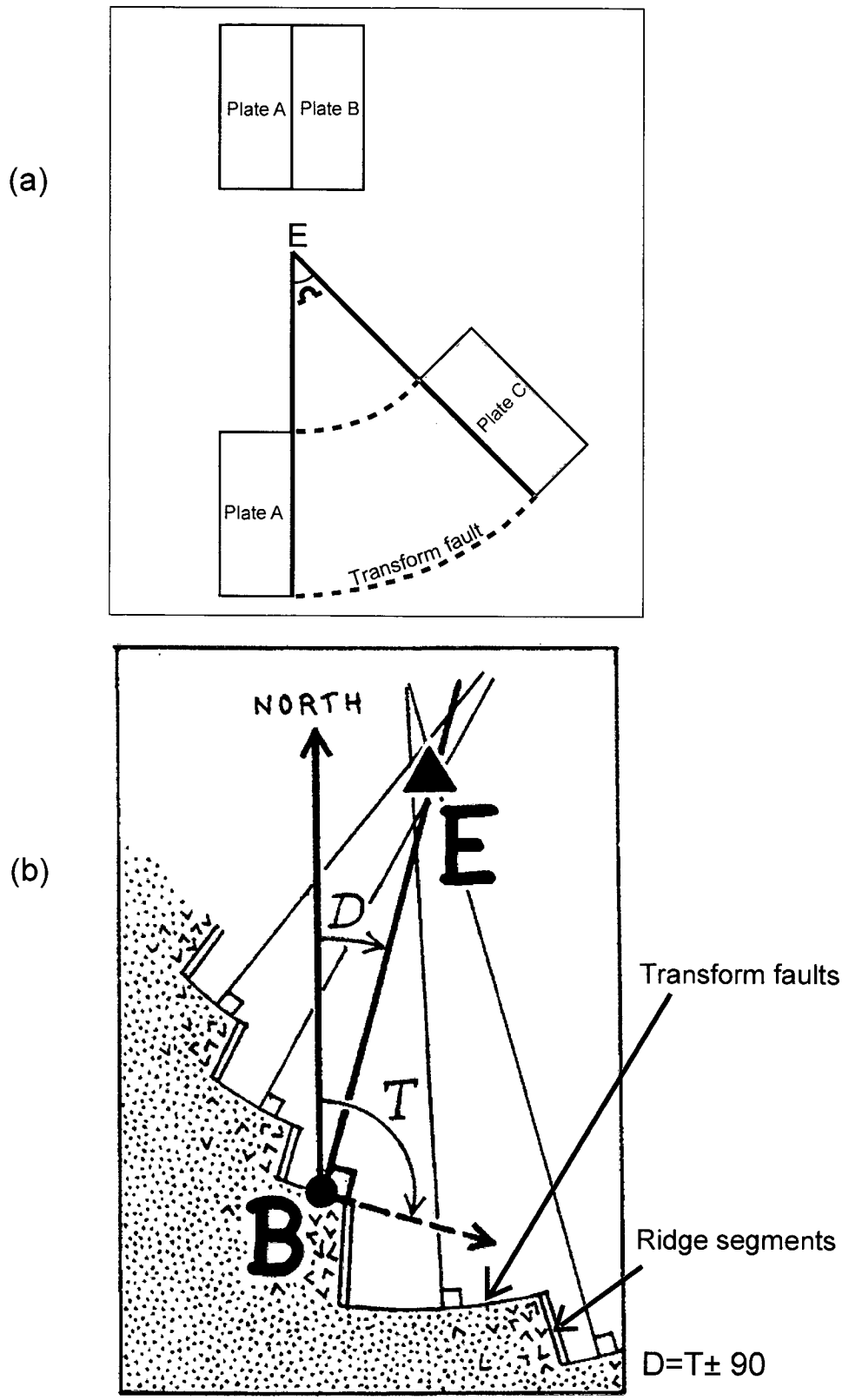

Fig. 3.10 Schematic diagrams representing the concept of Euler pole and Euler angle and their determination from the transform trends. (a) Plate A is fixed and Plate C is moving with respect to Plate A. The pole of rotation is the Euler pole (E) and the amount of angle rotated is the Euler angle (∩). (b) Locating an Euler pole E from the trends T of Transforms. Lines nearly intersecting at E are great circles perpendicular to transform.

available and the magnetic lineations are of too short extent to reliably compute variations of spreading velocity along the ridge axis. From analysis of transform trends, the Euler poles can be determined by two approaches, the graphical method and numerical method. The graphical method for the determination of Euler pole yields approximate values only. But, the mathematical method can yield more precise values of Euler pole.

(i) Graphical method for estimation of Euler pole from transform trends

In determining the location of an Euler pole using the trend of transforms (Fig 3.10a, b), the basic data to be analyzed consists of the local azimuth angle T of the transform at each locality B. Since the Euler pole lies on a great circle perpendicular to the transform, a great circle passing through the point B can be drawn by considering a pole of great circle at local azimuth $D=T\pm 90$. In the same way, the great circles passing through each transform points can be drawn. The co-ordinate, which defines the intersection of these great circles, is the location of Euler pole.

(ii) Numerical method for estimation of Euler poles from transform trends

Ideally, all of the great circles from the different observed points of fracture zones should intersect at the exact position of the Euler pole, E. But, nature is too complicated to provide an ideal Euler pole, so that the points of intersection are scattered along a general trend of great circles. Among these, the best fit Euler pole is determined by the least square approach. A methodology to perform the least square method to the derived trial Euler pole was provided by Le Pichon (1968), based on the computed theoretical azimuth of each observation compared with the actual observation. The procedure for this approach is as follows:

(1) Select the trial Euler pole

(2) At a given point of observation, calculate the theoretical azimuth.

(3) Subtract the theoretical transform trend (T_{ex}) from the observed trend (T_{obs}) and square the difference (ε^2). This squared error is commonly used in plate tectonics, as a measure of misfit between an observation and the predicted value.

(4) As a combined measure of misfit at all points of observation, use the sum $\Sigma\ \varepsilon^2$ of the squared errors at all the points.

(5) Select other trial poles and repeat the process until getting a satisfied Euler pole, for which $\Sigma\varepsilon^2$ is a minimum. This is the best-fit pole in the sense of least squares.

During the course of this study, a FORTRAN program has been developed to estimate the Euler pole, following the numerical method of determining Euler poles from transform trends. This software is developed mainly based on the method of Le Pichon (1968) and Cox and Hart (1986). In this program, an Euler pole determined based on graphical method is provided as trial Euler pole along with the end co-ordinates of number of fracture zones and their observed azimuths. The program provides the refined Euler pole.

(d) Rotation of a point over a sphere

As explained in the previous sections, any point on the Earth's surface can be rotated with respect to a rotation axis. The motion of a point over the surface of a sphere can be described with the help of Euler rotation parameters. The rotated co-ordinates of a point with respect to the known Euler pole and Euler angle can be determined using two methods – graphical method and numerical method.

(i) Graphical method of rotation of a point over a sphere:

Let,

(i) $K(\lambda_k, \phi_k)$ be a point to be rotated on Plate A (eg. Indian plate in Fig. 3.11a)

(ii) $E(\lambda_E, \phi_E)$ be the Euler pole about which point K is to be rotated

(iii) Ω be the angle of rotation that reconstructs Plate A with reference to Plate B (eg. African plate in Fig. 3.11a).

(iv) $K'(\lambda_k, \phi_k)$ be the rotated point over plate A,

where,

λ is the latitude of the corresponding point and

ϕ is the longitude of the corresponding point.

Using an equal area projection, any finite rotation can be accomplished using five successive rotations about the axis 2 and axis 3 (Fig. 3.11a-f). The first two rotations align the Euler pole E with axis 3, the third rotation is the desired rotation, and the last two rotations return E (and the globe) to its original position. The rotated point over plate A is given as K'(λ_k, ϕ_k). This rotation can be accomplished graphically in the following way:

(i) Two maps of globe in a stereographic or equal area projection are prepared, one on a white paper and another on a tracing paper. The plot of globe on tracing paper is referred as rotating globe co-ordinate system and the plot on white paper is referred as projection co-ordinate system. The points E and K are plotted on tracing paper (Fig. 3.11a). To start with, both the tracing paper and white paper are superposed in such a way that both the projection and rotating globe co-ordinate system coincide.

(ii) The globe on tracing paper is rotated with reference to axis 3 of the projection co-ordinate system by an angle of – ϕ_E, this rotation will take Euler pole to the Index Meridian (Fig. 3.11b).

(iii) The globe on tracing paper is rotated with reference to axis 2 of the projection co-ordinate system, by an angle of -(90-λ_E), which will bring the Euler pole to the Projection pole +3 (Fig. 3.11c).

(iv) The globe on tracing paper is rotated with reference to axis 3 of the projection co-ordinate system, by an angle Ω, which is the Euler angle. This will bring the point K to K' (Fig. 3.11d).

(v) The globe on tracing paper is rotated with reference to axis 2 of the projection co-ordinate system (Fig. 3.11e), by an angle (90-λ_E). This rotation will bring the Euler pole along Index meridian back to its original latitude.

(vi) The globe on tracing paper is rotated with reference to axis 3 of the projection co-ordinate system (Fig. 3.11f), by an angle ϕ_E. This rotation will bring the Euler pole back to its original longitude in the same reference frame as in (a).

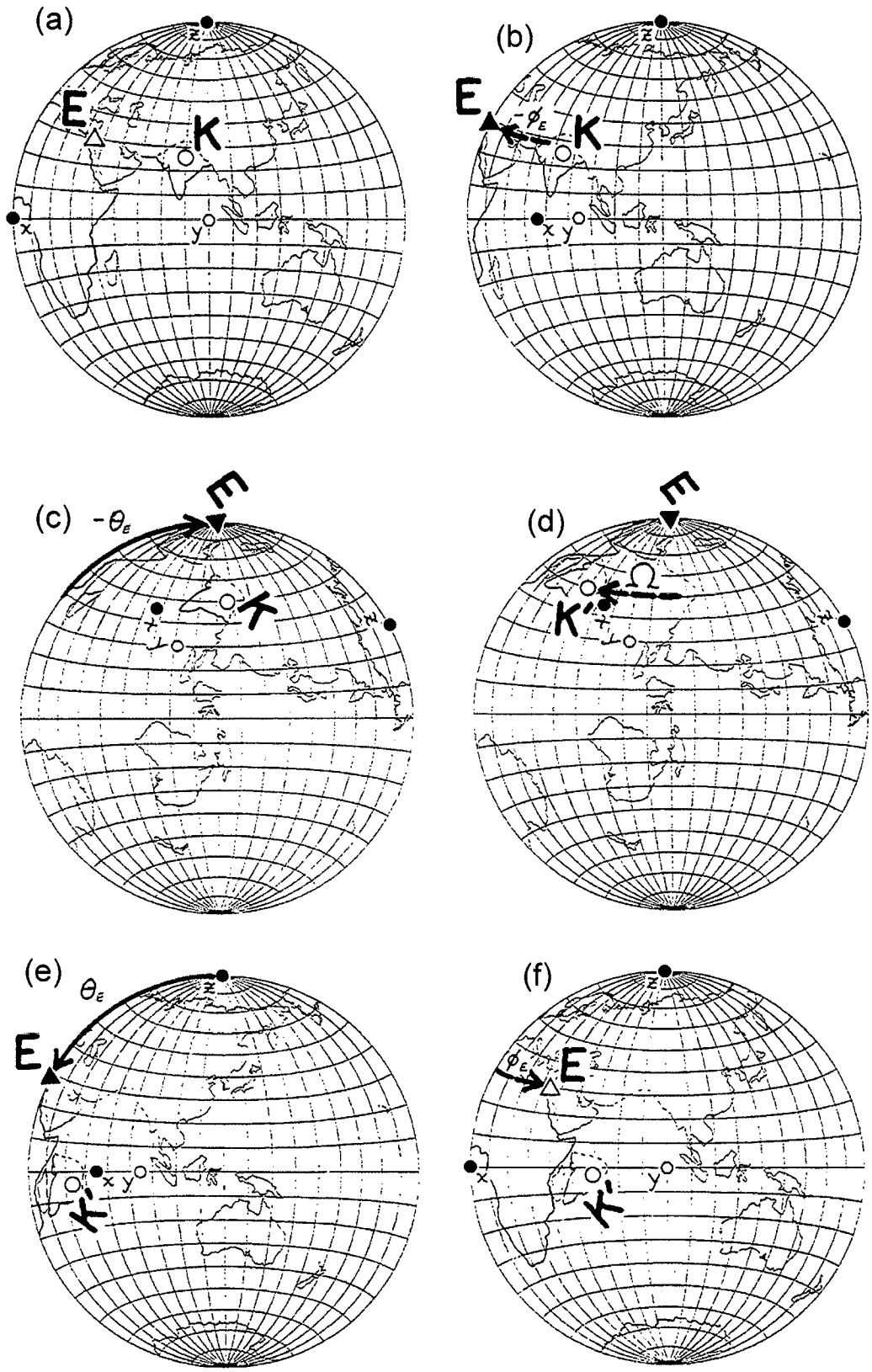

Fig. 3.11 Figures describing steps of rotation of a point around an Euler pole using an equal area projection map of the globe (modified after Cox and Hart, 1986). K: the point to be rotated; E: Euler pole; K' : the rotated position of K at various stages. Details of stages are described in the text.

(vii) The co-ordinates of K' is the rotated position of point K, which can be read from the globe.

(ii) Numerical method of rotation of a point over a sphere

Since too many points are involved in the plate kinematics, it is impossible to calculate the motion of each point one by one using graphical technique. Hence, rotations of plates are performed with the help of computers. The method, which is most suitable to the computers, is based on the matrix transformation of the three Cartesian components of position vectors. If point A is a point with Cartesian coordinates (A_x, A_y, A_z), prior to the rotation, then the components (B_x, B_y, B_z) after rotation to B can be obtained using the matrix multiplication.

B = R A, where R represents a 3 × 3 matrix

$$\begin{bmatrix} B_x \\ B_y \\ B_z \end{bmatrix} = \begin{bmatrix} R_{11} & R_{12} & R_{13} \\ R_{21} & R_{22} & R_{23} \\ R_{31} & R_{32} & R_{33} \end{bmatrix} \begin{bmatrix} A_x \\ A_y \\ A_z \end{bmatrix}$$

Applying the usual rule of matrix multiplication,

$$B_x = R_{11}A_x + R_{12}A_y + R_{13}A_z$$
$$B_y = R_{21}A_x + R_{22}A_y + R_{23}A_z$$
$$B_z = R_{31}A_x + R_{32}A_y + R_{33}A_z$$

The elements of the rotation vectors are

$R_{11} = E_xE_x(1-\cos\Omega) + \cos\Omega$ $R_{12} = E_xE_y(1-\cos\Omega) + \cos\Omega$ $R_{13} = E_xE_z(1-\cos\Omega) + \cos\Omega$

$R_{21} = E_yE_x(1-\cos\Omega) + \cos\Omega$ $R_{22} = E_yE_y(1-\cos\Omega) + \cos\Omega$ $R_{23} = E_yE_z(1-\cos\Omega) + \cos\Omega$

$R_{31} = E_zE_x(1-\cos\Omega) + \cos\Omega$ $R_{32} = E_zE_y(1-\cos\Omega) + \cos\Omega$ $R_{33} = E_zE_z(1-\cos\Omega) + \cos\Omega$

The multiplication of the rotation matrix **R** with the position matrix **A** gives the rotated position matrix, **B** in Cartesian co-ordinates, which can be converted into spherical polar co-ordinates.

3.3.4 *Adopted magnetic chron nomenclature and allied conventions*

In this study, the geomagnetic polarity time scale and the magnetic chron nomenclature proposed by Cande and Kent (1995) have been adopted (Table

3.3). Further, mainly based on Cox and Hart (1986) following conventions have been used in connection with denoting a particular geomagnetic polarity interval or the seafloor spreading magnetic anomaly created during that polarity interval;

(i) In geomagnetic polarity time scale, the term 'chron' have been used to denote the broad time interval within which the geomagnetic polarity remained constant. Each chron is designated by identification (numbers suffixed with alphanumeric characters), where the present normal chron is identified as chron 1 and preceding (older) normal chrons are designated successively with increasing numbers such as chron 2, chron 3 etc. This convention of identification of chrons by only numbers is followed for the Cretaceous-Tertiary-Quaternary Superchron (Note: here the term 'Superchron, denotes a large time interval during which the polarity bias is constant or nearly so). For still older Cretaceous-Jurassic Superchron, the letter 'M' is prefixed to the number label of the chron. Sometimes the suffix of 'n' or 'r' is further added to the chron identification to denote the episodes of normal or reverse polarity respectively. Wherever such a suffix is not added it is considered to represent a normal chron. For example, chron 27n (or, chron 27) represent the time interval for a normal episode and chron 27r represent the time interval for the reverse episode of magnetic polarity interval preceding (older in age) the normal chron 27n.

(ii) The boundaries of a chron are identified by adding the further suffix of 'y' to denote the younger end and the suffix 'o' to denote the older end of the chron.

(iii) The seafloor spreading magnetic anomaly caused by a magnetized block formed during a particular chron is designated by relating to the corresponding chron. For example, the magnetic anomaly caused by magnetized block formed during chron 28n is denoted as 'anomaly 28n' (or, in abbreviated form as 'A28n'). As a consequence of this form of anomaly designation, the temporal references, such as; 'time of anomaly 28n', 'time of A28n', 'anomaly 28n time' or 'A28n time' thus corresponds to chron 28n.

(iv) The boundaries of magnetized blocks thus are synonymous with chron boundaries. Therefore, the lineations drawn by joining the boundaries corresponding to the same chron on adjacent magnetic profile can be

considered to represent an isochron.

3.3.5 *Preparation of maps and profiles*

In the present study, large number of descriptive as well as interpretative maps and profiles has been presented. These maps have been prepared in Mercator projection of different scales using the Generic Mapping Tools (GMT) software (Wessel and Smith, 1995). Profiles and contours of different data as well as the colour shaded relief image and contours of satellite derived free-air gravity anomalies have also been prepared using the same GMT software. Many tectonic elements have been digitized from various published figures and maps using the ARC/Info GIS package. Few data profiles / sections have been digitized from published figures using WINDIG software. The digitized data were stored as GMT compatible data files and integrated to various maps and sections using GMT package.

Table 3.3 Selected magnetic anomaly numbers and their bounding ages, extracted from the Geomagnetic Polarity Timescale of Cande and Kent (1995). Magnetic anomaly number followed by the suffix 'n' represents normal polarity interval.

Anomaly number	Younger boundary (Ma)	Older boundary (Ma)
16n	35.343	36.341
20n	42.536	43.789
21n	46.264	47.906
22n	49.037	49.714
23n1	50.778	50.946
23n2	51.047	51.743
24n1	52.364	52.663
24n2	52.757	52.801
24n3	52.903	53.347
25n	55.904	56.391
26n	57.554	57.911
27n	60.920	61.276
28n	62.499	63.634
29n	63.976	64.745
30n	65.578	67.610
31n	67.735	68.737
32n1	71.071	71.338
32n2	71.587	73.004
33n	73.619	79.075
34n	83.000	118.000

CHAPTER 4

Chapter 4

GEOPHYSICAL SIGNATURES AND INFERENCE ABOUT CRUST UNDERLYING THE OFFSHORE INDUS AND LAXMI BASINS

4.1 Introduction

The deep offshore regions in and around the study area are the Laxmi Basin, the Offshore Indus Basin, and the Arabian Basin (Fig. 4.1). The Arabian Basin is the conjugate of Eastern Somali Basin, which was formed by seafloor spreading across the Carlsberg Ridge. Earlier studies (Norton and Sclater, 1979; Besse and Courtillot, 1988; Royer et al., 1992) considered this seafloor spreading to have started at chron 28, and depicted the configuration of India and Seychelles in their paleogeographic reconstruction models of chron 28. Those reconstruction models of chron 28 suggest that there existed a wide deep offshore region between the Seychelles and the India/Pakistan continental slope at that time. It may be noted that the existence of the Laxmi Ridge was either not known or was not considered in those studies. However, the subsequent studies (Chaubey et al., 2002a; Royer et al., 2002; Miles and Roest, 1993) considered the existence of the Laxmi Ridge and shown that the oldest magnetic anomaly identified in the Arabian Basin is anomaly 28n, which is located immediately south of Laxmi Ridge (Fig. 4.1). This observation implies that

i) at chron 28n, Seychelles was juxtaposed with the Laxmi Ridge,

ii) if Seychelles was ever juxtaposed with India/ Pakistan mainland, then it was in the form of a Greater Seychelles, i.e., Seychelles together with the Laxmi Ridge,

iii) Greater Seychelles was juxtaposed with India/Pakistan mainland at a time prior to the time of anomaly 28n (i.e. earlier than ~62 Ma), and

iv) the wide deep offshore region between the present day Laxmi Ridge and the adjacent India/ Pakistan continental slope was created as a result of moving away of Greater Seychelles from India/Pakistan mainland.

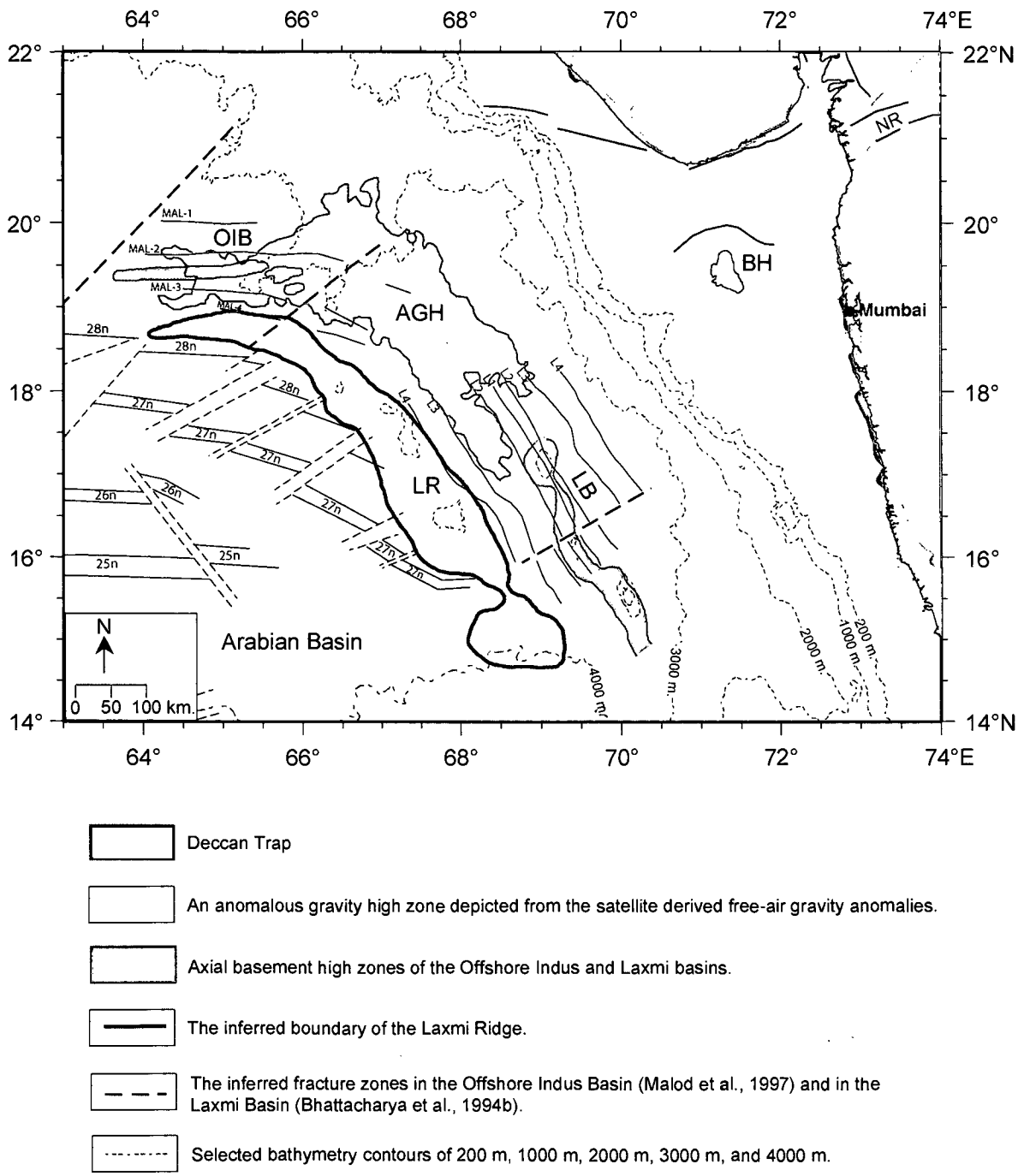

Deccan Trap

An anomalous gravity high zone depicted from the satellite derived free-air gravity anomalies.

Axial basement high zones of the Offshore Indus and Laxmi basins.

The inferred boundary of the Laxmi Ridge.

The inferred fracture zones in the Offshore Indus Basin (Malod et al., 1997) and in the Laxmi Basin (Bhattacharya et al., 1994b).

Selected bathymetry contours of 200 m, 1000 m, 2000 m, 3000 m, and 4000 m.

Fig. 4.1 Generalized map of the deep offshore regions adjoining west coast of India/ Pakistan, showing major tectonic elements. The solid black lines represent the mapped seafloor spreading type magnetic lineations inferred by Bhattacharya et al. (1994b), Malod et al. (1997) and Chaubey et al. (2002a). OIB: Offshore Indus Basin; LB: Laxmi Basin; LR: Laxmi Ridge; AGH: Anomalous Gravity High; BH: Bombay High; NR: Narmada Rift.

As described earlier in chapter 2, two views exist about the nature of the crust underlying the wide region between the Laxmi Ridge and the adjacent continental slope of India. Some researchers (Naini and Talwani, 1982; Kolla and Coumes, 1990; Miles et al., 1998; Todal and Eldholm, 1998; Lane et al., 2005; Krishna et al., 2006) believe that the crust underlying this region represents a thinned continental crust formed only by rifting, while the studies of others (Biswas and Singh, 1988; Bhattacharya et al., 1994b; Malod et al., 1997; Talwani and Reif, 1998; Bernard and Munschy, 2000; Bulychev et al., 2006) imply that at least the axial part of this region was formed by two-limbed seafloor spreading, which became extinct during chron 28n. It appears that most of these studies based their inference, about the nature of the crust underlying this region, on independent interpretation of one or other type of geophysical signatures rather than integrated analysis of all available data. In view of this, it is felt necessary to compile updated information about various geophysical signatures in the study area and to infer the nature of the crust underlying these regions based on integrated interpretation of those geophysical signatures. This chapter briefly describes those geophysical signatures and the inferences made from their integrated interpretation.

4.2 Geophysical signatures of the Offshore Indus and Laxmi basins

(a) Seafloor and basement features from seismic reflection profiles

The seismic investigations (Naini and Talwani, 1982; Kolla and Coumes, 1990; Malod et al., 1997; Collier et al., 2004a, b; Srinivas, 2004) carried out in the deep offshore regions adjoining to India/Pakistan mainland revealed the presence of various seafloor and basement features in the study area (Fig. 4.2). The major basement features among these are the Laxmi Ridge, the Palitana Ridge and the Panikkar Ridge. Sectional views of these features are available in some published seismic reflection sections from the Offshore Indus and Laxmi basins. The published seismic section from the Laxmi Basin is from Naini and Talwani (1982) and the two published seismic sections from the Offshore Indus Basin are from Malod et al. (1997) and Collier et al. (2004a, b). The locations of these three profiles have been shown in Fig. 4.2 and corresponding seismic sections in Fig. 4.3a-c. The sectional views of the basement highs representing

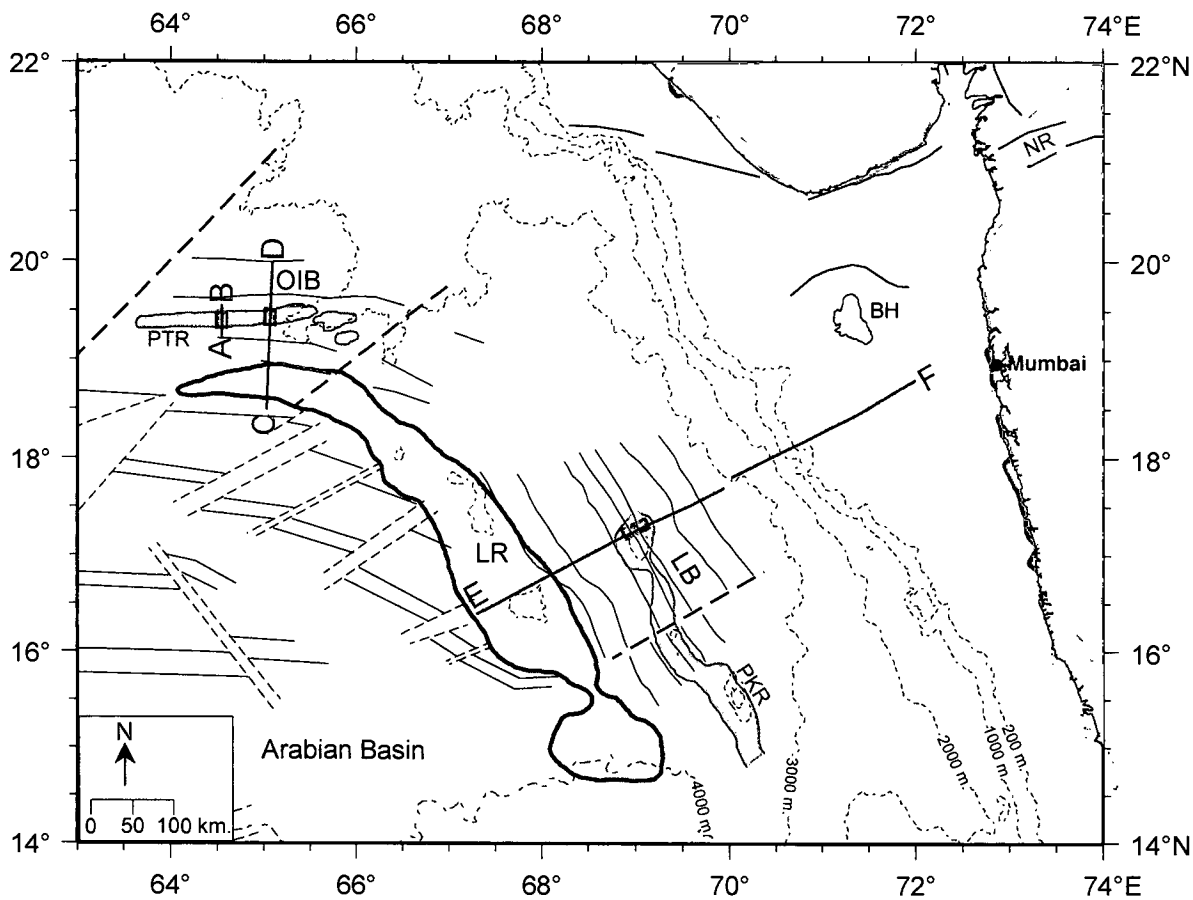

Axial basement high zones of the Offshore Indus and Laxmi basins.

Extent of the basement highs as depicted in the seismic reflection sections.

The inferred boundary of the Laxmi Ridge.

Fig. 4.2 Locations of the published seismic reflection profiles in the Offshore Indus and Laxmi basins. The seismic sections along the profiles AB, CD and EF are given in Fig. 4.3. PKR: Panikkar Ridge; PTR: Palitana Ridge. Other details are as in Fig. 4.1.

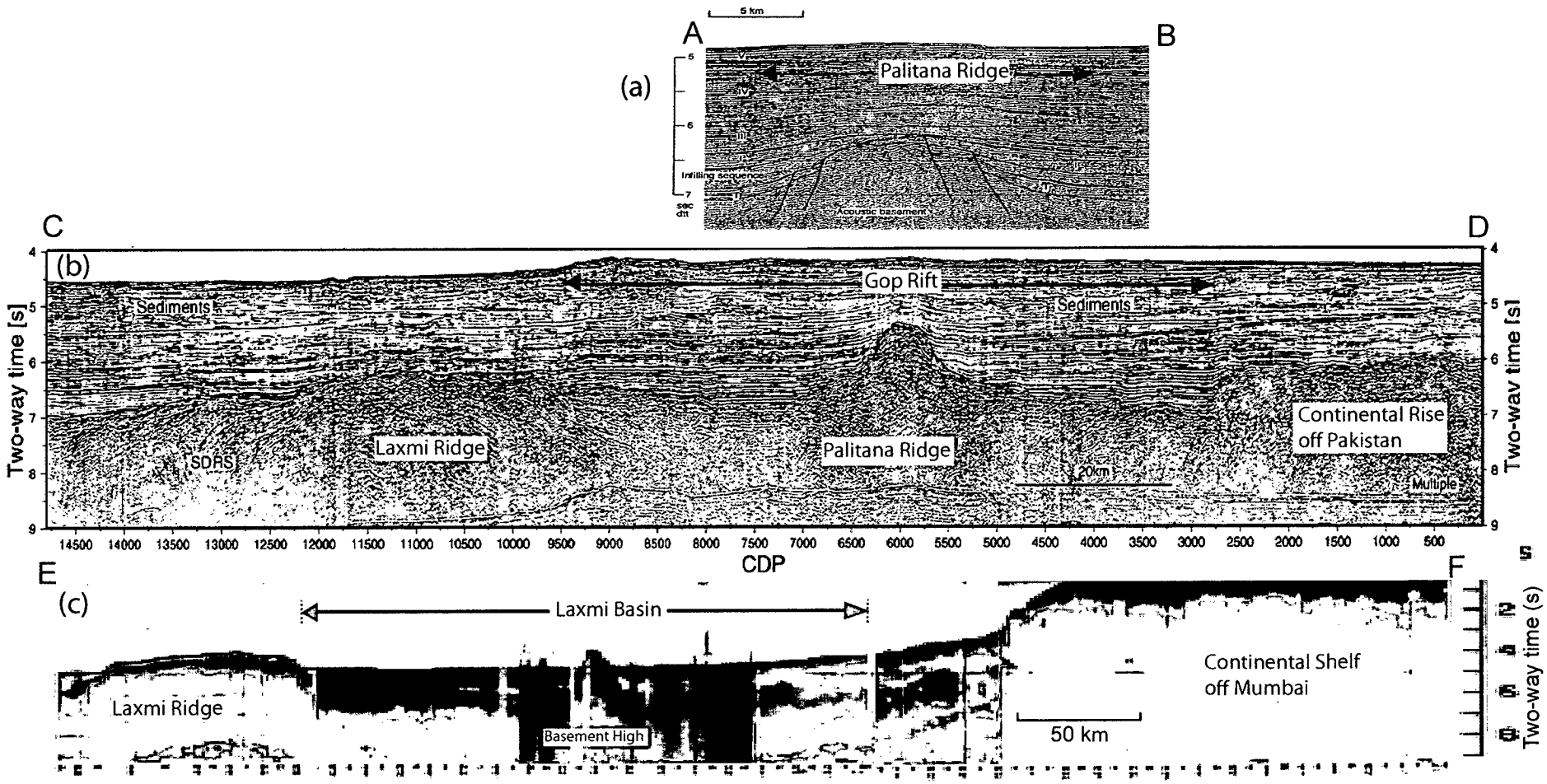

Fig. 4.3 Published seismic sections across the Offshore Indus Basin and the Laxmi Basin regions. Seismic reflection sections: (a) along profile AB (modified from Malod et al., 1997), (b) along profile CD (modified from Collier et al., 2004a, b) and (c) along profile EF (modified from Naini and Talwani, 1982). The basement high along the central part of the Laxmi Basin coincides with the axis of extinct spreading axis postulated by Bhattacharya et al. (1994a, b) and the location of Palitana Ridge coincides with the extinct spreading centre in the Offshore Indus Basin as postulated in the present study. Locations of the profiles are shown in Fig. 4.2.

the Laxmi Ridge as well as the axial basement high region of the Laxmi Basin are clearly observed from the seismic reflection section (Fig. 4.3c). In a similar way, the sectional view of the prominent basement high across the axial part of the Offshore Indus Basin is observed in both the seismic sections (Fig. 4.3a, b). The seismic results show (Fig. 4.2) that the basement expression of the southerly part of the Laxmi Ridge, which abuts the Laxmi Basin trends NW-SE and the northerly part of it, which abuts the Offshore Indus Basin region trends E-W. However, the seafloor topographic expression of the Laxmi Ridge is observed only over the NW-SE trending southerly segment. The axial basement high region of the Laxmi Basin is a NW-SE trending continuous basement feature, which at places outcrops as seamounts. The seismic and bathymetric results in the Offshore Indus Basin show that Palitana Ridge is an E-W trending continuous buried basement high feature. Interestingly, the Panikkar Ridge in the Laxmi Basin and the Palitana Ridge in the Offshore Indus Basin parallel the trend of the adjacent segments of the Laxmi Ridge. Further, the velocity-depth information derived from the seismic refraction results over the NW-SE trending (Naini and Talwani, 1982) and the E-W trending (Collier et al., 2004a, b) sectors of the Laxmi Ridge reveals the presence of deeper Moho than obtained for the Arabian Basin region.

(b) Gravity anomalies

The sea-surface gravity profiles (Naini and Talwani, 1982) in the Laxmi Basin revealed the presence of a short wave length gravity low superimposed on a broad wavelength gravity high. Axis of this short wave length gravity low coincides with the axial basement high feature seen in the seismic section. Subsequently, Bhattacharya et al. (1994b) observed that this prominent short wave length gravity low is a characteristic continuous feature within the Laxmi Basin and its trend is approximately NNW-SSE. The recent sea-surface gravity profile published by Collier et al. (2004b) interestingly depicted a similar feature in the Offshore Indus Basin, where also a basement high feature exist, which is associated with a short wave length gravity low atop a broad wave length gravity high.

In view of these similarities of gravity signatures, the available sea-surface gravity profiles have been compiled and studied to understand and compare the causative crustal structures of the Offshore Indus and Laxmi basins. For this

exercise, seventeen gravity profiles (Fig. 4.4) were selected. The gravity anomalies along these profiles were stacked after projecting them perpendicular to the trend of the Laxmi Ridge (Fig. 4.5). This stacking was done with respect to the inferred characteristic short wave length gravity low axis in both the basins. In the regions where gravity low axis could not be traced, the profiles were stacked based on the contiguity of the gravity signatures. Among the seventeen profiles, ten profiles are sea-surface gravity profiles archived in the NGDC and NIO databases. To fill the inter-profile wide gap areas, seven profiles have been extracted from the available (Sandwell and Smith, 1997; 2003) satellite derived free-air gravity anomalies. To test the reliability of the satellite gravity data to be used for the present study, the satellite derived free-air gravity anomalies have been extracted exactly along the location of sea-surface profile SK79-11. A comparison of gravity anomalies along these two profiles (Fig. 4.5) shows very good correlation between the satellite derived free-air gravity profile SK79-11(SG) and the sea-surface gravity profile SK79-11. In view of this, wherever additional gravity profiles were required for the correlation of characteristic gravity signatures, the satellite derived free-air gravity profiles have been extracted and used.

The stacked gravity profiles (Fig. 4.5) and the along track gravity anomalies (Fig. 4.6) show the presence of a major NW-SE trending broad free-air gravity low region existing between the Arabian Basin and the Laxmi Basin regions. This characteristic gravity signature shows that around 65°30'E this feature turns to WNW-ESE direction and extends westwards at least up to 63°40'E. A comparison of this gravity signature with the basement configuration of the regions showed that this signature correspond to the basement high region of the Laxmi Ridge. The broad wave length gravity high regions observed in the north and east of the Laxmi Ridge represent the gravity signatures of the Offshore Indus and Laxmi basins. In the Laxmi Basin region, the characteristic short wavelength gravity low atop the broad wavelength gravity high can be confidently correlated northwards at least till profile SK22-08. Similarly, in the Offshore Indus Basin region, similar gravity anomaly can be confidently correlated eastward till profile SG-05. In the region between profiles SK22-08 and SG-05, the continuation of this characteristic short wavelength gravity low axis

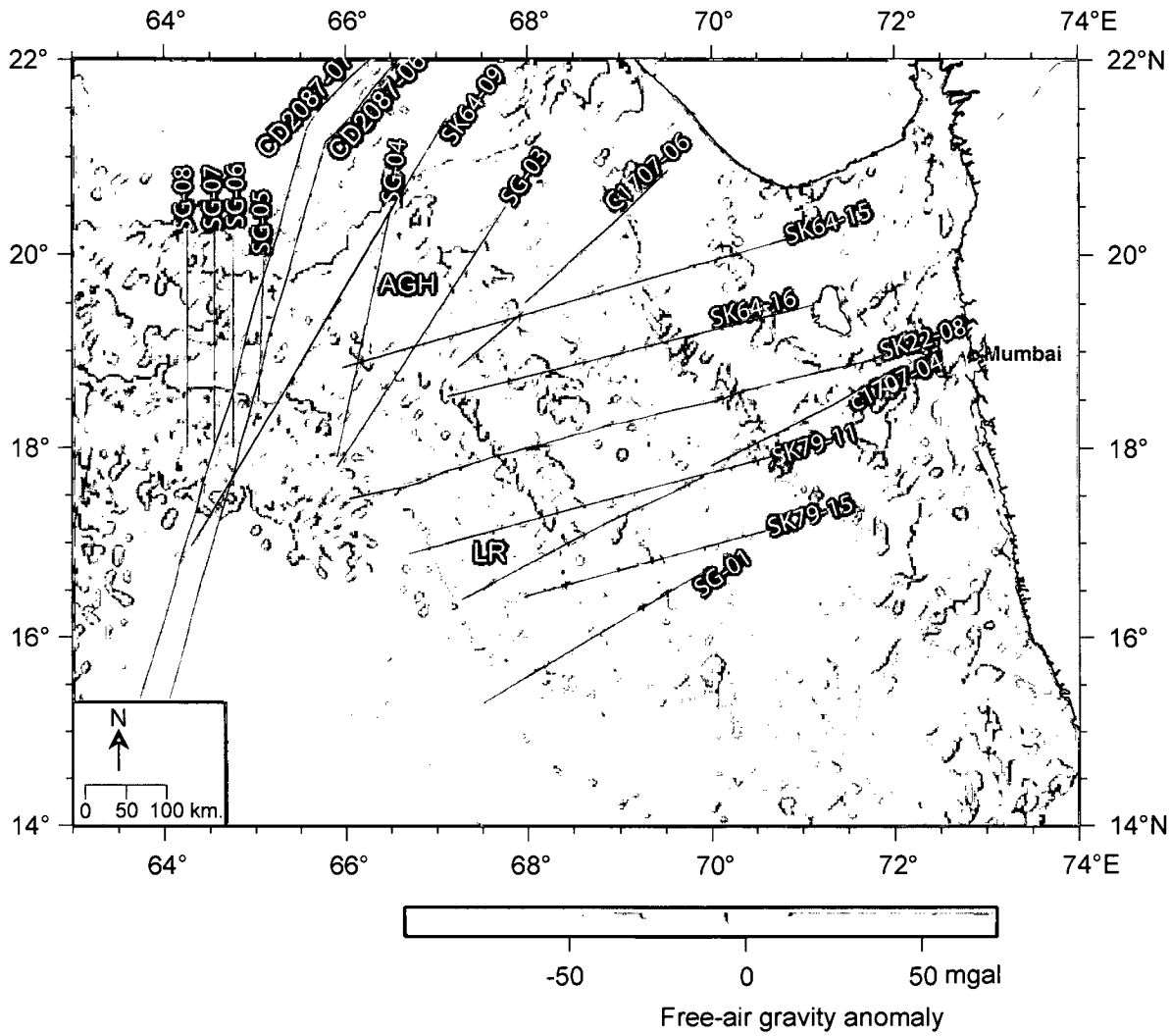

Fig. 4.4 Colour shaded-relief image of the satellite derived free-air gravity anomalies of the Laxmi Basin and Offshore Indus Basin regions. Black lines with white annotations are locations of selected gravity anomaly profiles used in this study to depict the characteristic gravity signatures of the region. Annotations along these profiles are profile identifiers. Profiles along which the free-air gravity anomalies have been extracted from satellite derived gravity anomalies are prefixed with SG. Other tracks are of sea-surface gravity anomalies along different ship tracks, the details of which are given in Table 3.1. Other details are as in Fig. 4.1.

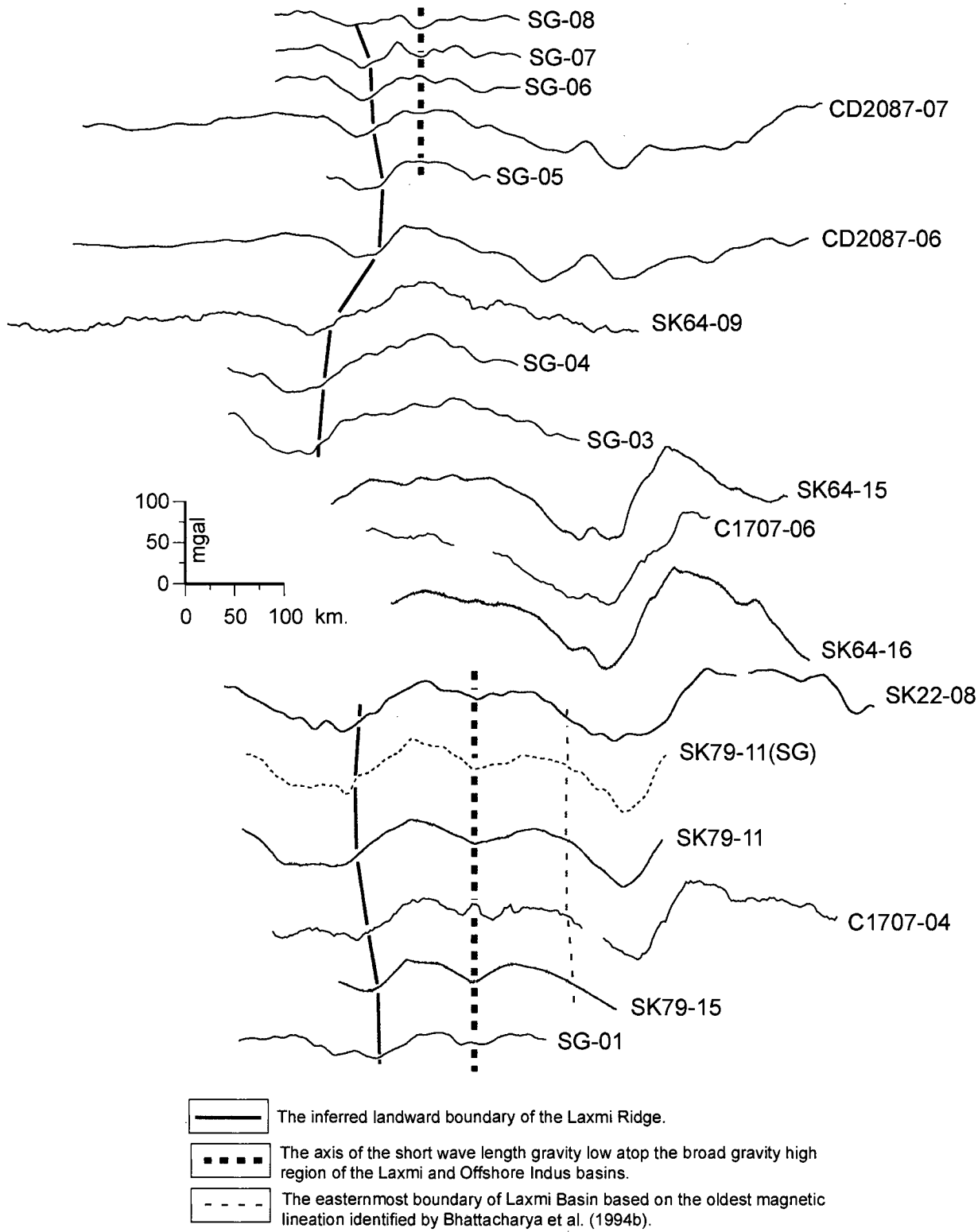

Fig. 4.5 Selected gravity profiles projected perpendicular to the trend of the Laxmi Ridge and stacked with respect to the axis of characteristic short wave length gravity low atop the broad gravity high region of the Laxmi and Offshore Indus basins. In the region where gravity low axis could not be traced, the profiles are stacked based on the contiguity of the other gravity signatures. Locations of these profiles are presented in Fig. 4.4. The excellent closeness may be noted between the sea-surface gravity anomaly along SK79-11 and the gravity anomly profile SK79-11(SG) which is based on satellite derived gravity data grids.

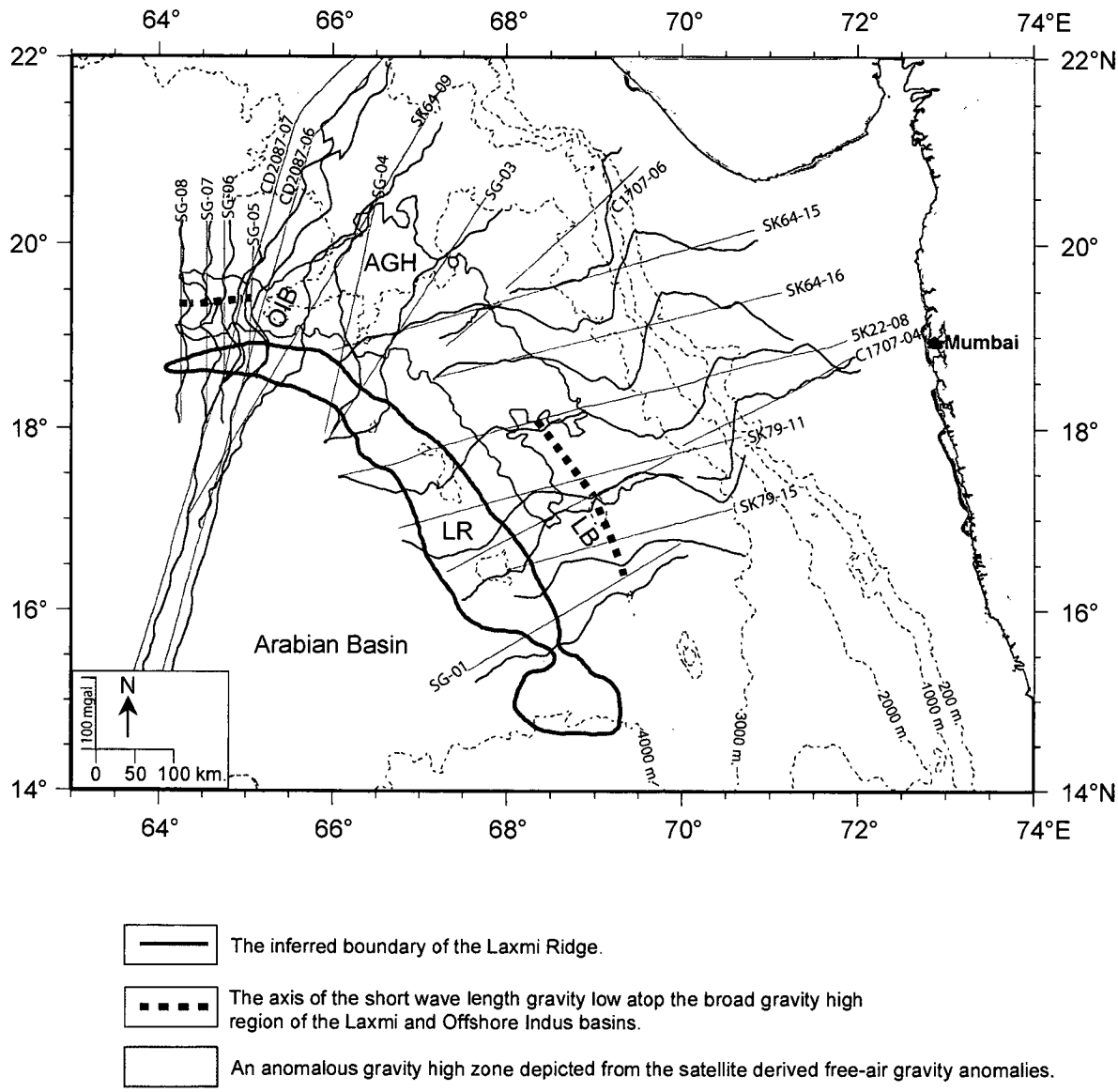

The inferred boundary of the Laxmi Ridge.

The axis of the short wave length gravity low atop the broad gravity high region of the Laxmi and Offshore Indus basins.

An anomalous gravity high zone depicted from the satellite derived free-air gravity anomalies.

Fig. 4.6 Map showing the gravity anomalies over the Laxmi Ridge, Laxmi Basin and Offshore Indus Basin regions, plotted perpendicular to the tracks.The gravity anomalies in both the Laxmi Basin and Offshore Indus Basin regions are characterized by a short wave length gravity low atop a broad wave length gravity high. Other details are as in Fig. 4.1.

could not be traced. Instead, it was observed that there exists an anomalous gravity high zone (AGH). The extent of this anomalous gravity high zone has been inferred in this study (Fig. 4.7a-d) based on the satellite derived free-air gravity anomalies. The free-air gravity anomaly contours (at 5-mgal interval) of this region clearly depict the presence of a gravity high region bounded by a steep gradient zone. This steep gradient zone around the anomalous gravity high has been considered to define its extent (Fig. 4.7a-d).

(c) Magnetic anomalies

The sea-surface magnetic profiles in the Laxmi Basin revealed the presence of fairly correlatable magnetic lineations (Bhattacharya et al., 1994b) between the Laxmi Ridge and the western continental slope of India. Bhattacharya et al. (1994b) observed that these magnetic lineations are symmetric about a central negative magnetic anomaly and the axis of symmetry coincides with a characteristic short wave length free-air gravity low atop a broad gravity high. Based on these observations, they inferred that the Laxmi Basin is underlain by oceanic crust created as a result of two-limbed seafloor spreading. Subsequently, Malod et al. (1997) mapped linear magnetic anomalies in the Offshore Indus Basin and inferred that these magnetic lineations represent oceanic crust formed as a result of two-limbed seafloor spreading process. However, the inferences of Bhattacharya et al. (1994b) and Malod et al. (1997) have been questioned in some of the subsequent studies (Todal and Eldholm, 1998; Miles et al., 1998) and were supported in several other studies (Bernard and Munschy, 2000; Talwani and Reif, 1998; Bulychev et al., 2006). The recent study carried out by Krishna et al. (2006) supported the postulation of Malod et al. (1997) that the Offshore Indus Basin is underlain by pre-Tertiary oceanic crust, however, they disagreed with the postulation of Bhattacharya et al. (1994b) that the Laxmi Basin is underlain by oceanic crust. In view of such different opinions, the available sea-surface magnetic profiles were compiled and studied to understand and compare the crustal structure causing the magnetic anomalies in the Offshore Indus and Laxmi basins.

For this exercise, seventeen sea-surface magnetic profiles (Fig. 4.8) archived in the NGDC database and NIO database have been selected. These magnetic profiles have been presented as plot along track map (Fig. 4.9a, b) and

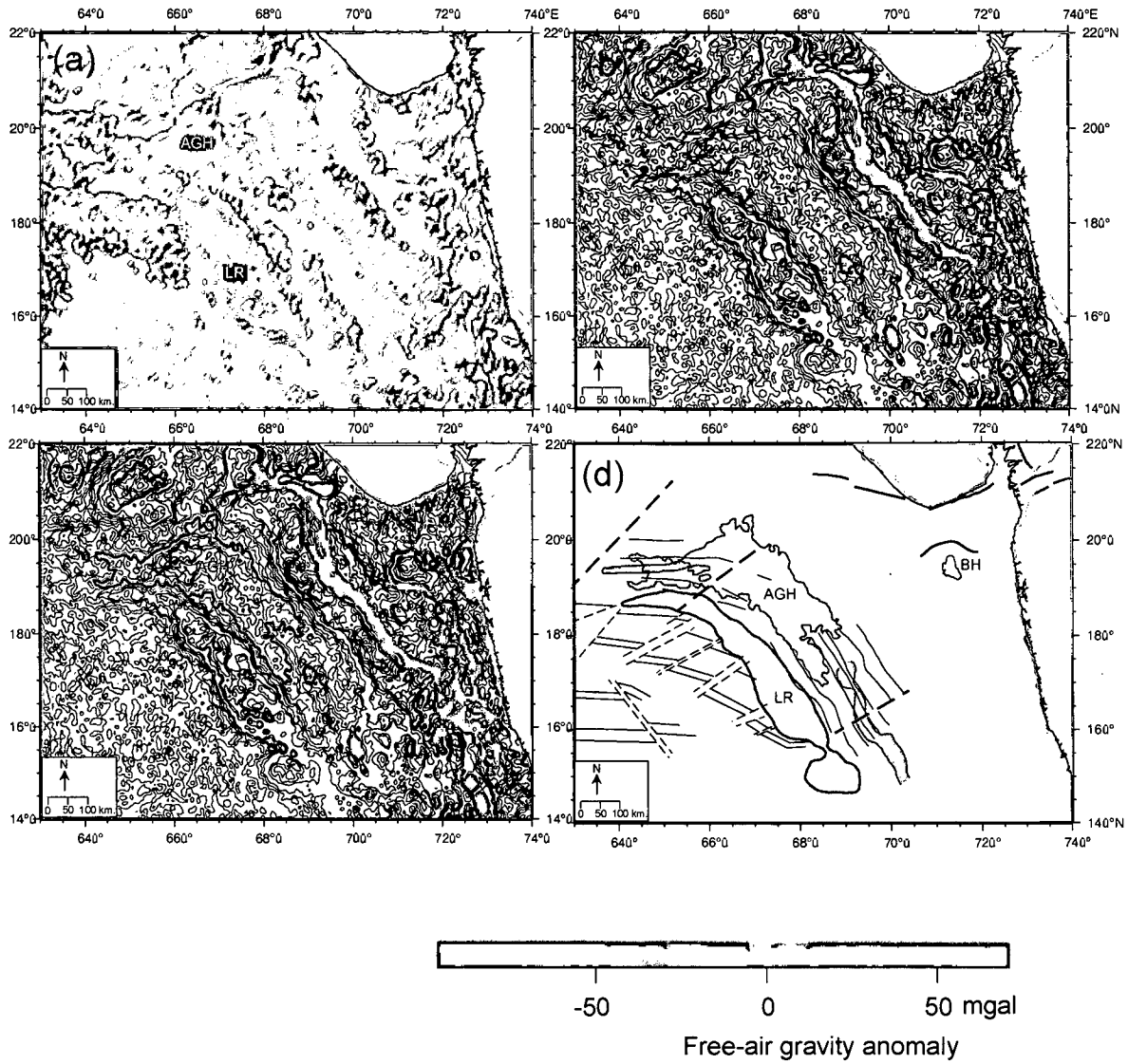

Fig. 4.7 The extent of the anomalous gravity high (AGH) zone northward of the Laxmi Ridge as deciphered from the satellite-derived free-air gravity anomalies. (a) AGH as reflected in the colour shaded-relief image of free-air gravity anomalies; (b) AGH as depicted by the free-air gravity anomaly contours of 5 mgal interval; (c) the extent of AGH (thick black line) as considered in this study to be defined by the steep slope of gravity contours and (d) the extent of the AGH (shaded yellow), along with the other tectonic elements in the adjoining regions. Other details are as in Fig. 4.1.

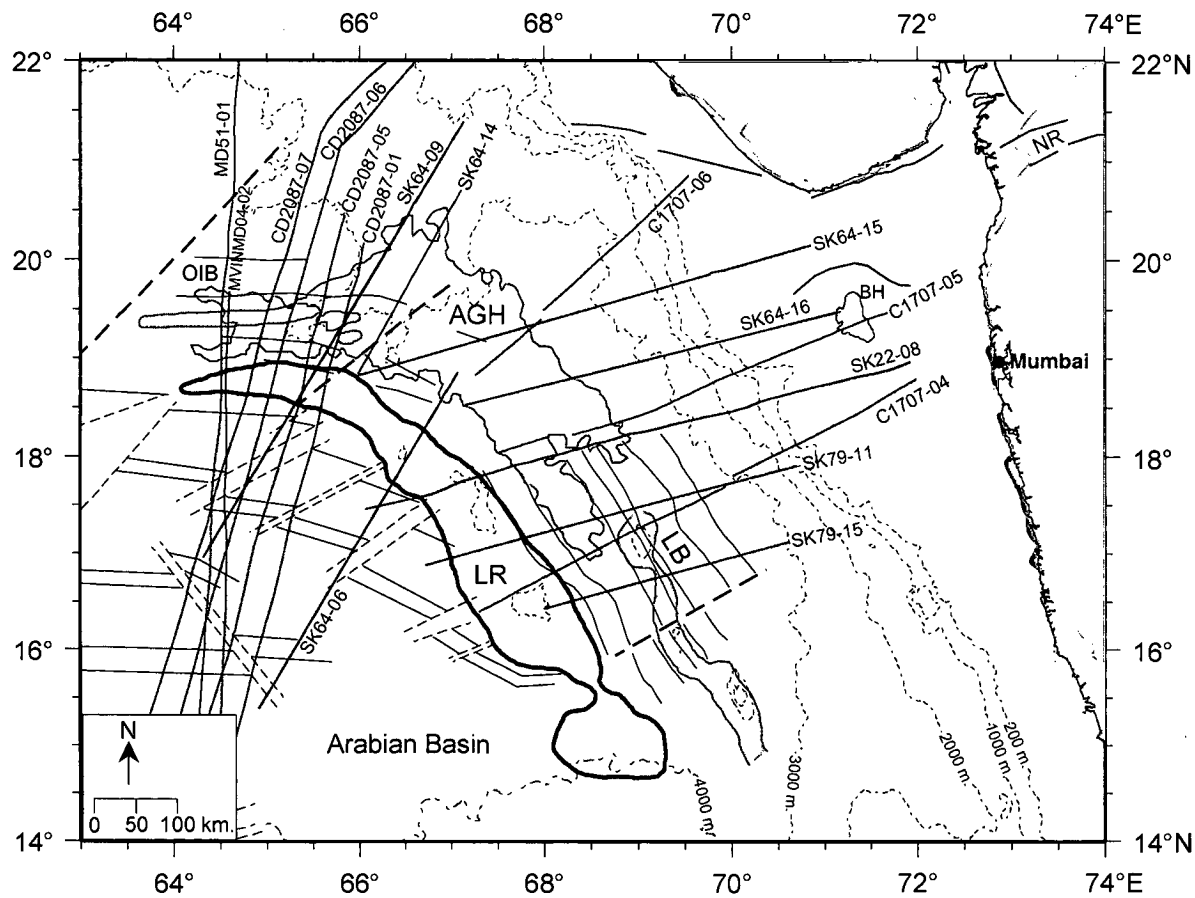

Fig. 4.8 Map showing locations of selected sea surface magnetic anomaly profiles across the Laxmi Basin and Offshore Indus Basin regions, which are stacked and presented in Fig. 4.10. Annotations along the tracks are profile identifiers. Other details are as in Fig. 4.1.

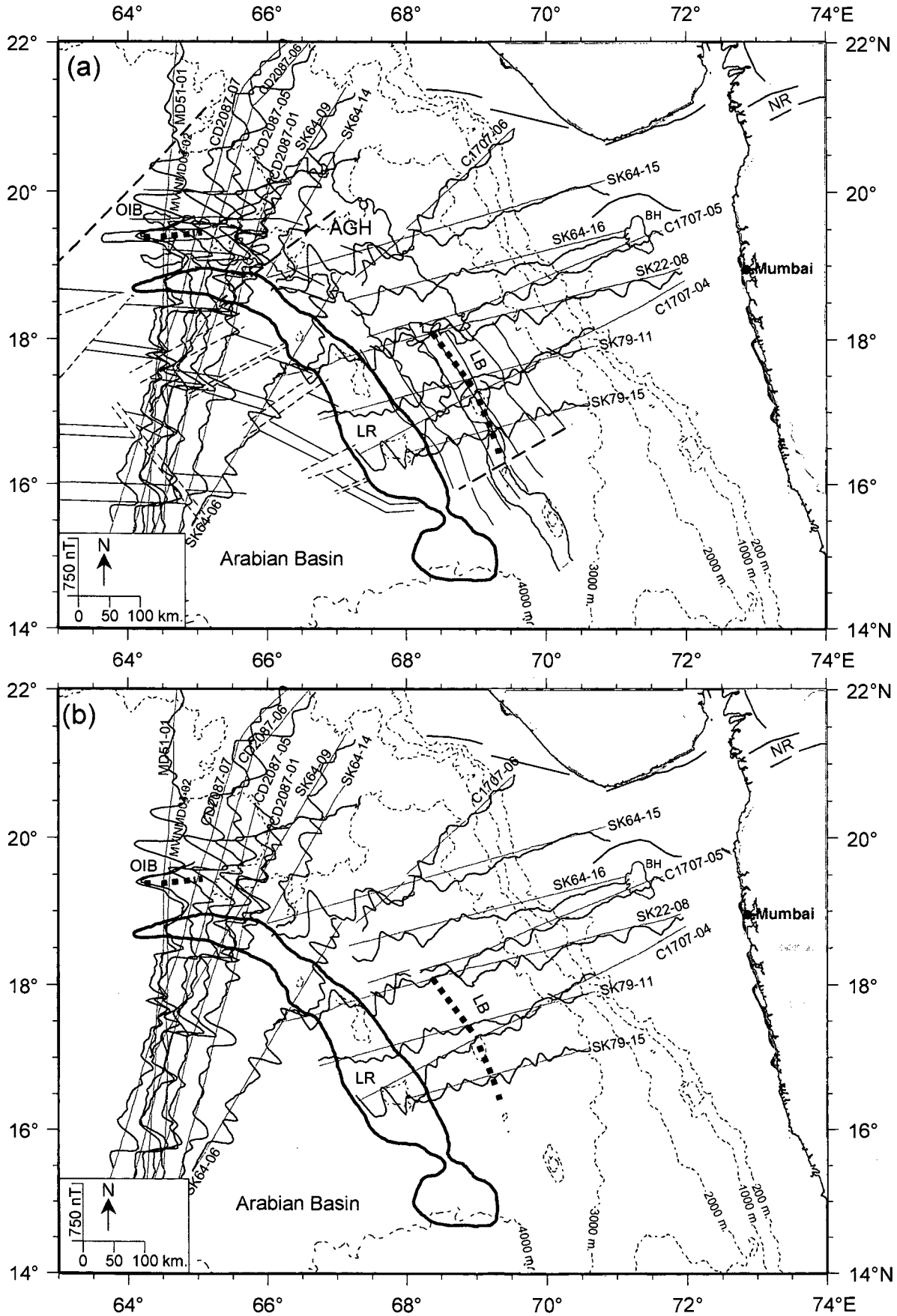

Fig. 4.9 Map showing the magnetic signatures in the Offshore Indus and Laxmi basins plotted perpendicular to ship's tracks. (a) along with major tectonic elements and selected bathymetry contours (b) along with the axis of the characteristic short wave length gravity low atop the broad gravity high of the Laxmi and Offshore Indus basins. Other details are as in Fig. 4.1 and Fig. 4.4.

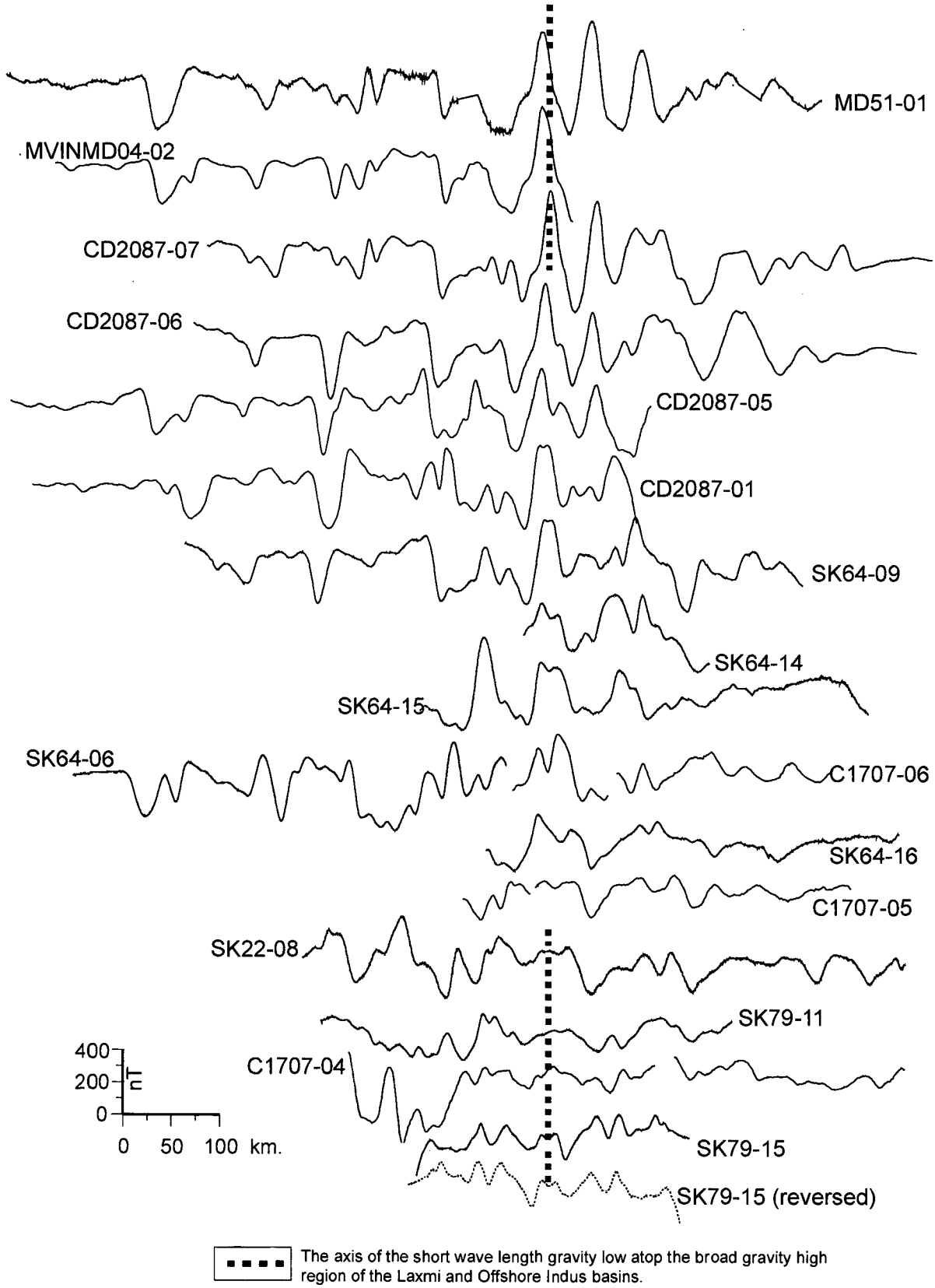

Fig. 4.10 Selected sea-surface magnetic profiles projected perpendicular to the strike of the inferred magnetic lineations and stacked with respect to the axis of the characteristic short wave length gravity low atop the broad wave length gravity high of the Offshore Indus and Laxmi basins. In the region where gravity low axis could not be traced, the profiles are stacked based on contiguity of prominent magnetic anomalies. Locations of these profiles are presented in Fig. 4.8.

as stacked profiles (Fig. 4.10). While stacking, the profiles were projected perpendicular to the strike of the inferred magnetic lineations and are aligned with respect to the axis of the characteristic short wave length gravity low atop the broad wavelength gravity high. As described earlier, the characteristic gravity low could not be traced between profiles SG-05 (the Offshore Indus Basin) and SK22-08 (the Laxmi Basin) due to the presence of an anomalous gravity high (AGH) zone. Therefore, the magnetic profiles located in this region have been aligned by considering the contiguity of the magnetic signatures along the profiles crossing with the characteristic gravity low axis.

It was observed that in the Laxmi Basin the sequence of positive and negative magnetic anomalies, flanking the axis of short wavelength gravity anomaly (along which the magnetic profiles are aligned), displays axial symmetry. As reported by Bhattacharya et al (1994b) this symmetry is particularly apparent (Fig. 4.10) from profile SK79-15 and SK79-15(reversed). In the Offshore Indus Basin area Malod et al. (1997) proposed such an axis of symmetry of magnetic anomalies; however, it was observed in the present study that the axis of symmetry proposed by them do not coincide with the axis of the characteristic short wave length gravity low or the location of Palitana Ridge.

d) Comparison of basement features and geophysical signatures

The gravity, magnetic and seismic information in the Offshore Indus and Laxmi basins and their association with the prominent basement features have been examined for their possible alikeness. Based on the seismic reflection and refraction information, it is clearly observed that both the basins show the presence of basement high features located approximately in the axial part of the basins. These axial basement high features parallel the trend of the adjacent segments of the Laxmi Ridge. These basement features in both the basins coincide with the axis of short wave length gravity low atop broad wavelength gravity high. These characteristic gravity lows merge with an intervening anomalous gravity high zone. The magnetic anomalies in both the basins reveal the presence of fairly correlatable linear and nearly parallel magnetic anomalies. In view of these observations, it appears that the crust underlying the Offshore Indus and Laxmi basins are similar in nature. Therefore, to infer the nature of the

crust underlying these regions, an integrated interpretation of these geophysical signatures was carried out.

4.3 Inference about the nature of crust underlying Offshore Indus and Laxmi basins

In this study, inference about the nature of the crust underlying the Offshore Indus and Laxmi basins have been made mainly based on crustal structure derived from forward modeling of gravity and magnetic anomalies. The gravity modeling was carried out following the procedure detailed in section 3.3.1. On obtaining a reasonable crustal configuration from gravity model, forward modeling of magnetic anomalies was carried out using the same crustal configuration. The magnetic anomalies are computed based on the procedure detailed in section 3.3.2.

a) Interpretation of gravity anomalies in the Offshore Indus Basin

To derive the crustal structure and density configuration in the Offshore Indus Basin and the adjoining regions, a ~500 km. long satellite derived free-air gravity profile (GCDH in Fig. 4.11a) that extend from the Arabian Basin to the continental rise off Pakistan has been used. This representative profile GCDH has been selected based on several consideration. First of all, this profile covers the well-correlatable magnetic lineations of the region. Secondly, over a part of this profile (segment CD) published latest seismic reflection results are available (Collier et al., 2004a, b) and refraction results are available (Collier et al., 2004b) over a nearby parallel profile RS (Fig. 4.11a).

As a first step for gravity modeling, an initial crustal model section (Fig. 4.11b) has been constructed by using the multichannel seismic reflection and seismic refraction results of Collier et al., (2004a, b). The seismic reflection results are more reliable for shallower regions (up to the basement), and seismic refraction results provide better information for deeper regions. Therefore while constructing this crustal section, shallower part was constrained from seismic reflection results and the deeper parts were constrained from seismic refraction results. To convert the depth to basement from the time to the depth units, an average velocity of 2.7 km/sec has been used for the sediments through out the profiles. This value was assumed following the empirical formula provided by

Malod et al (1997) for the Offshore Indus Basin and following the sediment velocity provided by Naini (1980) for the Arabian Basin. Since the velocity information from Collier et al. (2004a, b) is available only as analog velocity model section, therefore wherever available, the refraction information (Fig. 4.12a, b) of Naini and Talwani (1982) from the stations falling close to the gravity profile have also been considered while assigning the average interval velocities. In the Arabian Basin region, the velocity structure for a typical oceanic crust as provided by Naini and Talwani (1982) has been considered. While assigning the interval velocities for Laxmi Ridge region, the velocity information (Fig. 4.12a, b) from station L02V34 only has been considered, rather than using the velocities provided by Naini and Talwani (1982) for a generalized crustal structure of the Laxmi Ridge, as this station is over the Laxmi Ridge, it lies very close to the profile GCDH and refraction of Moho was obtained at this station. In the Offshore Indus Basin region, as such no refraction stations of Naini and Talwani (1982) provided information about the deeper crustal layers of the region. Therefore, only the refraction results of Collier et al. (2004b) have been considered for assigning the interval velocities for the layers. In the region of continental rise of Pakistan, the velocity structure of a typical continental crust has been assumed.

All the above mentioned assumed velocity information have been summarized as average crustal columns (Fig. 4.13a) and an initial crustal model (Fig. 4.13b) has been constructed using these average crustal columns. While constructing the crustal model the layer densities have been estimated based on the velocity-density relationship of Ludwig et al. (1970). Since the bathymetry and basement information are available only for CD segment of the profile GCDH, therefore in the gap areas (segments GC and DH), the bathymetry data have been extrapolated using the satellite derived topography data (Smith and Sandwell, 1997). In the gap areas the basement has been assumed to lie at the level of top of the layer with $\geq$ 5 km/sec velocity below the sedimentary layers. As seen from Fig. 4.11a, the gravity profile passes through four geological domains – the Arabian Basin, the Laxmi Ridge, the Offshore Indus Basin and the continental rise of Pakistan. In this initial crustal model, the probable lateral boundaries of each geological domain have been assumed mainly based on consideration of extent of different basement features and shapes of the gravity

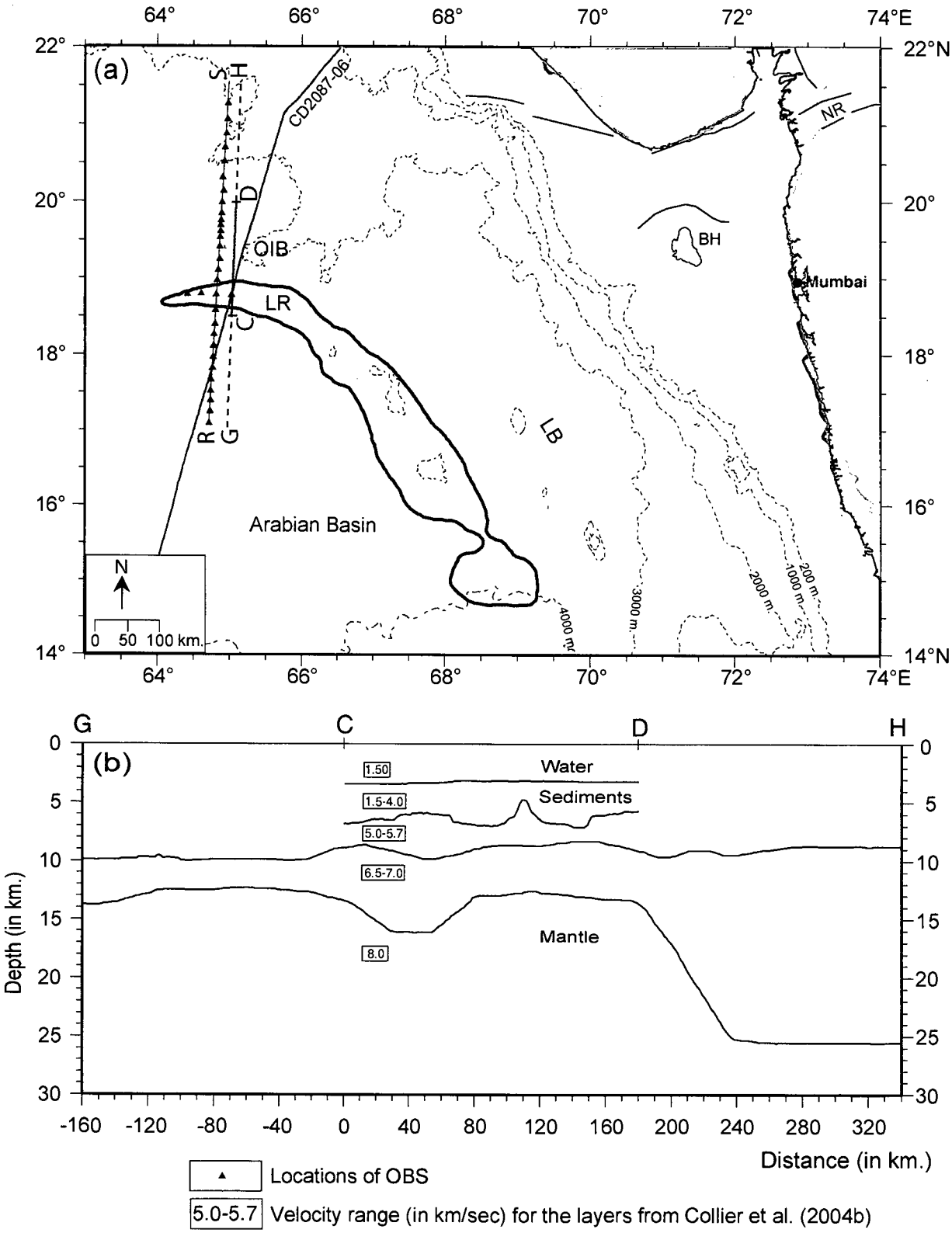

Fig. 4.11 Available seismic reflection, refraction (Collier et al., 2004a, b) and magnetic profiles from the Offshore Indus Basin close to the representative profile GCDH, which was used for inferring the nature of the underlying crust. (a) Locations of seismic refraction profile (RS), reflection profile (CD) and the nearest available magnetic profile (CD2087-06). (b) Seafloor and basement information from seismic reflection section CD and velocity-depth information projected onto profile GCDH from the results of refraction studies along profile RS. Other details are as in Fig. 4.1.

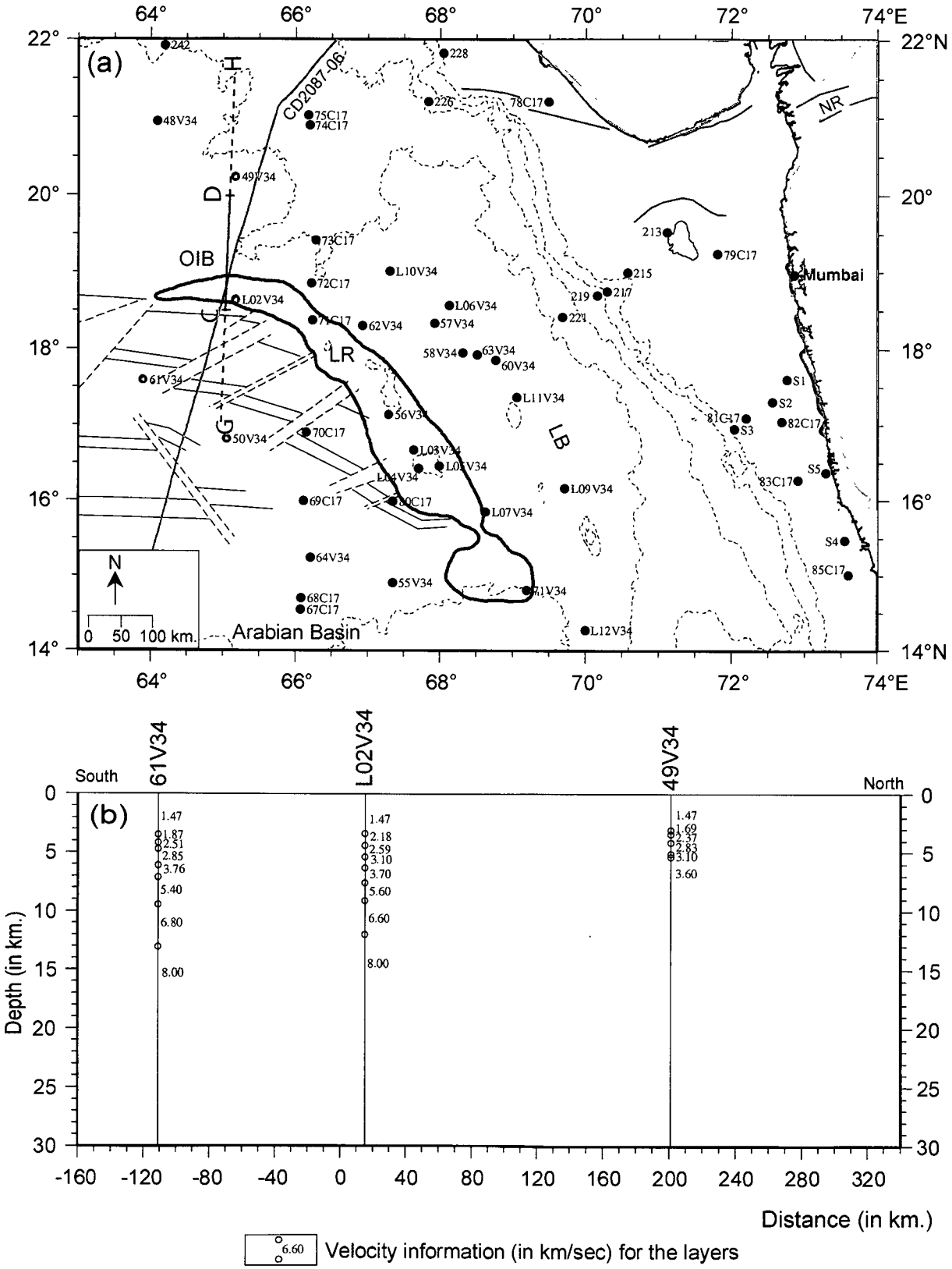

Fig. 4.12 The seismic refraction information in Offshore Indus Basin and the adjoining regions after Naini and Talwani (1982). (a) Locations of seismic refraction stations (solid black and red circles annotated with station ID) in and around the study area along with profiles used for gravity and magnetic modeling. (b) Velocity-Depth information along gravity profile GCDH, based on the seismic refraction information from the nearby stations shown as solid red circles. Other details are as in Fig. 4.1.

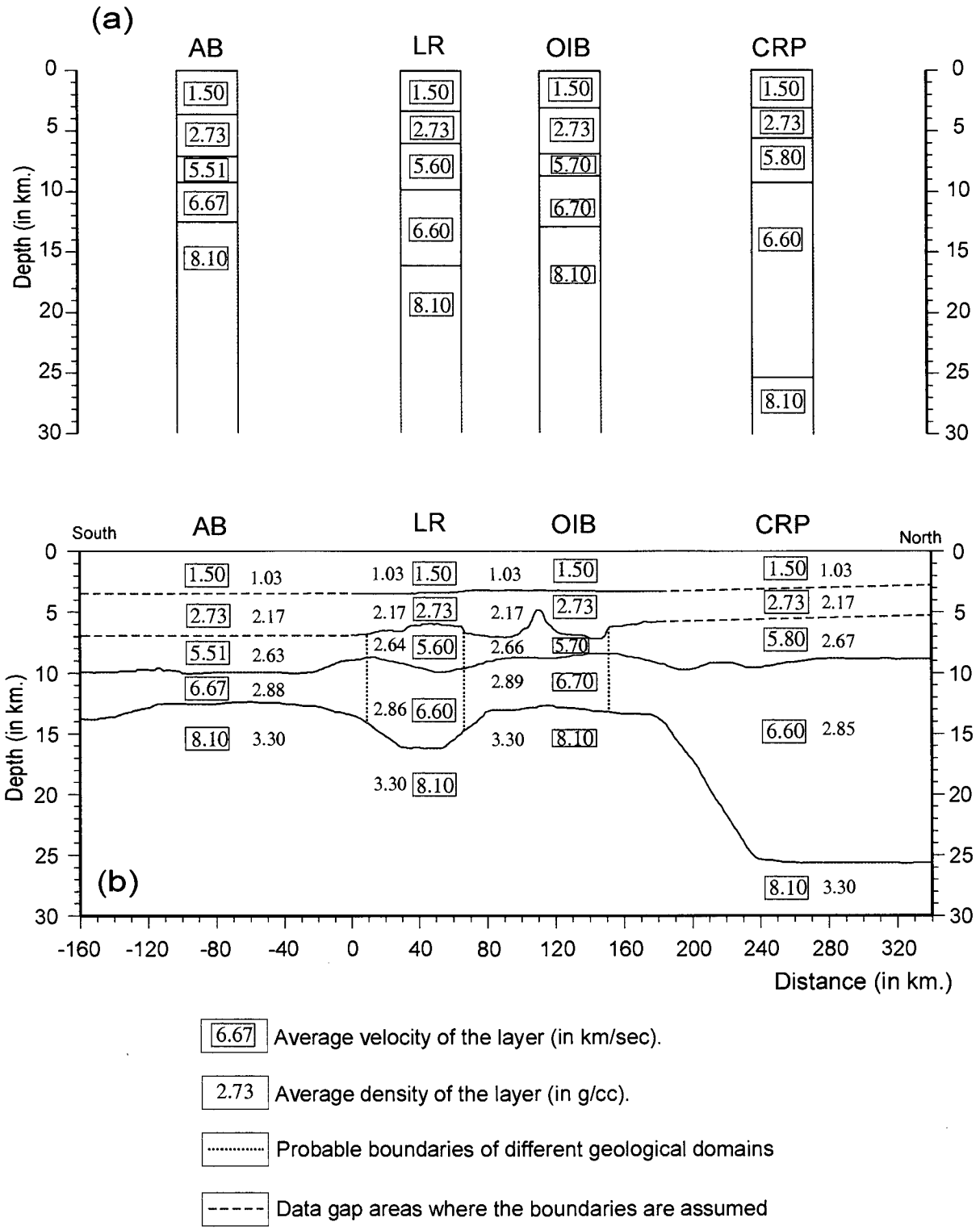

Fig. 4.13 The velocity-depth information along the profile GCDH that has been used for modeling the gravity data. (a) The average crustal columns representing the Arabian Basin (AB), Laxmi Ridge (LR), Offshore Indus Basin (OIB) and the continental rise of Pakistan (CRP). (b) The crustal structure section that has been used as the initial model while performing the gravity modeling.

anomalies. The initial crustal model was refined successively so as to obtain a reasonable good fit between the observed and computed anomalies. While refining the model, the relatively reliable constraints, such as the calculated densities of the layers, depth to seafloor and depth to basement configurations obtained from seismic reflection, have been kept unchanged, while the boundaries of the deeper crustal layers have been adjusted.

The derived crustal model (Fig. 4.14) suggests the presence of ~6 km thick crust below the sediments in the Arabian Basin region. This region consists of a two-layered crustal structure, where a 2.63 g/cc density upper crustal layer and a 2.88 g/cc density lower crustal layer, underlie the sediment layer of density 2.17 g/cc. The crust underlying this region of the Arabian Basin has already been established by many earlier studies as oceanic, which contain clearly identifiable magnetic lineations of seafloor spreading origin. Therefore these layers with density 2.63 g/cc and 2.88 g/cc can be considered as the layer 2 and layer 3 of the oceanic crust respectively. In the continental rise region off Pakistan, the crustal model suggests presence of ~14 km thick crust which increases in thickness landward. The assumed layer densities in this region are consistent with the upper and lower continental crusts, however the thickness ~14 km of this region is much less as compared to the thickness of about 30 km for the adjacent continental crust region. It is inferred that this crust underlying the continental rise region off Pakistan is underlain by thinned continental crust.

The derived crustal model suggest that the Laxmi Ridge region along this profile consists of a two-layered crustal structure, where a 2.64 g/cc density upper layer and a 2.86 g/cc density lower layer, underlie approximately 2.5 km thick layer of sediments. These density configurations appear to be consistent with the upper and lower continental crustal layers, which is isostatically balanced by deepening of Moho to a depth of 17 km. The total thickness of the crust underlying the Laxmi Ridge is ~11 km. Based on these inferences about the thickness and density configuration the Laxmi Ridge appear to represent a region of thinned continental crust.

The derived crustal model (Fig. 4.14) in the Offshore Indus Basin region suggests that the region can be considered to consist of a ~6 km thick two-layered crustal structure, where a 2.66 g/cc density upper layer and a 2.89 g/cc

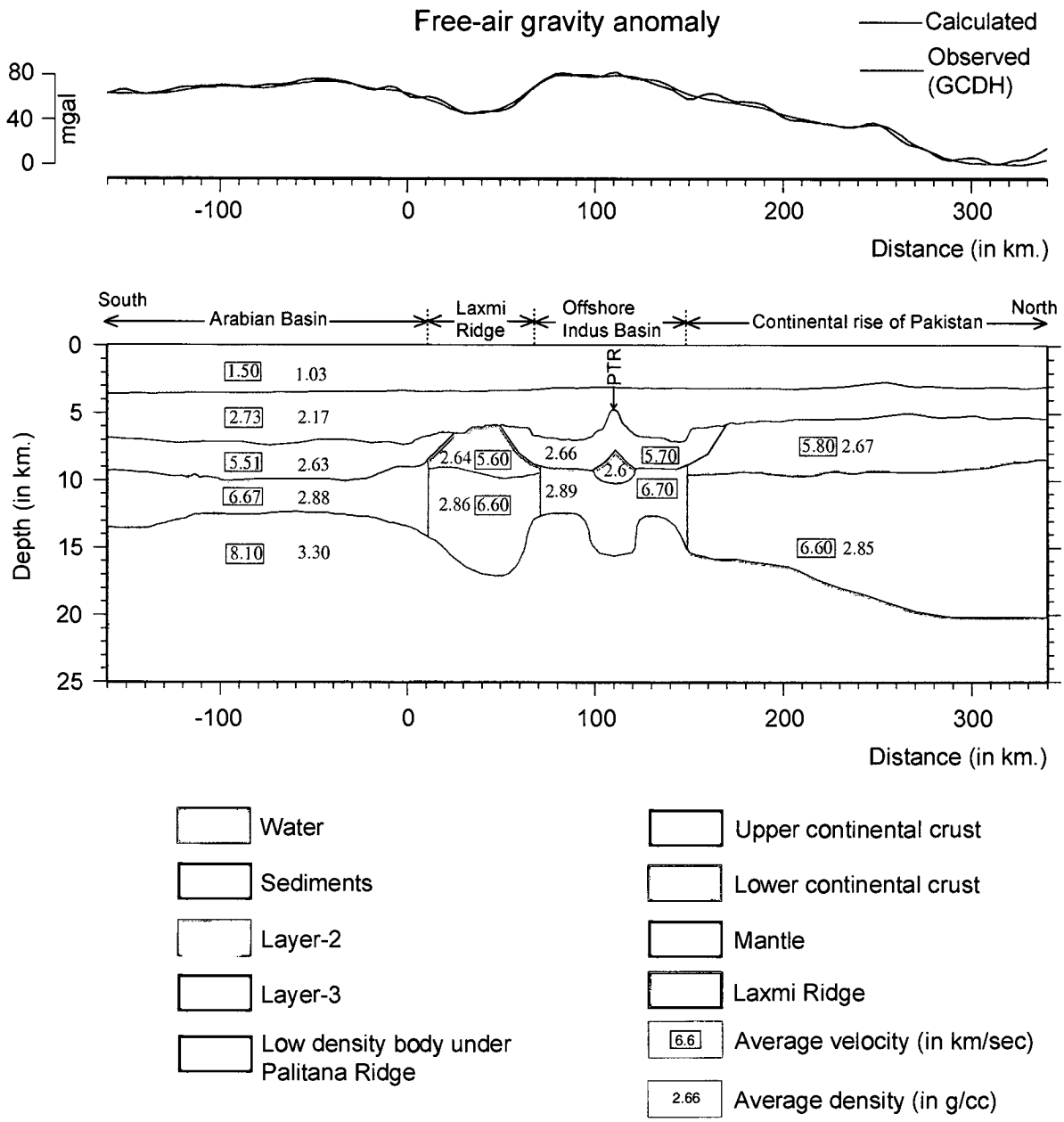

Fig. 4.14 Derived crustal structure across the Arabian Basin, Laxmi Ridge, Offshore Indus Basin and the continental rise of Pakistan based on forward modeling of gravity profile GCDH. The location of profile GCDH has been shown in Fig. 4.11. PTR: Palitana Ridge.

density lower layer, underlie approximately ~3.5 km thick layer of sediments. Interestingly, it is observed that except below the Palitana Ridge, the general depth to Moho in the Offshore Indus Basin region, almost is in the same level as that of the Arabian Basin. It appears that the density configurations, thickness of the crust as well as the similarity in Moho depth make the Offshore Indus Basin region comparable with the crustal configuration of the Arabian Basin, which is oceanic in nature. In that case the basement layer of the Offshore Indus Basin with density 2.66 g/cc and velocity 5.70 km/sec, can be equated to layer 2 of the oceanic crust. In the seismic refraction section of Collier et al. (2004b), a flat Moho has been depicted throughout the Offshore Indus Basin; however, the gravity modeling carried out in this study necessitated the Palitana Ridge region to be compensated by a deepening (~16 km) of Moho. This compensated structure was necessary to be introduced in order to explain the characteristic short wave length gravity low atop a broad wave length gravity high, which is associated with the Palitana Ridge region. Further, for better match with the observed gravity anomalies it became necessary also to introduce, just below the Palitana Ridge, a low-density body of density 2.6 g/cc beneath the layer of density 2.66 g/cc. As will be shown later, the Offshore Indus Basin region have been inferred to be underlain by an oceanic crust, where the Palitana Ridge is interpreted as an extinct spreading centre. In that case, existence of a low density body below the Palitana Ridge does not appear unreasonable as presence of similar solid low density body under an extinct spreading centre has been postulated by Jonas et al. (1991) to explain the observed gravity anomalies over extinct spreading centres. The gravity model suggests that under the Palitana Ridge the layer with density 2.66 g/cc rise upward. Considering this layer as layer 2 of the oceanic crust, such an upward rise do not appear to be uncommon as the recent seismic reflection studies carried out by Singh et al. (2006) over a segment of Mid-Atlantic Ridge clearly indicated upward rising of the base of Layer 2A towards the axis of the spreading centre. The derived crustal model further shows that a part of the basement layer (2.66 g/cc density layer) in the Offshore Indus Basin continues and falls over the inferred basinward edges of the continental crust over the Laxmi Ridge and the continental rise of Pakistan. As will be shown later, such an interpretation is necessary while carrying out the forward modeling of magnetic data and its integration with the gravity

interpretation. These regions may represent volcanics emplaced during the formation of 'Initial oceanic crust' as inferred in other continental margins by several researchers (Mutter et al., 1982; Talwani and Abreau, 2000). In view of all the above observations, it is tempted to believe that the Offshore Indus Basin region, in general can be considered to be underlain by an oceanic crust. However, to establish this inference, interpretation of magnetic data has been integrated with the gravity interpretation derived crustal structure.

(b) Interpretation of magnetic anomalies in the Offshore Indus Basin

If the Offshore Indus Basin region is underlain by an oceanic crust, then the magnetic anomalies along or close to this profile in the Offshore Indus Basin region should also be possible to be explained using the same crustal configuration derived from forward modeling of gravity data. As evidenced from the various seismic refraction studies, the ~6-7 km thick oceanic crust consists of two layers; viz. layer 2 and layer 3. The layer 2 consists of highly magnetic basalt flows where as the underlying layer 3 consist of weakly magnetic gabbroic oceanic crust. As a result, in general, the layer 2 has been considered as the major source of the seafloor spreading magnetic anomalies (Cox and Hart, 1986; Banerjee, 1984). Therefore, attempt has been made to examine the possibility of an oceanic nature of the crust underlying Offshore Indus Basin, based on forward modeling of magnetic anomalies. While carrying out modeling of magnetic data, the magnetic anomalies are considered to have been caused by juxtaposed blocks of normally and reversely magnetized crust, which lie within the layer 2 of the oceanic crust inferred from gravity model.

The magnetic parameters, which influence the shape and amplitude of the magnetic anomalies are the thickness of the magnetized layer, its susceptibility, the depth to the top of the magnetized layer, present location and strike of the magnetic bodies, paleo-location at the time of formation and the width of each normally and reversely magnetized blocks. Among these parameters, the thickness and the depth to the top of the magnetized layer have been defined by limits of the inferred layer-2 derived from gravity modeling. The synthetic magnetic anomalies are computed for a set of E-W striking juxtaposed normally and reversely magnetized blocks, presently observed at 20°N, 65°E (Fig. 4.15a). As it will be shown later, the central block is considered to correspond to anomaly

27n (~61 Ma) of geomagnetic polarity reversal timescale. Therefore, to obtain the paleo-location at the time of formation of this oceanic crust, a paleogeographic reconstruction of the region (Fig. 4.15b) has been carried out for 61 Ma in fixed hotspot reference frame using the finite rotation parameters of Müller et al. (1993). This model suggested that the Offshore Indus Basin area was in the southern hemisphere, near 11°S, 51°E, at the time of formation. The boundaries of the adjacent normally and reversely magnetized blocks have been defined in such a way that the computed synthetic magnetic anomalies give the best fit with the observed magnetic anomalies. For comparison of synthetic magnetic anomalies (Fig. 4.16) the projected profile CD2087-06 have been taken as the observed profile even though Collier et al. (2004b) in their paper have provided the plot of magnetic anomalies along profile CD. The reasons for not considering that profile are the following. First of all, the digital data for this profile are not available in public domain. Secondly, a comparison with two magnetic profiles CD2087-06 and CD 2087-07, located very close to profile CD, strongly suggested some inconsistency in the published magnetic profile of Collier et al. (2004b). Lastly, the profile CD2087-06 is of much longer extent and digital data along this profile is available from the NGDC database.

The magnetic modeling exercise (Fig. 4.16) shows that the observed magnetic anomalies along the profile in the Offshore Indus Basin can be considered to have been caused by juxtaposed normally and reversely magnetized blocks, which lie within the basement layer. The sequence of these magnetized blocks appear to be symmetrical about a central narrow normally magnetized block, where the axis of symmetry of the magnetized blocks coincides with the characteristic short wavelength gravity low atop a broad wavelength gravity high and the basement high feature of the Palitana Ridge. As discussed earlier, the basement layer (i.e. the layer with density 2.66 g/cc and velocity 5.70 km/sec) of the offshore Indus Basin can be equated to layer 2 of the oceanic crust. The parallel nature of the magnetic lineations and the symmetric arrangement of the magnetized blocks within the basement layer (inferred as layer 2 of the oceanic crust) support generation of the underlying crust by a two-limbed seafloor spreading. The continuation of magnetic anomalies (thereby magnetic bodies) a short distance over the Laxmi Ridge and basement of

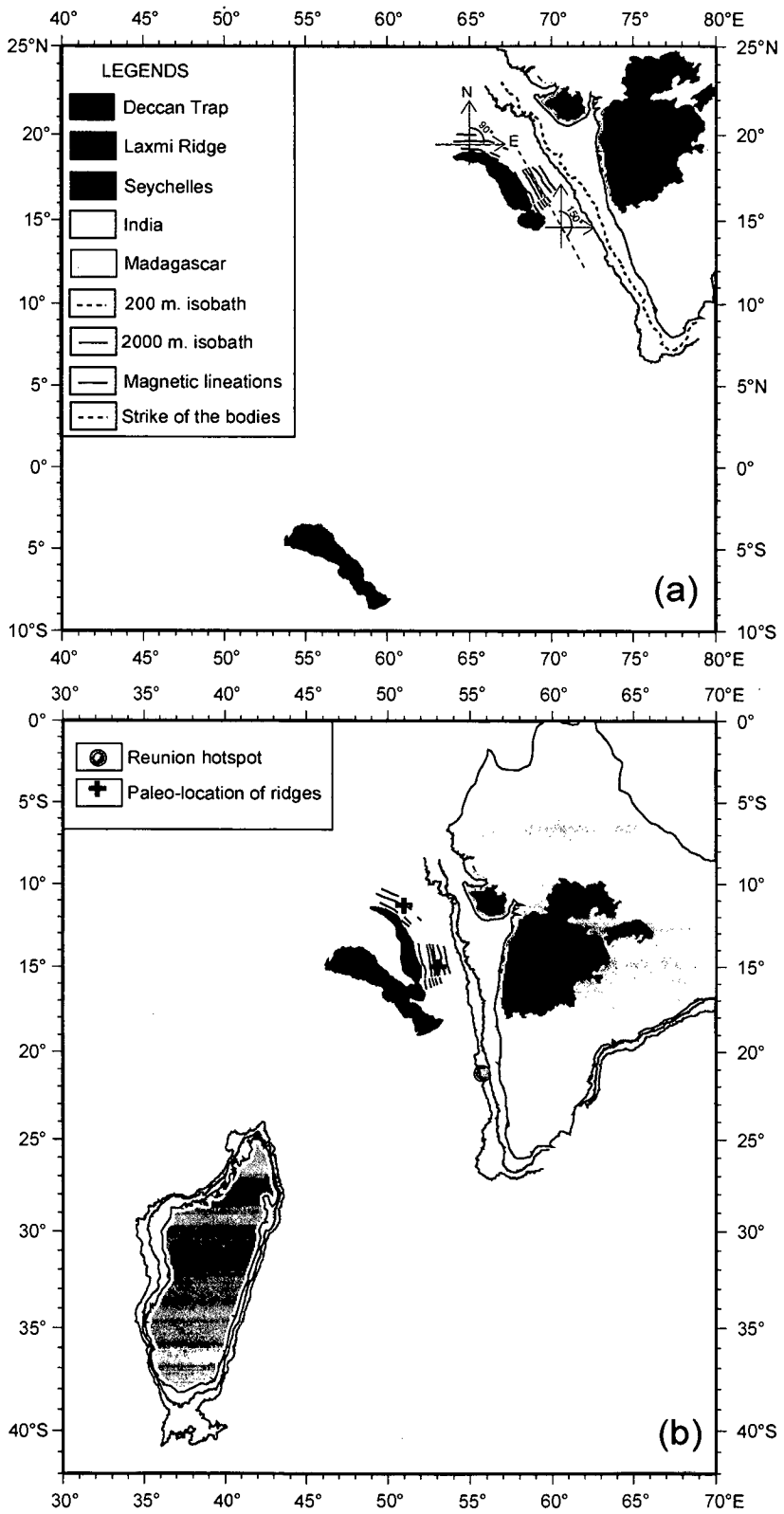

Fig. 4.15 Maps showing the locations and strike directions of the inferred paleo-spreading in the Offshore Indus and Laxmi basins as used for computation of synthetic magnetic anomalies. (a) Present location and strike of the ridges (b) Paleo-location of the ridges at anomaly 27n (61 Ma) time, as described by the finite rotation parameters of Müller et al. (1993) in fixed hotspot reference frame.

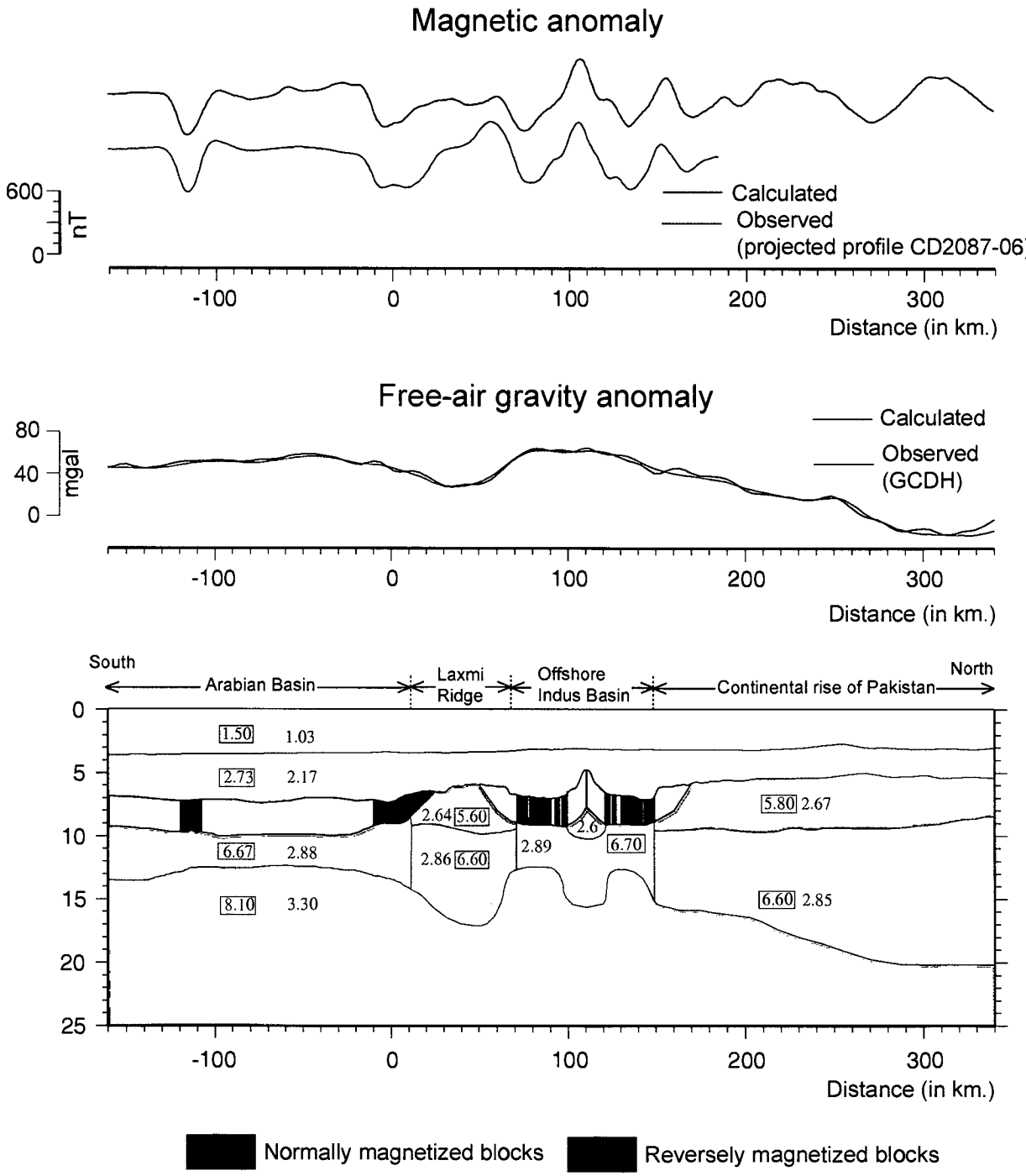

Fig. 4.16 Crustal structure along profile GCDH derived from integrated gravity and magnetic modeling. The forward modeling of the magnetic data shows that the magnetic anomalies in the Arabian Basin and Offshore Indus Basin can be explained in terms of juxtaposed normally and reversely magnetized blocks (susceptibility=0.01 cgs units) within the layer 2 derived by the gravity modeling. Synthetic magnetic profiles are computed for a ridge presently striking N90°E and obvserved at 20°N, 65°E which was formed at the location 11°S, 51°E. The computed magnetic anomalies are compared with the observed magnetic profile CD2087-06 (projected to an azimuth of 0°), which is located close to the gravity profile GCDH . The locations of the profiles have been shown in Fig. 4.11, other details are as in Fig. 4.14.

Pakistan continental rise perhaps represents the initial oceanic crust. In view of the above evidences from the gravity, magnetic and seismic information, it is interpreted that part of the Offshore Indus Basin, where the magnetic lineations have been mapped, is underlain by oceanic crust formed as a result of two-limbed seafloor spreading between Laxmi Ridge and continental rise of Pakistan and the axial basement high region (Palitana Ridge) represents the extinct spreading centre. It may be mentioned here that, earlier Malod et al. (1997) also reported existence of two-limbed seafloor spreading type magnetic anomalies in the Offshore Indus Basin region and thereby inferred an oceanic nature of the underlying crust. The interpretation of magnetic anomalies in the present study agrees with the inference of Malod et al. (1997) in one sense that the Offshore Indus Basin region is formed a two-limbed seafloor spreading, but differs on few important aspects. Firstly, the location of the axis of symmetry and thereby the location of the extinct spreading center is interpreted in this study at a location different than of Malod et al (1997). Secondly, the Palitana Ridge, which coincides with the axis of symmetry inferred in this study have been interpreted to represent the extinct spreading center, whereas Malod et al. (1997) considered the Palitana Ridge as an uplifted basement feature related to Miocene reactivation. Thirdly, as will be shown in a later section, the identification of the magnetic anomalies of the present study also differs from that of Malod et al. (1997).

(c) Interpretation of gravity anomalies in the Laxmi Basin

To derive the crustal structure and density configuration in the Laxmi Basin and the adjoining regions, an ~850 km long satellite derived free-air gravity profile RE-02(SG), that crosses the Arabian Basin, Laxmi Ridge, Laxmi Basin and the western continental shelf of India has been used (Fig. 4.17a). This profile has been selected since a recently published (Krishna et al., 2006) seismic reflection section RE-02 is available along this profile as a whole, and the location of the magnetic profile SK79-15 in the Laxmi Basin, which very clearly show the symmetric nature of the magnetic anomalies, is nearly coincident over large part of this profile.

As a first step, an crustal section (Fig. 4.17b) has been constructed by using the interpreted line drawings of the multichannel seismic reflection section

presented in Krishna et al. (2006) and seismic refraction results of Naini and Talwani (1982). As done in the case of Offshore Indus Basin region, shallower and deeper layers of this crustal section have been constrained from the seismic reflection and refraction results respectively. To convert the basement from the time section to the depth section, a velocity of 2.7 km/sec has been used for the sediments throughout the profile. The average interval velocities for all the layers in each geological domain have been estimated based on the interval velocity information of Naini and Talwani (1982). In the Arabian Basin region, the velocity structure for a typical oceanic crust as provided by Naini and Talwani (1982) has been considered. In the region of continental shelf of India, the velocity structure of a typical continental crust has been assigned. In the Laxmi Basin region, no sonobuoy refraction stations of Naini and Talwani (1982) provided information about the Moho depth. Their inference about the depth to the Moho under the Laxmi Ridge and Laxmi Basin regions were based on estimation of minimum depth to the Moho assuming a mantle velocity of 8.2 km/sec. Subsequent researchers, while performing gravity modeling, used that estimate of minimum depth to the Moho and a generalized regional average for the depth to other layers in the Laxmi Basin. Instead of such generalization, which appears to be less reasonable due to the structural complexity of the region, in the present study the seismic refraction information from only those stations have been used which are closer to profile RE-02(SG).

The most recent available seismic refraction results of Collier et al. (2004b) in the Offshore Indus Basin, which forms a part of the Eastern Basin of Naini and Talwani (1982), interestingly show that the depth to the Moho in the Arabian Basin and Offshore Indus Basin are almost in the same level. Therefore, in absence of well-constrained depth to the Moho information in the Laxmi Basin area, while constructing the initial crustal model the depth to the Moho has been assumed to lie in the same level as that in the adjacent Arabian Basin. This assumption was made considering the similarities of the Laxmi Basin and the Offshore Indus Basin in terms of basement features and geophysical signatures.

All the assumed velocity information has been summarized as average crustal columns (Fig. 4.18a) and initial crustal model (Fig. 4.18b) has been constructed using the above-mentioned average crustal columns. While

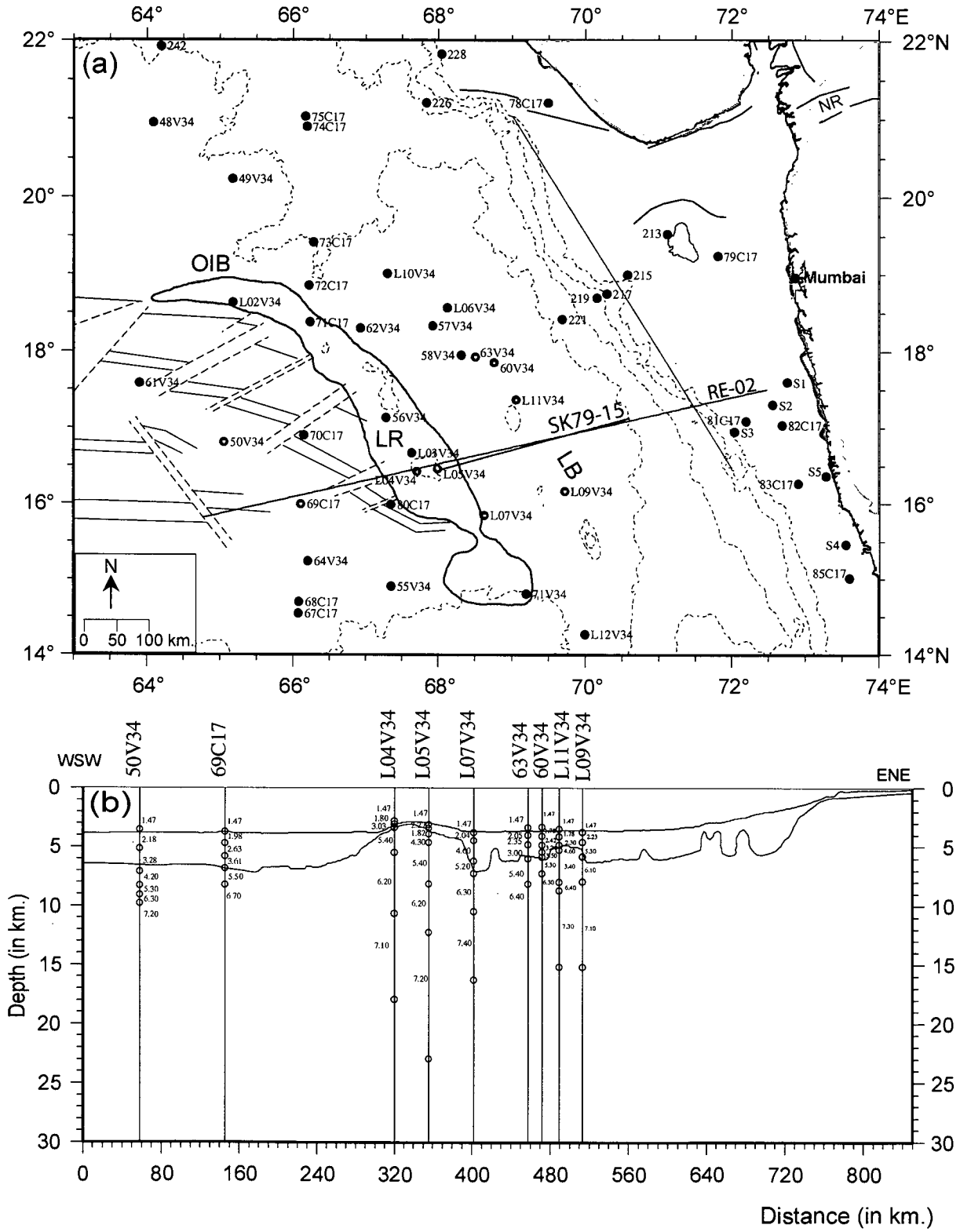

Fig. 4.17 The available seismic reflection and refraction information in the Laxmi Basin and the adjoining regions. (a) Locations of seismic refraction stations (after Naini and Talwani,1982) shown as red and black solid circles annotated with station ID, seismic reflection profile (RE-02 of Krishna et al., 2006). (b) The Velocity-Depth information along profile RE-02, based on the seismic refraction results from nearby refraction stations. Gravity data along profile RE-02 and magnetic data along nearly coincident profile SK79-15 have been used for modeling. Other details are as in Fig. 4.1.

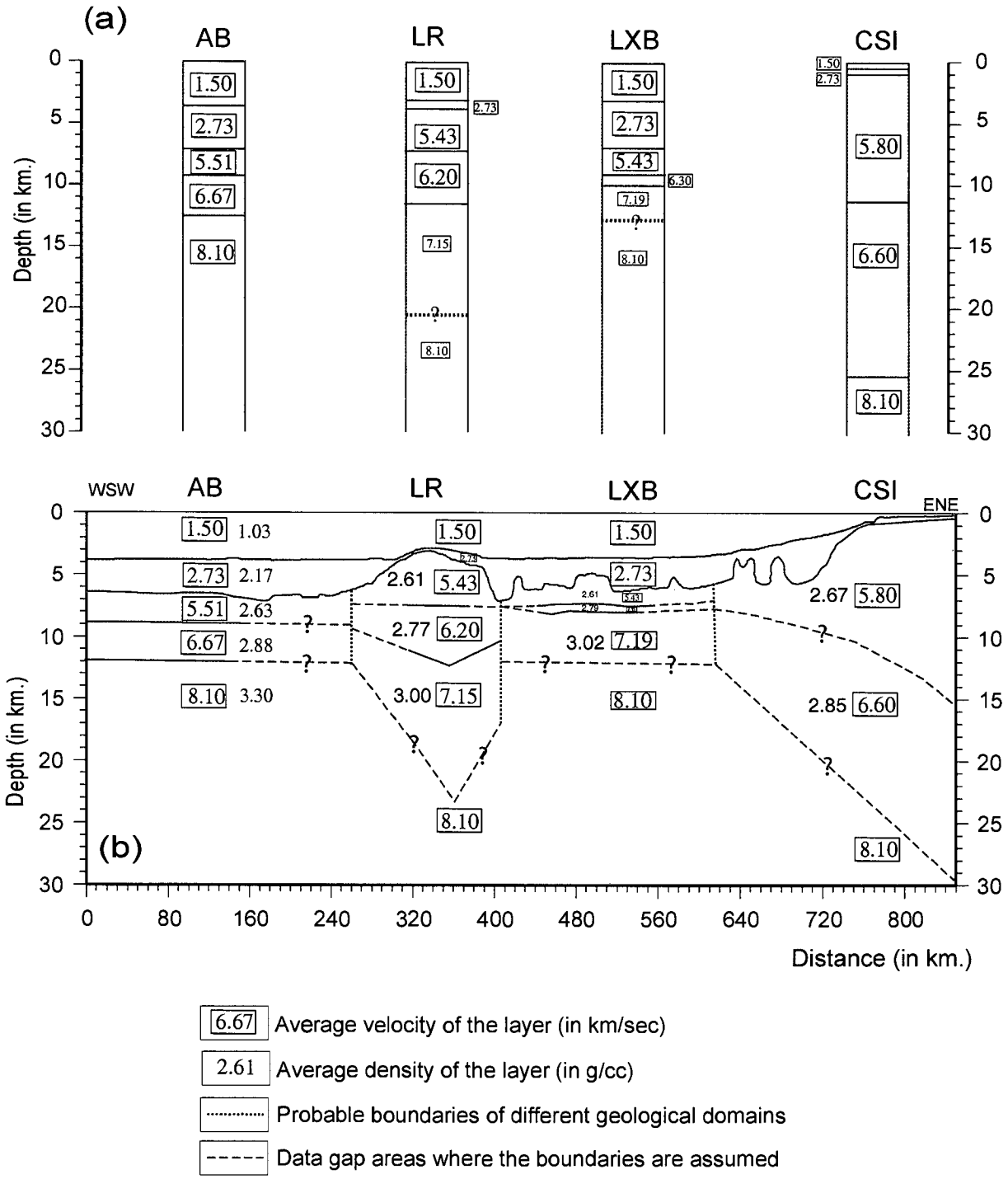

Fig. 4.18 The velocity-depth information along the profile RE-02, which has been used for modeling gravity data. a) The average crustal columns representing the Arabian Basin (AB), Laxmi Ridge (LR), Laxmi Basin (LXB) and the continental shelf of India (CSI). b) The crustal structure section that has been used as the initial model while performing the gravity modeling.

constructing the initial crustal model, the layer densities have been estimated using the velocity-density relationship of Ludwig et al. (1970). In this initial crustal model, the probable lateral boundaries of each geological domain have been assumed mainly based on consideration of extent of different basement features and shapes of the gravity anomalies. The initial crustal model was refined successively so as to obtain a reasonable good fit between the observed and computed anomalies. While refining the model, the relatively reliable constraints such as the calculated densities of the layers, depth to seafloor and depth to basement obtained from seismic reflection have been kept unchanged, while only the boundaries of the deeper crustal layers have been adjusted in order to obtain a fit between the observed and computed gravity anomalies. This approach has resulted in increasing the general depth to the Moho in the Laxmi Basin area. Further, while modeling, it was noticed that good fit between the observed and computed anomalies required consideration of few prominent short wave length observed anomalies too. Since short wavelength gravity anomalies have their origin in the shallower layers, therefore, at places slight refinement of the shallower layers became necessary. Examination of the interpreted line drawing of the basement and its comparison with the time section presented by Krishna et al. (2006), suggested scope to refine the depth to basement at places. In view of this, the inferred basement has been slightly refined at few places to obtain a better fit of the computed gravity anomalies with the observed gravity anomalies.

The derived crustal model (Fig. 4.19) suggests that the Arabian Basin region can be considered to consist of a ~5 km thick two-layered crustal structure, where a 2.63 g/cc density upper layer and a 2.88 g/cc density lower layer underlie the sediments. As mentioned earlier these layers with density 2.63 g/cc and 2.88 g/cc can be considered as the layer 2 and layer 3 of the oceanic crust respectively. The continental shelf/slope/rise region of India shows a two-layered crustal structure, where a layer of density 2.67 g/cc overlies a layer of density 2.85 g/cc. These layers with density configurations typical of upper and lower continental crust, are isostatically compensated at deeper levels with the landward increase in the Moho depth. In this region (between 630 – 670 km mark in Fig. 4.19), the interpreted line drawing of the basement shows two isolated peaks, which Krishna et al. (2006) have interpreted as volcanic intrusions.

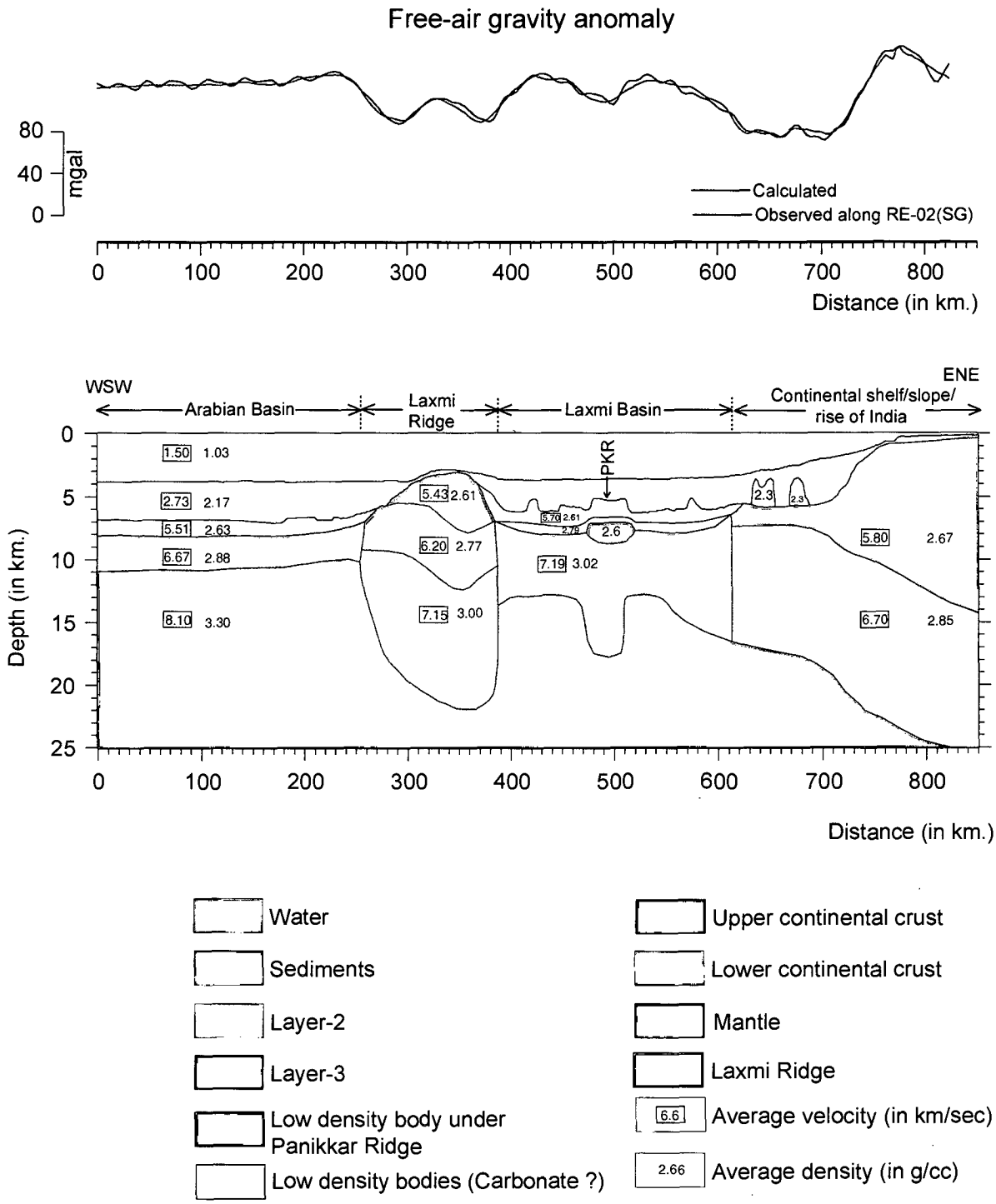

Fig. 4.19 Derived crustal structure across the Arabian Basin, Laxmi Ridge, Laxmi Basin and the western continental shelf of India based on forward modeling of the gravity profile RE-02(SG). The location of profile RE-02 has been shown in Fig. 4.17. PKR: Panikkar Ridge.

Although both these peaks are of nearly equal dimension, still only one of them appears to be associated with a short wavelength gravity anomaly. If the presence of these two features is true, then the gravity modeling carried out in this study necessitates these two bodies to be explained as low-density features with a density of 2.3 g/cc. In such a situation, it appears that these features cannot be interpreted as the volcanic intrusives as inferred by Krishna et al. (2006), because the volcanic intrusive bodies are usually of higher density than the surrounding continental crust. Probably, these features of lower density represent carbonate growth features over thinned continental crust, which later got buried under the sediments. The gravity model shows that the Laxmi Ridge can be represented as a distinct structural high underlain by a three-layered crustal structure under thin (~0.5 km) veneer of sediments. The three-layered crust of the Laxmi Ridge consists of an upper 2.61 g/cc density layer, middle 2.77 g/cc density layer and lower 3.00 g/cc density layer. The layer with density 3.00 g/cc can be considered as the middle-lower crust and the layer with density 2.61 g/cc as the upper continental crust. The layer of 2.77 g/cc probably represents the upper continental crust in which the rift related magmatic materials were emplaced. This increase in average density of the layer may be due to the presence of higher density volcanic material emplaced in the layer of 2.61 g/cc density. It appears that the density configurations is consistent with the layers of continental crust, which is isostatically compensated by a ~22 km deep Moho and the total thickness of the crust underlying the Laxmi Ridge is only about 19 km. Based on these inferences about the thickness, density configuration and its characteristic negative free-air gravity signature, the Laxmi Ridge appears to be underlain by a thinned continental crust as was inferred in several earlier studies.

The gravity modeling derived crustal structure (Fig. 4.19) of the Laxmi Basin region suggest that except below the Panikkar Ridge, the general depth to the Moho in this region is ~13 km and the total thickness of the crust under the Laxmi Basin region is ~7 km. The gravity model suggests that the Laxmi Basin area consists of a three-layered crustal structure under ~3.0 km thick sediment layer. The three-layered crust of the Laxmi Ridge consists of an upper 2.61 g/cc density layer, middle 2.79 g/cc layer and lower 3.02 g/cc layer. The densities of these layers are close to the densities of the layers of Laxmi Ridge, but the layer

thicknesses vary considerably between the crusts of the Laxmi Ridge and the Laxmi Basin. In the Laxmi Basin region, the thickness of each layers are much less than that of Laxmi Ridge region. As seen from the crustal configuration, the total thickness of the crust in the Laxmi Ridge is ~19 km, whereas that in the Laxmi Basin is only ~7 km. These layers with densities 2.61 g/cc, 2.79 g/cc and 3.02 g/cc can be considered to represent the layers 2A, 2B and 3 of oceanic crust.

The gravity modeling carried out in this study also necessitated the axial basement high region in the Laxmi Basin to be isostatically compensated by a deepening (~18 km) of Moho. This compensated structure was necessary to be introduced in order to explain the characteristic short wave length gravity low atop a broad wave length gravity high, which is associated with the axial basement high region in the Laxmi Basin. Further, for better match with the observed gravity anomalies, it appears to be necessary to introduce, just below the Panikkar Ridge, a low density body of 2.6 g/cc beneath the layer of density 2.79 g/cc. The inferred layer 2 of the oceanic crust under the axial basement high appears to rise up towards the centre of the axial basement high as in the case of Palitana Ridge. The derived crustal model further shows that a part of the basement layer (2.61 g/cc density layer) in the Laxmi Basin continues and falls over the inferred basinward edges of the continental crust over the Laxmi Ridge and the continental rise of India. As will be shown later, such an interpretation is necessary while carrying out the forward modeling of magnetic data and its integration with the gravity interpretation. This situation is similar to the situation modeled in the Offshore Indus Basin and thus similarly inferred to represent volcanics emplaced during the formation of 'Initial oceanic crust'

(d) Interpretation of magnetic anomalies in the Laxmi Basin

The interpretation of the gravity anomalies suggests that the Laxmi Basin region can be considered to be underlain by an oceanic crust. If this inference is correct, then the magnetic anomalies in the Laxmi Basin region also should be explained using the same crustal configuration derived based on modeling of gravity data. As is done in the case of Offshore Indus Basin, attempt has been made to examine the oceanic nature of the crust underlying the Laxmi Basin based on forward modeling of magnetic anomalies, where the magnetic

anomalies are considered to have been caused by juxtaposed blocks of normally and reversely magnetized crust, which lie within the gravity model derived inferred layer 2 of the oceanic crust.

The synthetic magnetic anomalies have been computed for a set of N30°W striking juxtaposed normally and reversely magnetized blocks, presently observed at 17°N, 69°E (Fig. 4.15a). As will be shown later, the central normally magnetized block correspond to anomaly 27n (~61.0 Ma) of geomagnetic polarity timescale. To obtain the paleo-location at the time of formation of this oceanic crust, a paleogeographic reconstruction of the region (Fig. 4.15b) has been carried out for 61 Ma in fixed hotspot reference frame using the finite rotation parameters of Müller et al. (1993). This model suggested that the Laxmi Basin area was in the southern hemisphere at ~15.0°S latitude at the time of formation. The bodies that caused the magnetic anomalies are considered to have a susceptibility of 0.01 cgs units, and the thickness and the depth to the top of the magnetized layer have been defined by limits of the inferred layer-2 derived from gravity modeling. The boundaries of the adjacent normally and reversely magnetized blocks have been obtained by a trial and error method in such a way that the synthetic magnetic anomalies computed using these symmetric magnetized blocks give the best fit with the observed magnetic anomalies.

The magnetic modeling exercise was carried out along profile SK79-15 as that displays very good axial symmetry and also is coincident over large part of the profile RE-02(SG) used for modeling the gravity data. The above exercise shows (Fig. 4.20) that the observed magnetic anomaly profile in the Laxmi Basin can be considered to have been caused by juxtaposed normally and reversely magnetized blocks, which lie within the basement layer. The sequence of these magnetized blocks appear to be symmetrical about a central narrow normally magnetized block, where the axis of symmetry coincides with the axis of the characteristic short wavelength gravity low atop the broad wavelength gravity high and the basement high feature (Panikkar Ridge). The parallel nature of the magnetic lineations and the symmetric arrangement of the magnetized blocks within the basement layer support generation of the underlying crust by two-limbed seafloor spreading. The continuation of magnetic anomalies (thereby magnetized bodies) a short distance over the Laxmi Ridge and basement of

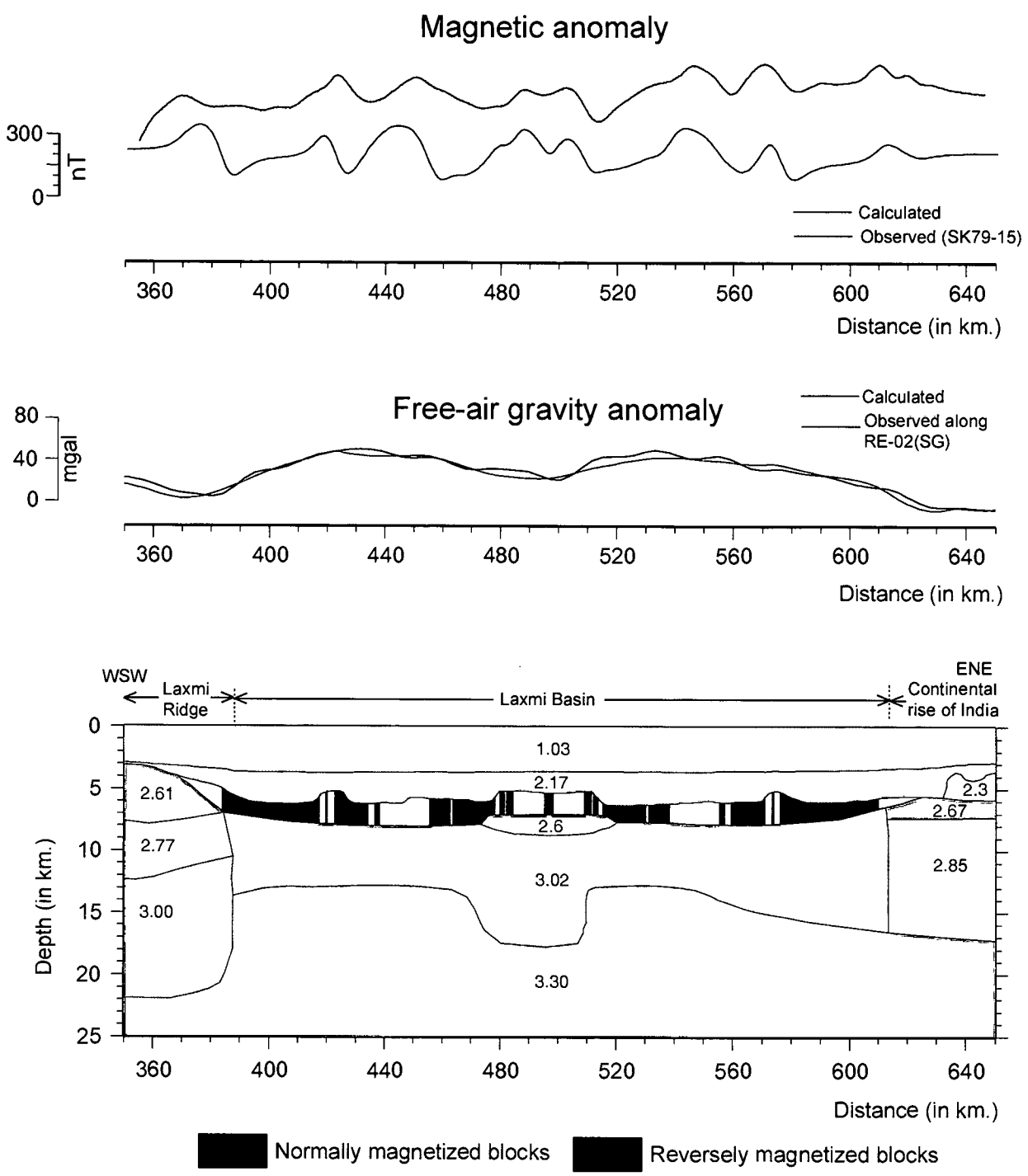

Fig. 4.20 Modelled crustal structure along part of profile RE-02 to show the crustal structure across the Laxmi Basin area from integrated gravity and magnetic modeling. The forward modeling of magnetic data shows that the magnetic anomalies in the Laxmi Basin can be explained in terms of juxtaposed normally and reversely magnetized blocks (susceptibility = 0.01 cgs units) within the layer-2 derived by the gravity modeling. Synthetic magnetic profiles are computed for a ridge presently striking N30°W and obvserved at 17°N, 69°E which was formed at the location 15°S, 53°E. The computed magnetic anomalies are compared with the magnetic profile SK79-15, which is located close to the gravity profile RE-02. The locations of the profiles have been shown in Fig. 4.17. Other details are as in Fig. 4.19.

Indian continental rise perhaps represents the initial oceanic crust. In view of the above evidences from the gravity, magnetic and seismic information, it is interpreted that part of the Laxmi Basin is underlain by oceanic crust formed as a result of two-limbed seafloor spreading between Laxmi Ridge and western India and the axial basement high region (Panikkar Ridge) represents the extinct spreading centre. The interpretation of the Laxmi Basin magnetic anomalies in the present study is similar to the interpretation of Bhattacharya et al. (1994b) that the Laxmi Basin region is formed by a two-limbed seafloor spreading. However, as will be shown in a later section, the identification of the magnetic anomalies of the present study differs from that of Bhattacharya et al. (1994b).

It has been observed that the magnetic anomalies in the Laxmi Basin have relatively lower amplitude as compared to the Offshore Indus Basin and the Arabian Basin. If the magnetic anomalies in both these nearby regions are of similar seafloor spreading origin, then the difference in amplitude needs explanation. As will be shown later, the magnetic lineations (i.e. the magnetized blocks) of the Arabian and Offshore Indus basins strike nearly E-W, whereas the magnetic lineations of the Laxmi Basin strike NNW-SSE. The observed amplitude difference appears to be due to this difference in the strike directions of the magnetized blocks in these two areas. This explanation is based on an exercise carried out in this study by computing the magnetic anomalies over the same block model of juxtaposed normally and reversely magnetized blocks (Fig. 4.21) but at different strike angles. The model clearly demonstrates that the set of E-W striking bodies (as in the Offshore Indus Basin) generate relatively higher amplitude anomalies as compared to the set of NNW-SSE striking bodies (as in the Laxmi Basin).

The inferred extinct spreading centre in both Offshore Indus and Laxmi basins are associated with prominent basement highs (viz. Palitana Ridge in the Offshore Indus Basin and Panikkar Ridge in the Laxmi Basin) and as will be shown later these spreading centres became extinct around chron 27ny (~61 Ma). It is interesting to note that similar basement highs are also present in the well-established Mascarene Basin extinct spreading centre, which became extinct almost during the same period. This observation is based on published

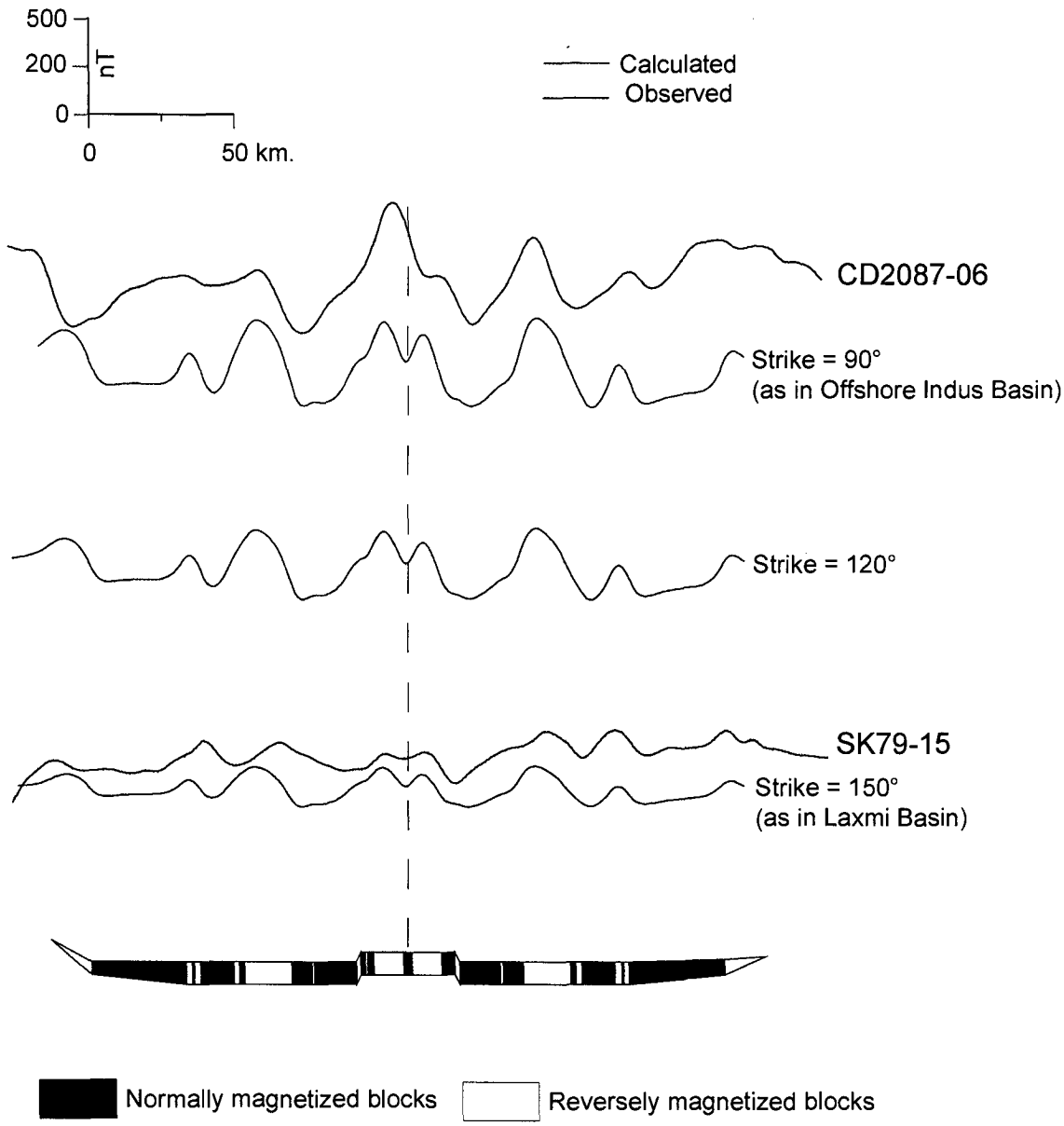

Fig. 4.21 Magnetic anomalies computed for the same magnetic block model but with different strike angles. The amplitude of the magnetic anomalies are higher when the strike of the magnetized blocks is 90°, as in the case of the Offshore Indus Basin and lower when the strike of the magnetized blocks is 150° as in the case of Laxmi Basin. Magnetic anomalies were computed for a model of about 1.75 km thick juxtaposed alternate normally and reversely magnetized blocks (susceptibility = 0.01 cgs units) which formed at 15°S, 53°E and presently located at 17°N, 69°E.

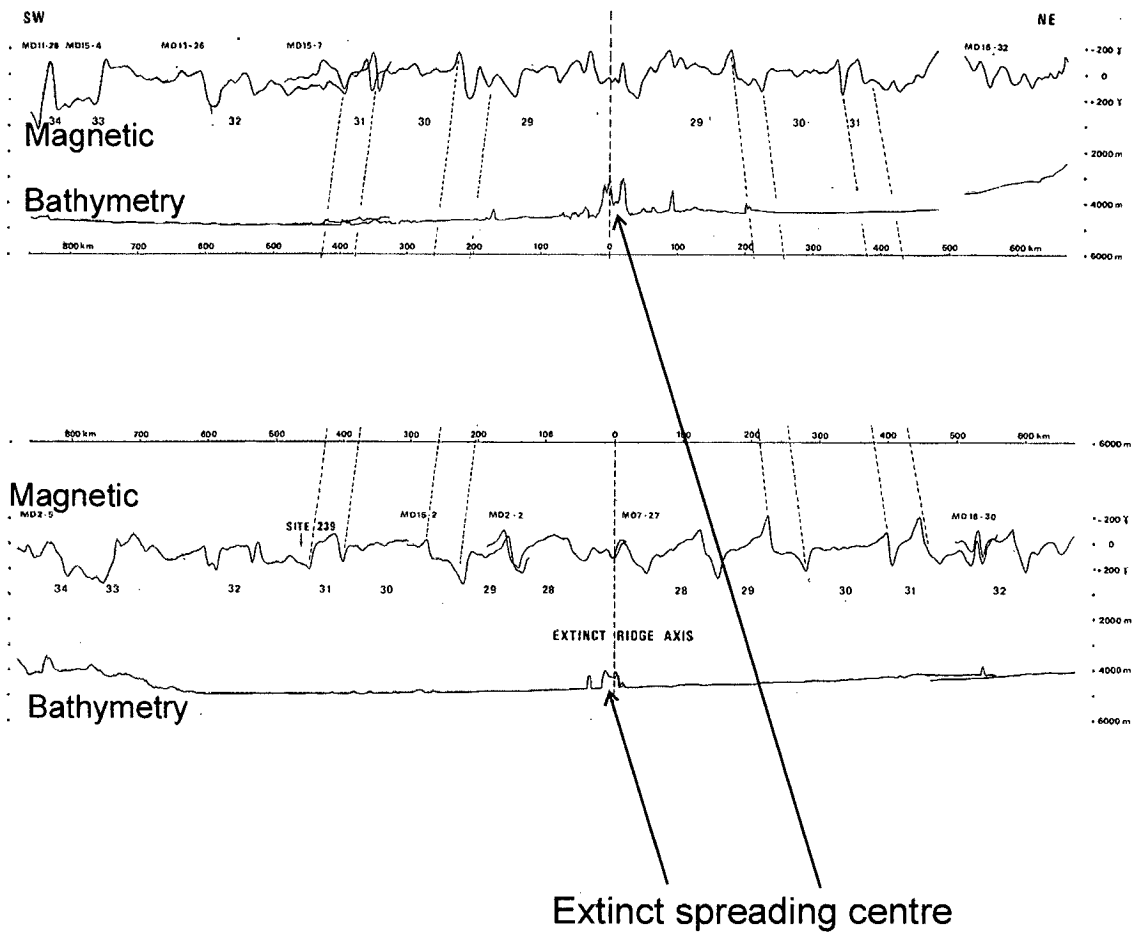

Fig. 4.22 Bathymetric and magnetic profiles across the extinct spreading centre in the Mascarene Basin. The extinct spreading axis corresponds to the vertical dashed line. Modified after Schlich (1982).

(Schlich, 1982) two bathymetric and magnetic profiles (Fig. 4.22) across the extinct spreading centre in the Mascarene Basin.

4.4 Identification of the inferred seafloor spreading magnetic lineations of the Offshore Indus and Laxmi basins

The geophysical studies carried out so far suggest a two-episode spreading history of the Arabian Sea. Commencing at chron 27n, the older phase ended at chron 21n and spreading of the younger phase started shortly before the time of formation of anomaly 11n. In the intervening period (i.e., between chrons 21n and 11n) spreading in the Arabian Sea is considered to have either completely ceased or reduced to an imperceptible level (Naini and Talwani, 1982; McKenzie and Sclater, 1971; Chaubey et al., 1993). In the Arabian Basin region, a well-developed anomaly 27n was mapped in the areas west of the Laxmi Ridge, which indicates that the oceanic crust generated at the time (hitherto believed) of opening of the Arabian Sea lies seaward, west of the Laxmi Basin. Further, the strike of the post-chron 27n anomalies (i.e. anomalies 27n to 21n) is approximately E-W, whereas the lineations within the Laxmi Basin trend NNW-SSE. This noticeable change in the trends of the pre-chron 27 anomalies of the Laxmi Basin and post-chron 27 anomalies of the adjacent Arabian Basin perhaps suggests reorganization of the spreading centres during the intervening period. Therefore, in line with the opinion of Bhattacharya et al. (1994b) it appears necessary to invoke a third, pre-chron 27, episode of seafloor spreading to explain the inferred oceanic crusts of the Laxmi and Offshore Indus basins.

As discussed by Bhattacharya et al. (1994b) possibility of the existence of pre-chron 27 oceanic crust in the northeastern Arabian Sea was indicated in several earlier studies. Scotese et al. (1988), in their paleogeographic reconstruction model, have inferred a piece of Late Cretaceous (chrons 29–34) oceanic crust in this area. Norton and Sclater (1979) in their chron 28 time reconstruction model, place the spreading centre north of and immediate adjacent to Seychelles, thereby showing a large gap of crust in the northern Arabian Sea of unexplained origin. Masson (1984) noted the anomalous reduced width of the northwestern Mascarene Basin, as compared to the oceanic crust generated during the same spreading regime in the southeastern Mascarene and Madagascar basins and concluded that about 500 km of crust is 'missing' in the

northwestern Mascarene Basin. To explain this missing crust, Masson suggested a model according to which the missing oceanic crust in the northwestern Mascarene Basin is accommodated by a pre-chron 28 phase of seafloor spreading between India and the Seychelles Plateau. This spreading was linked to the spreading in the southeastern Mascarene Basin by a fracture zone passing east of the Seychelles Plateau. Based on updated magnetic anomaly identification in the northwestern and southeastern Mascarene basin region, and a paleogeographic reconstruction model for chron 27n, Bernard and Munschy (2000) opined that the geometry of the Laxmi Basin corresponds to the missing oceanic crust in the northwestern Mascarene Basin. These inferences provide further support to the proposition that the Offshore Indus and Laxmi basins represent a part of the pre-chron 27 oceanic crust in the northeastern Arabian Sea, and therefore this age limit has been assumed for the purpose of identification of the observed magnetic lineations. As described in the previous sections, the magnetic anomalies in the Offshore Indus and Laxmi basins are akin to the oceanic crust formed as a result of two-limbed seafloor spreading, where the Palitana Ridge and the Panikkar Ridge represent the extinct spreading centres. Therefore, an attempt has been made in this study to identify these magnetic anomalies in terms of geomagnetic polarity reversal time scale. Further, an updated magnetic isochron map of the study area have been prepared, which depicts the conjugate magnetic isochrons on both the sides of those extinct spreading centres.

(a) Identification of magnetic lineations in the Offshore Indus Basin

The magnetic anomaly sequence in the Offshore Indus Basin region is very short, and therefore could not be easily compared with the geomagnetic polarity reversal time scale. After several trials, a good correlation (Fig. 4.23) has been obtained between the computed and observed magnetic anomalies by equating the anomalies in the Offshore Indus Basin to the chron 27n–31n interval of the geomagnetic polarity reversal time scale, where the ridge axis is considered at 61 Ma, slightly younger than chron 27no (61.276 Ma). The half spreading rate (Table 4.1) that is calculated based on this identification of the linear magnetic anomalies shows that the Offshore Indus Basin spreading centre was a slow (< 1cm/yr) spreading centre. The inferred oldest magnetic anomaly in

Table 4.1 Half spreading rates for the Offshore Indus Basin, calculated from the derived model of juxtaposed normally and reversely magnetized blocks. Ages of the magnetic lineations are after Cande and Kent (1995).

Chron	Young edge (Ma)	Old edge (Ma)	Duration (m.y.)	HSR (cm/yr)
27n*	60.920	61.276	0.276	~0.05
27r	61.276	62.499	1.223	0.85
28n	62.499	63.634	1.135	0.30
28r	63.634	63.976	0.342	0.30
29n	63.976	64.745	0.769	0.30
29r	64.745	65.578	0.833	0.30
30n	65.578	67.610	2.032	0.60
30r	67.610	67.735	0.125	0.60
31n	67.735	68.737	1.002	0.60

**Seafloor spreading does not appear to have taken place during the total duration of chron 27n in this basin; it appears to have become extinct around 61 Ma.*

this region is anomaly 31n, which suggest that spreading in this region was initiated at anomaly 31n time. The calculated half spreading rate of the region shows that during chrons 31n-30n, seafloor spreading took place with a half spreading rate of 0.6 cm/yr. Followed by this, the half spreading rate slowed down to 0.3 cm/yr from chron 29r onwards. This situation continued up to chron 28n. During chron 27r, the arrangement of magnetic anomalies necessitate considering a higher spreading rate. Subsequently, the spreading rate slowed down and the spreading in the region ceased, some time during chron 27n probably at 61 Ma.

Having inferred the magnetic lineations in the Offshore Indus Basin as anomalies sequence 27n-31n, attempt has been made to delineate the approximate boundaries of these normally and reversely magnetized blocks. Several authors (Roest et al., 1992; Chaubey et al., 2002a) have used the modulus of analytic signal technique (Nabighian, 1972, 1974) to pick the boundaries defining the blocks of juxtaposed normally and reversely magnetized crust. An attempt has been made to apply the same technique to the magnetic profiles in the Offshore Indus Basin region; however, it is observed that this method does not hold good both in the case of Offshore Indus Basin as well as in the Laxmi Basin. Probably, this may be due to the presence of narrow blocks of normally and reversely magnetized crust. This conclusion is based on exercises carried out to identify the boundaries of all magnetized blocks on the computed magnetic anomaly profile generated for the synthetic block models of both the regions. In view of this, a less disturbed representative profile in the Offshore Indus Basin has been selected and the approximate boundaries of the major blocks have been marked (Fig. 4.23) over this profile by comparing them with the corresponding computed anomaly profile, where locations of block boundaries have been marked with reference to model of magnetized blocks. Further, attempt has been made to pick these major block boundaries over other profiles (Fig. 4.24). These picks (block boundaries) have been transferred on a plot along track map (Fig. 4.25a) of the magnetic anomalies. Subsequently, the magnetic isochrons have been delineated (Fig. 4.25b) by connecting the corresponding picks on different profiles. Where an offset between two sets of magnetic

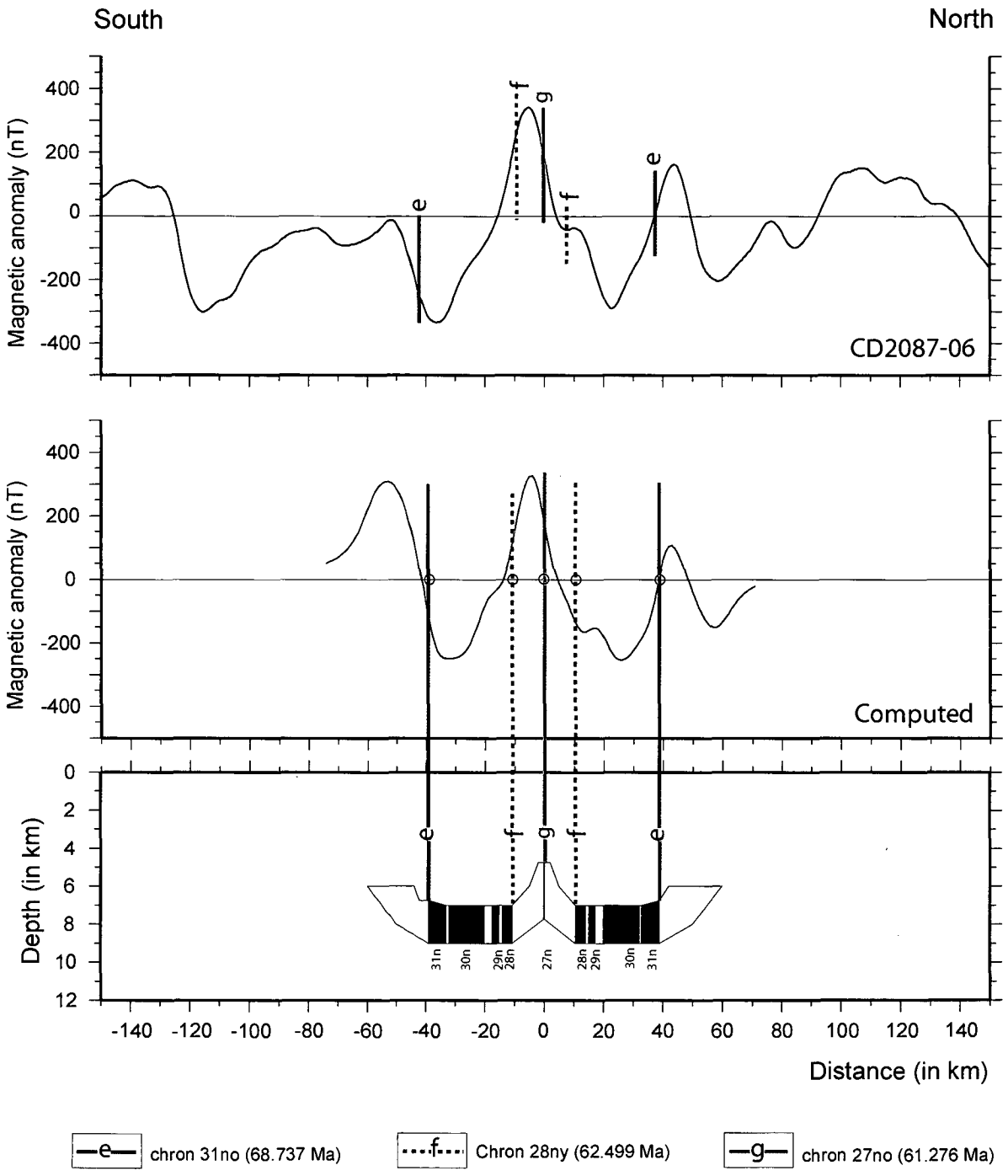

Fig. 4.23 Observed and computed magnetic anomalies along profile CD2087-06 across the Offshore Indus Basin to demonstrate delineation of boundaries of magnetized blocks on the profiles. The approximate boundaries of the magnetized blocks on the observed magnetic profiles have been marked by comparing them with the corresponding computed anomaly profile, where locations of block boundaries have been marked with reference to magnetized block model. The boundaries of magnetized blocks which could be reasonably approximated are labelled as e,f and g. Other details are as in Fig. 4.16.

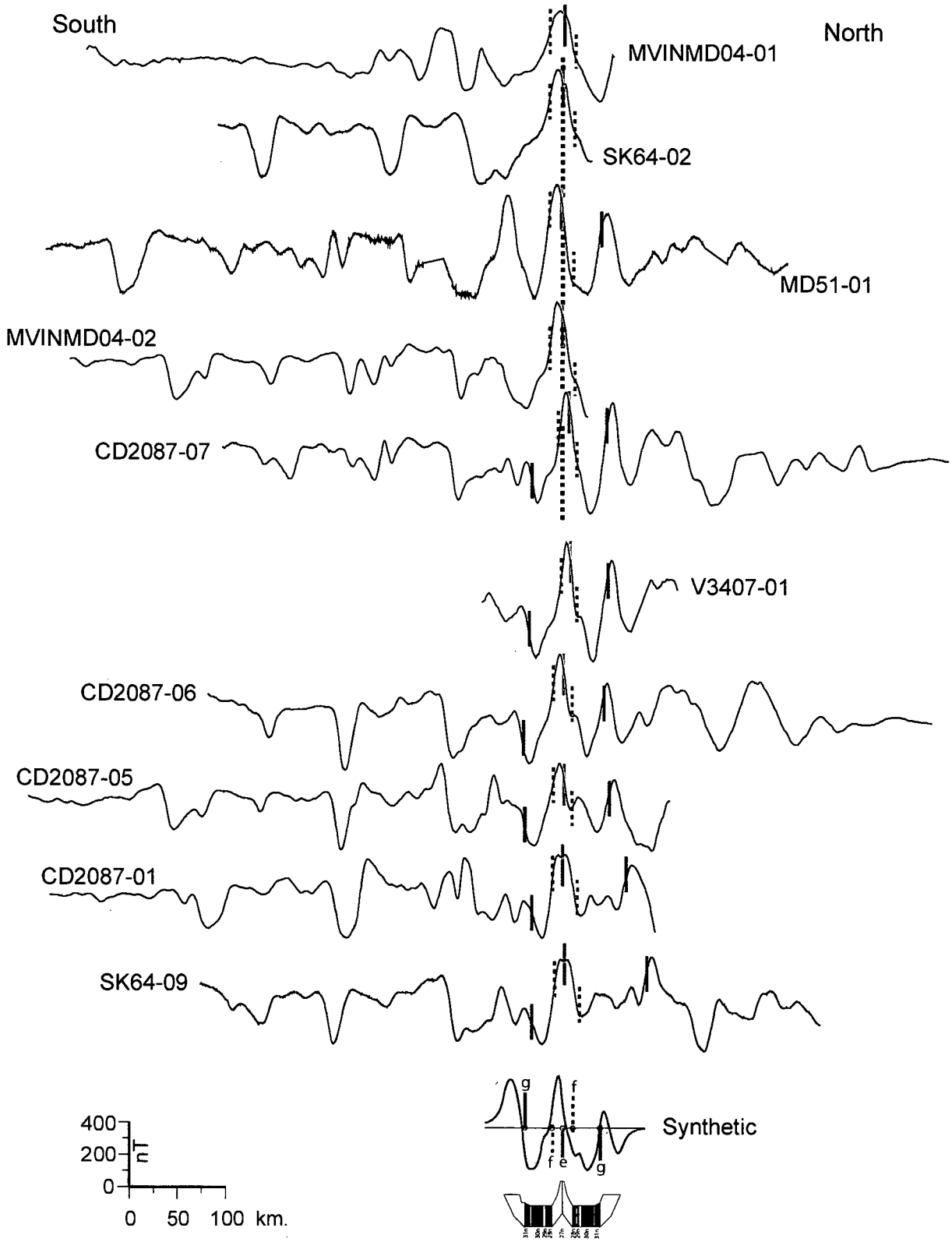

Fig. 4.24 Approximate boundaries of the normally and reversely magnetized blocks, picked over the magnetic profiles in the Offshore Indus Basin. The profiles were projected to an azimuth of 0° and stacked with respect to the axis of the characteristic short wave length gravity low atop the broad gravity high. Heavy dotted lines represent the axis of the characteristic gravity low. Other details are as in Fig. 4.23.

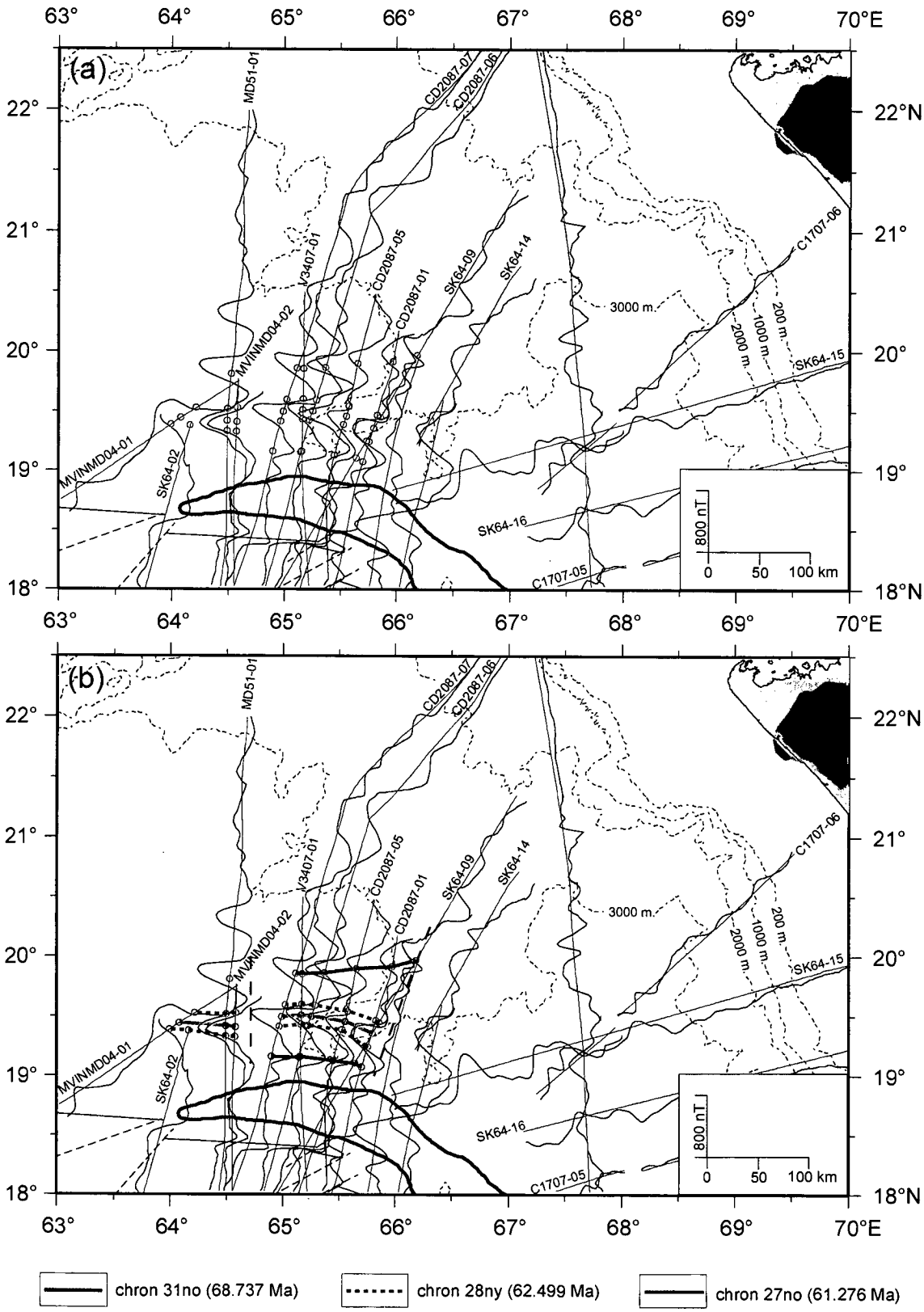

Fig. 4.25 Map showing inferred boundaries of magnetized blocks and magnetic isochrons along with magnetic anomalies in the Offshore Indus Basin plotted perpendicular to ship's tracks. (a) locations of the major boundaries of the normally and reversely magnetized blocks as shown in Fig. 4.25. (b) inferred magnetic isochrons. Other details are as in Fig. 4.24.

isochrons is apparent, fracture zones, orthogonal to these magnetic isochrons, have been invoked.

(b) Identification of magnetic lineations in the Laxmi Basin

Having interpreted the crust underlying the Laxmi Basin region as oceanic in nature, attempt has been made to identify the magnetic anomalies in this region. After several trials, a good correlation (Fig. 4.26) has been obtained between the computed and observed magnetic anomalies by equating the anomalies in the Laxmi Basin to chron 27n–33n interval of the geomagnetic polarity reversal time scale, where the ridge axis is considered at 61 Ma, slightly younger than chron 27no (61.276 Ma). The half spreading rate (Table 4.2) that is calculated based on this identification of these linear magnetic anomalies shows that the Laxmi Basin spreading centre was a slow spreading centre. The inferred oldest magnetic anomalies in this region are anomaly 33n, which suggest that the spreading in this region was initiated during chron 33n.

The calculated half spreading rate of the region shows that during chron 33n, seafloor spreading took place with a half spreading rate of 0.6 cm/yr. Followed by this, the half spreading rate increased to 0.8 cm/yr, which continued up to chron 32r1 time. The spreading rate slightly decreased to 0.7 cm/yr and slowed down to 0.2 cm/yr from chron 29r onwards. Interestingly, the period (~65.578 Ma) during which the spreading rate in the Offshore Indus and Laxmi basins slowed down was the time at which the Deccan Trap is considered to have erupted (Courtillot et al., 1986; Duncan, 1990). During chron 27r, the arrangement of the magnetic anomalies necessitate considering a higher spreading rate. Subsequently, the spreading rate slowed down and the spreading in the region ceased some time during chron 27n, probably around at 61 Ma. Based on this identification of the magnetic anomalies, it is observed that during times of anomalies 27n-28n, spreading was taking place simultaneously in the Offshore Indus, Laxmi and Arabian basins.

Having inferred the magnetic lineations in the Laxmi Basin as anomalies sequence 27n-33n, attempt has been made to delineate the approximate boundaries of these normally and reversely magnetized blocks. Since the analytic signal method was not found suitable in this region as in the case of Offshore

Table 4.2 Half spreading rates for the Laxmi Basin, calculated from the derived model of juxtaposed normally and reversely magnetized blocks. Ages of the magnetic lineations are after Cande and Kent (1995).

Chron	Young edge (Ma)	Old edge (Ma)	Duration (m.y.)	HSR (cm/yr)
27n*	60.920	61.276	0.276	~0.39
27r	61.276	62.499	1.223	0.85
28n	62.499	63.634	1.135	0.20
28r	63.634	63.976	0.342	0.20
29n	63.976	64.745	0.769	0.20
29r	64.745	65.578	0.833	0.20
30n	65.578	67.610	2.032	0.70
30r	67.610	67.735	0.125	0.70
31n	67.735	68.737	1.002	0.70
31r	68.737	71.071	2.334	0.70
32n1	71.071	71.338	0.267	0.70
32r1	71.338	71.587	0.249	0.80
32n2	71.587	73.004	1.417	0.80
32r2	73.004	73.291	0.287	0.80
32n3	73.291	73.374	0.083	0.80
32r3	73.374	73.619	0.245	0.80
33n	73.619	79.075	5.456	0.60

**Seafloor spreading does not appear to have taken place during the total duration of chron 27n in this basin; it appears to have become extinct around 61 Ma.*

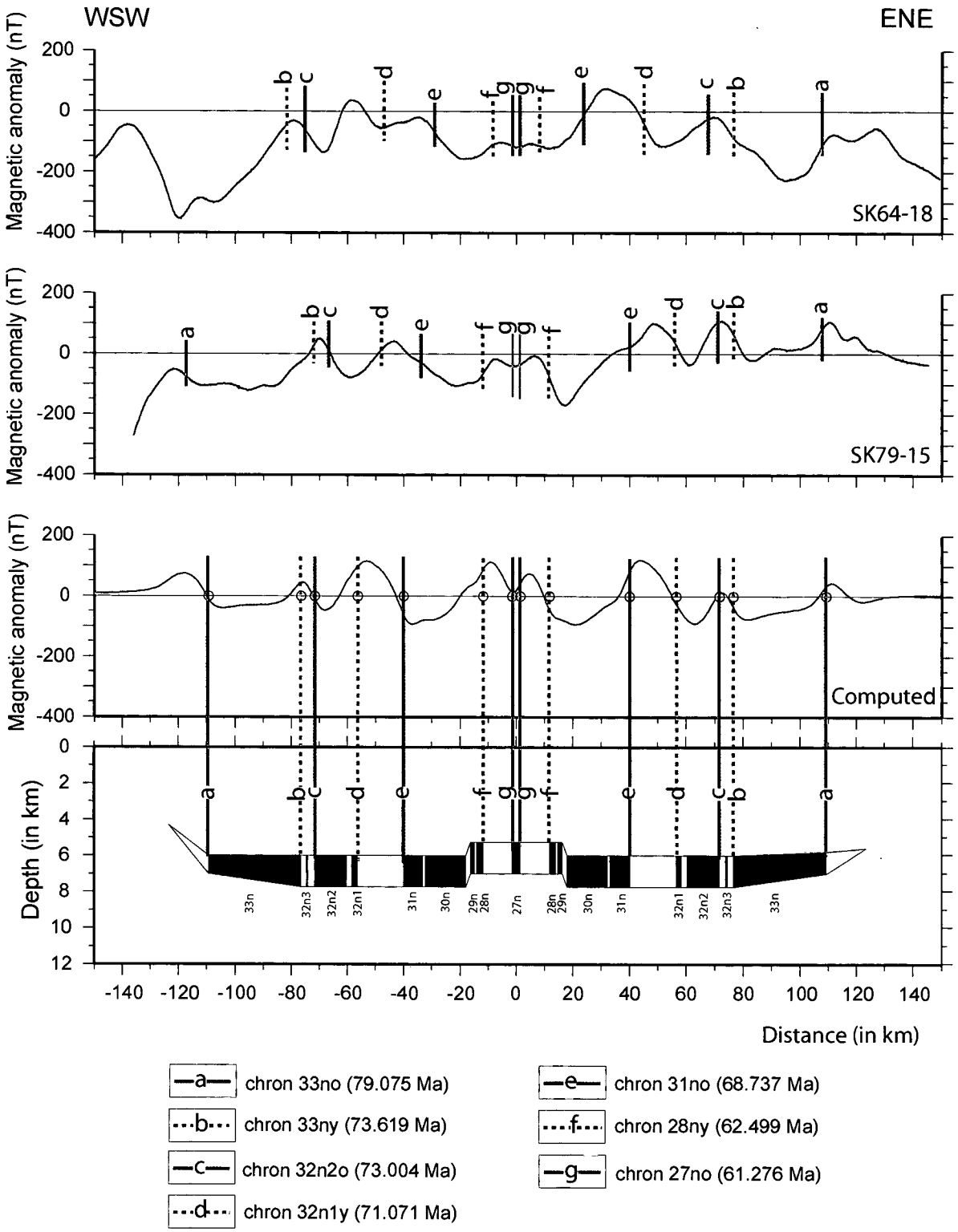

Fig. 4.26 Observed and computed magnetic anomalies along selected profiles across the Laxmi Basin to demonstrate the delineation of boundaries of magnetized blocks on the profiles. The approximate boundaries of the magnetized blocks on the observed magnetic profiles have been marked by comparing them with the corresponding computed anomaly profile, where locations of block boundaries have been marked with reference to magnetized block model. The boundaries of magnetized blocks which could be reasonably approximated are labelled as a,b,c,d.e.f and g. Other details are as in Fig. 4.20.

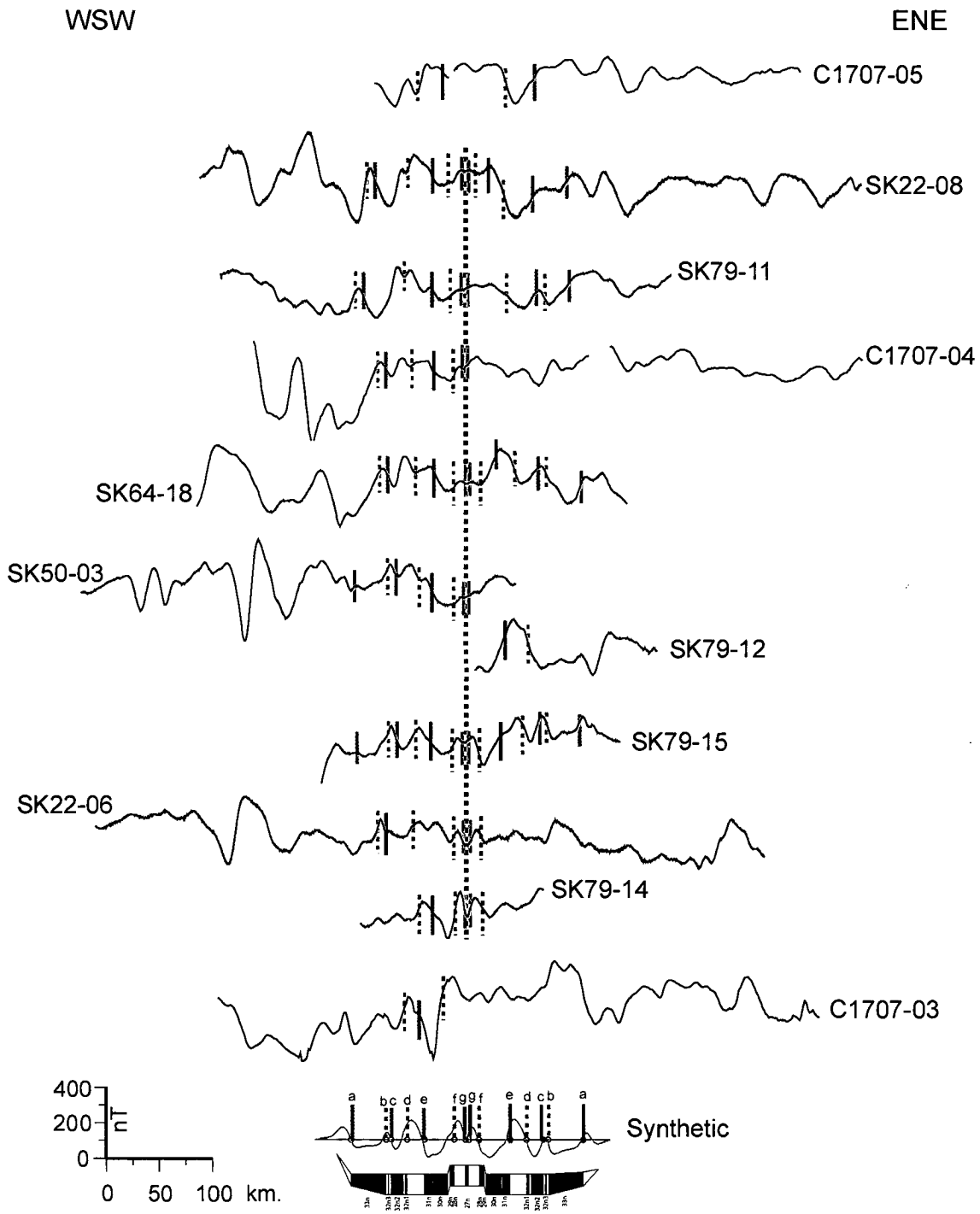

Fig. 4.27 Approximate boundaries of the normally and reversely magnetized blocks picked over the selected magnetic profiles in the Laxmi Basin region. The profiles were projected to an azimuth of 60° and stacked with respect to the axis of the characteristic short wave length gravity low atop the broad gravity high. Heavy dotted lines represent the axis of the characteristic gravity low. Other details are as in Fig. 4.26.

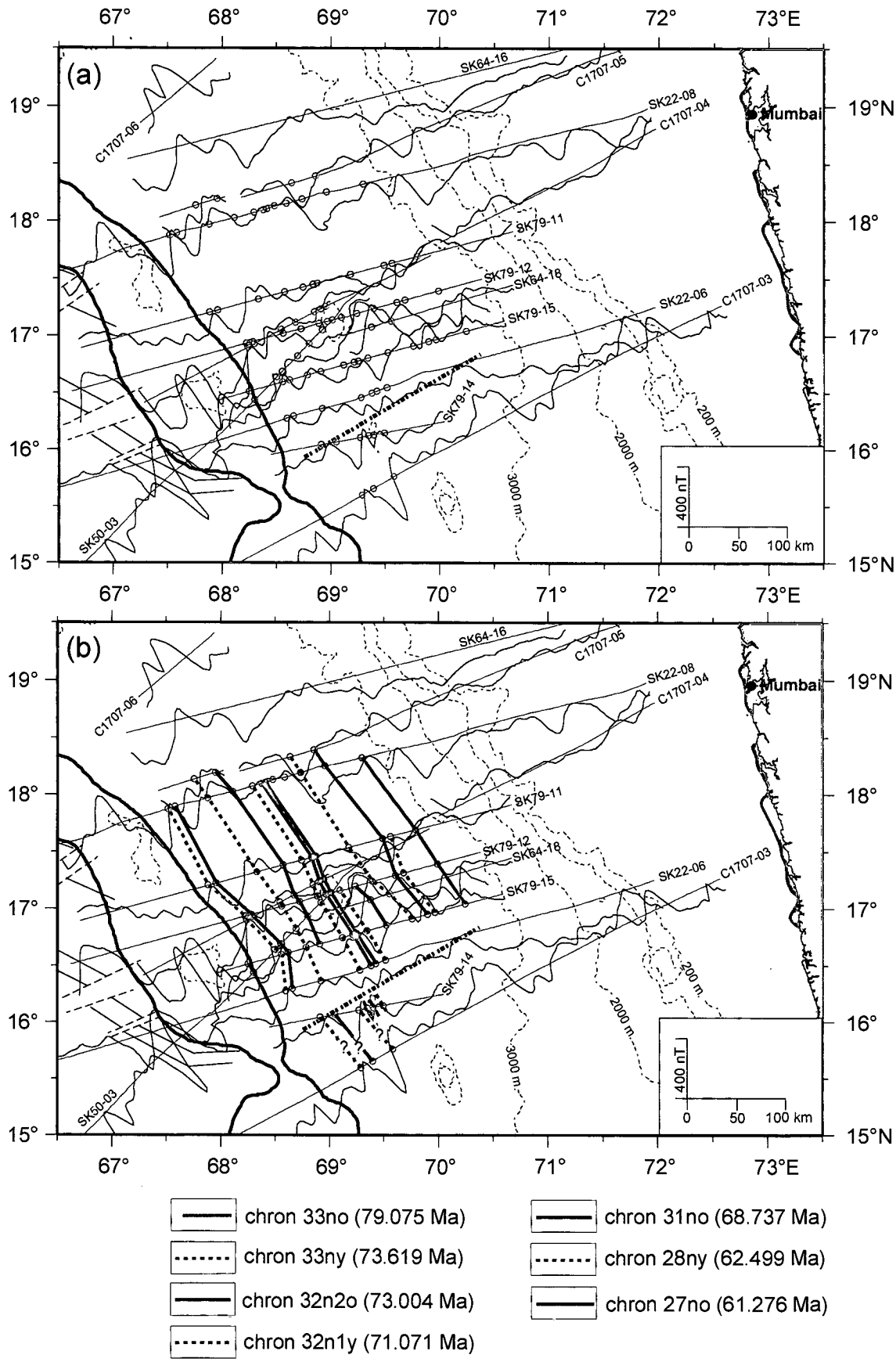

Fig. 4.28 Map showing inferred boundaries of magnetized blocks and magnetic isochrons along with magnetic anomalies in the Laxmi Basin plotted perpendicular to ship's tracks. (a) locations of the major boundaries of the normally and reversely magnetized blocks as shown in Fig. 4.26, (b) inferred magnetic isochrons.

Indus Basin region, therefore a less disturbed profile in the Laxmi Basin has been selected and the approximate boundaries of the major blocks are marked (Fig. 4.26) over this profile by comparing them with corresponding computed anomaly profile, where locations of block boundaries have been marked with reference to magnetized block model. Further, attempt has been made to pick these major block boundaries over other profiles (Fig. 4.27). These picks (block boundaries) have been transferred on plot-along track map (Fig. 4.28a) of the magnetic anomalies. Subsequently, the magnetic isochrons have been delineated (Fig. 4.28b) by connecting the corresponding picks on different profiles. Where an offset between two sets of magnetic isochrons is apparent, fracture zones, orthogonal to these magnetic isochrons, have been invoked.

(c) Updated magnetic isochron map of the studied area

In summary the updated magnetic isochron map of the study area as prepared (Fig. 4.29a, b) in the present study suggest that in the Laxmi Basin region, the magnetic isochrons range from chron 33no (79.075 Ma) to chron 27no (61.276 Ma), while in the Offshore Indus Basin these isochrons ranges from chron 31no (68.737 Ma) to chron 27no (61.276 Ma). In both the basins, the spreading appears to have ceased around 61 Ma. It further appears for a period of about 1.8 my (from 62.8 Ma to 61 Ma), prior to becoming extinct, the spreading centers of the Offshore Indus and Laxmi basins were active simultaneously with the spreading centers of the Arabian Basin.

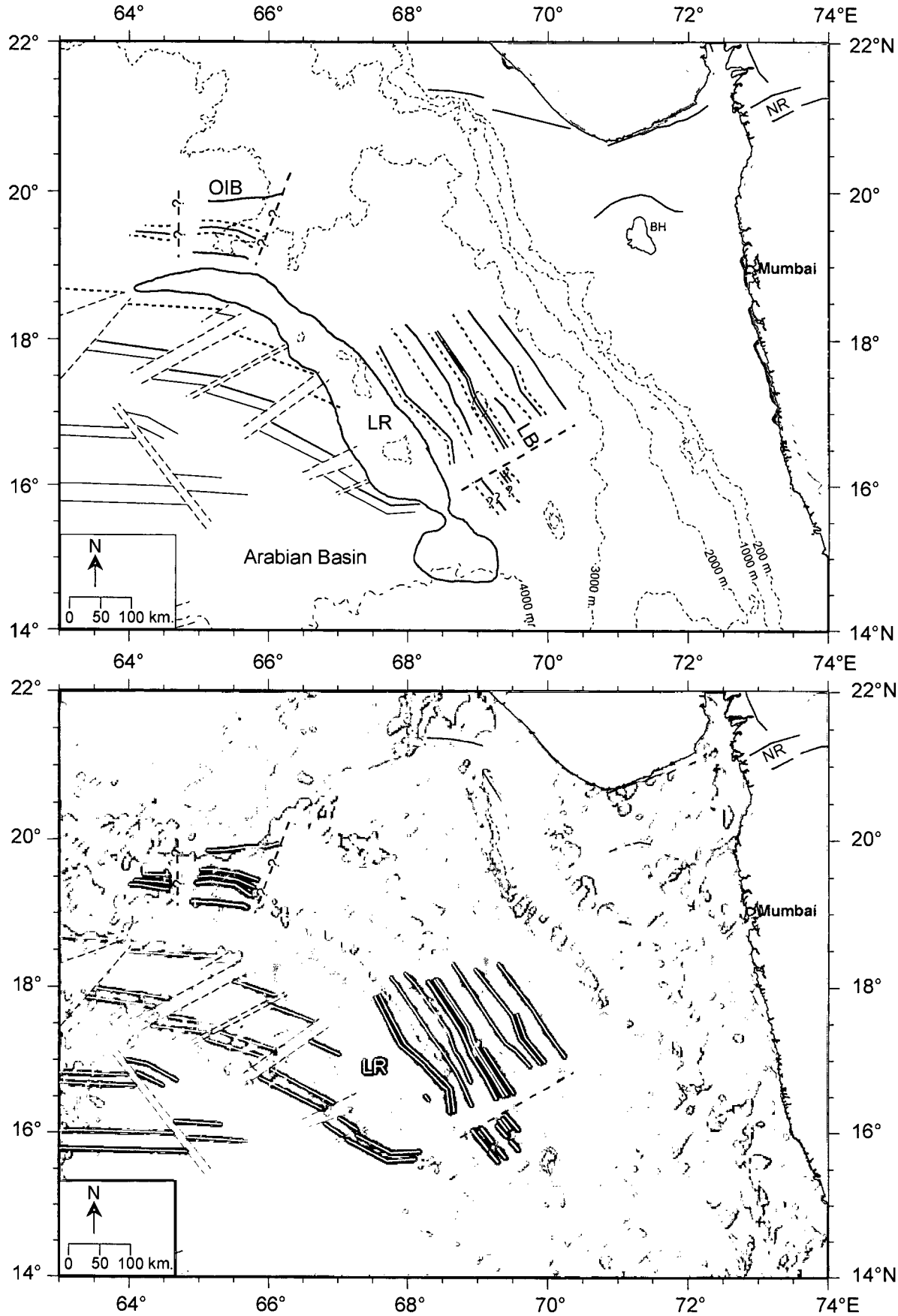

Fig. 4.29 Updated magnetic isochron map of the study area, (a) along with the selected bathymetry contours and the anomalous gravity high region, and (b) along with colour shaded-relief image of the satellite derived free-air gravity anomalies. White lines on colour shaded-relief image represent the mapped seafloor spreading magnetic lineations. Other details are as in Fig. 4.4.

CHAPTER 5

Chapter 5

EVALUATION AND IMPROVEMENT OF INDIA–MADAGASCAR–SEYCHELLES JUXTAPOSITION MODELS

5.1 Introduction

The western continental margin of India is considered to be a passive continental margin (Biswas, 1982, 1987), which evolved during the process of rifting and drifting of Madagascar, Seychelles and India. Even though researchers agree on the concept of a welded Madagascar–Seychelles–India continental block, but opinion differs regarding their immediate pre-drift juxtaposition and consequential early post drift relative positions. Probably lack of distinct and dependable "piercing points" such as onshore tectonic lineaments, which could have constrained this juxtaposition, is one of the reasons for those varied inferences. In case of India-Madagascar juxtaposition, the other reason could be the absence of India-Madagascar break-up related magnetic isochrons, which could have allowed arriving at consistent rotation parameters for constraining early India–Madagascar separation, as that break-up took place during Cretaceous long normal superchron. In case of India-Seychelles juxtaposition, one of the reasons may be lack of adequate understanding regarding the nature of the crust underlying the region north and east of Laxmi Ridge. In view of this, it is felt necessary to evaluate the various existing models for India-Seychelles-Madagascar relative motions for their juxtaposition and early drift period, and subsequently provide improved paleogeographic reconstruction models, which are compatible with the updated information about the tectonic elements from the conjugate regions. Extent of the continental blocks are important in the paleogeographic reconstruction studies, therefore at the beginning of this chapter the boundaries of continental blocks considered for paleogeographic reconstruction in this study have been defined.

5.2 The extent of continental blocks and continental slivers

The boundaries of the continental blocks to be considered for paleogeographic reconstruction usually are the continent-ocean boundaries. Unfortunately, in the study area, the continent-ocean boundary is poorly

constrained. As a result, different researchers used different criteria for defining the extent of the continental blocks under consideration. Norton and Sclater (1979) considered 2000 m isobath to define this boundary in the western continental margin of India, while Besse and Courtillot (1988) used 2500 m isobath. In contrary to this, Royer et al. (2002) considered the shelf break and Lawver and Gahagan (2005) used the steep gradients of the satellite altimetry data. In absence of other information, the foot of the slope can be considered to mark the ocean-continent boundary. A broad examination of bathymetric maps and sections around the continental blocks considered in this study suggests that the foot of the continental slope in these areas lies close to the 2000 m isobath. Therefore in the same way as Norton and Sclater (1979) the 2000 m isobath has been used in this study to define the boundaries of the continental blocks. The boundaries defined using this criterion may contain a part of the extended rift stage crust, which formed prior to seafloor spreading. Reconstruction models using unstretched extents of the continental blocks would provide better and closer fit of continental blocks, but the overall scenario more or less will remain the same as with the models developed using the 2000 m isobath outlines. The continental sliver of the Laxmi Ridge is an important tectonic element of the study area. Since the Laxmi Ridge presently lies at depth greater than 2000 m and most part of it is buried under sediment, therefore, for defining the boundary of the Laxmi Ridge different approach was taken.

(a) Boundary of Indian continental block

As described in the previous section, the 2000 m isobath has been considered (Fig. 5.1) to define the extent of Indian continental block. Between Cochin and Kutch-Saurashtra region, this boundary trend approximately in NW-SE direction and have a relatively smooth shelf-slope configuration. South of Cochin, trend of this boundary change and interestingly depicts the presence of a wide low gradient zone in the mid-continental slope region off Trivandrum. This low gradient zone broadly lies between 1000 m and 2000 m isobaths and covers an area of about 9000 sq km. Available bathymetric transects (Fig. 5.2a, b) across this zone suggest that low gradient zone is bounded by a steep ascending (by about 1000 m) seafloor to the adjacent continental shelf on easterly side and a comparable steep descending seafloor towards the deep sea in the westerly

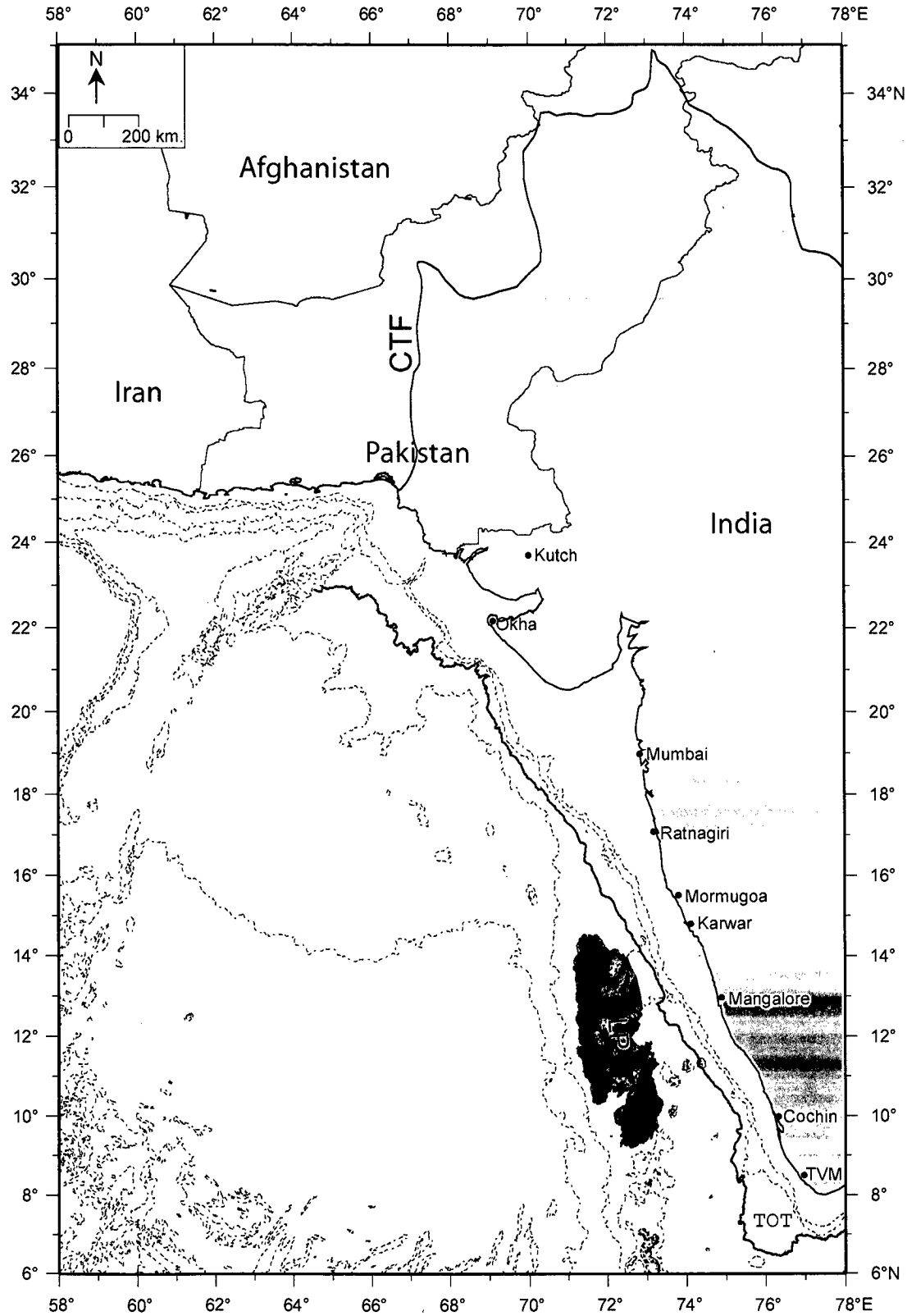

Fig. 5.1 The considered extent of Laccadive Plateau and western extent of the Indian continental block. The extent of the Laccadive Plateau is defined by 2000 m isobath. The western extent of Indian block is considered to consist of Indian mainland, part of Pakistan mainland existing east of Chaman Transform Fault and the 2000 m isobath (thick blue line) in the offshore. TOT: Terrace off Trivandrum; TVM: Trivandrum; LP: Laccadive Plateau; CTF: Chaman Transform Fault.

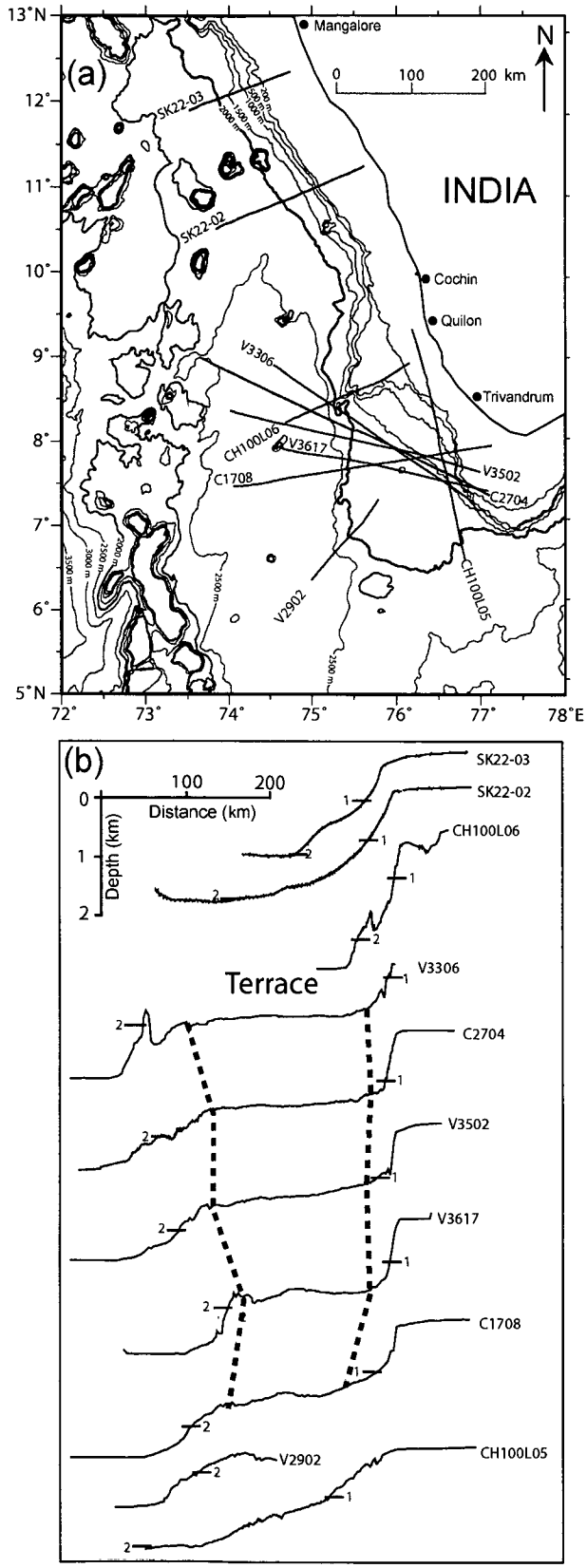

Fig. 5.2 Selected bathymetric profiles in the southwestern continental margin of India showing the presence of a terrace like feature in the mid-continental slope region off Trivandrum. (a) Map showing location of selected bathymetry profiles along with the bathymetry contours. (b) Selected bathymetric profiles showing the sectional view of the terrace off Trivandrum as compared to the normal shelf-slope configuration along the northern profiles (SK22-02 and SK22-03). The depth levels of 1 and 2 km are labeled on profiles.

side. This topography appears to be anomalous as compared to the general topography depicted by contours and two bathymetric transects (Fig. 5.2 a, b) across the normal shelf-slope configuration in the north. This wide zone is considered to qualify well as a 'terrace' following the definition of Lapedes (1978) and for further reference in this study this feature is denoted as Terrace off Trivandrum (TOT). In the region north of Kutch-Saurashtra region (Fig. 5.1), following the outline defined under PLATES Project (Coffin et al., 1998), the boundary of Indian continental block has been considered to lie along the Murray Ridge, the Chaman transform fault and the Himalayan subduction zone.

(b) Laxmi Ridge block

The Laxmi Ridge has widely been accepted (Naini and Talwani, 1982; Kolla and Coumes, 1990; Miles and Roest, 1993; Malod et al., 1997; Todal and Eldholm, 1998; Talwani and Reif, 1998; Miles et al., 1998; Collier et al., 2004a, b; Minshull et al., 2006) as a continental sliver. Available few seismic profiles (Naini and Talwani, 1982; Collier et al., 2004a, b) suggest this feature as a positive basement feature, which is covered by thin veneer sediments. Apparently due to use of large contour interval, the physiographic expression of the Laxmi Ridge is not clearly discernible from the bathymetry contours. As a result, the Laxmi Ridge appears as a series of isolated bathymetric highs defined by 3000 m and 3500 m isobaths. Even though a positive basement feature, the Laxmi Ridge, interestingly, is characterized by gravity low, both in free-air and isostatic gravity anomalies. Based on this observation, some researchers (Naini and Talwani, 1982; Todal and Eldholm, 1998; Miles et al., 1988) used the free-air or isostatic gravity anomalies to define the boundary of this inferred continental block. However, the boundaries defined by them varied from one another (Fig. 5.3a). In view of this, for the present study boundary of the Laxmi Ridge has been delineated primarily based on satellite derived free-air gravity anomalies. This approach was taken because the colour shaded-relief image (Fig. 5.3b) and the contours (Fig. 5.3c) of satellite derived free-air gravity anomalies appear to depict the characteristic gravity low associated with the Laxmi Ridge over its full extent. The boundary (Fig. 5.3d) of the Laxmi Ridge has been demarcated considering these gravity contours, extent of the mapped seafloor spreading magnetic lineations of the Arabian, Offshore Indus and Laxmi basins near the Laxmi Ridge,

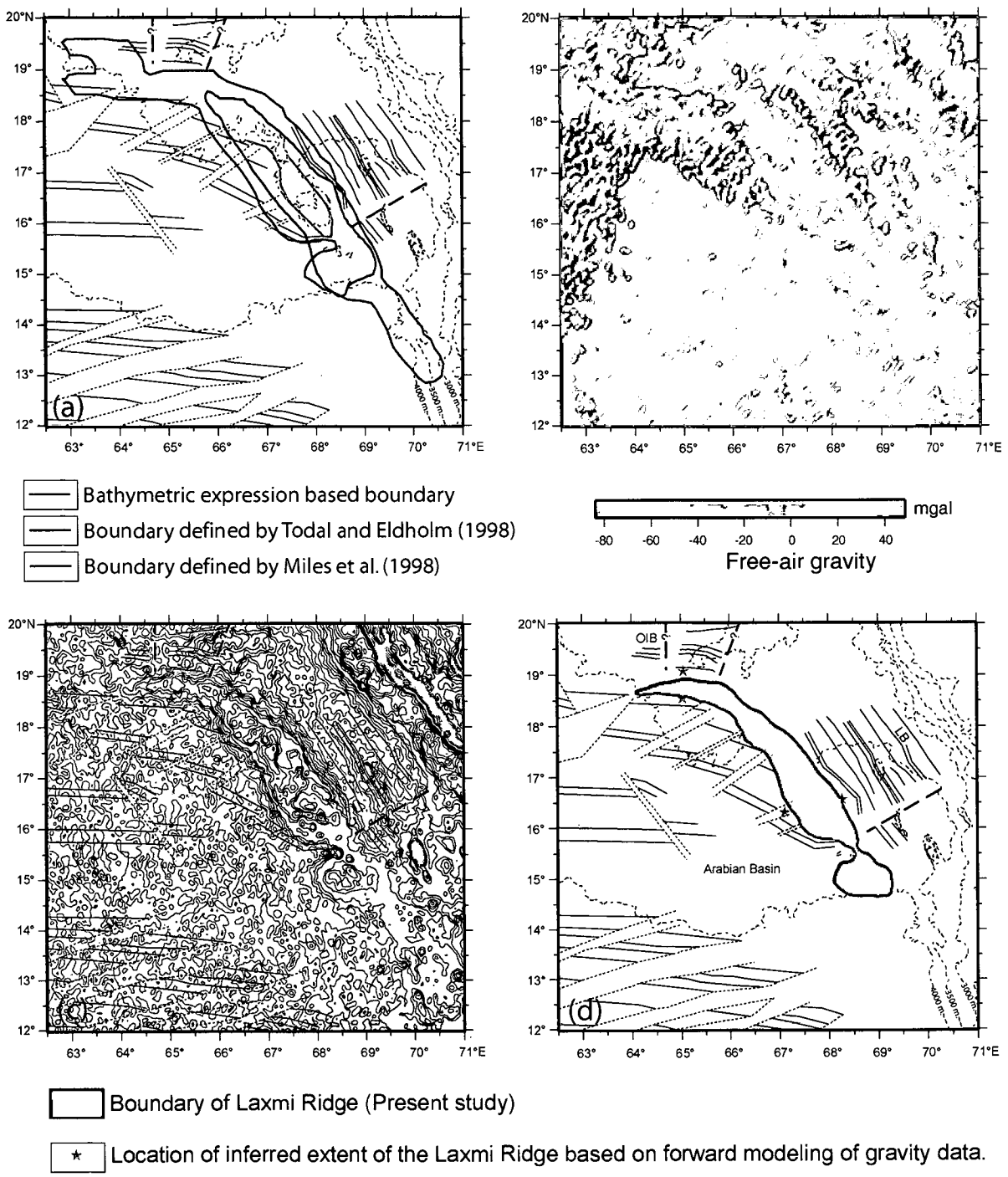

Fig. 5.3 The boundary defining the extent of the Laxmi Ridge continental sliver based on the satellite derived free-air gravity anomalies, mapped seafloor spreading type magnetic lineations and the derived crustal structure based on forward modeling of gravity profiles. (a) The boundaries proposed in the previous studies. (b) The colour shaded-relief image of the satellite derived free-air gravity anomalies (c) Contours of satellite derived free-air gravity anomalies in 5 mgal interval along with the location of boundaries derived based on forward modeling of selected gravity profiles and mapped seafloor spreading type magnetic lineations (d) The boundary of the Laxmi Ridge proposed in the present study, that has been used while performing the paleogeographic reconstruction.

and the crustal structure of the Laxmi Ridge derived based on the forward modeling of gravity data carried out in this study.

(c) Laccadive Plateau block

The Laccadive Plateau is a large submarine plateau structure, whose genesis is yet to be resolved. However, in this study the Laccadive Plateau is considered as a continental sliver as opined by many researchers (Krishnan, 1968; Naini and Talwani, 1982; Talwani and Reif, 1998; Chaubey et al., 2002b) and the compatibility of such a consideration in the early evolution model of Arabian Sea has been examined through the paleogeographic reconstructions. In view of this, as followed for the other continental blocks in this study, the 2000 m bathymetry contour surrounding the Laccadive Plateau region have been used to define the extent of the Laccadive Plateau continental block (Fig. 5.1).

(d) Seychelles block

In the Western Indian Ocean Seychelles-Mascarene Plateau is an arcuate system of shallow banks and small islands. It is approximately 2600 km long from its northwestern to southwestern end, and consists of the Seychelles Bank, the Mascarene Plateau (comprising the Saya de Malha Bank, the Nazareth Bank, the Cargados Carajos Bank), and Mauritius Island. The Seychelles Bank is separated from the Saya de Malha Bank by a 1500 m deep saddle (Mart, 1988). Based on the results of seismic refraction (Davies and Francis, 1964; Francis et al., 1966) and geological studies (Baker and Miller, 1963), the Seychelles Bank was found to consist of Precambrian granites and therefore established as a continental fragment. However, the extent of this continental fragment towards the Saya de Malha Bank and beyod over the Mascarene Plateau is not known as yet. In view of this, it became necessary for this study, to decide how much extent of the Seychelles-Mascarene Plateau will have to be considered as part of Seychelles continental block. In this study, the Seychelles continental block (Fig. 5.4) is considered to consist of the Seychelles Bank and part of the saddle between the Seychelles Bank and the Saya de Malha Bank. The saddle like region existing between the Seychelles Bank and the Saya de Malha Bank has been considered as continental, because seismic data coupled with the satellite gravity data (Hayling, 1992 quoted by Plummer, 1996) suggested the presence of

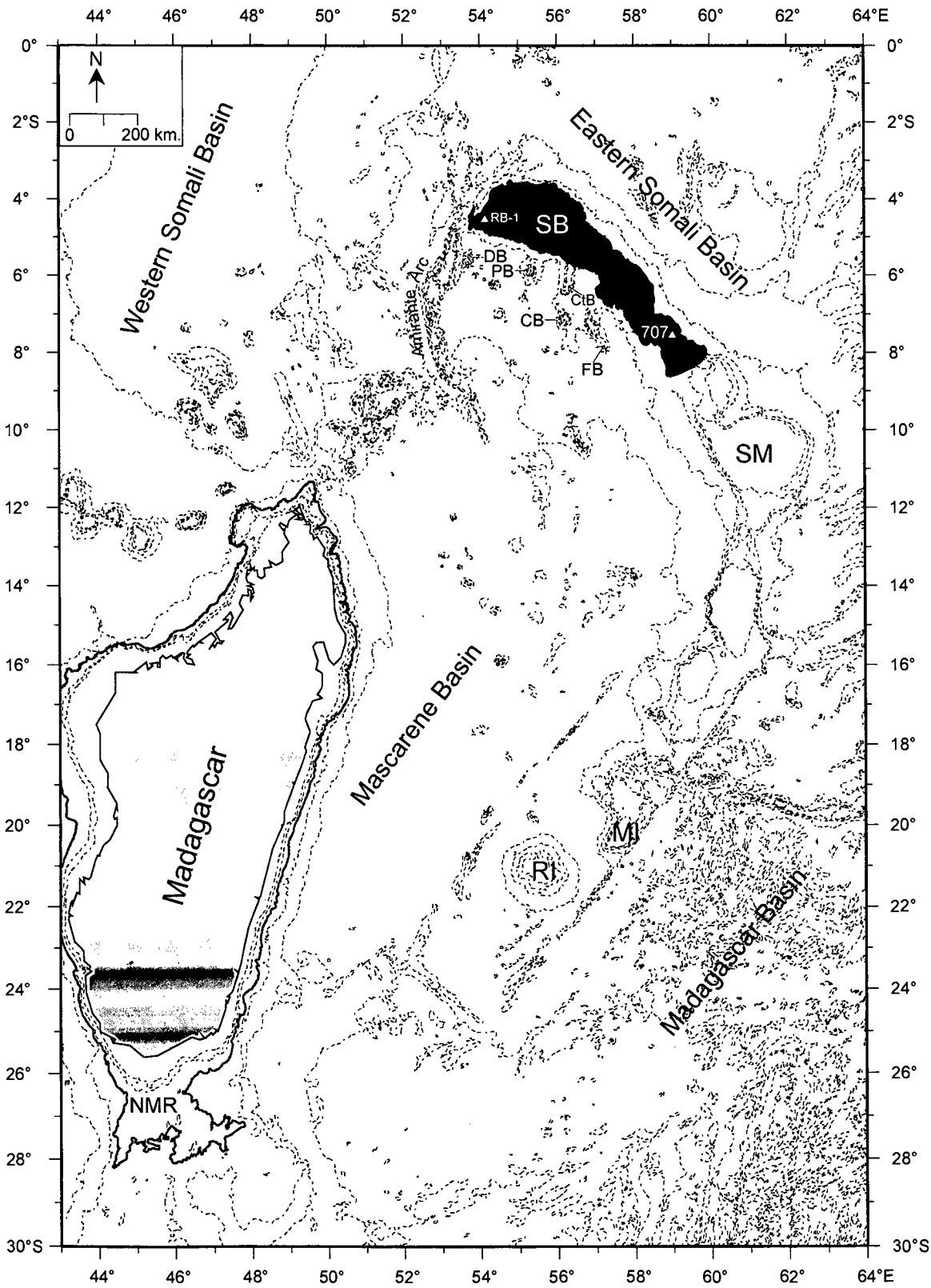

Fig. 5.4 The extent of Madagascar and Seychelles continental blocks defined by the 2000 m isobath (thick blue line). SB: Seychelles Bank; CtB: Constant Bank; CB: Coevity Bank; DB: Desroches Bank; FB: Fortune Bank; PB: Platte Bank; RB: Reith Bank; SM: Saya de Malha Bank; MI: Mauritius Island; RI: Reunion Island; NMR: Northern Madagascar Ridge.

tilted fault blocks of a rifted continental crust near the location of ODP-707. The Saya de Malha Bank has not been included as part of Seychelles as difference in opinion (Duncan and Hargraves, 1990; Plummer, 1996) exists about its genesis. The Mascarene Plateau has not been included as it is considered to have been formed as a result of the motion of African plate over the Reunion hotspot (Duncan, 1981; Morgan, 1981). The protrusions surrounding the Seychelles Bank, such as Amirante arc, Constant Bank, Coevity Bank, Platte Bank, Desrouche Bank and Fortune Bank, have not been included as their genesis still remain to be clearly understood.

(e) Madagascar block

As in the case of Indian continental block, the 2000 m. isobath has been considered as the boundary (Fig. 5.4) to define the extent of Madagascar continental block. It is observed that the northern part of the Madagascar Ridge get included within the extent of the so defined Madagascar continental block. Considering northern part of Madagascar Ridge as a part of Madagascar does not appear unreasonable as based on paleogeographic reconstruction studies, Sahabi (1993) and Reeves et al. (2002) suggested a continental origin of northern Madagascar Ridge. Several other publications (Goslin et al., 1980; Schlich, 1982) also suggested that the northern Madagascar Ridge probably represents area of thinned continental crust. It is interesting to note that the eastern limit of the Madagascar continental block is characterized by an unusual steep and straight edge over considerable length. This straight edge has been interpreted by several authors (Barron, 1987; Lawver et al., 1999) as an evidence of transform motion between India and Madagascar that is believed to have been taken place between 160 and 105 Ma.

5.3 India-Madagascar juxtaposition models

(a) Existing models for India–Madagascar juxtaposition at chron 34ny

For tracing the India–Madagascar separation one need to start with the India–Madagascar juxtaposition. The aspect of paleogeographic juxtaposition of India and Madagascar has been directly addressed or indirectly depicted in number of studies. The qualitative juxtaposition models (Crawford, 1978; Katz and Premoli, 1979; Agrawal et al., 1992; Windley et al., 1994; Menon and

Santosh, 1995; Dissanayake and Chandrajith, 1999; Pradeepkumar and Krishnanath, 2000; Torsvik et al., 2000; Anil Kumar et al., 2001) are based on the colinearity of inferred comparable onshore shear zones, geological domains or continental scale MAGSAT and gravity anomalies (Fig. 5.5a-l). On the other hand quantitative models are based on estimated finite rotation parameters. Based on the evaluation of those qualitative models by Yoshida et al. (1999) and other recent studies (Chetty and Bhaskar Rao, 2004; Radhakrishna et al., 2004), it appears that there is a broad agreement about the comparable geological units and shear zones of southern India and Madagascar, however precise conjugate correspondence of these features is still awaited. As according to Norton and Sclater (1979) the separation of India and Madagascar started shortly before anomaly 34 (83.0 Ma) time, therefore, in the following paragraph, some of the quantitative models (Norton and Sclater, 1979; Morgan, 1981; Besse and Courtillot, 1988; Müller et al., 1993) with focus on India–Madagascar relative position for the time of this anomaly 34 have been briefly discussed and shown that the relative position of India and Madagascar vary in different models.

For this purpose four paleogeographic reconstructions (Fig. 5.6a-d) have been prepared, for the time of younger bound of anomaly 34n (i.e. chron 34ny; 83.0 Ma), using finite rotation parameters provided in four studies (Norton and Sclater, 1979; Morgan, 1981; Besse and Courtillot, 1988; Muller et al., 1993). Since the age corresponding to various magnetic isochrons in those studies are based on different geomagnetic timescales, therefore, for using those finite rotation parameters in this study, the ages have been re-assigned according to the geomagnetic time scale of Cande and Kent (1995). It is generally agreed that the magnetic anomaly 34n identified in the southern Mascarene Basin represents the oldest magnetic anomalies formed shortly after the India–Madagascar separation. Therefore, the paleo-ridge positions at chron 34ny and paleo-transforms have been marked using the available (Schlich, 1982; Dyment, 1991; Bernard and Munschy, 2000) magnetic anomaly identifications close to Madagascar in the Mascarene Basin and considered them fixed to the African plate while generating reconstruction maps.

In the reconstruction (Fig. 5.6a) following Norton and Sclater's (1979) model, it is observed that the 2000 m isobaths off Indian coast as well off

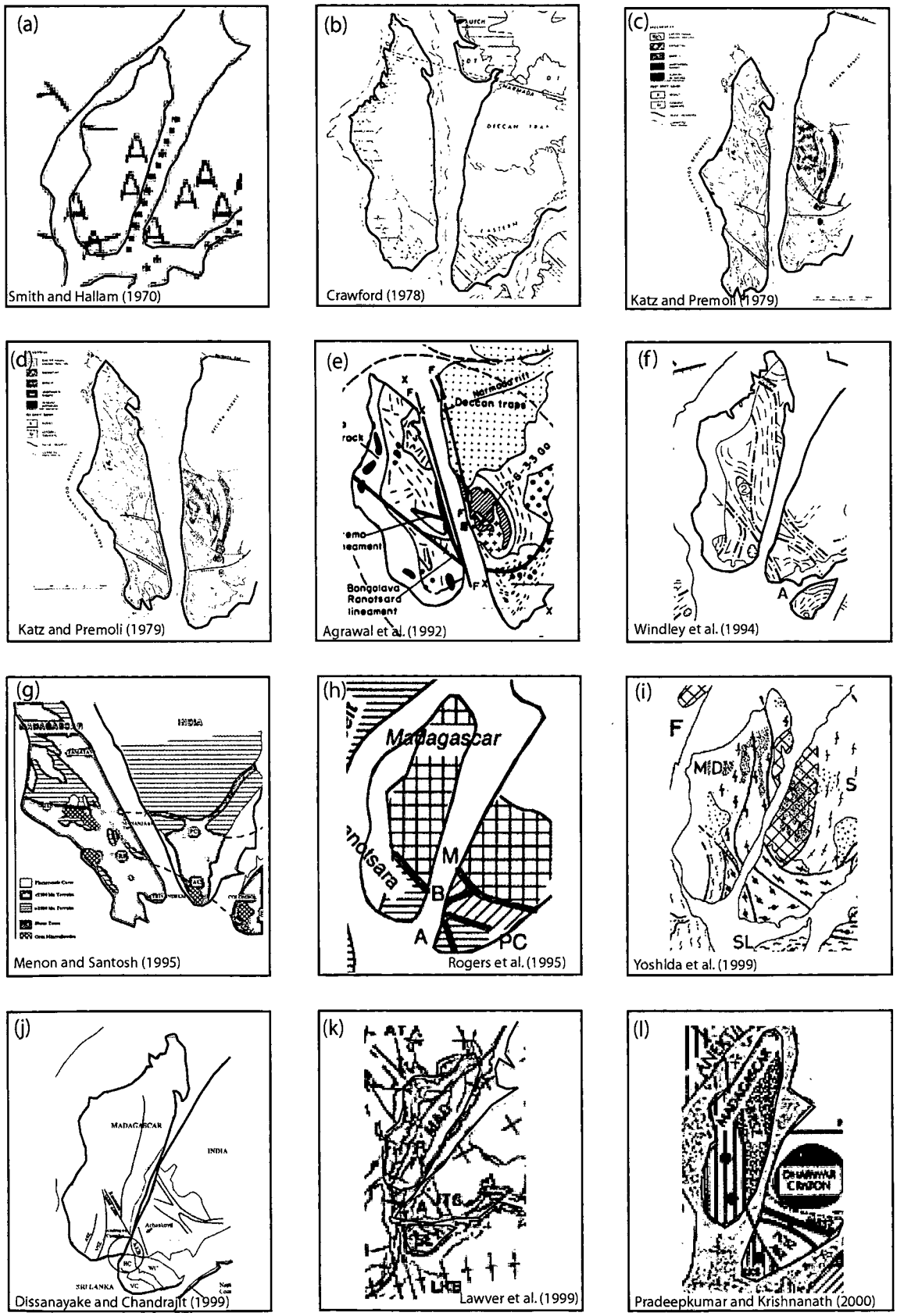

Fig. 5.5 Qualitative models proposed in various studies describing the India-Madagascar juxtaposition in the Gondwanaland configuration, arranged chronologically in terms of their year of publications. Models a, g, h, j and l are based on similarities in geological domains, while models b, c, d, f, i and k are based on colinearity of inferred comparable onshore shear zones. The model e is based on continental scale MAGSAT and gravity anomalies.

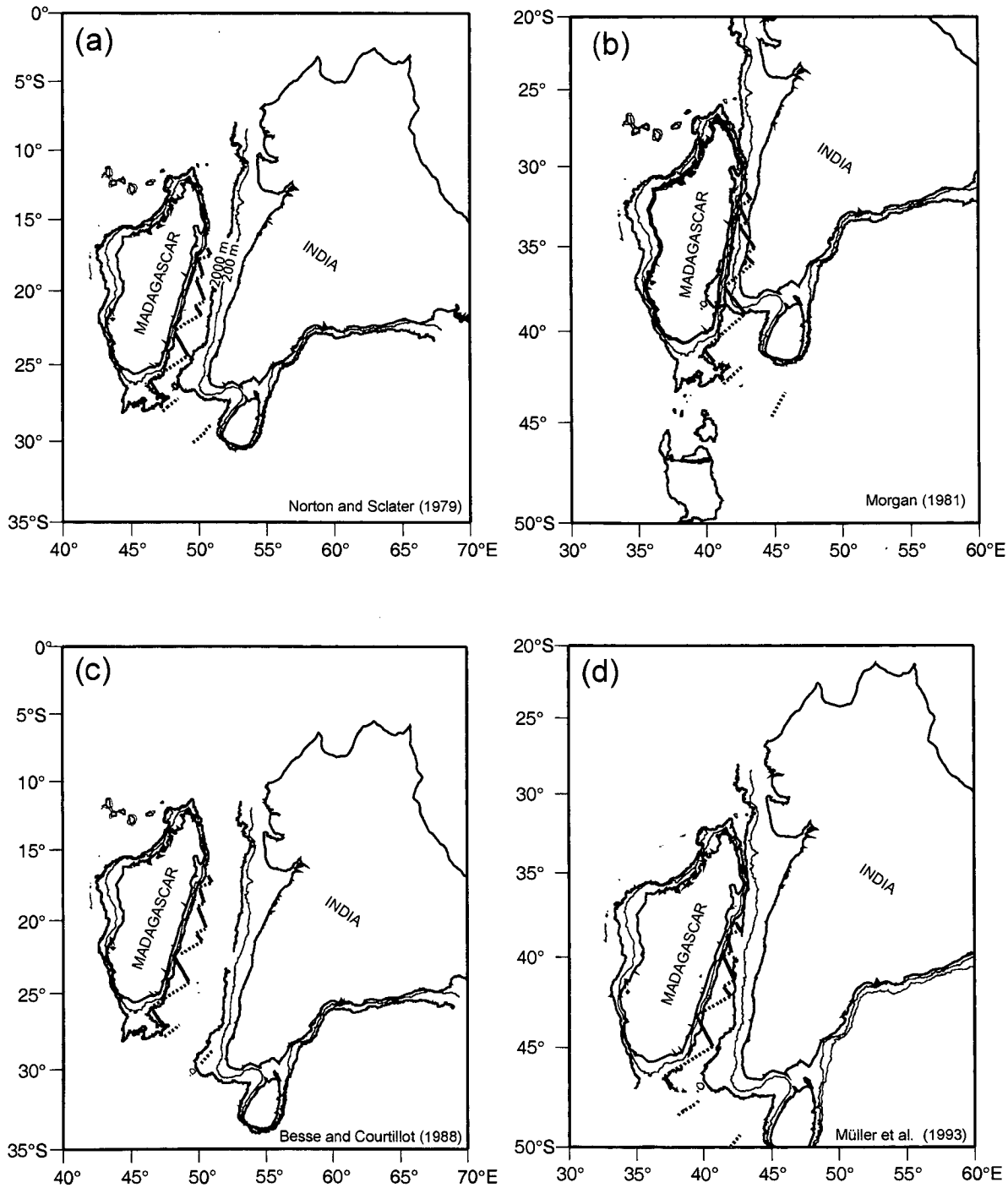

Fig. 5.6 Various paleogeographic reconstruction models to show the varied juxtaposition of India with Madagascar at chron 34ny (83.0 Ma). Models (a), and (c) are in fixed Africa reference frame while models (b) and (d) are in fixed hotspot reference frame. Locations of chron 34ny paleo-spreading ridge segments are shown as thick red lines and transform segments by dashed lines. The 200 m and 2000 m isobaths surrounding India and Madagascar are shown by thin black lines and thick blue lines respectively.

Madagascar coast are symmetric about the chron 34ny ridge position and there is not much offset between the southern tips of India and Madagascar. The reconstruction following Morgan's (1981) model provides a close-fit (Fig. 5.6b) for India and Madagascar without any intervening gap at 83.0 Ma itself and the paleo-ridge overlaps Indian landmass at places. Further, in this reconstruction, it is also observed that the southern tip of Madagascar is much south of the southern tip of India and the 2000 m isobath off the Indian coast overlaps the Madagascar mainland. Reconstructions following model of Besse and Courtillot (1988) depict (Fig. 5.6c) the 83.0 Ma paleo-ridge positions closer to 2000 m isobath off Madagascar as compared to the same off Indian coast. The reconstruction model (Fig. 5.6d) following Müller et al. (1993) shows that the 2000 m isobaths off India as well off Madagascar are more or less symmetric about the paleo-ridge position, but towards north Madagascar is much closer to India. It thus appears that the models of Besse and Courtillot (1988) and Morgan (1981) are not appropriate for the India–Madagascar relative motion as they place the chron 34ny ridge axis asymmetrically with respect to the conjugate 2000 m isobaths. Based on the above exercise, it is believed that the model of Norton and Sclater (1979) provides a better approximation of the India–Madagascar pre-chron 34ny relative motion as it can also accommodate the microcontinental fragments in the pre-drift India–Madagascar juxtaposition model.

(b) Improved model for India-Madagascar juxtaposition in the immediate pre-drift scenario

Fig. 5.7a presents a reconstruction map of India–Madagascar juxtaposition for chron 34ny (83.0 Ma), which has been prepared using the rotation parameters of Norton and Sclater (1979). As evidenced from this reconstruction map, it is believed that the shape of the 2000 m bathymetry contours off the southwest Indian coast and southeast Madagascar coast strongly suggest the conjugate nature of the terrace off Trivandrum and the bathymetry notch in the northern Madagascar Ridge. As mentioned earlier, it is generally believed that the separation of India and Madagascar started shortly before chron 34ny and based on dated onshore volcanics this separation is considered to have been initiated around 88–91 Ma (Storey et al., 1995; Torsvik et al., 2000; Pande et al., 2001; Anil Kumar et al., 2001). If that is the case, then India and Madagascar were

much closer as compared to their position in the chron 34ny reconstruction (Fig. 5.7a). In view of this, attempt has been made to reconstruct Madagascar and India for a pre-chron 34ny close-fit configuration. Since the finite rotation parameters to describe this motion are not readily available in the Norton and Sclater (1979) model, so it was tried to bring a closer fit of India and Madagascar by extrapolation, considering the same pole and rate of rotation as of chron 34ny. This exercise provided a closer fit of India and Madagascar at 86.5 Ma and interestingly depicted a near fit (with slight overlap) of the terrace off Trivandrum with the bathymetric notch of the northern Madagascar Ridge. Attempt has been made to improve this fit by trial and error and believed to have obtained a reasonably good fit (Fig. 5.7b) of those terrace and notch for the same 86.5 Ma using a slightly modified Euler pole (Table 5.1) of Norton and Sclater (1979) in fixed Madagascar reference frame. As mentioned by Storey et al. (1995), the eastern part of the northern Madagascar Plateau and a bathymetric high on the west side of the southern tip of India was inferred by Dyment (1991) to be conjugate with respect to the Mascarene Basin spreading ridge. In view of this, it is tempted to believe that this terrace off Trivandrum (TOT) and the bathymetric notch (BN) of northern Madagascar Ridge are the conjugate features inferred by Dyment (1991). It may be mentioned here that so far not enough chron 34ny magnetic isochrons have been mapped in the vicinity of the northern Madagascar Ridge but published maps do suggest the existence of traces of several fracture zones. Considering the disposition of this terrace (TOT) and bathymetric notch (BN) with respect to the trends of paleo-ridge and paleo-transform segments in the reconstruction map (Fig. 5.6a) it may not be unreasonable to believe that the shape of those conjugate features were controlled by the ridge and transform segments of the paleo-ridge which existed at 86.5 Ma.

According to Storey et al. (1995) the Madagascar Ridge is believed to be a volcanic emplacement related to the motion of the African plate over the Marion hotspot since 90 Ma. However, as explained earlier, the crust underlying the northern domain of the Madagascar Ridge is considered to be anomalous as it is neither purely continental nor of oceanic affinity. Perhaps the terrace off Trivandrum also has a similar nature of crust as the conjugate areas of the northern Madagascar Ridge and probably represents areas of thinned continental

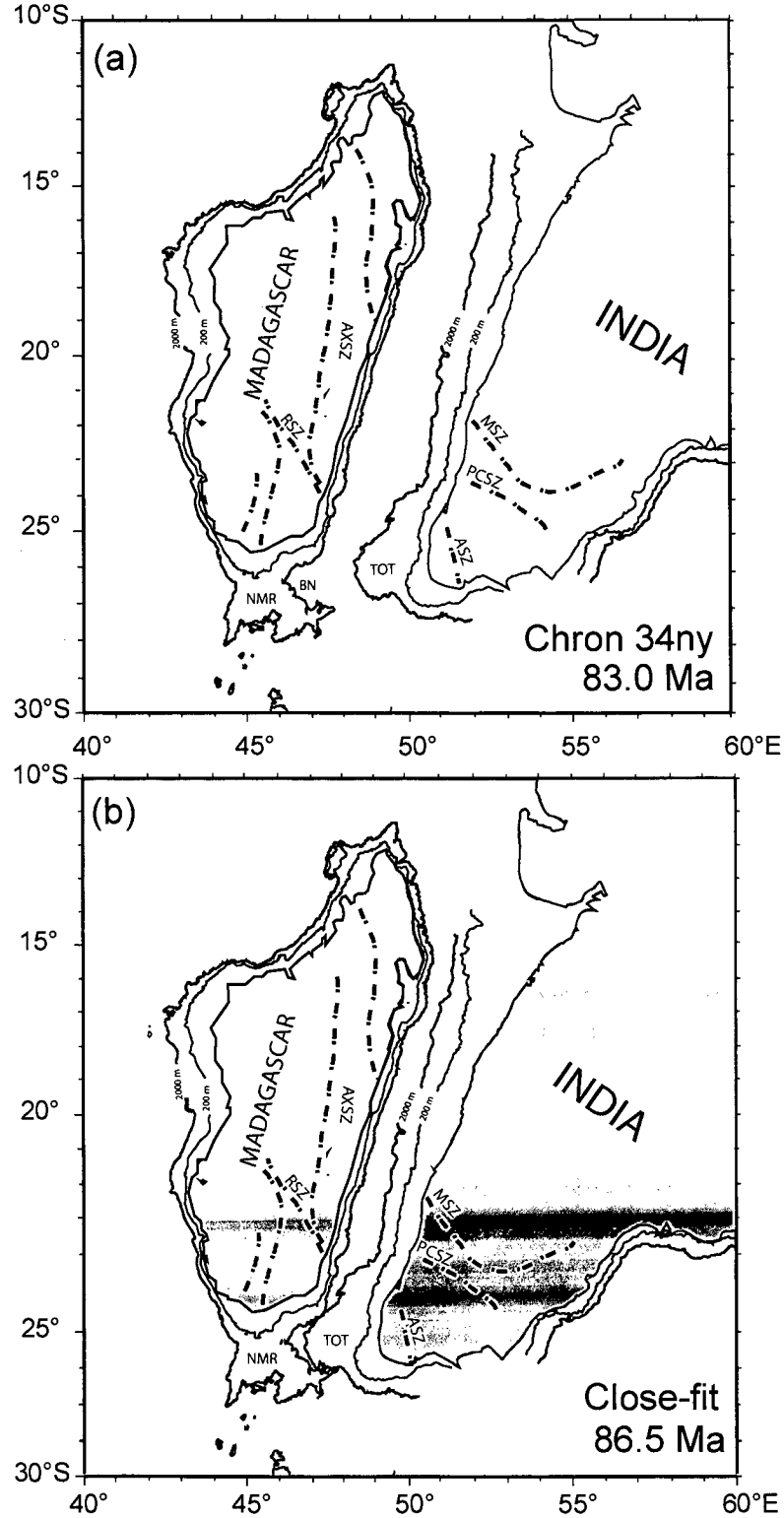

Fig. 5.7 Paleogeographic reconstruction of India and Madagascar in fixed Madagascar reference frame. (a) at 83.0 Ma following Norton and Sclater (1979) rotation parameters, (b) a plausible close-fit at 86.5 Ma following the additional rotation parameters suggested in this study (Table 5.1). Land portions of India and Madagascar are shaded, surrounding 200 m isobaths are shown by thin black lines and 2000 m isobaths are shown by thick blue lines. Locations of onshore shear zones simplified after Meissner et al. (2002) and Windley et al. (1994). TOT: Terrace off Trivandrum, BN: Bathymetric notch; NMR: Northern Madagascar Ridge, ASZ: Achankovil Shear Zone, PCSZ: Palghat-Cauvery Shear Zone, MSZ: Moyar Shear Zone, RSZ: Ranotsara Shear Zone, AXSZ: Axial Shear Zone.

crust on which at places Marion hotspot related volcanics might have been emplaced.

5.4 India-Seychelles juxtaposition models

(a) India-Seychelles juxtaposition as implied from existing models

Based on the marine magnetic investigations, several researchers depicted the configuration of India and Seychelles in their paleogeographic reconstruction models of chron 28, and they considered Seychelles to have been welded with Indian block prior to this period. However, most of these studies, apparently due to their emphasis on broader perspective, did not provide specific attention to the Seychelles continental block in their paleogeographic reconstruction models older than chron 28.

The most recent information about the mapped seafloor spreading magnetic lineations in the conjugate Arabian and Eastern Somali basins are available from Chaubey et al. (2002a). They inferred that the oldest magnetic lineations available in the Arabian Basin correspond to chron 28ny (62.499 Ma). In the north this lineation is located immediately south of the Laxmi Ridge and its conjugate is located immediately north of the Seychelles. Therefore, the conjugate Arabian and Eastern Somali basins can be considered to have been formed since chron 28ny as a result of rifting and subsequent drifting between the Seychelles and the Laxmi Ridge. Using these mapped magnetic lineations, Royer et al. (2002) have estimated the finite rotation parameters to describe this relative motion between the Laxmi Ridge and the Seychelles. However, the oldest period for which they have provided the finite rotation parameter is for chron 27ny (60.920 Ma), and the paleogeographic reconstruction model at this time shows (Fig. 5.8a) that a triangular wedge of oceanic crust exists between the Laxmi Ridge and Seychelles continental blocks. In the present study, an attempt has been made to estimate the finite rotation parameter for obtaining a close-fit juxtaposition model of the Laxmi Ridge and Seychelles by closing this triangular wedge of oceanic crust. An age of 62.8 Ma has been assigned for this close-fit. This time was estimated from the width of the normally magnetized block corresponding to chron 28ny, which exists southward of the Laxmi Ridge with following considerations that; (i) this crust was created only during younger part

of the chron 28n and (ii) the spreading rate during this period was same as that during the subsequent chron 27n in the Arabian Basin. This model for close-fit juxtaposition shows (Fig. 5.8b) that the Seychelles and Laxmi Ridge were welded together and remained in the form of Greater Seychelles (Seychelles+Laxmi Ridge block) during the period older than 62.8 Ma. From this reconstruction model, it is observed that at that time there existed a substantial swath of deep offshore region between the Greater Seychelles and the Indian continental block. The observation of course does not clarify whether during the period older than 62.8 Ma, the relative position of the Laxmi Ridge (as also the Greater Seychelles) with respect to India, remained unchanged or not. An exercise carried out in this study suggests consideration of a Laxmi Ridge (or Greater Seychelles) much closer to India than their relative position at 62.8 Ma. In this exercise, a paleogeographic reconstruction model for chron 34ny (83.0 Ma) have been made, where the Laxmi Ridge (or Greater Seychelles) have been retained in the same position relative to India as was at 62.8 Ma. It shows (Fig. 5.9) that the northern part of the Greater Seychelles moves west of Madagascar mainland and the southern part overlap with the Madagascar continental block. This observation thus strongly suggest that the Greater Seychelles was closer towards the Indian continental block during the period prior to 62.8 Ma and the deep offshore regions existing between the Greater Seychelles and the Indian continental block have been shaped by the relative motion between these two features.

(b) Improved model for close-fit India-Seychelles juxtaposition

As shown in the preceding section, the gap of deep offshore region (comprising mainly the Offshore Indus and Laxmi basins), between the Greater Seychelles and Indian continental block need to be closed for the period older than 62.8 Ma. This closing could be done either by considering the region to have been formed only by rifting or by rifting followed by seafloor spreading, during the period older than chron 28ny (62.499 Ma). As described in previous chapter, the nature of the crust underlying the Offshore Indus Basin and Laxmi Basin regions have been interpreted in this study as oceanic crust created by two-limbed seafloor spreading, which became extinct at around 61 Ma. Based on those results, it is tempted to believe that the moving away of Greater Seychelles from

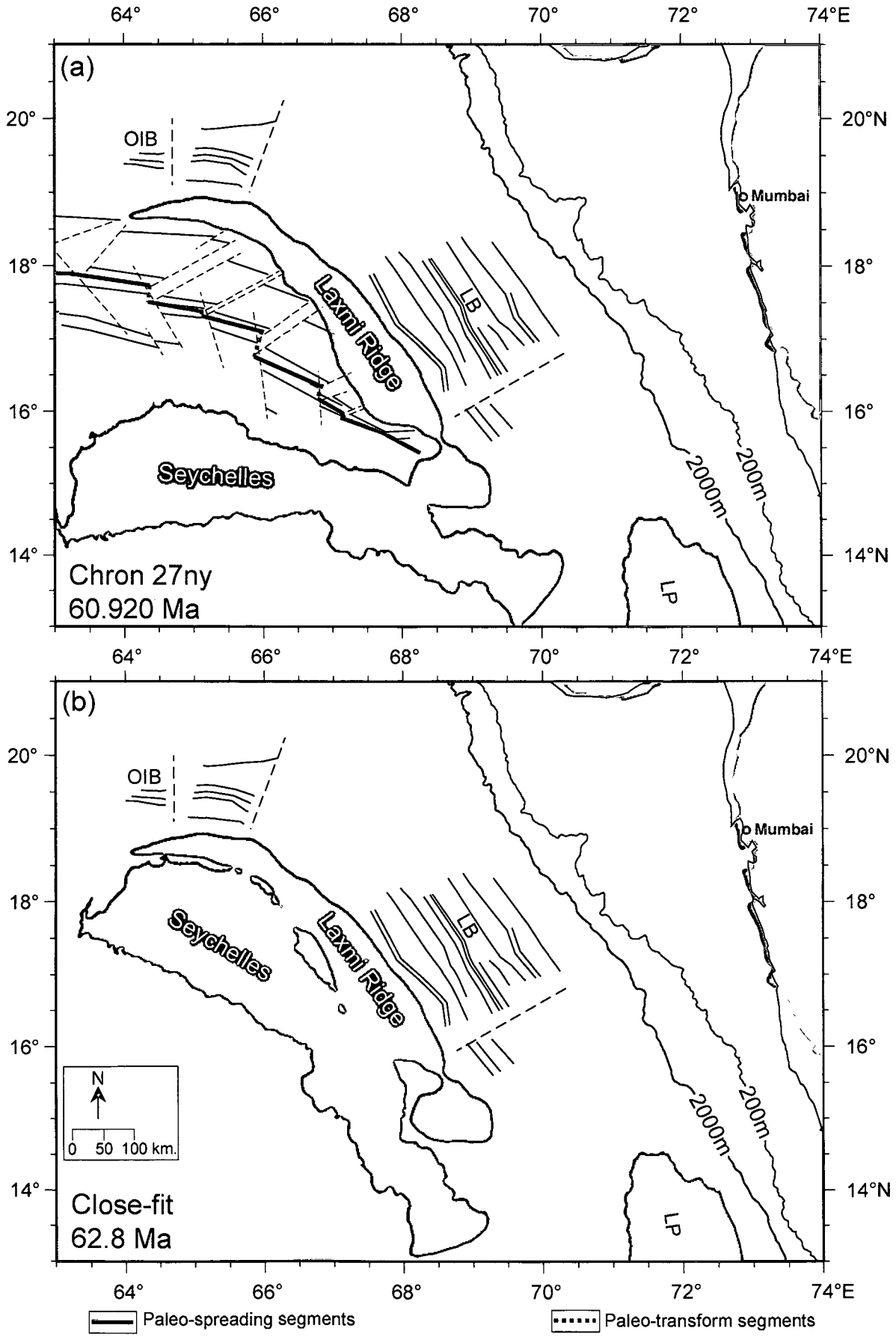

Fig. 5.8 The paleogeographic reconstruction models for configuration of Seychelles and Laxmi Ridge in fixed India reference frame. (a) at chron 27ny time following Royer et al. (2002) and (b) a close-fit Seychelles-Laxmi Ridge juxtaposition scenario as suggested in this study. OIB: Offshore Indus Basin; LB: Laxmi Basin; LP: Laccadive Plateau.

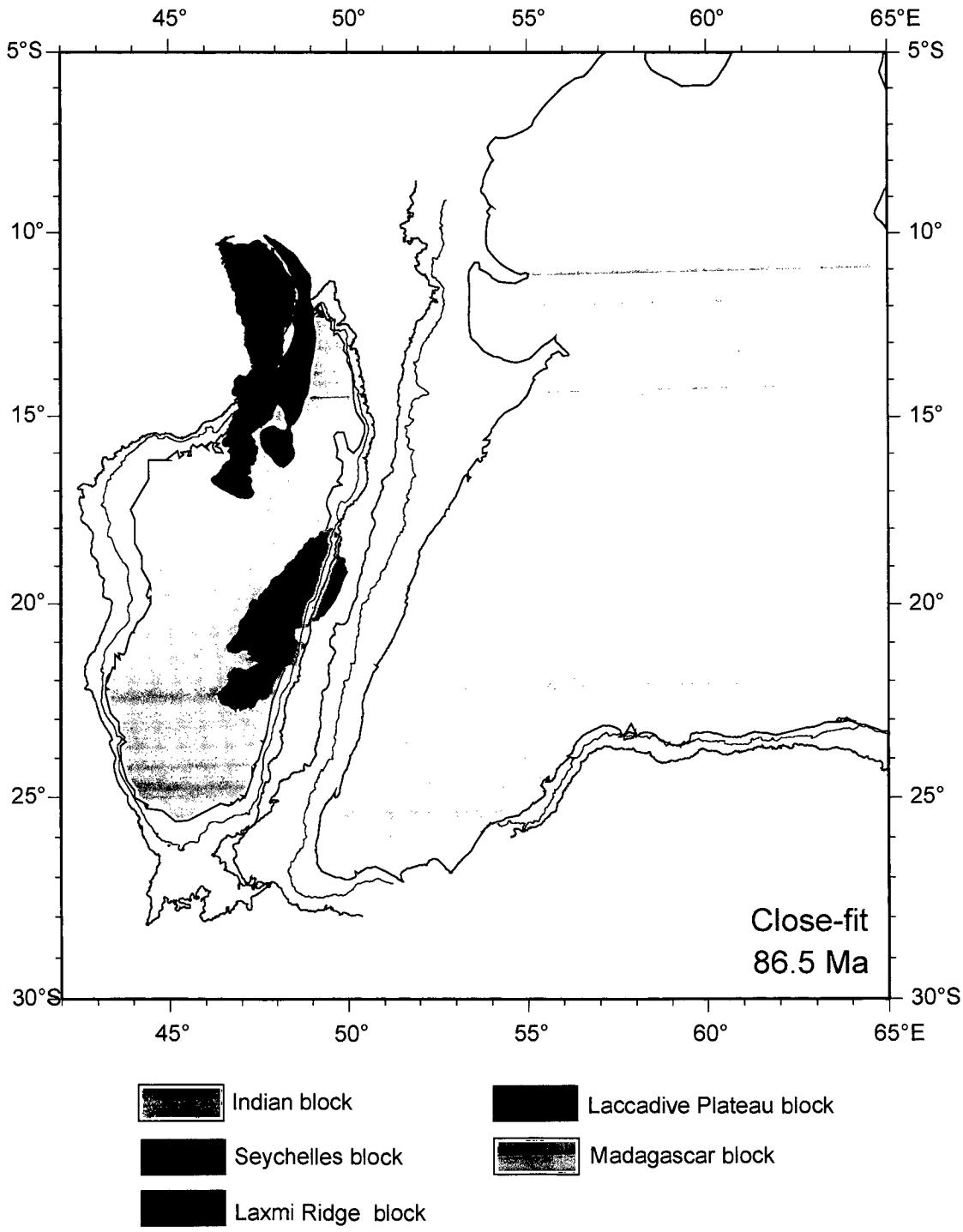

Fig. 5.9 Paleogeographic reconstruction model for India-Madagascar close-fit juxtaposition at 86.5 Ma in fixed Madagascar reference frame. In this model, the Laccadive Plateau and the Laxmi Ridge have been kept in their present position relative to India. Seychelles is shown with the Laxmi Ridge as both were together at that time. Overlapping of Laxmi Ridge (as well Seychelles) and the Laccadive Plateau with Madagascar suggests that the Laxmi Ridge and the Laccadive Plateau were much closer to Indian mainland at that time and have drifted to their present position subsequently.

Indian continental block was resulted due to an episode of rifting followed by two-limbed seafloor spreading. Therefore, attempt have been made to estimate the finite rotation parameters, which can describe the relative motion of Greater Seychelles with Indian continental block, from the mapped seafloor spreading magnetic lineations of the Laxmi and Offshore Indus basins inferred in the present study.

The updated magnetic isochron map of the study area (Fig. 5.10) shows that the magnetic isochrons in the Offshore Indus Basin are in the E-W direction while those in Laxmi Basin region are in NNW-SSE direction. This implies that the direction of spreading in Offshore Indus and Laxmi basins were quite different. The Laxmi Basin region appears to have been created by the relative motion between Laxmi Ridge and India and the Offshore Indus Basin region appears to have been created by the relative motion between Laxmi Ridge and Pakistan. These differing directions of spreading in the Laxmi and Offshore Indus basins observations necessitate assuming a three-plate scenario to describe the India-Greater Seychelles juxtaposition by closing the Offshore Indus and Laxmi basins. It is therefore necessary to look for the three plates, the three plate boundaries separating them and the triple junction connecting these plate boundaries. The spreading centres in the Offshore Indus and Laxmi basins obviously represent the two plate boundaries of this triple junction. It appears that considering the Narmada Rift, as the third arm of the triple junction is not unreasonable due to several reasons. Although there exists three rift systems (Kutch Rift, Cambay Rift and Narmada Rift) in the western part of adjacent Indian mainland, but location and orientation wise, the Narmada Rift appear to be a more reasonable candidate for this third arm. The timing of initiation of Narmada Rift at Late Cretaceous, also appear to be compatible to this three plate scenario as the spreading in the Laxmi Basin and Offshore Indus Basin arms were inferred to be taken place during the same period. In such a scenario, the paleo-ridge positions in the Offshore Indus and Laxmi basins may represent the ridge axes of a ridge-ridge-rift (R-R-r) triple junction, while the Narmada Rift may represent a failed rift of that system. Such a proposition, although qualitatively, have also been forwarded by Malod et al. (1997). If the above assumption about the presence of a triple junction is correct, then it becomes necessary to consider the

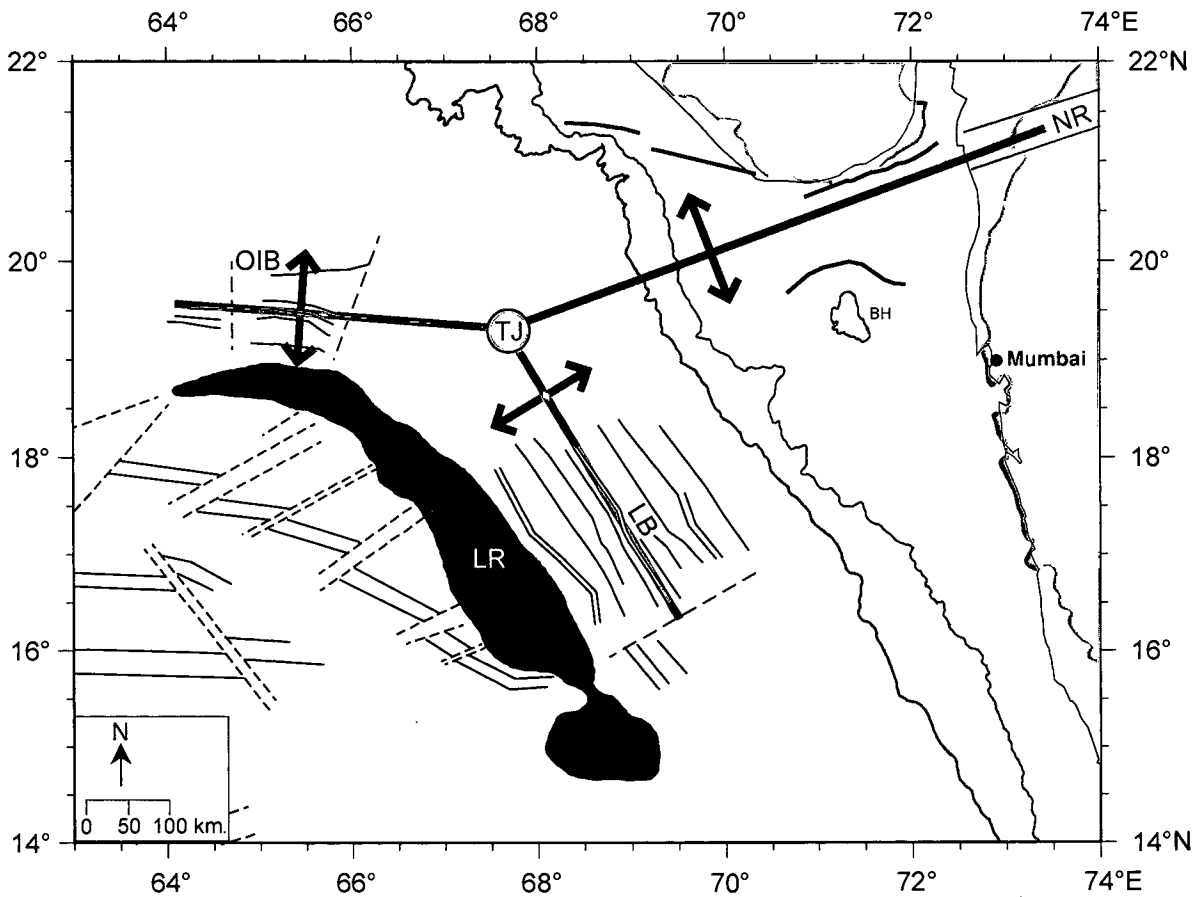

Ridge axis of the Offshore Indus and Laxmi basins representing the two arms of a probable triple junction.

Rift axis through Narmada Rift representing one arm of a probable triple junction.

Direction of spreading/ extension by rifting along the arms of a probable triple junction

Fig. 5.10 Updated magnetic isochron map of the study area depicting different spreading directions in the Laxmi and Offshore Indus basins. Considering different directions of the spreading centres in these basins along with the adjacent failed Narmada Rift, a Ridge-Ridge-rift triple junction appears to have existed in this region between 86.5 Ma to 61 Ma. TJ: Triple junction. Other details are as in Fig. 4.1.

Indian continental block at that time (prior to 61 Ma) as two separate blocks across the Narmada Rift. Such two blocks have been considered in this study as the northern Indian block (NIB) and the southern Indian block (SIB). In view of such considerations the oceanic crust in the Offshore Indus and Laxmi basins can be explained as results of relative motions by seafloor spreading of Greater Seychelles from the northern Indian block and the southern Indian block respectively. The relative motion between NIB and SIB was accommodated by extension of continental crust along the Narmada Rift. In the present study, these three relative motions have been described in terms of quantitative paleogeographic reconstruction models and an improved model have been provided for the India-Seychelles juxtaposition in their pre-drift juxtaposition scenario.

In the case of India-Seychelles juxtaposition, the paleogeographic reconstruction models in the fixed southern Indian block frame or in fixed northern Indian block frame can be prepared either by closing the Laxmi Basin and Narmada Rift without considering the Offshore Indus Basin, or by closing the Laxmi Basin and Offshore Indus Basin without considering the Narmada Rift. In the case of Offshore Indus Basin, the sequence of magnetic anomalies is very short and well-constrained fracture zone are not available which makes estimation of Euler parameters by transform trend method difficult. In view of this, the reconstruction models have been prepared by closing the Laxmi Basin and Narmada Rift. However, the mapped seafloor spreading linear magnetic anomalies in the Offshore Indus Basin have been used to validate the reliability of the model in such a way that the corresponding conjugate magnetic isochrons coincide with the paleo-ridge axis in the Offshore Indus Basin.

The finite rotation parameters (Table 5.3) describing the relative motion of northern Indian block from the southern Indian block have been estimated based on trial and error. The timing of 86.5 Ma have been assumed for the close-fit juxtaposition of these two blocks as that time is considered in this study as the time of initiation of drifting of India-Madagascar-Greater Seychelles continental blocks from each other. Extension across Narmada Rift has been assumed to have been ceased at 61 Ma as according to present study that was the time at which cessation of seafloor spreading in the other two arms of the system (i.e.,

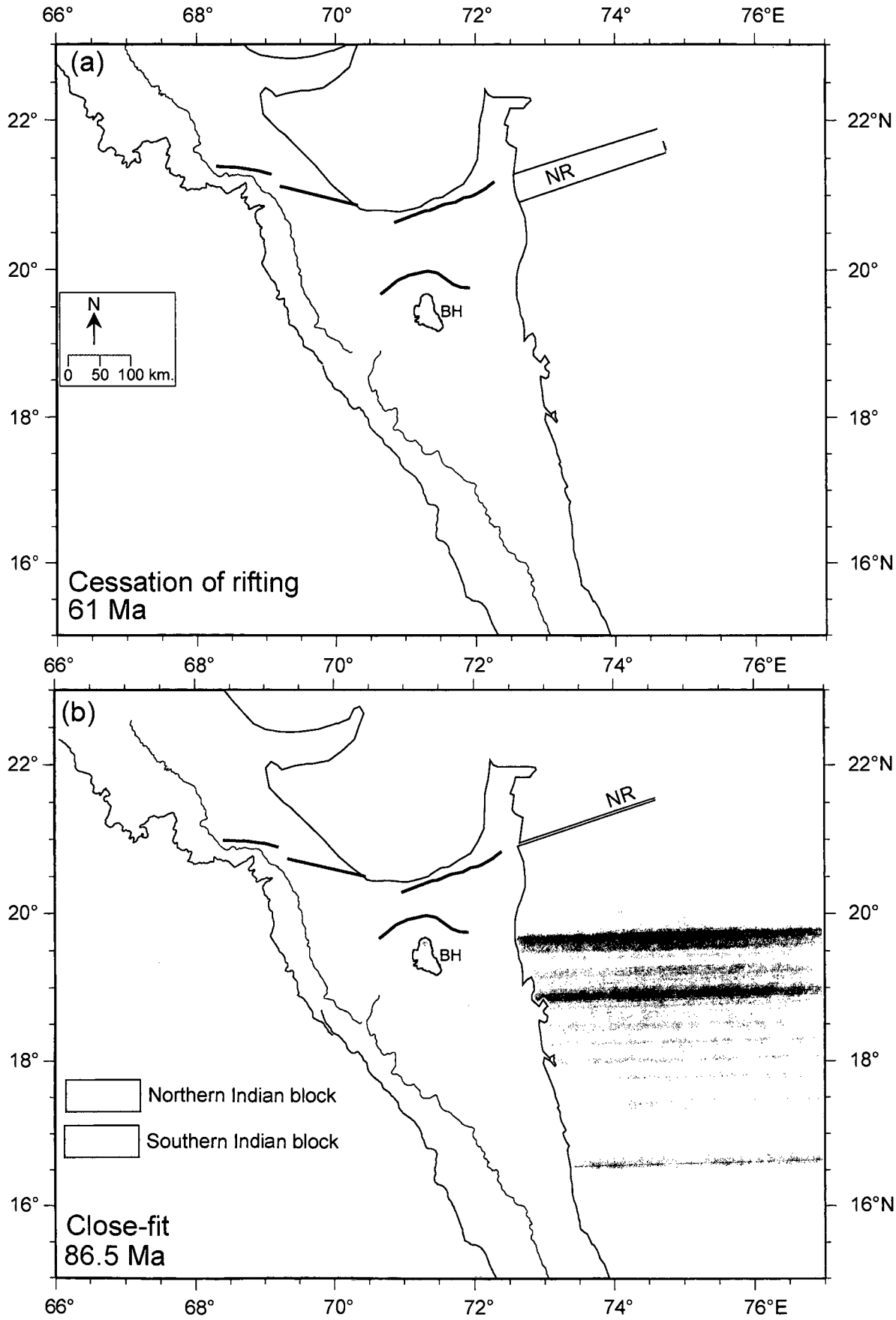

Fig. 5.11 The paleogeographic reconstruction models depicting the juxtaposition of northern Indian block with the southern Indian block in the fixed southern Indian block reference frame. (a) at ~61 Ma, when Narmada Rift became a failed rift arm. (b) at 86.5 Ma, when extension (rifting) started along Narmada Rift.

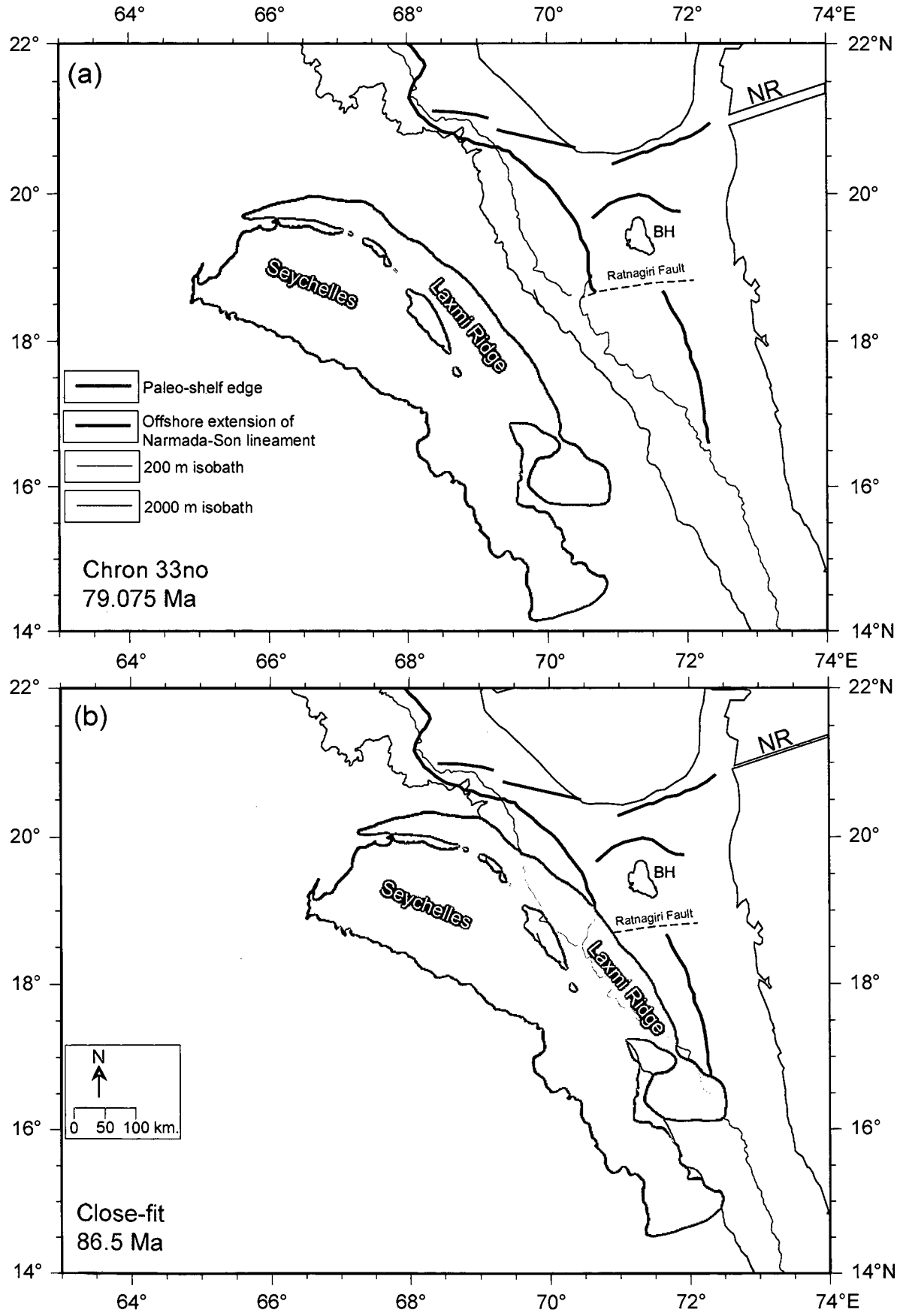

Fig. 5.12 Paleogeographic reconstruction models of Greater Seychelles and India in fixed southern Indian block reference frame. (a) for chron 33no and (b) for close-fit juxtaposition at ~86.5 Ma.

across the Laxmi and Offshore Indus basins) took place. Following this consideration, for the period younger to 61 Ma, the northern and southern Indian blocks have been maintained as a single welded continental block (Fig. 5.11a, b).

The finite rotation parameters, which describe the relative motion of Greater Seychelles with southern Indian block, have been estimated using the mapped magnetic isochrons in the Laxmi Basin. The Laxmi Basin consists of well-developed linear magnetic anomalies, however, it appears that the locations of fracture zone in this region is not well constrained. Therefore, based on the procedure detailed in the section 3.3.3d, the finite rotation parameters (Table 5.4) describing the relative motion of Greater Seychelles with the southern Indian block have been estimated for different chrons by assuming hypothetical fracture zones orthogonal to the mapped magnetic lineations. As the oldest magnetic isochron inferred in the Laxmi Basin region corresponds to chron 33no (79.075 Ma), so the finite rotation parameters could be obtained only up to chron 33no. However, the paleogeographic reconstruction for chron 33no (Fig. 5.12a) shows that a still closer-fitting India-Greater Seychelles juxtaposition could be obtained in a pre-chron 33no configuration. In view of this attempt was made to obtain finite rotation parameters for a pre-chron 33no close fitting India-Greater Seychelles configuration. In absence of any other information to constrain this juxtaposition, following assumptions were used as constraints;

i) Greater Seychelles was closely fit to India at the same time (ie. at 86.5 Ma), when Madagascar was also closely fitted with India.

ii) The Greater Seychelles has to be accommodated in the well constrained India- Madagascar juxtaposition model (for 86.5 Ma), which was proposed in this study and in Yatheesh et al. (2006). Further in that 86.5 Ma reconstruction, Seychelles has also to reasonably closely fit to Madgascar.

Taking these constraints into consideration, by trial and error finite rotation parameters were obtained for a close fit Greater Seychelles – India model at 86.5 Ma. However, from that model (Fig. 5.12a) it was observed that a large part of the Laxmi Ridge overlaps the 2000 m isobath of the Indian block and at places, it overlaps even the continental shelf. This overlap is observed near the continental

Table 5.1 Suggested additions to the finite rotation parameters of Norton and Sclater (1979) to obtain a close-fit India (IND) and Madagascar (MAD) in fixed Madagascar reference frame ($_{MAD}ROT_{IND}$). Other details are as in Table 3.2.

Chron	Age (Ma)	Finite rotation parameters		
		Lat. (deg.)	Long. (deg.)	Angle (deg.)
34ny	83.0	18.70	25.80	-56.00
Close-fit	86.5	18.70	26.40	-58.36

Table 5.2 Suggested additions to the finite rotation parameters of Royer et al. (2002) to obtain a close-fit Seychelles (SEY) and Laxmi Ridge (LAX) in fixed Laxmi Ridge reference frame ($_{LAX}ROT_{SEY}$). Other details are as in Table 3.2.

Chron	Age (Ma)	Finite rotation parameters		
		Lat. (deg.)	Long. (deg.)	Angle (deg.)
27ny	60.920	18.83	24.86	35.41
Close-fit	62.800	20.75	-47.00	24.75

Table 5.3 Finite rotation parameters estimated to describe the relative motions of the northern Indian block (NIB) to the southern Indian block (SIB) in fixed southern Indian block reference frame ($_{SIB}ROT_{NIB}$), by closing the Narmada rift. Other details are as in Table 3.2.

Chron	Age (Ma)	Finite rotation parameters		
		Lat. (deg.)	Long. (deg.)	Angle (deg.)
Cessation of rifting	61.0	90.00	0.00	0.00
Close-fit	86.5	26.00	94.00	1.00

Table 5.4 Finite rotation parameters estimated based on the mapped magnetic lineations in the Laxmi Basin region inferred in the present study. The rotation parameters are for the relative motion of Laxmi Ridge (LAX) with southern Indian block (SIB), in fixed southern Indian block ($_{SIB}ROT_{LAX}$) reference frame. Other details are as in Table 3.2.

Chron	Age (Ma)	Finite rotation parameters		
		Lat. (deg.)	Long. (deg.)	Angle (deg.)
Cessation of drifting	61.000	90.0	0.0	0.000
27no	61.276	54.8	12.9	0.050
28ny	62.499	54.8	12.9	0.250
31no	68.737	54.8	12.9	0.625
32n1y	71.071	54.8	12.9	0.950
32n2o	73.004	54.8	12.9	1.400
33ny	73.619	54.8	12.9	1.600
33no	79.075	54.8	12.9	2.230
Close-fit	86.500	65.0	6.0	3.800

Table 5.5 Finite rotation parameters estimated to describe the relative motions of the Laccadive Plateau (LCP) to the southern Indian block (SIB) in fixed southern Indian block reference frame ($_{SIB}ROT_{LCP}$), by closing the Laccadive Basin. Other details are as in Table 3.2.

Chron	Age (Ma)	Finite rotation parameters		
		Lat. (deg.)	Long. (deg.)	Angle (deg.)
Cessation of drifting	61.0	90.00	0.00	0.00
Close-fit	86.5	17.00	71.00	16.00

shelf off Mumbai – Saurashtra coast. As could be seen from Fig. 5.12b, even in that overlap situation the eastward limit of the Laxmi Ridge does not reach the zone of steep dips and faults (Rao and Srivastava, 1981; Srivastava and Mathur, 1984; Murty et al., 1981), which represents the boundaries of the paleo-shelf edge. This paleo-shelf edge represents the seaward extent of the Indian continental block in a better way. Further, the Laxmi Ridge is a region of extended crust; hence its unstretched extent will be much narrower. Similar way the present day shelf-slope region west of Bombay high is also a zone of extended crust, which will be much narrower in its unstretched condition. In view of these, it is opined that the close fit juxtaposition of Greater Seychelles – India at 86.5 Ma as obtained in the present study is not unreasonable.

5.5 India–Laccadive Plateau juxtaposition models

Between the Laccadive Plateau and the Indian mainland, there exists a triangular shaped deep offshore region (the Laccadive Basin). The nature of the crust underlying this region has not yet been clearly understood. If the Laccadive Plateau is a continental block as believed in some studies, then it has to be accommodated in the close fit India-Seychelles-Madagascar juxtaposition models. If the present day position of the Laccadive Plateau with respect to Indian block is maintained in the India–Madagascar paleogeographic reconstruction for chron 34ny (83.0 Ma), then a major portion of the Laccadive Plateau overlaps the Madagascar continental block (Fig. 5.9). This observation implies that the Laccadive Plateau, if it is of continental origin, then it was much closer to Indian block than its present location and the Laccadive Basin has opened due to drifting away of the Laccadive Plateau from Indian block. Whether this drifting was due to rifting only or rifting followed by seafloor spreading is not clear. Whatever may be the mechanism for this divergence, if there was a divergence of blocks then the motion can be described by finite rotation parameters. Therefore the finite rotation parameters for this motion have been estimated (Table 5.5) based on trial and error, assuming that; (i) the Laccadive Plateau was fitted closely with Indian block at the same time when Madagascar-Greater Seychelles blocks were closely fitted to India and, (ii) the drifting of Laccadive plateau stopped at the same time when drifting of the Laxmi Ridge away from Indian block stopped (Fig. 13a, b).

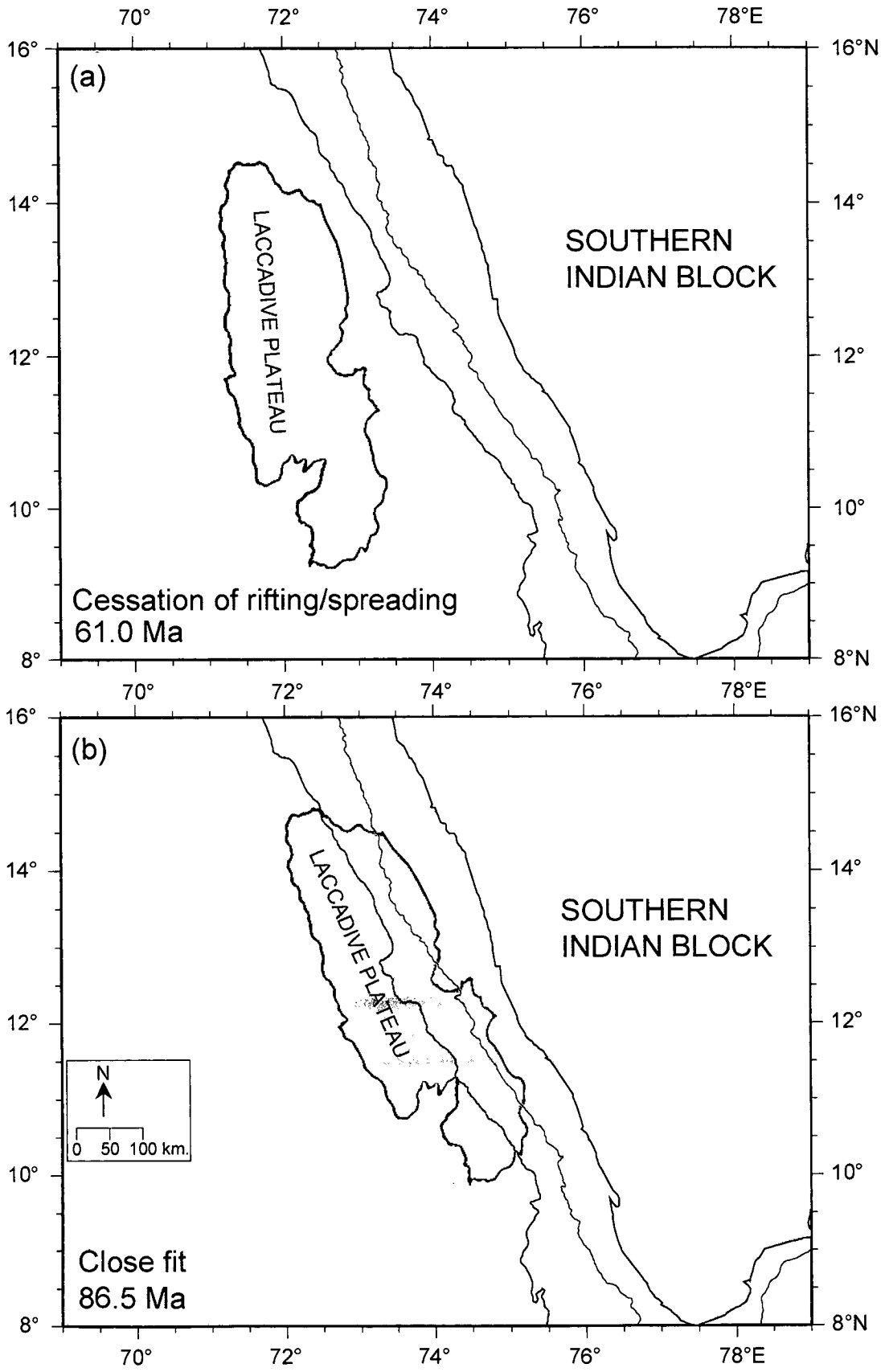

Fig. 5.13 The paleogeographic reconstruction models depicting the close fit juxtaposition of Laccadive Plateau with the southern Indian block in the fixed southern Indian block reference frame; (a) at 61 Ma when drifting of the Laccadive Plateau from the southern Indian block appears to have ended and (b) close-fit juxtaposition at 86.5 Ma.

5.6 India-Seychelles-Madagascar juxtaposition model at 86.5 Ma

Based on the exercises carried out to understand the relative motions among the various continental blocks in the study area, it appears that considering their close-fit juxtaposition at 86.5 Ma is quite reasonable. Using these rotation parameters, a paleogeographic reconstruction model has been prepared in fixed Madagascar reference frame. This reconstruction (Fig. 5.14), depict the configuration of India, Madagascar, Seychelles, Laxmi Ridge and Laccadive Plateau in a close-fit scenario at 86.5 Ma. The finite rotation parameters describing the relative motion among these continental blocks as derived or updated in this study have been presented in Table 5.1 to Table 5.5. This reconstruction has been done in two steps. First, in order to get the configuration of Greater India (SIB+NIB+SEY+LAX+LCP), the northern Indian block (NIB), Seychelles (SEY), Laxmi Ridge (LAX) and Laccadive Plateau (LCP) have been rotated to southern Indian block (SIB) using the respective finite rotation parameters of the blocks with respect to the southern Indian block (SIB). Subsequently, the Greater India thus reconstructed has been rotated to Madagascar using the finite rotation parameters (Table 5.1) describing the relative motion of India with respect to Madagascar.

In this close-fit juxtaposition model (Fig. 5.14) the Seychelles, the Laxmi Ridge and the Laccadive Plateau is accommodated, but at places some overlap could be seen. Such overlap do not appear to pose a serious challenge to the proposed reconstruction model, as the extent of these continental slivers surely were much lesser in their original pre-thinning state. It is agreeable that these blocks would have fitted slightly better and closer within their unstretched dimension but the overall scenario would have remained the same.

In Fig. 5.15 the geographical extent of some onshore and offshore tectonic elements from India and Madagascar have been shown in the close fit India-Seychelles-Madagascar juxtaposition model. As described in section 3.2.7, Indian and Madagascar mainland consists of number of Precambrian lineaments, which have been considered by several authors (Katz and Premoli, 1979; Windley et al., 1994; Lawver et al., 1999; Yoshida et al., 1999) for forwarding qualitative models for India-Madagascar juxtaposition. Many researchers (Windley et al., 1994; Menon and Santosh, 1995; Rogers et al., 1995; Yoshida et

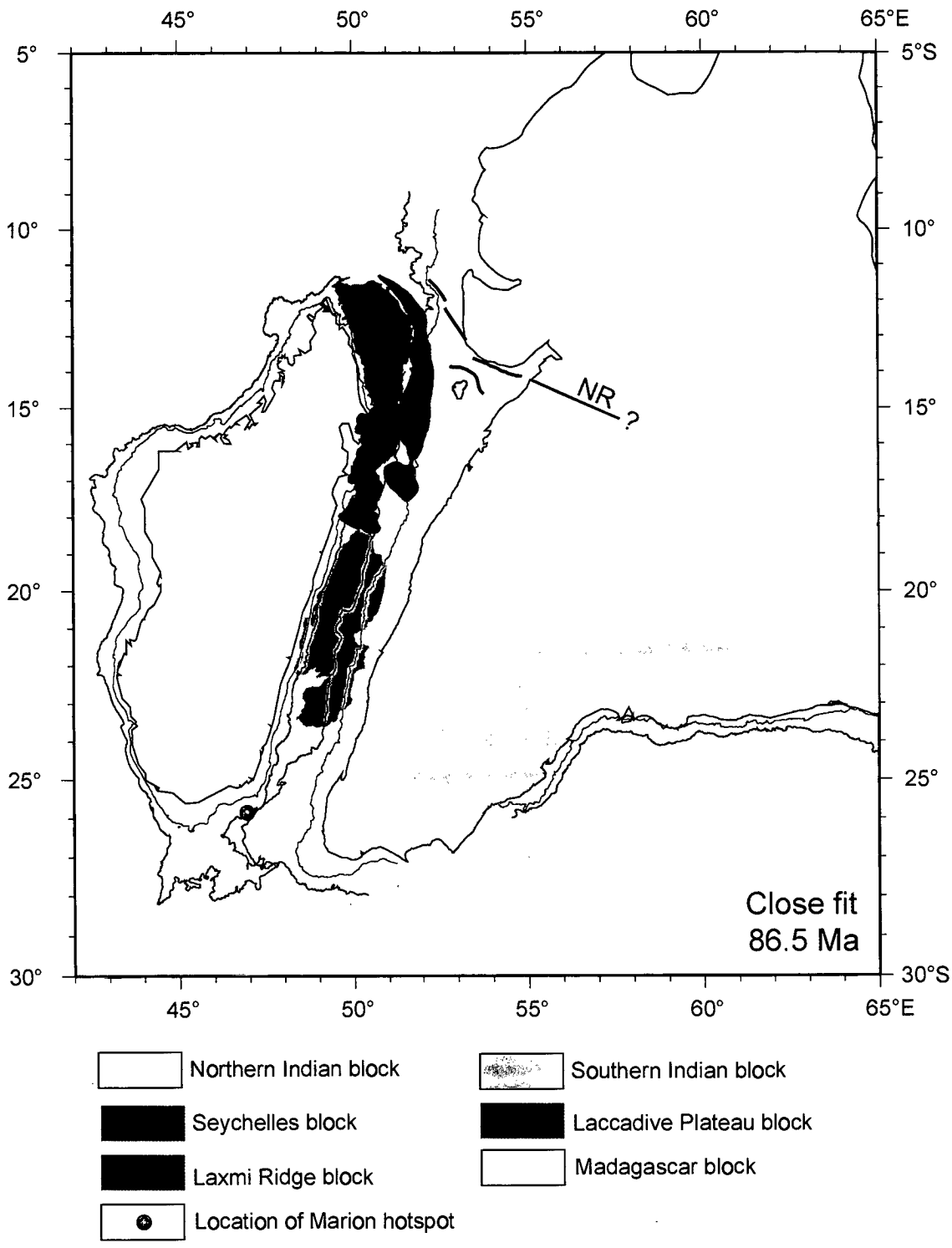

Fig. 5.14 Paleogeographic reconstruction model (in fixed Madagascar frame) describing the configuration of India and Madagascar in the close-fit juxtaposition scenario, where the Seychelles, the Laxmi Ridge and the Laccadive Plateau have been accommodated as the intervening microcontinental slivers. NR: Narmada Rift.

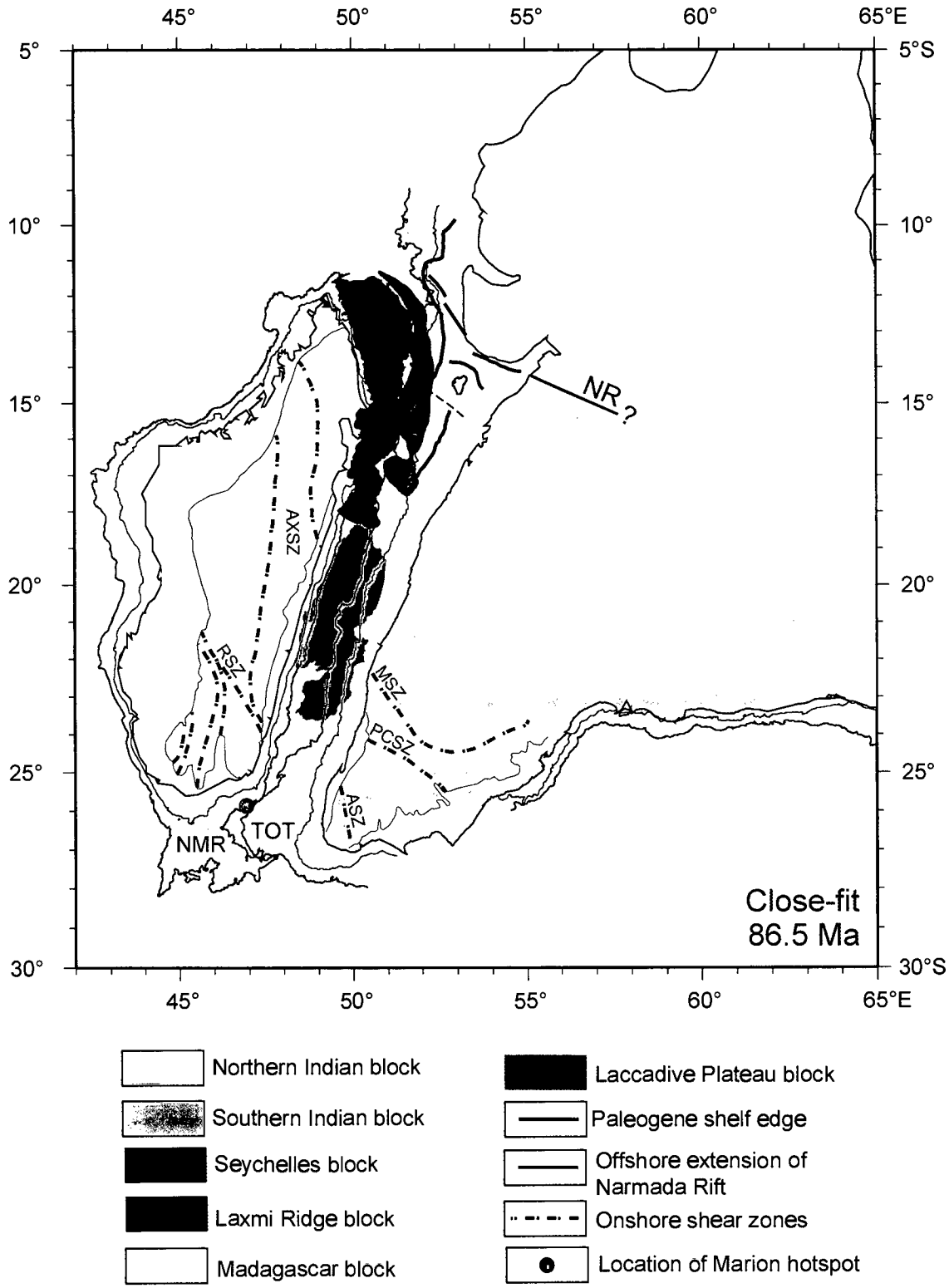

Fig. 5.15 Paleogeographic reconstruction model (in fixed Madagascar reference frame) describing the configuration of India and Madagascar at close fit juxtaposition scenario, along with the available inormation of onshore and offshore tectonic elements. NR: Narmada Rift; ASZ: Achankovil Shear Zone; MSZ : Moyar Shear Zone; PCSZ : Palghat-Cauvery Shear Zone; RSZ: Ranotsara Shear Zone; AXSZ: Axial Shear Zone; TOT: Terrace off Trivandrum; NMR: Northern Madagascar Ridge.

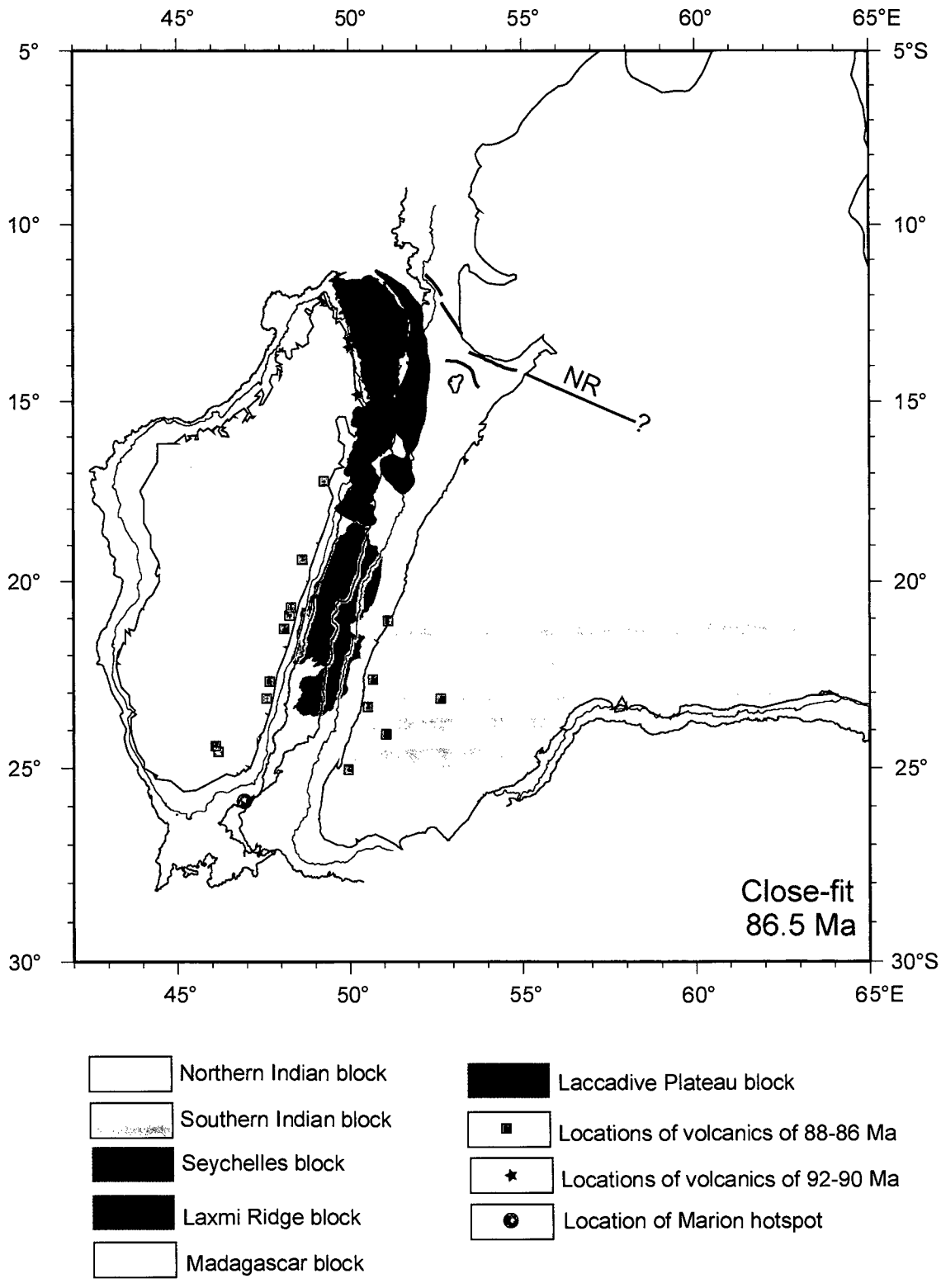

Fig. 5.16 Paleogeographic reconstruction model (in fixed Madagascar reference frame) describing the configuration of India, Seychelles and Madagascar at close fit juxtaposition scenario, along with location and age information of volcanics, which are considered to be related to rifting of these continental blocks.

al., 1999; Pradeepkumar and Krishnanath,. 2000) have suggested that the Achankovil Shear Zone of India can be correlated with the Ranotsara Shear Zone of Madagascar, and these shear zones are collinear in the India-Madagascar juxtaposition scenario. The model of close-fit juxtaposition as obtained in this study, appear to constrain the relative disposition of those onshore shear zones in the immediate pre-drift tectonic scenario.

Several researchers have reported the presence of ~90.0 Ma volcanics in the eastern side of Madagascar and western side of India. These volcanics from Indian side are the St. Mary islands (Valsangkar et al., 1981; Torsvik et al., 2000; Pande et al., 2001), the Cretaceous dykes of Karnataka (Anil Kumar et al., 2001) and the North Kerala dykes (Radhakrishna et al., 1999). The ^{40}Ar-^{39}Ar age determinations carried out by Storey et al. (1995) in the east coast of Madagascar derived an age of volcanics ranging 84-89 Ma. The ^{40}Ar-^{39}Ar age determinations (Storey et al., 1995) and the U-Pb age determinations (Torsvik et al., 2000) in the northeastern region of Madagascar derived an age of volcanics ranging 90-92 Ma (Fig. 5.16). Considering these volcanics to have been formed as a result of rift-related magmatism preceding the continental break-up, it appears that the rifting between Seychelles and Madagascar might have been initiated around 92 Ma, as noticed from the volcanics of northeastern Madagascar while the rifting between India/ Laccadive Plateau and Madagascar might have been initiated slightly later, probably around 88 Ma, as evidenced from the volcanics of east coast of Madagascar. Therefore, these observations imply that the rifting between Seychelles and Madagascar might have propagated from north to south.

Several researchers (Barron, 1987; Lawver et al., 1999) considered the unusual steep and straight edge of eastern Madagascar as an evidence of transform motion between India and Madagascar, which is believed to have taken place between 160 and 105 Ma. It is therefore necessary to examine the compatibility of the proposed model of juxtaposed conjugate TOT and BN and the transform motion between India and Madagascar, because a locked-in TOT and BN would have prevented such a transform motion. It may be noted that the inferred transform motion between India and Madagascar had taken place about 18 my prior to the locked-in TOT and BN model, which have been proposed for

India–Madagascar juxtaposition in an immediate pre-drift scenario at 86.5 Ma. At that time, the regions, which later developed into TOT and BN, might have existed simply as adjacent crusts across the transform boundary subsequent to the transform motion. Later, this area probably thinned when it came under the influence of Marion hotspot, and the bathymetric protrusion (TOT) and notch (BN) were formed by the initial geometry of the spreading axis when spreading was initiated between India and Madagascar.

CHAPTER 6

Chapter 6

EARLY OPENING HISTORY OF THE ARABIAN SEA

6.1 Introduction

In this chapter, an attempt has been made to describe the plate tectonic evolution the Arabian Sea region from 86.5 Ma to 61.0 Ma, through a sequence of paleogeographic reconstruction maps. Based on the present study, this period is considered to correspond to the early opening of the Arabian Sea, which formed the tectonic fabric of the continental margin of the western India and the adjacent deep offshore regions. As inferred in this study, the evolution of this region from 86.5 Ma to 61.0 Ma is due to relative motions among southern Indian block (SIB), northern Indian block (NIB), Laxmi Ridge (LAX), Seychelles (SEY), Laccadive Plateau (LCP) and Madagascar (MAD). The finite rotation parameters (Table 6.1) describing the relative motions among these continental blocks from 86.5 Ma to 61.0 Ma have been mostly estimated in the present study. The reconstruction models presented are for 86.5 Ma (close-fit), 83.0 Ma (chron 34ny), 79.075 Ma (chron 33no), 68.737 Ma (chron 31no), 62.499 Ma (chron 28ny), and 60.920 Ma (chron 27ny). These reconstructions were made in fixed Madagascar reference frame and the legends of symbols used in the paleogeographic reconstruction models are given in Table 6.2.

6.2 Paleogeographic reconstruction models

(a) Close-fit (86.5 Ma; Late Cretaceous)

The first reconstruction model (Fig. 6.1) is for 86.5 Ma. As inferred in this study, this was the time when all the continental blocks under consideration were fitted together very closely in their immediate pre-drift configuration. At that time several continental rifts, which probably were initiated several million years before, and a short spreading centre which got just initiated, separated the smaller continental fragments of Seychelles, Laxmi Ridge and Laccadive Plateau from the neighbouring large continental blocks of India and Madagascar. Madagascar was separated from Seychelles and Laccadive Plateau by long continental rifts and from the southwestern tip of India by the short segment of spreading center. Marion Hotspot was located at that time over the northern

Madagascar Ridge and probably under its influence the short seafloor spreading system got initiated in the nearby region. The rift axis between Seychelles and Madagascar probably were connected with a spreading centre north of Indian continental block through a long transform fault. In the region between Greater Seychelles (SEY+LAX) and India, a triple junction situation existed, where three continental rifts joined together to form a rift-rift-rift (r-r-r) triple junction. The rift, which was extending northwards (i.e. between Greater Seychelles and northern Indian block) from this triple junction developed later into Offshore Indus Basin and the rift which was extending southwards (i.e. between Greater Seychelles and southern Indian block) from this triple junction developed later into Laxmi Basin. Another rift system, which is inferred to have existed at this time between the Laccadive Plateau and the southern Indian Block, in due course developed into the Laccadive Basin.

(b) Chron 34ny (~83.0 Ma; Late Cretaceous)

A paleogeographic reconstruction (Fig. 6.2) was made for chron 34ny (~83.0 Ma) as this was the time corresponding to the oldest identified magnetic lineations in the Mascarene Basin. The seafloor spreading, which at 86.5 Ma was initiated between the southwestern tip of India and the northern Madagascar Ridge have by this time progressed northwards and created the oceanic crust of the southern Mascarene Basin and separated the bathymetric notch in the northern Madagascar Ridge and the terrace off Trivandrum. By this time the rifts radiating from the Triple junction between the Greater Seychelles and India propagated some distance outwards and the rift between India and the Laccadive Plateau propagated some distance southward. Crustal extension continued along all segments of these continental rifts.

(c) Chron 33no (~79.0 Ma; Late Cretaceous)

A paleogeographic reconstruction (Fig. 6.3) for chron 33no (~79.0 Ma) has been made because this is the time corresponding to the oldest magnetic lineation inferred in the Laxmi Basin. Seafloor spreading system by this time developed along the entire length of the Mascarene Basin and Seychelles was totally separated from Madagascar. However, as the spreading in the Mascarene Basin propagated from south, so more oceanic crust was accreted in the

southern Mascarene Basin as compared to its northern part. The rift axis of the Laxmi Basin evolved into a spreading center in its northern end but continued its southward propagation as a rift. Crustal extension continued along the Offshore Indus Basin and the Narmada Rift, while these rifts continued their outward propagation. As a result of development of a spreading center in the Laxmi Basin, the triple junction became a ridge-rift-rift (R-r-r) triple junction. Laccadive Plateau continued to move away from southern Indian block either by crustal extension along the intervening rift or by seafloor spreading along a ridge axis, which evolved from that rift axis.

(d) Chron 31no (~68.7 Ma; Late Cretaceous)

The paleogeographic reconstruction (Fig. 6.4) for chron 31no (~68.7 Ma) has been made as this is the time corresponding to the oldest magnetic lineation inferred in the Offshore Indus Basin. By this time, the entire rift axis in the Offshore Indus Basin evolved into a spreading center, and as a result, the triple junction has become a ridge-ridge-rift (R-R-r) triple junction. In the Laxmi Basin area also spreading ridge developed almost up to the northern extremities of the Laccadive Plateau. The seafloor spreading continued in the Mascarene Basin and the Laccadive Basin developed into a triangular shaped basin.

(e) Chron 28ny (~62.5 Ma; Late Paleocene)

The paleogeographic reconstruction (Fig. 6.5) for chron 28ny (~62.5 Ma) has been made since this is the time corresponding to the oldest magnetic lineation inferred in the Arabian Basin. At this stage two significant developments took place; the Greater Seychelles broke into Seychelles and Laxmi Ridge by development of a new spreading center, while spreading in the northwestern Mascarene Basin ceased. This new spreading center between Seychelles and Laxmi Ridge will later develop into the Carlsberg Ridge. This break-up between the Laxmi Ridge and Seychelles started while seafloor spreading in the Laxmi and Offshore Indus basins was continuing. Probably the proximity of the Reunion Hotspot was a reason for these developments. The Seychelles and Laxmi Ridge was getting separated by a spreading center in the northern part and by a rift in the southern part and that rift axis was connected with the spreading system in the southeastern Mascarene Basin by a long transform offset.

(f) Chron 27ny (~61.0 Ma; Late Paleocene)

The last paleogeographic reconstruction (Fig. 6.6) presented is for chron 27ny (~61.0 Ma). The continued spreading across the Carlsberg Ridge by this time created a triangular wedge of oceanic crust between the Laxmi Ridge and the Seychelles. However, by this time, the drifting away of the Laccadive Plateau and the Laxmi Ridge from India stopped and both these continental fragments reached their present position relative to India. The reason for cessation of this drifting perhaps was due to cessation of spreading along the Laxmi Basin and Offshore Indus Basin spreading centers, cessation of rifting/ spreading in the Laccadive Basin and the rifting in the Narmada Rift. Subsequently, the Narmada Rift became a failed rift and the spreading centres of the Laxmi Basin and the Offshore Indus Basin became extinct spreading centres.

Table 6.1 Finite rotation parameters describing relative motions between various plates used in the present study. The given rotation angles are those required to reconstruct the plate positions backwards in time. Angle is positive when the motion of the moving plate is counter clockwise with respect to the fixed plate when viewed from outside the earth. Ages are after Cande and Kent (1995).

Chron	Age (Ma)	Finite rotation parameters			Reference
		Lat. (deg.)	Long. (deg.)	Angle (deg.)	
(a) Seychelles (SEY) and Laxmi Ridge (LAX) in fixed Laxmi Ridge reference frame ($_{LAX}ROT_{SEY}$)					
16n	35.842	13.30	54.10	20.800	Norton and Sclater (1979)
21ny	46.264	18.64	43.37	22.559	Royer et al. (2002)
22ny	49.037	18.94	39.62	23.195	Royer et al. (2002)
23n1y	50.778	18.55	38.73	26.157	Royer et al. (2002)
24n1y	52.364	19.17	34.18	26.232	Royer et al. (2002)
25ny	55.904	19.41	29.02	30.111	Royer et al. (2002)
26ny	57.554	19.61	25.62	30.729	Royer et al. (2002)
27ny	60.920	18.83	24.86	35.411	Royer et al. (2002)
Close-fit	62.800	20.75	-47.00	24.750	This study
(b) Laxmi Ridge (LAX) and southern Indian block (SIB) in fixed southern Indian block reference frame ($_{SIB}ROT_{LAX}$)					
27ny	60.920	90.00	0.00	0.000	This study
27no	61.276	54.80	12.90	0.050	This study
28ny	62.499	54.80	12.90	0.250	This study
31no	68.737	54.80	12.90	0.625	This study
32n1y	71.071	54.80	12.90	0.950	This study
32n2o	73.004	54.80	12.90	1.400	This study
33ny	73.619	54.80	12.90	1.600	This study
33no	79.075	54.80	12.90	2.230	This study
Close-fit	86.500	65.00	6.00	3.800	This study

Table 6.1 (contd.)

Chron	Age (Ma)	Finite rotation parameters			Reference
		Lat. (deg.)	Long. (deg.)	Angle (deg.)	
(c) Northern Indian block (NIB) and southern Indian block (SIB) in fixed southern Indian block reference frame ($_{SIB}ROT_{NIB}$)					
Cessation of rifting	60.920	90.00	0.00	0.000	This study
Close-fit	86.500	26.00	94.00	1.000	This study
(d) Laccadive Plateau (LCP) and southern Indian block (SIB) in fixed southern Indian block (SIB) reference frame ($_{SIB}ROT_{LCP}$)					
Cessation of rifting	60.920	90.00	0.00	0.000	This study
Close-fit	86.500	17.00	71.00	16.000	This study
(e) Southern Indian Block (SIB) and Madagascar (MAD) in fixed Madagascar reference frame ($_{MAD}ROT_{SIB}$)					
16ny	35.842	13.30	54.10	-20.800	Norton and Sclater (1979)
22ny	49.040	12.90	45.30	-30.100	Norton and Sclater (1979)
28ny	62.499	18.80	26.20	-38.400	Norton and Sclater (1979)
34ny	83.000	18.70	25.80	-56.000	Norton and Sclater (1979)
Close-fit	86.500	18.70	26.40	-58.360	This study

Table 6.2 Legend of symbols used to denote various features in the paleogeographic reconstruction maps (from Fig. 6.1 to Fig. 6.6) along with their brief description.

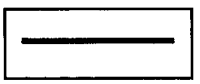
Rift axis

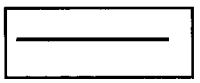
Ridge axis

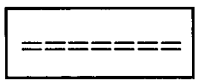
Extinct spreading centre


Transform fault

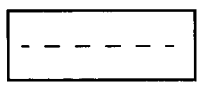
Probable fracture/ fault zone

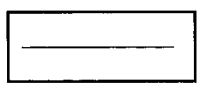
200 m isobath

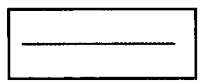
2000 m isobath


Oceanic crust created during 86.5 Ma - 79.0 Ma


Oceanic crust created during 79.0 Ma - 63.6 Ma


Oceanic crust created during 63.6 Ma - 61.0 Ma


Rift stage crust

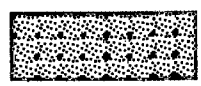
Oceanic/ rift stage (??) crust of the Laccadive Basin


Deccan Trap

Marion hotspot

Reunion hotspot

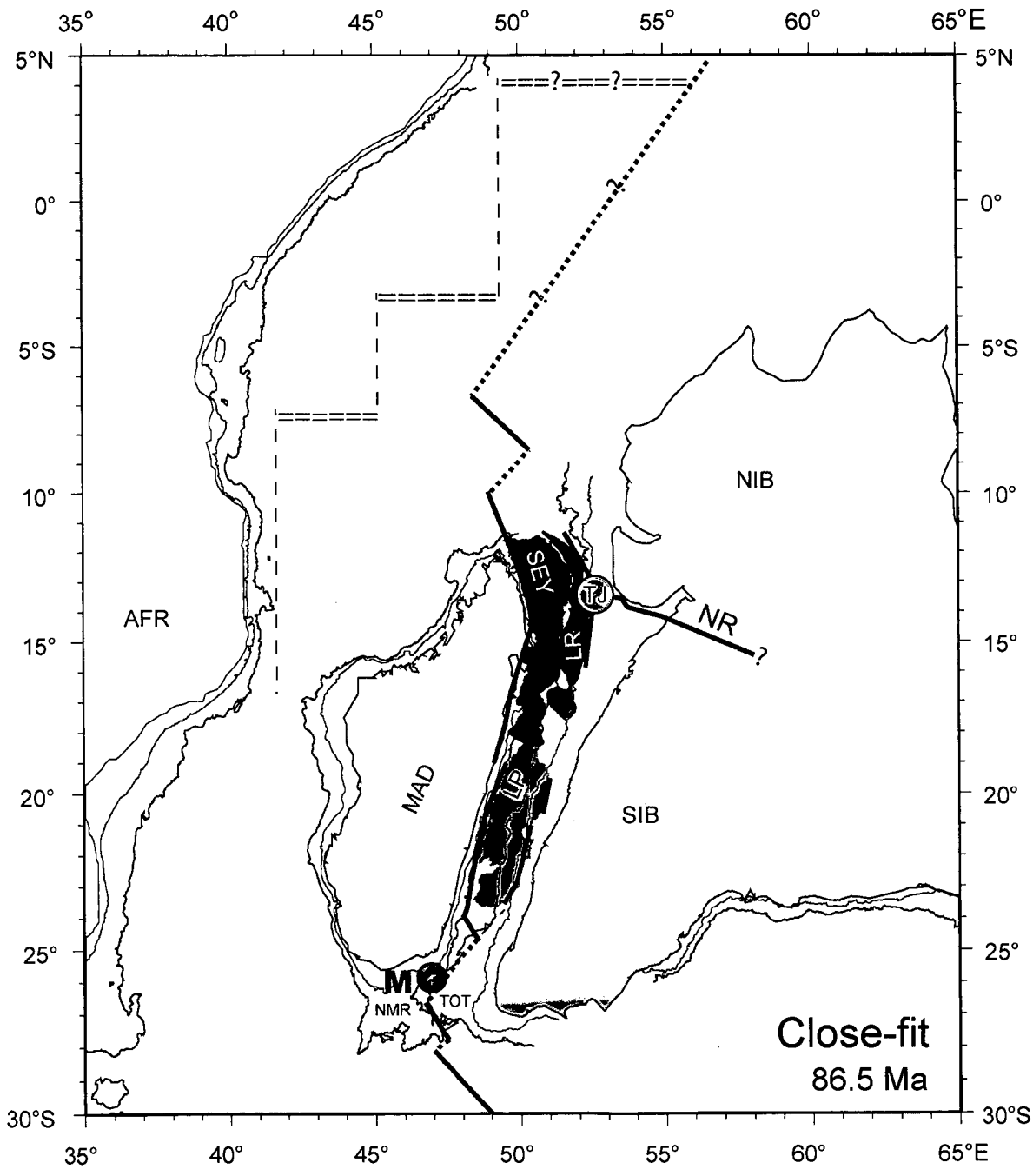

Fig. 6.1 Paleogeographic reconstruction of the Western Indian Ocean region for close-fit juxtaposition (86.5 Ma, Late Cretaceous) with schematic depiction of the evolution of the ocean basins and associated tectonic features. This is the inferred time at which the spreading appears to have been initiated between southern Indian block and Madagascar. AFR: Africa; MAD: Madagascar; SEY: Seychelles; LR: Laxmi Ridge; LP: Laccadive Plateau; SIB: Southern Indian block; NIB: Northern Indian block; NR: Narmada Rift; TJ: Triple junction. Symbols used are explained in Table 6.2.

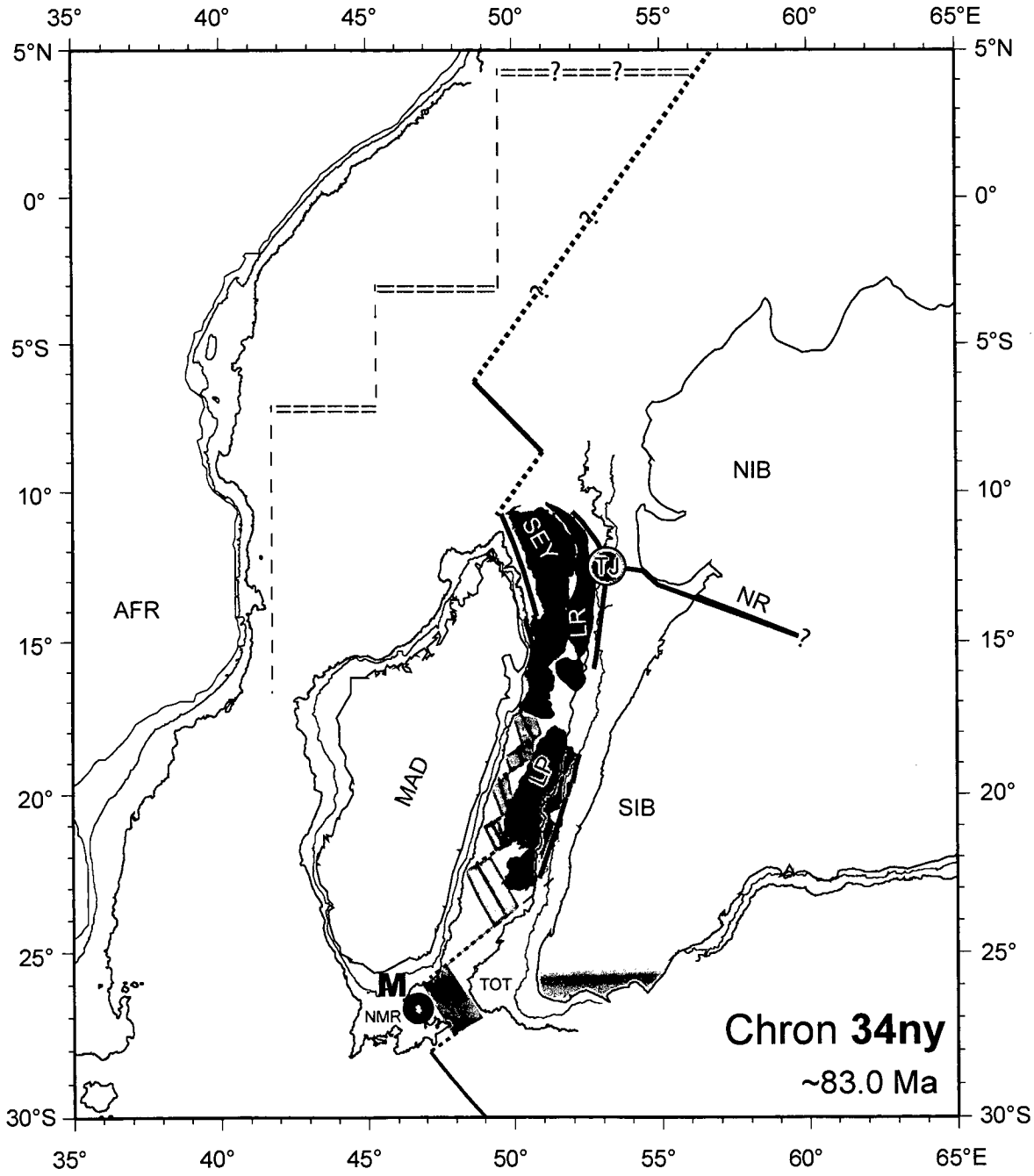

Fig. 6.2 Paleogeographic reconstruction of the Western Indian Ocean region for Chron 34ny (~83.0 Ma, Late Cretaceous) with schematic depiction of the evolution of the ocean basins and associated tectonic features. By this time, a spreading system has progressed northwards along the eastern margin of Madagascar, which will later evolve into Mascarene Basin and break Seychelles away from Madagascar. Other details are as in Fig. 6.1.

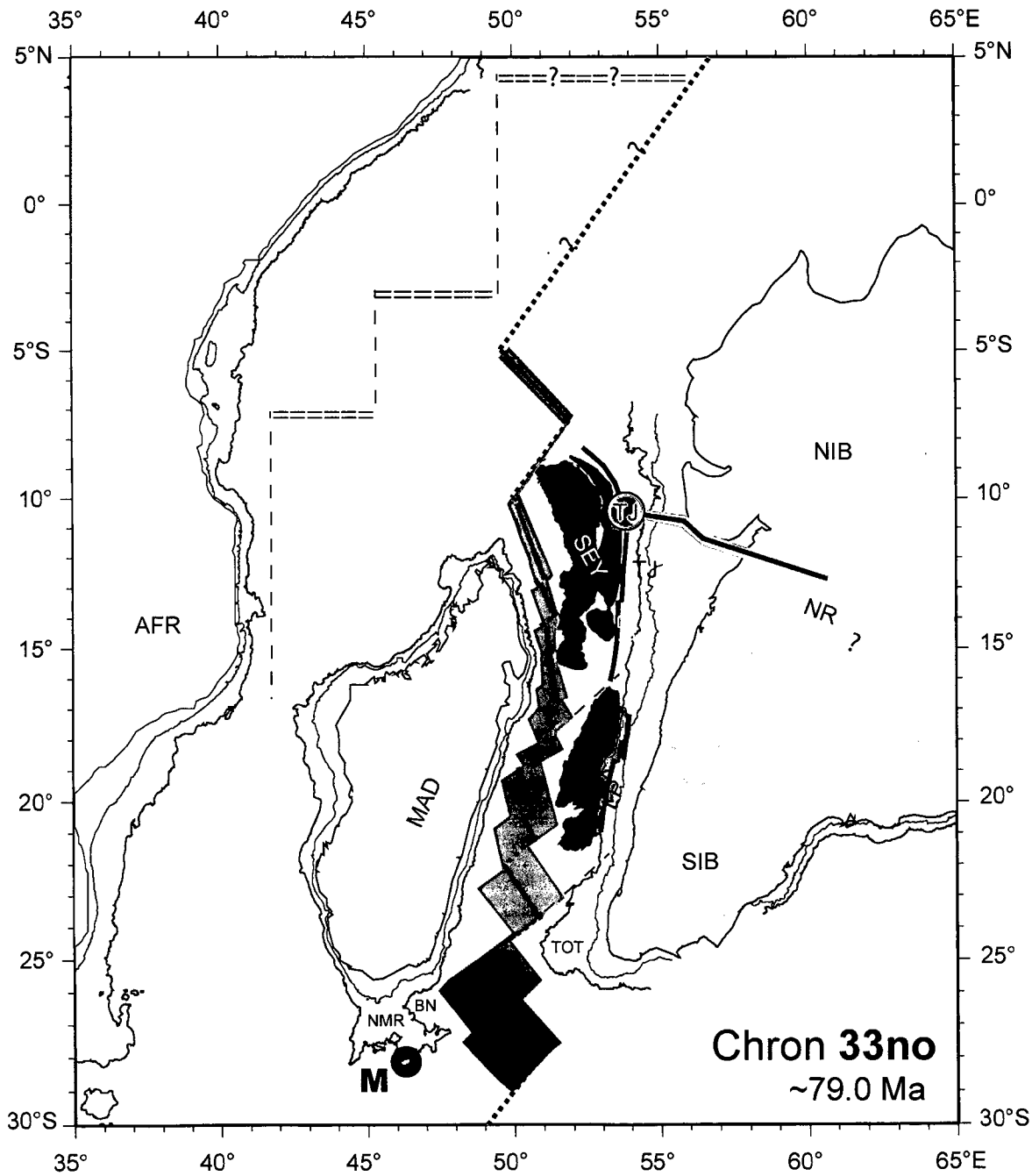

Fig. 6.3 Paleogeographic reconstruction of the Western Indian Ocean region for Chron 33no (~79.0 Ma, Late Cretaceous) with schematic depiction of the evolution of the ocean basins and associated tectonic features. This is the inferred time at which the spreading appears to have been initiated in the Laxmi Basin between the Greater Seychelles and southern Indian block. Other details are as in Fig. 6.1.

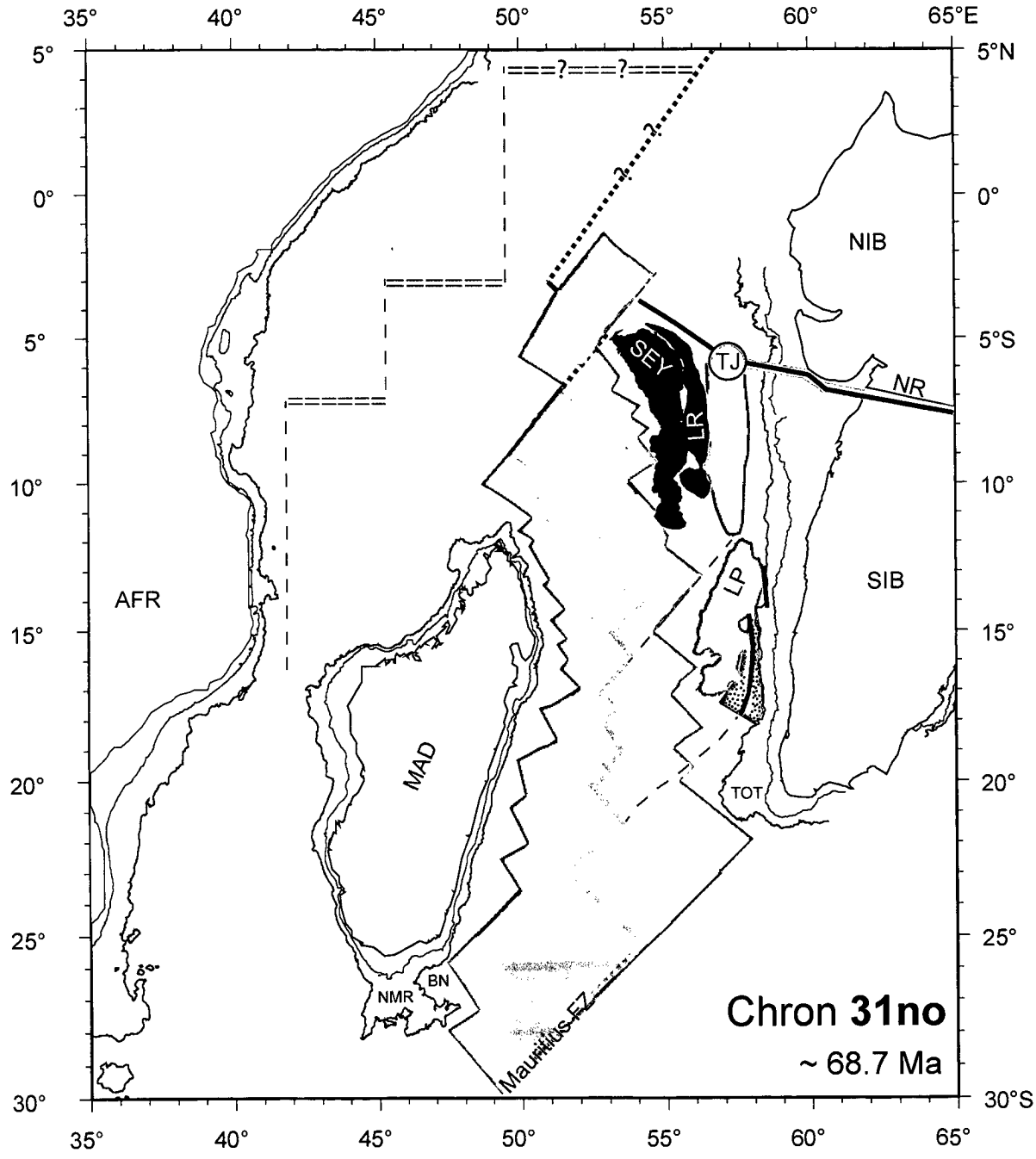

Fig. 6.4 Paleogeographic reconstruction of the Western Indian Ocean region for Chron 31no (~68.7 Ma, Late Cretaceous) with schematic depiction of the evolution of the ocean basins and associated tectonic features. This is the inferred time at which the spreading appears to have been initiated in the Offshore Indus Basin between the Greater Seychelles and northern Indian block. Other details are as in Fig. 6.1.

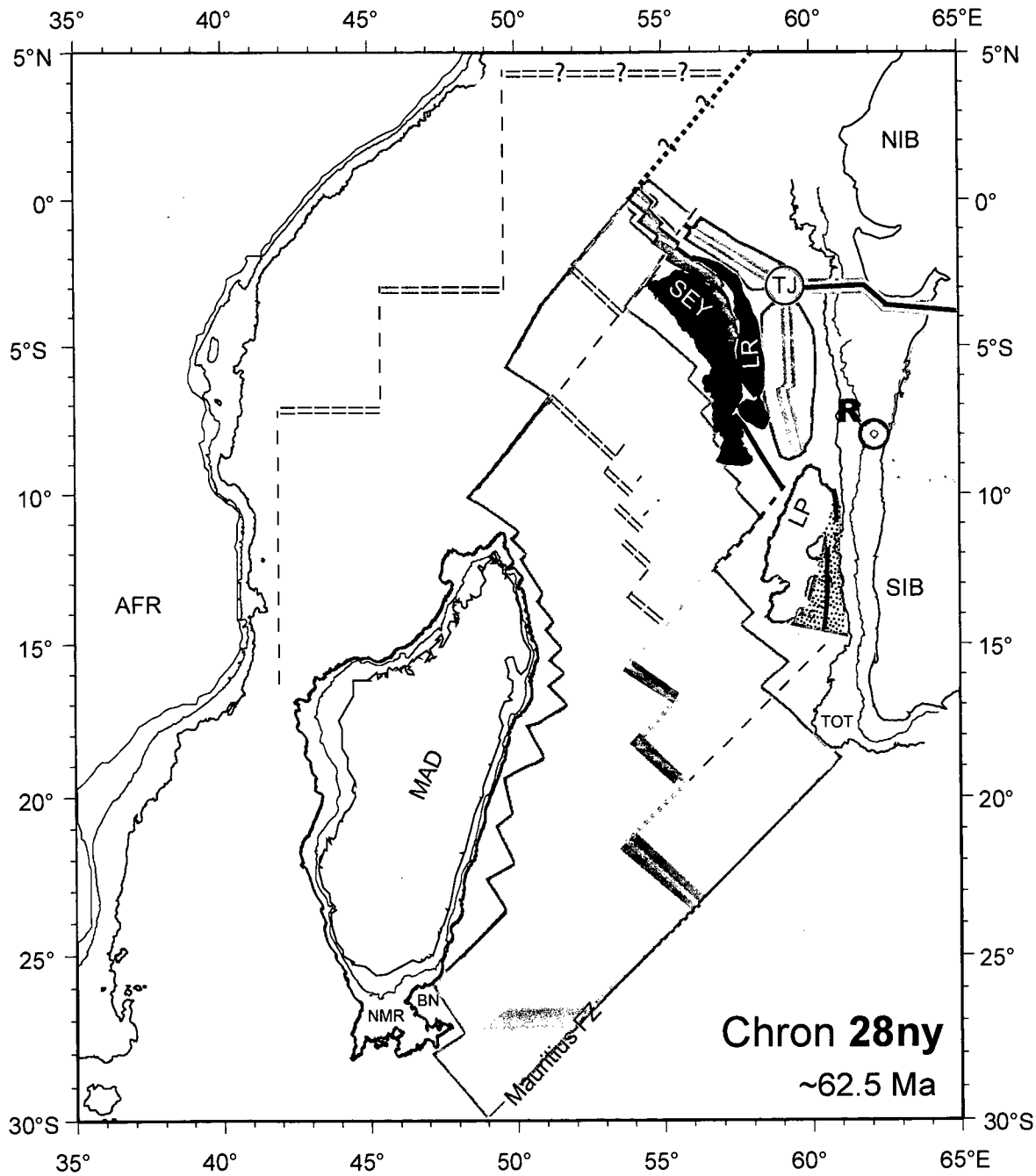

Fig. 6.5 Paleogeographic reconstruction of the Western Indian Ocean region for Chron 28ny (~62.5 Ma, Late Paleocene) with schematic depiction of the evolution of the ocean basins and associated tectonic features. This is the inferred time at which the spreading appears to have been initiated across the Paleo-Carlsberg Ridge between the Seychelles and Laxmi Ridge. Other details are as in Fig. 6.1.

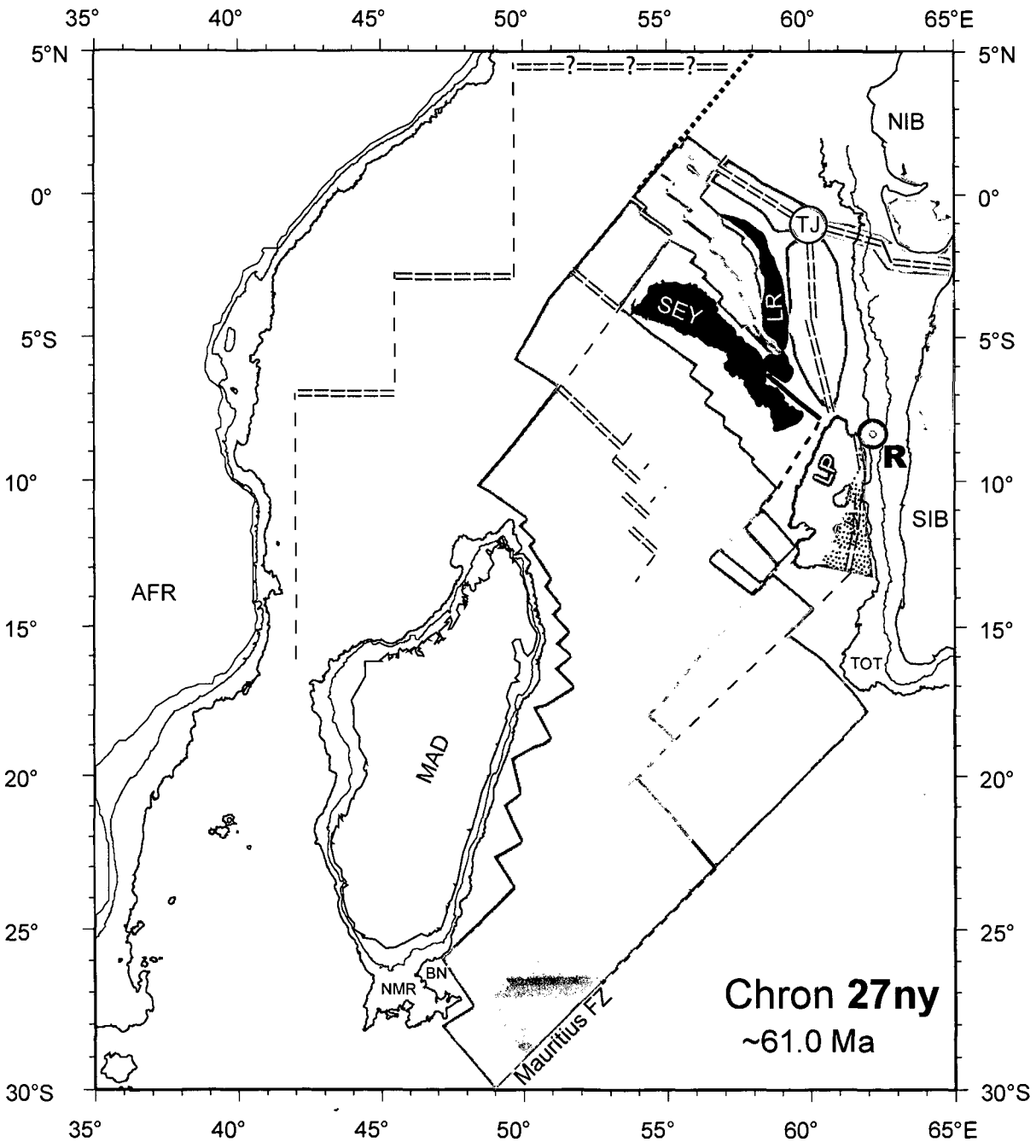

Fig. 6.6 Paleogeographic reconstruction of the Western Indian Ocean region for Chron 27ny (~61.0 Ma, Late Paleocene) with schematic depiction of the evolution of the ocean basins and associated tectonic features. This is the inferred time at which the spreading / rifting in the Laxmi Basin, Offshore Indus Basin, Laccadive Basin and Narmada Rift ceased. Other details are as in Fig. 6.1.

CHAPTER 7

Chapter - 7

SUMMARY AND CONCLUSIONS

7.1 Introduction

The present study deals with the deep offshore regions between Laxmi-Laccadive ridges and the continental shelves of western India and southern Pakistan, which mainly contain the Offshore Indus and Laxmi basins. It is aimed to reconstruct the early drift stage dispositions of various continental fragments and other regional tectonic elements of these areas and thus enhance understanding of the early opening of the Arabian Sea region in the framework of plate tectonic evolution. The main data used for the present study are sea-surface magnetic, gravity and bathymetric profiles; satellite derived free-air gravity anomalies, GEBCO bathymetry contours, published regional scale tectonic element identifications and available finite rotation parameters of relative motion among India, Seychelles, Madagascar and Laxmi Ridge. The compiled data and interpretations are presented in the form of profiles and maps. The inferred early plate tectonic evolution of the study area has been described through a set of paleogeographic reconstruction maps. This chapter presents a brief summary of the present work, salient inferences and scope for further work.

7.2 Summary

In the Arabian Sea region, the Arabian Basin and its conjugate Eastern Somali Basin are believed to have been formed by seafloor spreading process along Carlsberg Ridge since early Tertiary time. According to this model, the Laxmi and Laccadive ridges broadly mark the landward boundary of this early Tertiary oceanic crust on the Indian side. However, there exists substantial swath of deep offshore region, between Laxmi-Laccadive ridges and the continental shelves of western India and southern Pakistan, whose genesis and evolution remains to be confidently established. These deep offshore regions mainly contain the Laxmi and Offshore Indus basins and various views exist about the nature of the crust underlying these basins. In view of this, updated information about the basement features and various geophysical signatures in the study area have been compiled and interpreted to understand the nature of the crust

underlying these regions. The data suggested interesting similarities of geophysical signatures and basement features in the Offshore Indus Basin and Laxmi Basin regions. Both the basins are characterized by the presence of a short wave length gravity low atop a broad wavelength gravity high that coincide with a basement high feature and the axis of symmetry of the magnetic anomalies. To evaluate these inference and to understand the crustal structure of the regions, integrated interpretation of gravity and magnetic data have been carried out using forward modeling of anomalies under constrains of available seismic information.

The crustal configuration of the Offshore Indus Basin derived based on the forward modeling of gravity data reveals the presence of ~6 km thick two-layered crust with densities 2.66 g/cc and 2.89 g/cc under ~3.5 km thick sediments of density 2.17 g/cc. This derived density and crustal configuration suggest that the nature of the underlying crust can be considered as oceanic, where the upper layer of 2.66 g/cc and the lower layer of 2.89 g/cc can be considered to represent the layer 2 and layer 3 of the oceanic crust. The crustal configuration of the Laxmi Basin derived based on the forward modeling of gravity data reveals the presence of ~7 km thick three-layered crust with densities 2.66 g/cc, 2.78 g/cc and 3.02 g/cc under ~3.0 km thick sediments of density 2.17 g/cc. This derived density and crustal configuration suggest that the nature of the underlying crust can also be considered as oceanic, where the layers with densities 2.66 g/cc, 2.78 g/cc and 3.02 g/cc correspond to the layer 2A, layer 2B and layer 3 of the oceanic crust. If these inferences about the nature of the crust underlying the Offshore Indus and Laxmi basins are correct, then the magnetic anomalies in both the basins should be able to explain in terms of juxtaposed normally and reversely magnetized blocks of oceanic crust fitting in the inferred layer-2 of the oceanic crust. To examine this possibility, forward modeling of the magnetic data was carried out, which suggested that the magnetic anomalies in both the basins could be explained in terms of juxtaposed normally and reversely magnetized blocks akin to oceanic crust created by two-limbed seafloor spreading. In view of this, following the procedure for analysis of seafloor spreading magnetic anomalies, the arrangement of magnetized blocks in the model have been interpreted in terms of geomagnetic polarity time scale to identify the magnetic

anomalies and thus obtain the age of the underlying oceanic crust. The interpretation suggested that the magnetic anomalies in the Offshore Indus Basin could be considered to correspond from chron 27no (61.276 Ma) to chron 31no (68.737 Ma) while that in the Laxmi Basin could be considered to correspond from chron 27no (61.276 Ma) to chron 33no (79.075 Ma). Slightly after chron 27no, i.e. at about 61 Ma, spreading in both the basins appear to have ceased and they became extinct spreading centres.

Having identified the magnetic anomalies, an updated magnetic isochron map of the study area has been prepared, which depicts the conjugate magnetic isochrons on both the sides of those extinct spreading centers. The conjugate magnetic isochrons have been used to estimate the finite rotation parameters, which describe the relative motion of Laxmi Ridge with India/Pakistan mainland that resulted in the formation of Offshore Indus and Laxmi basins. The other finite rotation parameters required to describe the early opening history of the Arabian Sea are the relative motions of India with Madagascar and Laccadive Plateau with India. Towards obtaining the most reasonable finite rotation parameter, which describes the relative motion of India with Madagascar, available finite rotation parameters provided by various researchers have been evaluated in light of available tectonic element information. It was observed that the finite rotation parameters provided by Norton and Sclater (1979) is the most reasonable model for relative motion of India with Madagascar. It is further inferred that the terrace like feature located in the mid-continental slope region off Trivandrum is conjugate to the northern Madagascar ridge, and these features are scars related to India-Madagascar separation, which was initiated at 86.5 Ma. The finite rotation parameters describing the relative motion of Laccadive Plateau with India has been obtained based on trial and error, as no such information is available.

Having obtained the finite rotation parameters to describe the relative motions of India-Madagascar, Laxmi Ridge-India, Seychelles-Laxmi Ridge and Laccadive Plateau-India, the plate tectonic evolution of the study area for the period 86.5 Ma to ~61.0 Ma have been demonstrated by paleogeographic reconstruction models. These reconstructions provided a new view about the dispositions of India, Seychelles and Madagascar during the early drift stages wherein the Laxmi Ridge and Laccadive Plateau could be accommodated as

continental slivers. The reconstruction models are given for six distinct stages, viz. close-fit juxtaposition (86.5 Ma), chron 34ny (83.0 Ma), chron 33no (79.075 Ma), chron 31no (68.737 Ma), chron 28ny (62.499 Ma) and chron 27ny (60.920 Ma). Reconstruction model for 86.5 Ma has been provided since this is the time of initiation of drifting among the different continental blocks. Reconstruction model for chron 34ny has been provided since this is the oldest magnetic isochron present in the Mascarene Basin, which is believed to have been formed as a result of India-Seychelles block with Madagascar. The reconstruction models for 33no and 31no have been provided since they are the oldest inferred magnetic lineations in the Laxmi Basin and Offshore Indus Basin respectively. Chron 28ny has been selected since this is the oldest magnetic anomaly identified in the Arabian Basin. The reconstruction for chron 27ny has been given since this is the time at which the spreading centres in the Laxmi Basin, Offshore Indus Basin as well as Mascarene Basin became extinct and the subsequent spreading continued in the Carlsberg Ridge which resulted in the formation of conjugate Arabian and Eastern Somali Basins.

7.3 Salient inferences

i. The similarities of the geophysical signatures in the Offshore Indus Basin and Laxmi Basin have been established.

ii. The nature of the crust underlying the Offshore Indus and Laxmi basins have been established as oceanic crust, formed as a result of two-limbed seafloor spreading between Laxmi Ridge and India/Pakistan.

iii. The timing for the initiation and extinction of two-limbed seafloor spreading process in the Offshore Indus Basin and Laxmi Basin has been inferred.

iv. The genesis of Palitana Ridge in the Offshore Indus Basin and axial basement high in the Laxmi Basin, have been established as extinct spreading centres.

v. Approximate boundary of the normally and reversely magnetized blocks of oceanic crust in the Offshore Indus and Laxmi basins have been delineated and finite rotation parameters describing the relative motion of Laxmi Ridge with India/ Pakistan have been estimated using conjugate magnetic isochrons.

vi. Conjugate nature of the terrace like feature located in the mid-continental slope region off Trivandrum with the northern Madagascar Ridge has been established. The genesis of these features has been established in terms of India-Madagascar separation, which was initiated at about 86.5 Ma.

vii. The dispositions of India, Seychelles and Madagascar during the early drift stages have been deciphered wherein the continental slivers of Laxmi Ridge and Laccadive Plateau also have been accommodated.

7.4 Scope for further work

The present study provided several clues to the hitherto unanswered problems about the origin and evolution of various tectonic elements in the deep offshore regions adjoining to west coast of India/Pakistan. However, more studies and selected ground truth data will be required to enhance the confidence in these inferences. Following are some suggested geophysical studies, which may be pursued further.

a) Detailed deep penetration seismic reflection and refraction investigation of the Laxmi Basin and the Laccadive Basin to obtain the improved velocity-depth information of the crustal layers.

b) Investigation of the Laccadive Basin region with closely spaced magnetic traverses to map the presence of magnetic lineations, if any.

c) Investigation of the inferred oceanic crust region of the Laxmi and Offshore Indus basins with closely spaced magnetic traverses to map the evolution of the extinct spreading ridge segments in detail.

d) Deep penetration seismic reflection and refraction investigation of the areas landward of the oceanic crust region of the Laxmi Basin to examine the existence of rifted/ thinned continental crust and its seaward extent.

REFERENCES

List of References

1. Acton, G., Gordon, R.G., 1989. Limits on the age of the Deccan Traps of India from paleomagnetic and plate reconstruction data and the uncertainties. Journal of Geophysical Research, 94, 17713-17720.

2. Agrawal, P.K., Pandey, O.P., Negi, J.G. 1992. Madagascar: a continental fragment of the paleo-super Dharwar Craton of India. Geology, 20, 543-546.

3. Alvarez, L.W., Alvarez, W., Asaro, F., Michel, H.V., 1980. Extraterrestrial cause for the Cretaceous-Tertiary extinction. Science, 208, 1095-1108.

4. Anand, S.P., Rajaram, M., 2003. Study of aeromagnetic data over part of Eastern Ghat Mobile Belt and Baster Craton. Gondwana Research, 6 (4), 859-865.

5. Anil Kumar, Bhaskar Rao, Y.J., Padmakumari, V.M., Dayal, A.M., Gopalan, K., 1988. Late Cretaceous mafic dykes in the Dharwar Craton. Proceedings of Indian Academy of Science (Earth and Planetary Science), 97(1), 107-114.

6. Anil Kumar, Pande, K., Venkatesan, T.R., Bhaskar Rao, Y.J., 2001. The Karnataka Late Cretaceous dykes as products of the Marion hotspot at the Madagascar - India breakup event: evidence from $^{40}Ar/^{39}Ar$ geochronology and geochemistry. Geophysical Research Letters, 28(14), 2715-2718.

7. Avraham, Z.B., Bunce, E.T., 1977. Geophysical study of the Chagos-Laccadive Ridge, Indian Ocean. Journal of Geophysical Research, 82(8), 1295-1305.

8. Babenko, K.M., Panaev, V.A., Svistunov, Yu.I., Schlezinger, A.Ye, 1981. Tectonics of the eastern part of the Arabian Sea, according to seismic data. Geotectonics, 18, 37-62.

9. Baker, B.H., Miller, J.A., 1963. Geology and geochronology of the Seychelles Islands and structure of the floor of the Arabian Sea. Nature, 199, 346-348.

10. Baksi, A.K., 1988. Critical evaluation of the age of the Deccan Traps, India: Implications for the flood basalt volcanism and faunal extinction: Reply. Geology, 16, 758-759.

11. Baksi, A.K., 1994. Geochronological studies on the whole-rock basalts, Deccan Traps, India: evaluation of the timing of volcanism relative to the K-T boundary. Earth and Planetary Science Letters, 121, 43-56.

12. Baksi, A.K., Farrar, E., 1991. $^{40}Ar/^{39}Ar$ dating of the Siberian Traps, USSR: evaluation of the ages of the two major extinction events relative to episode of flood basalt volcanism in the USSR and Deccan Traps, India. Geology, 19, 461-464.

13. Banerjee, S.K. 1984. The magnetic layer of the ocean crust - how thick is

it? Tectonophysics, 105, 15-27.

14. Bansal, A.R., Fairhead, J.D., Green, C.M., Fletcher, K.M.U., 2005. Revised gravity for offshore India and the isostatic compensation of submarine features. Tectonophysics, 404, 1-22.

15. Barron, E.J., 1987. Cretaceous plate tectonic reconstructions. Paleogeography, Paleoclimatology and Paleoecology, 59, 3-29.

16. Basu, A.R., Renne, P.R., Dasgupta, D.K., Teichmann, F., Poreda, R.J., 1993. Early and late igneous pulses and high ^{3}He plume origin for the Deccan Flood Basalts. Science, 261, 902-906.

17. Bernard, A., Munschy, M., 2000. Le bassin des Mascareignes et le bassin de Laxmi (ocen Indien occidental) se sont-ils formes a l'axe d'un meme centre d'expansion? Comptes Rendus de l'Academie des Sciences - Series IIA - Earth and Planetary Sciences, 330(11), 777-783.

18. Besse, J., Courtillot, V., 1988. Paleogeographic maps of the continents bordering the Indian Ocean since the Early Jurassic. Journal of Geophysical Research, 93(B10), 11791-11808.

19. Bhattacharya, G.C., Chaubey, A.K., 2001. Western Indian Ocean - a glimpse of the tectonic scenario. In: Sengupta, R., Desa, E. (Eds.). The Indian Ocean - A Perspective, Oxford & IBH Pub. Company Ltd., 691-729.

20. Bhattacharya, G.C., Chaubey, A.K., Murty, G.P.S., Gopala Rao, D., Scherbakov, V.A., Lygin, V.A., Philipenko, A.I., Bogomyagkov, A.P., 1992. Marine magnetic anomalies in the northeastern Arabian Sea. Oxford-IBH, New Delhi, 503-509.

21. Bhattacharya, G.C., Chaubey, A.K., Murty, G.P.S., Srinivas, K., Sarma, K.V.L.N.S., Subrahmanyam, V., Krishna, K.S., 1994b. Evidence for seafloor spreading in the Laxmi Basin, northeastern Arabian Sea. Earth and Planetary Science Letters, 125, 211-220.

22. Bhattacharya, G.C., Murty, G.P.S., Srinivas, K., Sudhakar, M., Nair, R.R., 1994a. Swath bathymetric investigation of the seamounts located in Laxmi Basin, Eastern Arabian Sea. Marine Geodesy, 17, 169-182.

23. Bhattacharya, G.C., Subrahmanyam, V., 1986. Extension of the Narmada-Son lineament on the continental margin off Saurashtra, Western India as obtained from magnetic measurements. Marine Geophysical Researches, 8, 329-344.

24. Bhattacharya, G.C., Subrahmanyam, V., 1991. Geophysical study of a seamount located on the continental margin of India. Geo Marine Letters, 11, 71-78.

25. Biswas, S.K., 1982. Rift basins in western margin of India and their hydrocarbon prospects with special reference to Kutch Basin. American Association of Petroleum Geologists Bulletin, 66, 1497-1513.

26. Biswas, S.K., 1987. Regional tectonic framework, structure and evolution of the western marginal basins of India. Tectonophysics, 135, 307-327.

27. Biswas, S.K., 1989. Hydrocarbon exploration in western offshore basins of India. In: Recent Geoscientific Studies in the Arabian Sea off India, Geological Survey of India, Special Publication 24, 185-194.

28. Biswas, S.K., Singh, N.K., 1988. Western continental margin of India and hydrocarbon potential of deep-sea basins. 7th Offshore Southeast Asia Conference, 170-181.

29. Boast, J., Nairn, A.E.M., 1982. An outline of the Geology of Madagascar. In: Nairn, A.E.M., Stehli, F.G. (Eds.), The Ocean Basins and Margins. Plenum Press, New York, 6, 649-696.

30. Bott, M.H.P., 1995. Rifted passive margins. In: Olsen, K.H. (Ed.), Continental Rifts: Evolution, Structure, Tectonics. Elsevier, 409-426.

31. Bulychev, A.A., Gilod, D.A., Mazo, E.L., Schreider, A.A., 2006. Features of the crustal structure of the Arabian Sea. Oceanology, 46 (3), 418-429.

32. Cande, S.C., Kent, D.V., 1995. Revised calibration of the geomagnetic polarity time scale for the Late Cretaceous and Cenozoic. Journal of Geophysical Research, 100, 6093-6095.

33. Chaubey, A.K., Bhattacharya, G.C., Murty, G.P.S., Desa, M., 1993. Spreading history of the Arabian Sea: some new constraints. Marine Geology, 112, 343-352.

34. Chaubey, A.K., Bhattacharya, G.C., Murty, G.P.S., Srinivas, K., Ramprasad, T., Rao, D.G., 1998. Early Tertiary seafloor spreading magnetic anomalies and paleo-propagators in the northern Arabian Sea. Earth and Planetary Science Letters, 154, 41-52.

35. Chaubey, A.K., Dyment, J., Bhattacharya, G.C., Royer, J.Y., Srinivas, K., Yatheesh, V., 2002a. Paleogene magnetic isochrons and palaeo-propagators in the Arabian and Eastern Somali basins, NW Indian Ocean. In: Clift, P.D., Croon, D., Gaedicke, C., Craig, J. (Eds.), The Tectonic and Climatic Evolution of the Arabian Sea Region. Geological Society, London, Special Publication, 195, 71-85.

36. Chaubey, A.K., Rao, D.G., Srinivas, K., Ramprasad, T., Ramana, M.V., Subrahmanyam, V., 2002b. Analyses of multichannel seismic reflection, gravity and magnetic data along a regional profile across the central-western continental margin of India. Marine Geology, 182(3-4), 303-323.

37. Chetty, T.R.K., Bhaskar Rao, Y.J., 2004. Structural framework of south India and the significance of major shear zones. Joint AOGS 1st Annual Meeting and 2nd APHW Conference, Asia Oceania Geosciences Society, Singapore, 54-55.

38. Coffin, M.F., Gahagan, L.M., Lawver, L.A., 1998. Present-day plate boundary digital data compilation, Technical Report, 174, University of

Texas Institute for Geophysics.

39. Collier, J.S., Minshull, T.A., Kendall, J.M., Whitmarsh, R.B., Rumpker, G., Joseph, P., Sampson, P., Lane, C.I., Sansom, V., Vermeesch, P.M., Hammond, J., Wookey, J., Teanby, N., Ryberg, T., Dean, S.M., 2004b. Rapid continental breakup and microcontinent formation in the Western Indian ocean. EOS Transactions, American Geophysical Union, 85, 481-496.

40. Collier, J.S., Minshull, T.A., Whitmarsh, R.B., Kendall, J.M., Lane, C.I., Sansom, V., Rumpker, G., Ryberg, T., 2004a. Geophysical investigation of a conjugate pair of rifted margins formed at high extension rate: Laxmi Ridge - northern Seychelles Bank, Western Indian Ocean. InterMARGINS Workshop: "Modeling the extensional Deformation of the Lithosphere" (IMEDL). Pontresina (Swiss Alps), Poster, 30.

41. Collins, A.S., Kroner, A., Razakamanana, T., Windley, B.F., 2000a. The tectonic architecture of the East African Orogen in Central Madagascar – a structural and geochronological perspective. 18th Colloquium of African Geology, Graz, Austria.

42. Collins, A.S., Razakamanana, T., Windley, B.F., 2000b. Neoproterozoic extensional detachment in central Madagascar: implications for the collapse of the East African Orogen. Geological Magazine, 137 (1), 39-51.

43. Collins, A.S., Windley, B.F., 2002. The tectonic evolution of central and northern Madagascar and its place in the final assembly of Gondwana. Journal of Geology, 110, 325-339.

44. Corti, G., Wijk, J.V., Bonini, M., Sokoutis, D., Cloetingh, S., Innocenti, F., Marietti, P., 2003. Transition from continental break-up to punctiform seafloor spreading: How fast, symmetric and magmatic. Geophysical Research Letters, 30(12,1604), doi:10.1029/2003GL017374.

45. Courtillot, V., Besse, J., Vandamme, D., Montigny, R., Jaeger, J.J., Capetta, H., 1986. Deccan flood basalts at the Cretaceous/ Tertiary boundary? Earth and Planetary Science Letters, 80, 361-374.

46. Courtillot, V., Feraud, G., Maluski, H., Vandamme, D., Moreau, M.G., Besse, J., 1988. Deccan flood basalts and Cretaceous/Tertiary boundary. Nature, 333, 843-846.

47. Cox, A., Hart, R.B., 1986. Plate Tectonics: How it works. Blackwell Scientific Publications, 392 p.

48. Crawford, A.R., 1978. Narmada-Son lineament of India traced into Madagascar. Journal of Geological Society of India, 19 (4), 144-153.

49. Das, S.R., Ray, A.K., 1976. Fracture pattern, hot springs and lineaments of the west coast. Journal of Geological Survey of India, 125 Year News Letter, 1-6.

50. Davies, D., Francis, T.J.G., 1964. The crustal structure of the Seychelles

Bank. Deep Sea Research, 11, 921-927.

51. Davis, R.A., Fitzgerald, D.M., 2004. Beaches and Coasts. Blackwell Publishing Company, Malden, USA, 419 p.

52. Dickin, A.P., Fallick, A.E., Halliday, A.N., Macintyre, R.M., Stephens, W.E., 1987. An isotopic and geochronological investigation of the younger igneous rocks of the Seychelles microcontinent. Earth and Planetary Science Letters, 81, 46-56.

53. Dietz, R.S., Holden, J.C., 1970. Reconstruction of Pangaea: breakup and dispersion of continents, Permian to Present. Journal of Geophysical Research, 75, 4939-4963.

54. Dissanayake, C.B., Chandrajith, R., 1999. Sri Lanka - Madagascar Gondwana linkage: evidence for a Pan-African mineral belt. Journal of Geology, 107, 223-235.

55. Droz, L., Bellaiche, C., 1991. Seismic facies and geologic evolution of the central portion of the Indus Fan. In: Wimer, P., Link, M.H. (Eds.). Seismic facies and sedimentary processes of submarine fans and turbidite systems, Springer Verlag, 383-420.

56. Duncan, R.A., 1981. Hotspots in the Southern Oceans - an absolute frame of reference for the motion of the Gondwana continents. Tectonophysics, 74, 29-42.

57. Duncan, R.A., 1990. The volcanic record of the Reunion hotspot. In: Duncan, R.A., Backman, J., Peterson, C. et al. (Eds.). Proceedings of ODP Scientific Results. Ocean Drilling Programme, College Station, TX, 115, 3-10.

58. Duncan, R.A., Hargraves, R.B., 1990. $^{40}Ar/^{39}Ar$ Geochronology of basement rocks from the Mascarene Plateau, the Chagos Bank, and the Maldives Ridge. In: Duncan, R.A., Backman, J., Peterson, L.C. et al. (Eds.). Proceedings of ODP Scientific Results, Texas A&M University, 115, 43-51.

59. Duncan, R.A., Pyle, D.G., 1988. Rapid eruption of the Deccan flood basalts at the Cretaceous / Tertiary boundary. Nature, 333, 841-843.

60. Dyment, J., 1991. Structure et évolution de la lithosphère océanique dans l'océan Indien: apport des données magnétiques. Doctorate Thesis, Université Louis Pasteur.

61. Dyment, J., 1996. Birth and death of an ocean basin: evolution of the Mascarene Basin between 83 and 60 Ma (chrons 34-27). International Symposium on Geology and Geophysics of the Indian Ocean. Goa, India, 46-47.

62. Dyment, J., 1998. Evolution of the Carlsberg Ridge between 60 and 45 Ma: ridge propagation, spreading asymmetry, and the Deccan-Reunion hotspot. Journal of Geophysical Research, 103, 24067-24084.

63. Eldholm, O., Skogseid, J., Planke, S., Gladezenco, T.P., 1995. Volcanic margins concept. In: Banda et al. (Eds.), Rifted Continent-Ocean Boundaries. Kluwer Academic Publishers, Dordrecht, NATO ASI Series, 1-16.

64. Fisher, R.L., Engel, C.G., Hilde, T.C.W., 1968. Basalts dredged from the Amirante Ridge, Western Indian Ocean. Deep Sea Research, 15, 521-534.

65. Fisher, R.L., Sclater, J.G., McKenzie, D.P., 1971. The evolution of the Central Indian Ridge, Western Indian Ocean. Geological Society of America Bulletin, 82, 553-562.

66. Fitton, J.G., 1983. Active versus passive continental rifting: evidence from the West African Rift system. Tectonophysics, 94(1-4), 473-481.

67. Francis, T.J.G., Davies, D., Hill, M.N., 1966. Crustal structure between Kenya and the Seychelles. Philosophical Transactions of Royal Society of London, Series A, 259, 240-261.

68. Francis, T.J.G., Shor, G.G., 1966. Seismic refraction measurements in the Northwest Indian Ocean. Journal of Geophysical Research, 71, 427-449.

69. Golombek, M.P., Tanaka, K.L., Franklin, B.J., 1996. Extension across Tempe Terra, Mars, from measurements of fault scarp widths and deformed craters. Journal of Geophysical Research, 101, 26119–26130.

70. Gombos, A.M., Powell, W.G., Norton, I.O., 1995. The tectonic evolution of western India and its impact on hydrocarbon occurrences: An overview. Sedimentary Geology, 96(1-2), 119-129.

71. Goslin, J., Recq, M., Schlich, R., 1981. Structure profonde du plateau de Madagascar: relations avec le plateau de crozet. Tectonophysics, 76, 75-97.

72. Goslin, J., Segoufin, J., Schlich, R., Fischer, R.L., 1980. Submarine topography and shallow structure of the Madagascar Ridge, Western Indian Ocean. Geological Society of America Bulletin, 91, 741-753.

73. Hofmann, C., Feraud, G., Courtillot, V., 2000. ^{40}Ar-^{39}Ar dating of mineral separates and whole rocks from the Western Ghats lava pile: further constraints on duration and age of the Deccan Trap. Earth and Planetary Science Letters, 180, 13-27.

74. Intergovernmental Oceanographic Commission, International Hydrographic Organization, British Oceanography Data Centre, 2003. Centenary Edition of the GEBCO Digital Atlas, published on CD-ROM on behalf of the Intergovernmental Oceanographic Commission and the International Hydrographic Organization as part of the General Bathymetric Chart of the Oceans. British Oceanographic Data Centre, Liverpool, UK.

75. Jonas, J., Hall, S., Casey, J. F., 1991. Gravity anomalies over extinct

spreading centers: a test of gravity models of active centers. Journal of Geophysical Research, 96, 11,759–11,777.

76. Jones, E.J.W., 1999. Marine Geophysics. John Wiley and Sons Ltd., Chichester, 466 p.

77. Katz, M.B., Premoli, C., 1979. India and Madagascar in Gondwanaland based on matching Precambrian lineaments. Nature, 279, 312-315.

78. Khanna, M., Walton, E.K., 1992. Geological evolution of the Seychelles western shelf with special reference to the Karoo Supergroup. Indian Journal of Petroleum Geology, 1(1), 52-74.

79. Kolla, V., Coumes, F., 1987. Morphology, internal structure, seismic stratigraphy and sedimentation of Indus Fan. American Association of Petroleum Geologists Bulletin, 71(6), 650-677.

80. Kolla, V., Coumes, F., 1990. Extension of structural and tectonic trends from the Indian subcontinent into the eastern Arabian Sea. Marine and Petroleum Geology, 7, 188-196.

81. Kothari, V., Waraich, R.S., Baruah, R.M., Lal, N.K., Zutshi, P.L., 2001. A reassessment of the hydrocarbon prospectivity of Kerala-Konkan deep water basin, western offshore, India. PETROTECH Poster.

82. Krishna, K.S., Murty, G.P.S., Srinivas, K., Rao, D.G., 1992. Magnetic studies over the northern extension of the Pratap Ridge complex, eastern Arabian Sea. Geo Marine Letters, 12, 7-13.

83. Krishna, K.S., Rao, D.G., Sar, D., 2006. Nature of the crust in the Laxmi Basin (14°-20°), western continental margin of India. Tectonics, 25(TC1006), doi:10.1029/2004TC001747.

84. Krishnan, M.S., 1968. Geology of India and Burma. Higgin-Bothams, Madras, 536 p.

85. Kroner, A., Brown, L., 2005. Structure, composition and evolution of the South Indian and Sri Lankan Granulite Terrains from deep seismic profiling and other geophysical and geological investigations: a LEGENDS initiative. Gondwana Research, 8 (3), 317-335.

86. Kumar, R., 1986. Fundamentals of Historical Geology and stratigraphy of India. Wiley Eastern Limited, 254 p.

87. Lane, C.I., Collier, J.S., Minshull, T.A., Whittmarsh, R.B., Sansom, V., 2003. Structure of the Laxmi Ridge ocean-continent transition zone. EOS Transactions, American Geophysical Union, 84(46), F1343.

88. Lane, C.I., Minshull, T.A., Collier, J.S., Whittmarsh, R.B., Sansom, V., Evain, M.M., 2005. Extensive magmatism during the formation of the Laxmi Ridge rifted margin, NW Indian Ocean. Geophysical Research Abstracts, 7.

89. Lapedes, D.N., 1978. McGraw-Hill Dictionary of Scientific and Technical Terms. McGraw-Hill Book Company, New York, 1771p.

90. Laughton, A.S., Matthews, D.H., Fisher, R.L., 1970. The structure of the Indian Ocean. In: Maxwell, A.E. (Eds.), The Sea. Wiley-Interscience, New York, 4, 543-586.

91. Lawver, L.A., Gahagan, L.M., 2005. Steep satellite altimetry gradients as a proxy to the edge of the continental crust, American Geophysical Union, Spring Meeting, Abstract.

92. Lawver, L.A., Gahagan, L.M., Dalziel, W.D., 1999. A tight fit-Early Mesozoic Gondwana, a plate reconstruction perspective. In: Motoyoshi, Y., Shiraishi, K. (Eds.). Origin and Evolution of Continents, Memoir of National Institute of Polar Research, Special Issue, 53, 214-229.

93. Le Pichon, X., 1968. Seafloor spreading and continental drift. Journal of Geophysical Research, 73, 3,661-3,697.

94. Ludwig, W.J., Nafe, J. E., Drake, C. L., 1970. Seismic refraction. In: A.E. Maxwell (Ed.). The Sea. Wiley-Interscience, New York, 53-84.

95. Macnab, R.F., 1966. Magnetic effects of two-dimensional structures. BIO Computer note 66-1-C, Bedford Institute of Oceanography.

96. Mahadevan, T.M., 1994. Deep continental structure of India: A review. Geological Society of India, Bangalore, 569 p.

97. Malod, J.A., Droz, L., Mustafa Kamal, B., Patriat, B., 1997. Early spreading and continental to oceanic basement transition beneath the Indus-deep sea fan: northeastern Arabian Sea. Marine Geology, 141, 221-235.

98. Mart, Y., 1988. The tectonic setting of the Seychelles, Mascarene and Amirante Plateaus in the western equatorial Indian Ocean. Marine Geology, 79, 261-274.

99. Masson, D.G., 1984. Evolution of the Mascarene Basin, Western Indian Ocean and the significance of the Amirante arc. Marine Geophysical Researches, 6, 365-382.

100. Matthews, D.H., 1966. The Owen Fracture Zone and the northern end of the Carlsberg Ridge. Philosophical Transactions of Royal Society of London, Series A 259, 172-186.

101. Matthews, D.H., Davies, D., 1966. Geophysical studies of the Seychelles Bank. Philosophical Transactions of Royal Society of London, Series A, 259, 227-239.

102. McKenzie, D., Sclater, J.G., 1971. The evolution of the Indian Ocean since the Late Cretaceous. Geophysical Journal of Royal Astronomical Society, 25, 437-528.

103. Meissner, B., Deters, P., Srikantappa, C., Kohler, H., 2002.

Geochronological evolution of the Moyar, Bhavani and Palghat shear zones of southern India: implications for east Gondwana correlations. Precambrian Research, 114, 149-175.

104. Menon, R.D., Santosh, M., 1995. A Pan-African gemstone province of East Gondwana. In: Yoshida, M., Santosh, M. (Eds.). India and Antarctica during the Precambrian. Geological Society of India, Bangalore, 357-371.

105. Miles, P.R., Munschy, M., Segoufin, J., 1998. Structure and early evolution of the Arabian Sea and East Somali Basin. Geophysical Journal International, 15, 876-888.

106. Miles, P.R., Roest, W.R., 1993. Earliest seafloor spreading magnetic anomalies in the north Arabian Sea and the ocean-continent transition. Geophysical Journal International, 115, 1025-1031.

107. Minshull, T.A., Lane, C.I., Collier, J.S., Whitmarsh, R.B., 2006. Rifting and magmatism at the western margin of India. Geophysical Research Abstracts, 8, 08653.

108. Mishra, D.C., Arora, K., Tiwari, V.M., 2004. Gravity anomaly and the associated tectonic features over the Indian Peninsular Shield and adjoining ocean basins. Tectonophysics, 379, 61-76.

109. Morgan, W.J., 1972. Deep mantle convection plumes and plate motions. American Association of Petroleum Geologists Bulletin, 56, 203-213.

110. Morgan, W.J., 1981. Hotspot tracks and the opening of the Atlantic and Indian Oceans. In: Emiliani (Ed.), The Sea. Wiley Interscience, New York, 7, 443-487.

111. Müller, R.D., Gaina, C., Roest, W.R., Hansen, D.L., 2001. A recipe for microcontinent formation. Geology, 29(3), 203-206.

112. Müller, R.D., Royer, J.Y., Lawver, L.A., 1993. Revised plate motions relative to the hotspot from combined Atlantic and Indian Ocean hotspot tracks. Geology, 21, 275-278.

113. Murty, A.V.S., Arasu, R.T., Dhanawat, B.S., Subrahmanyam, V.S.R., 1999. Some aspects of deepwater exploration in the light of new evidences in the western Indian offshore. Third International Petroleum conference and exhibition, PETROTECH, 457-462.

114. Murty, K.V.S., Prasad, B.N., Rawat, G.S., 1981. Structure of continental margin off Bombay. In: Rao, R.P. (Ed.). Workshop on Geological Interpretation of Geophysical Data. ONGC, Dehradun, 41-48.

115. Mutter, J.C., Talwani, M., Stoffa, P.L., 1982. Origin of seaward-dipping reflectors in oceanic crust off the Norwegian margin by "subaerial sea-floor spreading". Geology, 10(7), 353-357.

116. Nabighian, M.N., 1972. The analytic signal of two-dimensional magnetic bodies with polygonal cross-section: Its properties and use for automated

anomaly interpretation. Geophysics, 37 (3), 507-517.

117. Nabighian, M.N., 1974. Additional comments on the analytic signal of two-dimensional magnetic bodies with polygonal cross section. Geophysics, 39 (1), 85-92.

118. Naini, B.R., 1980. Geological and Geophysical study of the continental margin of western India, and the adjoining Arabian Sea including the Indus cone. Ph.D. Thesis, Columbia University.

119. Naini, B.R., Talwani, M., 1977. Sediment distribution and structures in the Indus Cone and the western continental margin of India (Arabian Sea). EOS Transactions, American Geophysical Union, 58, 405.

120. Naini, B.R., Talwani, M., 1982. Structural framework and the evolutionary history of the continental margin of western India. In: Watkins, J.S., Drake, C.L. (Eds.), Studies in Continental Margin Geology. Memoir 34, American Association of Petroleum Geologists, 167-191.

121. Nair, K.M., Singh, N.K., Ram, J., Gavarshetty, C.P., Muraleekrishnan, B., 1992. Stratigraphy and sedimentation of Bombay Offshore Basin. Journal of Geological Society of India, 40, 415-442.

122. Naqvi, S.M., 2005. Geology and Evolution of the Indian Plate: From Hadean to Holocene-4 Ga to 4 Ka. Capital Publishers, New Delhi, 450p.

123. Narain, H., Kaila, K.L., Verma, R.K., 1968. Continental margins of India. Canadian Journal of Earth Sciences, 5(4), 1051-1065.

124. National Research Council, 1979. Ad hoc panel to investigate the geological and geophysical research needs and problems of continental margins. Natural Academy Science, Washington, 1–302.

125. Negi, J.G., Agrawal, P.K., Pandey, O.P., Singh, A.P., 1993. A possible K-T boundary bolide impact site offshore near Bombay and triggering of rapid Deccan volcanism. Physics of Earth and Planetary Interiors, 76, 189-197.

126. Norton, I.O., Sclater, J.G., 1979. A model for the evolution of the Indian Ocean and the break-up of Gondwanaland. Journal of Geophysical Research, 84(B12), 6803-6830.

127. Open University Course Team, 1995. The Ocean Basins: Their Structure and Evolution. The Open University Press, England, 171 p.

128. Pande, K., Sheth, H.C., Bhutani, R., 2001. ^{40}Ar -^{39}Ar age of the St. Mary Islands volcanics, southern India: record of India - Madagascar break-up on the Indian subcontinent. Earth and Planetary Science Letters, 193, 39-46.

129. Pandey, O.P., Agrawal, P.K., Negi, J.G., 1995. Lithospheric structure beneath Laxmi Ridge and Late Cretaceous geodynamic events. Geo Marine Letters, 15, 85-91.

130. Pepper, J.F., Everhart, G.M., 1963. The Indian Ocean: the geology of its bordering lands and the configuration of its floor. In: Miscellaneous Geologic Investigations. U.S. Geological Survey, 1-33.

131. Plummer, P.S., 1995. Ages and geological significance of the igneous rocks from Seychelles. Journal of African Earth Science, 20(2), 91-101.

132. Plummer, P.S., 1996. The Amirante ridge/trough complex: response to rotational transform rift/drift between Seychelles and Madagascar. Terra Nova, 8, 34-47.

133. Plummer, P.S., Belle, E.R., 1995. Mesozoic tectono-stratigraphic evolution of the Seychelles microcontinent. Sedimentary Geology, 96, 73-91.

134. Pradeepkumar, A.P., Krishnanath, R., 2000. A Pan-African 'Humite Epoch' in East Gondwana: implications for Neoproterozoic Gondwana geometry. Journal of Geodynamics, 29, 43-62.

135. Radhakrishna, T., Dallmeyer, R.D., Joseph, M., 1994. Paleomagnetism and $^{36}Ar/^{40}Ar$ vs $^{39}Ar/^{40}Ar$ isotope correlation ages of dyke swarms in Central Kerala, India: tectonic implications. Earth and Planetary Science Letters, 121, 213-226.

136. Radhakrishna, T., Joseph, M., Mathai, J. Southern Granulite Terrain and constraints for the Precambrian continental assemblies. Joint AOGS 1st Annual Meeting and 2nd APHW Conference, Asia Oceania Geosciences Society, Singapore, 55-56.

137. Radhakrishna, T., Joseph, M., Thampi, P.K., Mitchell, J.G., 1990. Phanerozoic mafic dyke intrusions from the high grade terrain from southwestern India: K-Ar isotope and geochemical implications. In: Parker, A.J., Rickwood, P.C., Tucker, D.H. (Eds.). Mafic Dykes and Emplacement Mechanisms. Balkema, Rotterdam, 363-372.

138. Radhakrishna, T., Maluski, H., Mitchell, J.G., Joseph, M., 1999. ^{40}Ar-^{39}Ar and K/Ar geochronology of the dykes from the South Indian Granulite Terrain. Tectonophysics, 304, 109-129.

139. Raju, D.S.N., Bhandari, A., Ramesh, P., 1999. Relative sea level fluctuations during Cretaceous and Cenozoic in India. Bulletin of ONGC, 36, 185-202.

140. Ramana, M.V., Rajendraprasad, B., Hansen, R.D., 1987. Geophysical and geological surveys along the northeastern flank of Mount Error, Northwestern Indian Ocean. Marine Geology, 76, 153-162.

141. Ramaswamy, G., Rao, K.L.N., 1980. Geology of the continental shelf of the west coast of India. In: Miall, A.D. (Ed.), Facts and Principles of Petroleum Occurrence. Canadian Society of Petroleum Geologists, Canada, Memoir 6, 801-821.

142. Rampino, M.R., Stothers, R.B., 1988. Flood basalt volcanism during the last 250 million years. Science, 241, 663-667.

143. Rao, D.G., Bhattacharya, G.C., 1977. Marine magnetic anomalies off the southwest coast of India and their analysis. Journal of Geological Society of India, 18, 504-508.

144. Rao, D.G., Bhattacharya, G.C., Subbaraju, L.V., Ramana, M.V., Subrahmanyam, V., Raju, K.A.K., Ramprasad, T., Chaubey, A.K., 1987. Regional marine geophysical studies of the southwestern continental margin of India. In: Rao, T.C.S., Natarajan, R., Desai, B.N., Swamy, G.N., Bhatt, S.R. (Eds.), Contributions in Marine Sciences - Dr. S.Z. Qasim Sastyabdapurti Felicitation Volume. NIO, Goa, Goa, 427-437.

145. Rao, D.G., Ramana, M.V., Bhattacharya, G.C., Subbaraju, L.V., Raju, K.A.K., Ramprasad, T., 1992. Marine geophysical studies along a transect across the continental margin off Bombay coast, west of India. In: Desai, B.N. (Ed.), Oceanography of the Indian Ocean. IBH Publications, New Delhi, 493-501.

146. Rao, R.P., Srivastava, D.C., 1981. Seismic stratigraphy of west Indian offshore. In: R.P. Rao (Ed.). Workshop on Geological Interpretation of Geophysical Data. ONGC, Dehradun, 1-9.

147. Rao, R.P., Srivastava, D.C., 1984. Regional seismic facies analysis of western offshore, India. Bulletin of ONGC, 21, 83-96.

148. Rao, T.C.S., Bhattacharya, G.C., 1975. Seismic profiler & magnetic studies off Quilon, southwest India. Indian Journal of Marine Sciences, 4, 110-114.

149. Rathore, S.S., Vijayan, A.R., Prabhu, B.N., Misra, K.N., 1997. K-Ar dating of basement rocks of Bombay Offshore Basin. Second International Petroleum Conference and exhibition. New Delhi.

150. Reddy, S.I., Roychowdhury, K., Drolia, R.K., Ashalata, B., Mittal, G.S., Subrahmanyam, C., Singh, R.N., 1988. On the structure of the western continental margin off Mangalore coast, India. Journal of Association of Exploration Geophysicists, 9, 181-189.

151. Reeves, C., Leven, J., 2001. The evolution of the west coast of India from a perspective of global Tectonics. Journal of Geophysics, 22(1), 17-23.

152. Reeves, C.V., Sahu, B.K., de Wit, M., 2002. A re-examination of the paleo-position of Africa's eastern neighbours in Gondwana. Journal of African Earth Science, 34, 101-108.

153. Roest, W.R., Hamed, A., Verhoef, J., 1992. The seafloor spreading rate dependence of the anomalous skewness of marine magnetic anomalies. Geophysical Journal International, 109, 653-669.

154. Rogers, J.J.W., Miller, J.S., Clements, A.S., 1995. A Pan African zone linking East and West Gondwana. In: Yoshida, M., Santosh, M. (Eds.). India and Antarctica during the Precambrian. Geological Society of India, Bangalore, 11-23.

155. Royer, J.Y., Chaubey, A.K., Dyment, J., Bhattacharya, G.C., Srinivas, K., Yatheesh, V., Ramprasad, T., 2002. Paleogene plate tectonic evolution of the Arabian and Eastern Somali basins. In: Clift, P.D., Croon, D., Gaedicke, C., Craig, J. (Eds.), The Tectonic and Climatic Evolution of the Arabian Sea Region. Geological Society, London, Special Publication, 195, 7-23.

156. Royer, J.Y., Müller, R.D., Gahagan, L.M., Lawver, L.A., Mayes, C.L., Nurnberg, D., Sclater, J.G., 1992. A global isochron chart. Technical Report, 117, University of Texas Institute for Geophysics.

157. Sacks, P.E., Nambiar, C.G., Walters, L.J., 1997. Dextral Pan-African shear along the southwestern edge of the Achankovil shear belt, South India: constraints on Gondwana reconstructions. Journal of Geology, 105, 275-284.

158. Sahabi, M., 1993. Un mode`le ge´ne´ral de l'e´volution de l'oce´an Indien. Ph.D. Thesis, Universite Bretagne.

159. Sandwell, D.T., Smith, W.H.F., 1997. Marine gravity anomaly from Geosat and ERS I satellite altimetry. Journal of Geophysical Research, 102, 10039-10054.

160. Sandwell, D.T., Smith, W.H.F., 2003. World Gravity Image version 11.2, 2 minute resolution, 72S to 72N. ftp://topex.ucsd.edu/pub/global_grav_2min/

161. Satyanarayana, Y., Murty, G.R.K., De, C., 1997. Marine magnetic studies over the Laccadive Ridge, Indian Ocean. Journal of Geological Society of India, 49(1), 39-46.

162. Schlich, R., 1974. Seafloor spreading history and deep sea drilling results in the Madagascar and Mascarene Basins, Western Indian Ocean. Initial Report of the Deep Sea Drilling Project, 25, 663-678.

163. Schlich, R., 1982. The Indian Ocean: aseismic Ridges, spreading centres and basins. In: Nairn, A.E.M., Stehli, F.G. (Eds.), The Ocean Basins and Margins. Plenum Press, NewYork, 6, 51-147.

164. Schlich, R., Fondeur, C., 1974. Anomalies magnetiques cretacees dans le bassin des Mascareignes (Ocec Indien). C.R. Academy of Science, Paris, 278B, 541-544.

165. Schlich, R., Simpson, E.S.W., Gieskes, J., Girdley, W.A., Leclaire, L., Marshall, B., Moore, C., Muller, C., Sigal, J., Vallier, T.L., White, S.M., Zobel, B., 1974. Site 239. Initial Report of the Deep Sea Drilling Project, 25, 25-63.

166. Scotese, C.R., Gahagan, L.M., Larson, R.L., 1988. Plate tectonic reconstructions of the Cretaceous and Cenozoic ocean basins. Tectonophysics, 155, 27-48.

167. Seibold, E., Berger, W.H., 1993. The Seafloor: An Introduction to Marine Geology. Springer Verlag, 356 p.

168. Shaynurov, R.V., Terekhov, A.A., 1991. Gravitational and magnetic fields of the Central Arabian Sea and their correlation with tectonic structure. Oceanology, 31, 83-89.

169. Shipboard Scientific Party, 1972. Site 219. In: Whitmarsh, R.B., Weser, O.E., Ross, D.A. (Eds.), Initial Report of Deep Sea Drilling Project, 23.

170. Singh, A.P., 1999. The deep crustal accretion beneath the Laxmi Ridge in the northeastern Arabian Sea: the plume model again. Journal of Geodynamics, 27, 609-622.

171. Singh, A.P., 2002. Impact of Deccan volcanism on deep crustal structure along western part of Indian mainland and adjoining Arabian Sea. Current Science, 82(3), 316-325.

172. Singh, N.K., Lal, N.K., 1993. Geology and Petroleum prospects of Konkan-Kerala Basin. In: Biswas, S.K., Dave, A., Garg, P., Pandey, J., Maithani, A., Thomas, N.J. (Eds.). Proceedings of Second seminar on Petroliferous Basins of India, Indian Petroleum Publishers, 2, 461-469.

173. Singh, S.C., Crawford, W., Carton, H., Seher, T., Combier, V., Cannat, M., Canales, J.P., Dusunur, D., Escartin, J., Miranda, J.M., 2006. Discovery of axial magma chamber reflections and faults beneath the lucky strike volcano and hydrothermal field at the mid-Atlantic Ridge. Nature, 442 (7106), 1029-1032.

174. Smith, A.G., Hallam, A., 1970. The fit of the southern continents. Nature, 225, 139-144.

175. Smith, W.H.F., Sandwell, D.T., 1997. Global Seafloor topography from satellite altimetry and ship depth soundings. Science, 277, 1956-1962.

176. Srinivas, K., 2004. Seismic reflection and bathymetric study over deep offshore regions off the central west coast of India. Ph.D. Thesis, Goa University, India.

177. Srivastava, D.C., Mathur, P.N., 1984. Seismic facies of the carbonate sequences of the Mahim area, Bombay Offshore Basin. Bulletin of ONGC, 21 (2), 89-93.

178. Storey, M., Mahoney, J.J., Saunders, A.D., Duncan, R.A., Kelley, S.P., Coffin, M.F., 1995. Timing of hotspot-related volcanism and the breakup of Madagascar and India. Science, 267, 852-855.

179. Subrahmanyam, V., Rao, D.G., Ramana, M.V., Krishna, K.S., Murty, G.P.S., Rao, M.G., 1995. Structure and tectonics of the southwestern continental margin of India. Tectonophysics, 249, 267-282.

180. Talwani, M., Abreu, V., 2000. Inferences regarding initiation of oceanic crust formation from the U.S. East Coast margin and conjugate Atlantic margins. In: Mohriak, W., Talwani, M. (Eds.), Atlantic Rifts and Continental Margins. American Geophysical Union, Washington, DC, Geophysical Monograph, 115, 211-233.

181. Talwani, M., Ewing, J., Sheridan, R.E., Holbrook, W.S., Glover, L., 1995. The EDGE experiment and the US east coast magnetic anomaly. In: Banda, E., Thorne, M., Talwani, M. (Eds.). Rifted Ocean-Continent Boundaries. Kluwer, Dordrecht, 155-181.

182. Talwani, M., Heirtzler, J.R., 1964. Computation of Magnetic anomalies caused by two-dimensional structures of arbitrary shape. In: Parks, G.A. (Ed.), Computers in the Mineral Industries. Stanford University, 464-480.

183. Talwani, M., Kahle, H.G., 1975. Free-air gravity anomaly maps of the Indian Ocean, Geological-Geophysical Atlas of the Indian Ocean. In: Udintsev, G.E. (Ed.), Moscow, 81-104.

184. Talwani, M., Reif, C., 1998. Laxmi Ridge- a continental sliver in the Arabian Sea. Marine Geophysical Researches, 20, 259-271.

185. Talwani, M., Worsel, J.L., Landisman, M., 1959. Rapid gravity computation for two-dimensional bodies with application to the Mendocino submarine fracture zone. Journal of Geophysical Research, 64, 49-59.

186. Tewari, V.M., Rao, V.V., 2003. Structure and tectonics of the Proterozoic Aravalli-Delhi Geological Province, NW Indian Peninsular Shield. In: Mahadevan, T.M., Arora, B.R., Gupta, K.R. (Eds.). Indian Continental Lithosphere, Geological Society of India, Memoir 53, 57-78.

187. Todal, A., Eldholm, O., 1998. Continental margin off western India and Deccan Large Igneous Province. Marine Geophysical Researches, 20, 273-291.

188. Torsvik, T.H., Tucker, R.D., Ashwal, L.D., Carter, L.M., Jamtveit, V., Vidyadharan, K.T., Venkataramana, P., 2000. Late Cretaceous India - Madagascar fit and timing of breakup related magmatism. Terra Nova, 12, 220-224.

189. Trujillo, A.P., Turman, H., 2005. Essentials of Oceanography. Prentice Hall, Englewood Cliffs, NJ, 552p.

190. Udintsev, G.B., Fisher, R.L., Kanaev,V.F., Laughton, A.S., Simpson, E.S.W., Zhiv, D.F., 1975. Geological-Geophysical Atlas of the Indian Ocean. Academy of Science, U.S.S.R., Moscow, 151p.

191. Valdiya, K.S., 2001. River response to continuing movements and the scarp development in central Sahyadri and adjoining coastal belt. Journal of Geological Soceity of India, 57, 13-30.

192. Valsangkar, A.B., Radhakrishnamurthy, C., Subbarao, K.V., Beckinsale, R.D., 1981. Paleomagnetism and Potassium-Argon age studies of acid igneous rocks from the St. Mary Islands. Geological Society of India, Memoir 3, 265-275.

193. Vandamme, D., Courtillot, V., Besse, J. Montigny, R., 1991. Paleomagnetism and age determination of the Deccan Traps (India): Results of a Nagpur-Bombay traverse and Review of Earlier work.

Reviews of Geophysics, 29(2), 159-190.

194. Verzhbitsky, E.V., 2003. Geothermal regime and genesis of the Ninety-East and Chagos-Laccadive Ridges. Journal of Geodynamics, 35, 289-302.

195. Wessel, P., Smith, W.H.F., 1995. New version of the Generic Mapping Tools released. EOS Transactions of American Geophysical Union, 76, 329.

196. White, R., McKenzie, D., 1989. Magmatism at rift zones: the generation of volcanic continental margins and Flood Basalts. Journal of Geophysical Research, 94(B6), 7685-7730.

197. Whittmarsh, R.B., 1974. Some aspects of plate tectonics in the Arabian Sea. In: Initial Reports of the Deep Sea Drilling Project. US Govt. Printing Office, Washington, 23, 35-115.

198. Widdowson, M., 1997. Tertiary paleosurfaces of the SW Deccan, western India: implications for passive margin uplift. In: Widdowson, M. (Ed.), Paleosurfaces: Recognition, Reconstruction and Paleoenvironmental Interpretation. Geological Society, London, Special Publication, 120, 221-248.

199. Widdowson, M., Gunnell, Y., 1999. Lateritization, geomorphology and geodynamics of a passive continental margin: the Konkan and Kanara coastal low lands of western Peninsular India. International Association of Sedimentologists, Special Publication, 27, 245-274.

200. Widdowson, M., Pringle, M.S., Fernandez, O.A., 2000. A post K-T boundary (Early Paleocene) age for Deccan type feeder dykes, Goa, India. Journal of Petrology, 41(7), 1177-1194.

201. Windley, B.F., Razafiniparany, A., Razakamanana, T., Ackermand, D., 1994. Tectonic framework of the Precambrian of Madagascar and its Gondwana connections. Geologische Rundschau, 83, 642-659.

202. Yatheesh, V., Bhattacharya, G.C., Mahender, K., 2006. The terrace like feature in the mid-continental slope region off Trivandrum and a plausible model for India-Madagascar juxtaposition in immediate pre-drift scenario. Gondwana Research, 10, 179-185.

203. Yoshida, M., Rajesh, H.M., Santosh, M., 1999. Juxtaposition of India and Madagascar: A perspective. Gondwana Research, 2 (3), 449-462.

ANNEXURE

Available online at www.sciencedirect.com
SCIENCE DIRECT®
Gondwana Research 10 (2006) 179–185
www.elsevier.com/locate/gr

The terrace like feature in the mid-continental slope region off Trivandrum and a plausible model for India–Madagascar juxtaposition in immediate pre-drift scenario

V. Yatheesh [a,*], G.C. Bhattacharya [b], K. Mahender [c]

[a] National Centre for Antarctic and Ocean Research, Headland Sada, Vasco-da-Gama, Goa 403 804, India
[b] Geological Oceanography Division, National Institute of Oceanography, Dona Paula, Goa 403 004, India
[c] Department of Earth Science, Goa University, Taleigao Plateau, Goa 403 206, India

Received 2 April 2005; accepted 24 November 2005
Available online 26 May 2006

Abstract

Bathymetry of the southwestern continental margin of India reveals the presence of an anomalous terrace like feature in the mid-continental slope region off Trivandrum. The genesis of this terrace of large areal extent (~9000 sq. km.) is yet to be established. Based on exercises with several existing paleogeographic reconstruction models and updated compilation of identified offshore tectonic elements, this study attempts to identify a plausible model of India–Madagascar juxtaposition in immediate pre-drift scenario, which provides idea about genesis of this terrace. It is inferred that the terrace off Trivandrum and an anomalous bathymetric notch located in the northern Madagascar Ridge are conjugate features related to India–Madagascar separation and the rifted and sheared segments of the pre-drift plate boundary have shaped their outlines. The drifting of India from Madagascar is suggested to have commenced at about 86.5 Ma.

Keywords: Terrace; Madagascar Ridge; India–Madagascar juxtaposition; Paleogeographic reconstruction; Shear zones

1. Introduction

The continental shelf of west coast of India (Fig. 1), limited by the 200 m isobath, has variable width. Towards the north this shelf is relatively wider, being more than 300 km in the areas north off Mumbai coast, whereas towards the south this width gradually narrows down to about 50 km off Trivandrum. As compared to the continental shelf, the continental slope in most of this region is relatively narrow and parallels the trend of the continental shelf edge. However, the continental slope region off Trivandrum (Fig. 1) interestingly depicts the presence of an anomalous broad terrace like feature, which has not drawn much attention of the researchers so far. The western continental margin of India, to which this terrace belongs, is considered to be a passive continental margin (Biswas, 1982, 1987), which evolved during the process of rifting and drifting of Madagascar, Seychelles and India. Even though researchers agree on the concept of a welded Madagascar–Seychelles–India continental block, but opinion differs regarding their immediate pre-drift juxtaposition and consequential early post drift positions. Probably lack of distinct and dependable "piercing points" such as onshore tectonic lineaments, which could have constrained this juxtaposition, is one of the reasons for those varied inferences. The other reason could be the absence of India–Madagascar break-up related magnetic isochrons, which could have allowed arriving at consistent rotation parameters for constraining early India–Madagascar separation, as that break-up took place during Cretaceous long normal superchron.

It was also observed that the outline of this terrace appears in the post anomaly 34 paleogeographic reconstructions of Norton and Sclater (1979) as well as of Besse and Courtillot (1988). However, those studies, apparently due to their emphasis on broader perspective, did not pay specific attention to this terrace or looked for its conjugate feature. Rao and Bhattacharya (1975) analyzed magnetic and seismic data in the northern part (off

* Corresponding author. Fax: +91 832 2520877.
E-mail address: yatheesh@ncaor.org (V. Yatheesh).

1342-937X/$ - see front matter © 2006 International Association for Gondwana Research. Published by Elsevier B.V. All rights reserved.
doi:10.1016/j.gr.2005.11.021

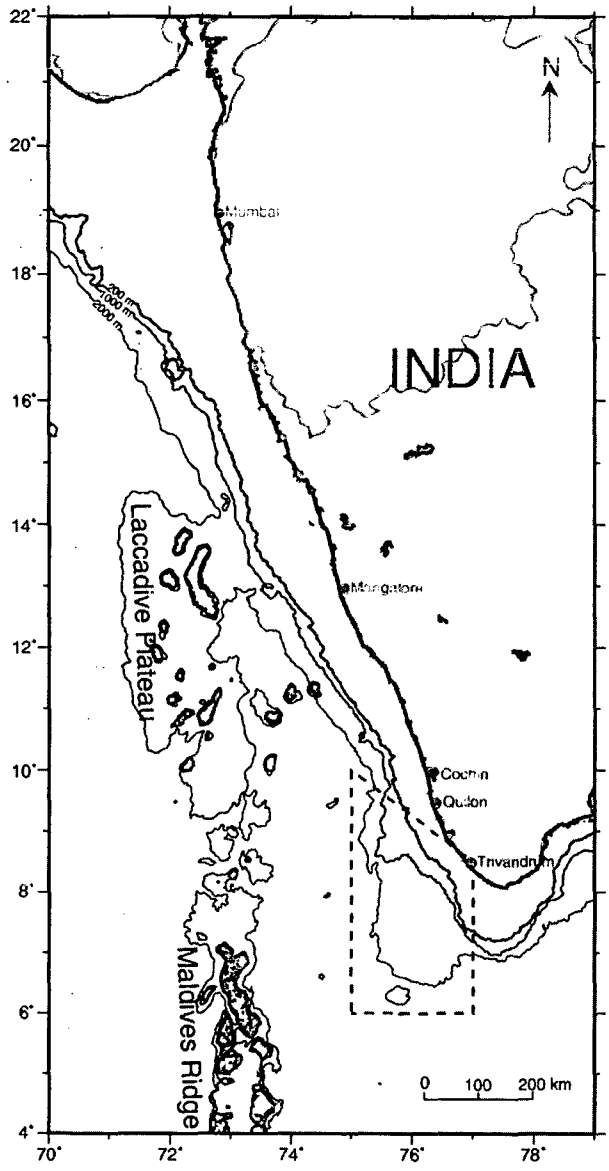

g. 1. Generalized map of the southwestern continental margin of India along with ected (200, 1000 and 2000 m) bathymetric contours obtained from recent GEBCO gital data set (Intergovernmental Oceanographic Commission et al., 2003). The shed box indicates the area of the terrace like feature located off Trivandrum.

uilon) of this terrace and attributed its genesis to block faulting the basement. As mentioned by Storey et al. (1995), the stern part of the northern Madagascar Plateau and a bathymetric high on the west side of the southern tip of India was ferred by Dyment (1991) to be conjugate with respect to the ascarene Basin spreading ridge. However, subsequent searchers could not identify those inferred conjugate features d make their use to constrain the India–Madagascar juxtasition, since they were not depicted in publication. In view of is, an attempt has been made in this paper to identify those njugate features distinctly through exercises with several ailable paleogeographic reconstruction models and use those njugate features to arrive at a close fit model of the India–adagascar juxtaposition in their immediate pre-drift scenario.

2. The topography of the terrace like feature off Trivandrum

The bathymetry contour map (Fig. 1), shows a conspicuously wide low gradient zone in the mid-continental slope region off Trivandrum. This zone broadly lies between 1000 and 2000 m isobaths and covers an area of about 9000 sq. km. Eight available bathymetric transects (Figs. 2 and 3) across this zone suggest this terrace as a relatively flat zone bounded by a steep ascending (by about 1000 m) seafloor to the adjacent continental shelf on the easterly side and a comparable steep descending seafloor towards the deep sea in the westerly side. This topography appears to be anomalous as compared to the general topography depicted by contours and two bathymetric transects (Fig. 3) across the normal shelf–slope configuration in the north. This wide zone is considered to qualify well as a 'terrace' following the definition of Lapedes (1978) and for further reference in this study we denote this feature as 'Terrace off Trivandrum (TOT)'.

3. India–Madagascar juxtaposition at anomaly 34 time — varied inferences

For tracing the India–Madagascar separation one need to start with the India–Madagascar juxtaposition. The aspect of paleogeographic juxtaposition of India and Madagascar has been directly addressed or indirectly depicted in number of studies. The

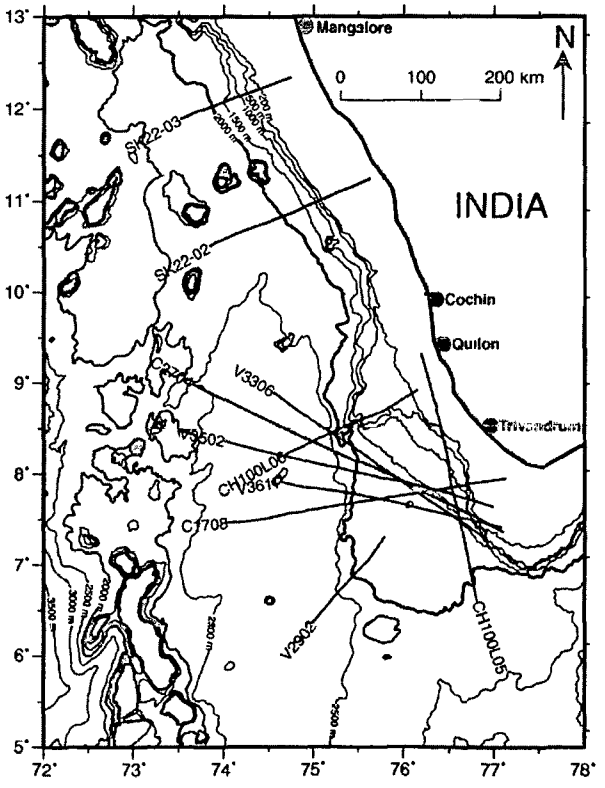

Fig. 2. Map showing location of selected bathymetry profiles across the southwestern continental margin of India along which the sectional views have been presented in Fig. 3. These bathymetry profiles have been obtained from the National Geophysical Data Centre (1998) and National Institute of Oceanography (NIO) databases. Other details as in Fig. 1.

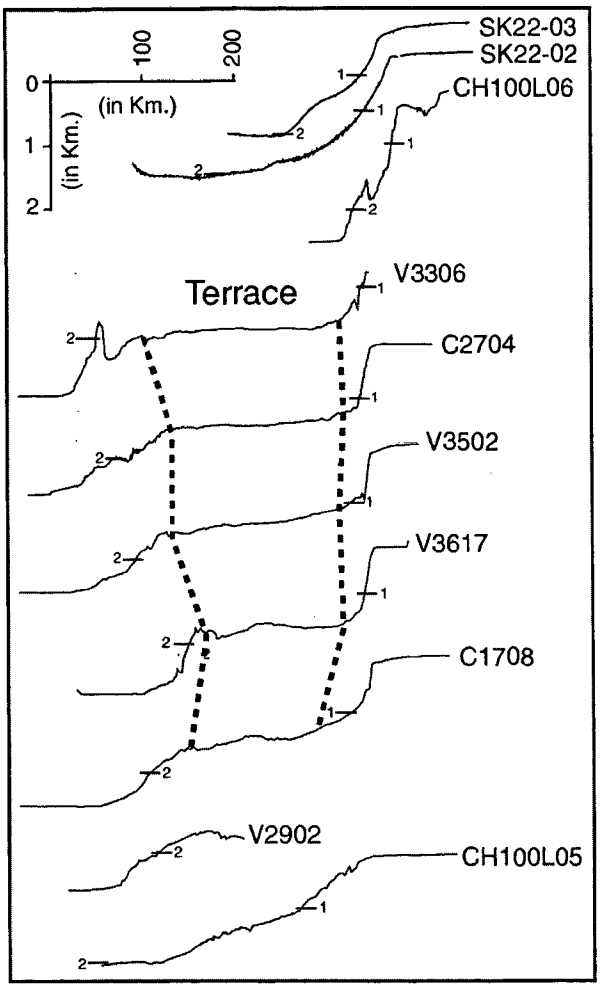

Fig. 3. Selected bathymetric profiles across the southwestern continental margin of India showing the distinct sectional view of the terrace off Trivandrum as compared to the normal shelf–slope configuration along the northern profiles (SK22-02 and SK22-03). The locations of these profiles are shown in Fig. 2 and the depth levels of 1 and 2 km are labeled on the profiles.

qualitative juxtaposition models (Crawford, 1978; Katz and Premoli, 1979; Agrawal et al., 1992; Windley et al., 1994; Menon and Santosh, 1995; Dissanayake and Chandrajith, 1999; Pradeepkumar and Krishnanath, 2000; Torsvik et al., 2000; Anil Kumar et al., 2001) are based on the colinearity of inferred comparable onshore shear zones, geological domains or continental scale MAGSAT and gravity anomalies. On the other hand quantitative models are based on estimated finite rotation parameters. Based on the evaluation of those qualitative models by Yoshida et al. (1999) and other recent studies (Chetty and Bhaskar Rao, 2004; Radhakrishna et al., 2004) it appears that there is a broad agreement about the comparable geological units and shear zones of southern India and Madagascar, however precise conjugate correspondence of these features is still awaited. According to Norton and Sclater (1979) the separation of India and Madagascar started shortly before anomaly 34 time. Therefore, in the following paragraph, we briefly discuss some of those quantitative models (Norton and Sclater, 1979; Morgan, 1981; Besse and Courtillot, 1988; Muller et al., 1993) with focus on India–Madagascar relative position for the time of this anomaly 34 and show that the relative position of India and Madagascar vary in different models.

The paleogeographic reconstructions (Fig. 4a–d) prepared for this study are for the time of younger bound of anomaly 34 (i.e. anomaly 34ny). These reconstructions have been prepared using finite rotation parameters of different published models (Norton and Sclater, 1979; Morgan, 1981; Besse and Courtillot, 1988; Muller et al., 1993). Since the age corresponding to various magnetic isochrons in those studies are based on different geomagnetic timescales, therefore, for using those finite rotation parameters in this study, we have re-assigned the ages according to Cande and Kent's (1995) geomagnetic time scale. It is generally agreed that the magnetic anomaly 34 identified in the southern Mascarene Basin represents the oldest anomalies formed shortly after the India–Madagascar separation. Therefore, the paleo-ridge positions at anomaly 34ny and paleo-transforms have been marked using the available (Schlich, 1982; Dyment, 1991; Bernard and Munschy, 2000) magnetic anomaly identifications close to Madagascar in the Mascarene Basin and considered them fixed to the African plate while generating reconstruction maps. We considered the 2000 m isobath obtained from recent GEBCO digital data set (Intergovernmental Oceanographic Commission et al., 2003) to define the continent–ocean boundary off India and Madagascar.

In the reconstruction (Fig. 4a) following Norton and Sclater's (1979) model, we observed that the 2000 m isobaths off Indian coast as well off Madagascar coast are symmetric about the anomaly 34ny time ridge position and there is not much offset between the southern tips of India and Madagascar. The reconstruction following Morgan's (1981) model provides a close fit (Fig. 4b) for India and Madagascar without any intervening gap at 83.0 Ma itself and the paleo-ridge overlaps Indian landmass at places. Further, in this reconstruction, we also observed that the southern tip of Madagascar is much south of the southern tip of India and the 2000 m isobath off the Indian coast overlaps the Madagascar mainland. Reconstructions following model of Besse and Courtillot (1988) depict (Fig. 4c) the 83.0 Ma paleo-ridge positions closer to 2000 m isobath off Madagascar as compared to the same off Indian coast. The reconstruction model (Fig. 4d) following Muller et al. (1993) shows that the 2000 m isobaths off India as well off Madagascar are more or less symmetric about the paleo-ridge position, but towards north Madagascar is much closer to India. It appears that the models of Besse and Courtillot (1988) and Morgan (1981) are not appropriate for the India–Madagascar relative motion as they place the anomaly 34ny time ridge axis asymmetrically with respect to the conjugate 2000 m isobaths. Based on our exercise, we believe that the model of Norton and Sclater (1979) provides a better approximation of the India–Madagascar pre-anomaly 34ny time relative motion as it can accommodate the microcontinental fragments in the pre-drift India–Madagascar juxtaposition model.

4. Terrace off Trivandrum in a close fit India–Madagascar configuration

Fig. 5a presents a reconstruction map of India–Madagascar juxtaposition for anomaly 34ny time (83.0 Ma), which we

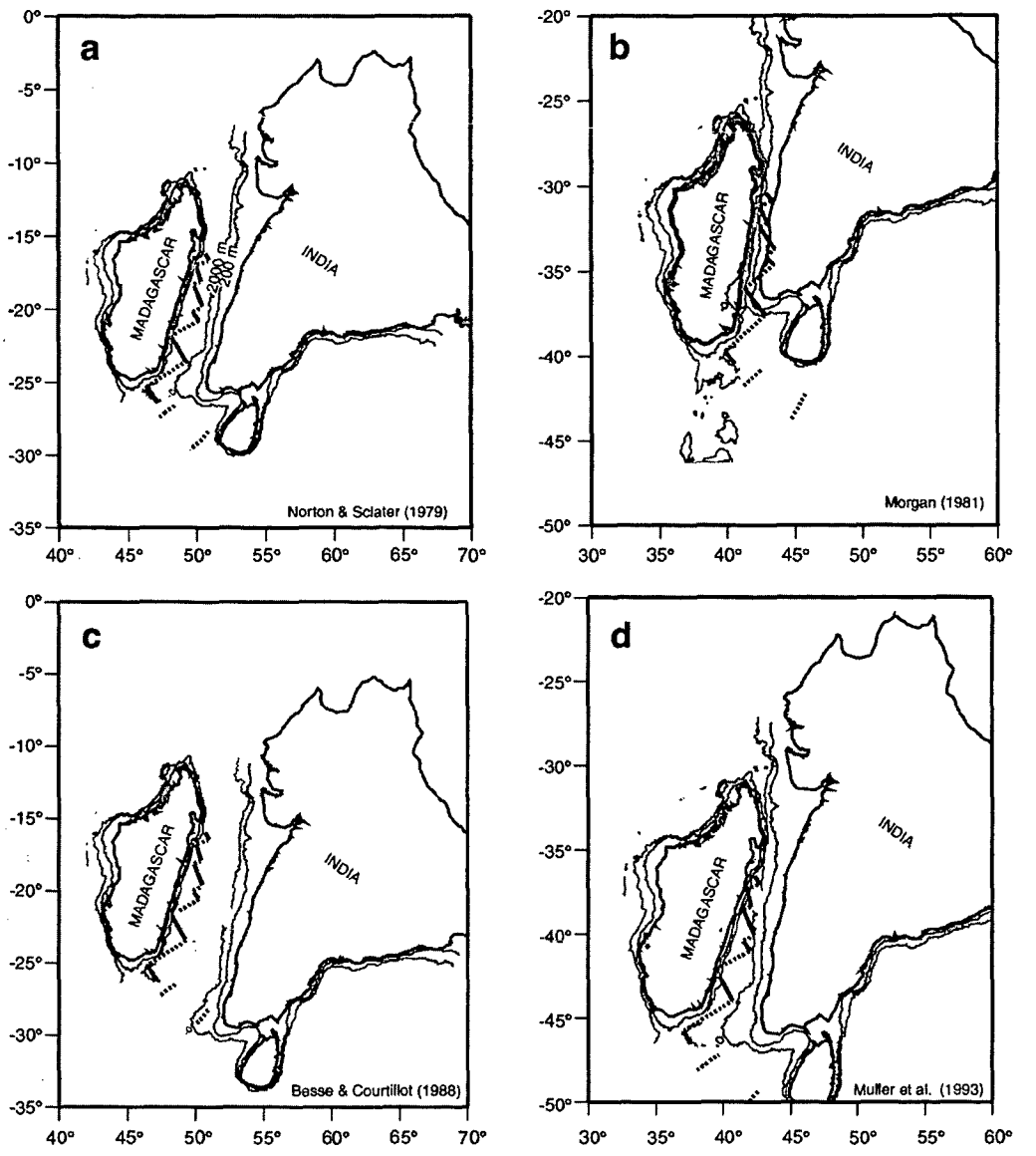

g. 4. Various paleogeographic reconstruction models to show the varied juxtaposition of India with Madagascar at anomaly 34 ny (83.0 Ma). Models a, and c are in ed Africa reference frame while models b and d are in fixed hotspot reference frame. Locations of anomaly 34ny time paleo-spreading ridge segments are shown as ck black lines and transform segments by dashed lines. The 200 m and 2000 m isobaths surrounding India and Madagascar are shown by thin lines.

epared using the rotation parameters of Norton and Sclater 979). As evidenced from this reconstruction map, we believe at the shape of the 2000 m bathymetry contours off the uthwest Indian coast and southeast Madagascar coast strongly ggest the conjugate nature of the terrace off Trivandrum and e bathymetry notch in the northern Madagascar Ridge. As entioned earlier, it is generally believed that the separation of dia and Madagascar started shortly before anomaly 34 ny time d based on dated onshore volcanics this separation is nsidered to have been initiated around 88–91 Ma (Storey et , 1995; Torsvik et al., 2000; Pande et al., 2001; Anil Kumar et , 2001). If that is the case, then India and Madagascar were ich closer as compared to their position in the anomaly 34ny ne reconstruction (Fig. 5a). In view of this we tried to construct Madagascar and India for a pre-anomaly 34ny time close fit configuration. Since the finite rotation parameters to describe this motion are not readily available in the Norton and Sclater (1979) model, so we tried to bring a closer fit of India and Madagascar by extrapolation, considering the same pole and rate of rotation as of anomaly 34ny time. This exercise provided a closer fit of India and Madagascar at 86.5 Ma and interestingly depicted a near fit (with slight overlap) of the terrace off Trivandrum with the bathymetric notch of the northern Madagascar Ridge. We tried to improve this fit by trial and error and believed to have obtained a reasonably good fit (Fig. 5b) of those terrace and notch for the same 86.5 Ma using a slightly modified Euler pole (Table 1) of Norton and Sclater (1979). In view of this, we are tempted to believe that this terrace off Trivandrum (TOT) and the bathymetric notch (BN) of northern Madagascar Ridge are the conjugate features

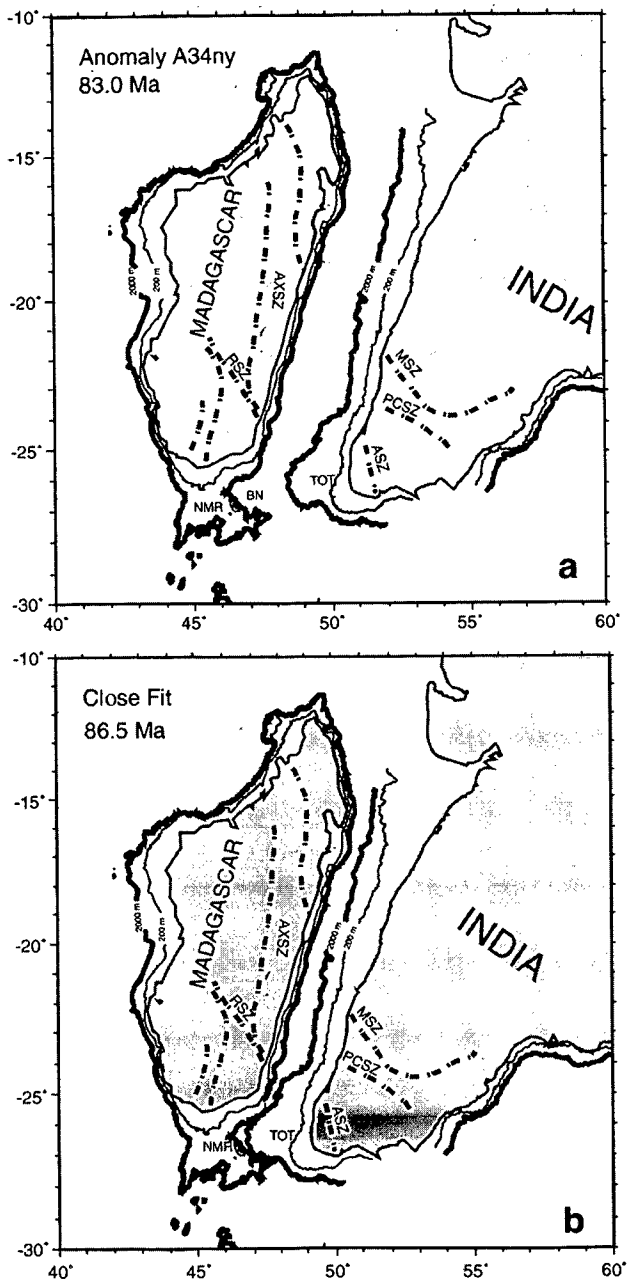

Fig. 5. Paleogeographic reconstruction of India and Madagascar in fixed Africa reference frame; (a) at 83.0 Ma following Norton and Sclater (1979) rotation parameters, (b) a plausible close fit at 86.5 Ma following the additional rotation parameters suggested in this study (Table 1). Madagascar is in its present position. Land portions of India and Madagascar are shaded, surrounding 200 m isobaths are shown by thin lines and 2000 m isobaths are shown by thick lines. Locations of onshore shear zones simplified after Meissner et al. (2002) and Windley et al. (1994). TOT: Terrace off Trivandrum, BN: Bathymetric notch; NMR: Northern Madagascar Ridge, ASZ: Achankovil Shear Zone, PCSZ: Palghat–Cauvery Shear Zone, MSZ: Moyar Shear Zone, RSZ: Ranotsara Shear Zone, AXSZ: Axial Shear Zone.

inferred by Dyment (1991). It may be mentioned here that so far not enough anomaly 34ny magnetic isochrons have been mapped in the vicinity of the northern Madagascar Ridge but

Table 1
Suggested addition to the finite rotation parameters of Norton and Sclater (1979) to obtain a closer fit India and Madagascar in fixed Africa reference frame

Anomaly	Age (Ma)	Finite rotation parameters		
		Latitude (Deg.)	Longitude (Deg.)	Angle (°CCW)
34ny	83.0	18.7	25.8	−56.00
Close fit	86.5	18.7	26.4	−58.36

CCW: Counter Clock-Wise.

published maps do suggest the existence of traces of several fracture zones. Considering the disposition of this terrace (TOT) and bathymetric notch (BN) with respect to the trends of paleo-ridge and paleo-transform segments in the reconstruction map (Fig. 4a) it may not be unreasonable to believe that the shape of those conjugate features were controlled by the ridge and transform segments of the paleo-ridge which existed at 86.5 Ma.

According to Storey et al. (1995) the Madagascar Ridge is believed to be a volcanic emplacement related to the motion of the African plate over the Marion hotspot since 90 Ma. However, based on the difference in the nature of the crust, the Madagascar Ridge is considered to be divided, roughly by a transition zone along 32°S latitude, into a northern domain and a southern domain (Goslin et al., 1980; Schlich, 1982; Bhattacharya and Chaubey, 2001). The velocity–depth distribution of the southern domain is closely related to that of a mean oceanic crust, but the crust underlying the northern domain is considered to be anomalous as it is neither purely continental nor of oceanic affinity. Perhaps the terrace off Trivandrum also has a similar nature of crust as the conjugate areas of the northern Madagascar Ridge and probably represents areas of

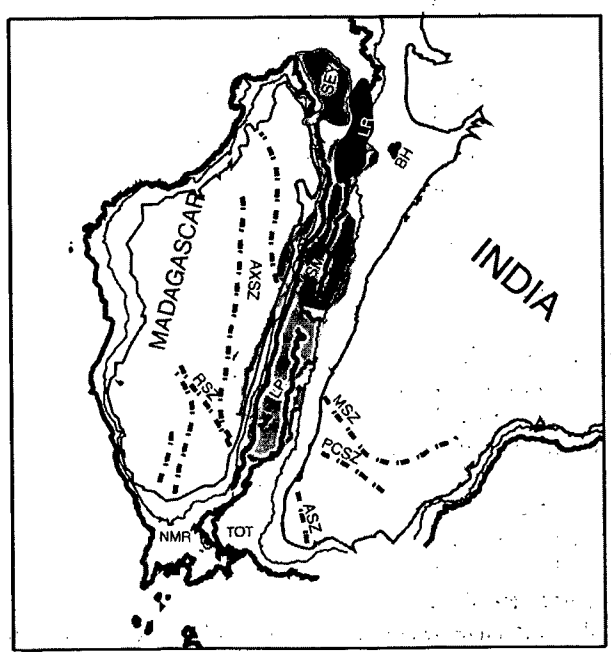

Fig. 6. A schematic model showing possibility of accommodating Seychelles Bank [SEY] and other probable microcontinental slivers (Laccadive Plateau [LP], Laxmi Ridge [LR], Saya de Malha Bank [SM]) in the gap between the 2000 m bathymetry contours in a close fit India–Madagascar configuration at 86.5 Ma. BH: Bombay High. Other details are as in Fig. 5.

ıinned continental crust on which at places Marion hotspot ɛlated volcanics might have been emplaced.

Several authors (Barron, 1987; Lawver et al., 1999) onsidered the unusual steep and straight edge of eastern Madaascar as an evidence of transform motion between India and ſadagascar, which was believed to have taken place between 60 and 105 Ma. It is therefore necessary to examine the comatibility of our proposed model of juxtaposed conjugate TOT nd BN and the transform motion between India and Madaascar, because a locked-in TOT and BN would have prevented ıch a transform motion. It may be noted that the inferred ansform motion between India and Madagascar had taken lace about 18 m.y. prior to the locked-in TOT and BN model hich we have proposed for an India–Madagascar immediate re-drift scenario at about 86.5 Ma. The region which later ɛveloped into TOT and BN might have existed simply as ljacent crusts across the transform boundary subsequent to the ansform motion. Later, this area probably thinned when it came ıder the influence of Marion hotspot, and the bathymetric otrusion (TOT) and notch (BN) were formed by the initial ɛometry of the spreading axis when spreading was initiated ɛtween India and Madagascar. Assumption of such an initial ɔreading geometry in this region appears to be reasonable based ı disposition of the TOT with respect to the reconstructed lahanoro and Mauritius Fracture zones along with their interɔning magnetic anomaly 34 (Fig. 4a).

Our proposed close fit (Fig. 5b) depicts the existence of a ide gap between the conjugate 2000 m isobaths in the areas ɔrth of TOT. On the other hand we have not shown the disɔsition of Seychelles microcontinent in this model and we also ɛed to provide space for accommodation of Laxmi Ridge, Saya ı Malha Bank, and Laccadive Plateau, in case they are icrocontinental slivers as believed by some authors (Krishnan, 68; Naini and Talwani, 1982; Plummer and Belle, 1995; Todal d Eldhom, 1998; Talwani and Reif, 1998; Bhattacharya and ıaubey, 2001; Collier et al., 2004; Lane et al., 2005), which isted between India and Madagascar in pre-drift scenario. We ɛl accommodation of these features is possible in our 86.5 Ma dia–Madagascar close fit model and to depict that possibility ɔ presented a schematic map (Fig. 6) where major portion of ɛse features (outlined by the simplified surrounding present 00 m isobath) have been accommodated in the gap available tween the conjugate reconstructed 2000 m bathymetric conırs. Since these features are inferred as thinned continental ıst, therefore, their present extents perhaps are much larger ın their original pre-thinning state. Therefore, we feel they uld be more conveniently accommodated in the gap in their ɔ-thinning dimension. As mentioned earlier, perhaps there was ne crustal extension in the regions of the TOT and BN before ı spreading event, and therefore, the unstretched TOT and BN ıuld have fitted slightly better and closer, but the overall ɔnario would have remained the same.

Summary and conclusions

We believe to have presented a better constrained model for a se fit juxtaposition of India and Madagascar in the immediate pre-drift tectonic scenario. This model suggests that the bathymetric protrusion of the terrace like feature off Trivandrum (TOT) fits well in shape and size with the bathymetric notch (BN) located in the northern Madagascar Ridge and they lock well in a close fit India–Madagascar configuration. This fit can be obtained for an 86.5 Ma reconstruction using a slightly modified finite rotation parameters of Norton and Sclater (1979) for relative motion of India with Africa. This model also appears to accommodate Seychelles, Laxmi Ridge, Saya de Malha Bank and Laccadive Plateau as intervening microcontinental slivers. In view of these, it is inferred that the terrace off Trivandrum and the bathymetric notch of the northern Madagascar Ridge represent scars related to the India–Madagascar break-up, the outlines of which were shaped by the rifted and transforms segments of the initial spreading geometry and the drifting of India from Madagascar was initiated around 86.5 Ma.

Acknowledgement

The authors are grateful to Dr. P.C. Pandey, Director, National Centre for Antarctic and Ocean Research, Goa and Dr. S.R. Shetye, Director, National Institute of Oceanography (NIO), Goa for encouragement and support to carry out this work. We thank Dr. S. Rajan for his interest in this work and Shri. T.M. Mahadevan for helpful suggestions. The paper greatly benefited from the constructive reviews of Dr. Alok Bagchi and an anonymous reviewer. We thank Prof. M. Santosh and Dr. T.R.K. Chetty for helpful suggestions, which improved the manuscript. All figures were drafted with GMT software (Wessel and Smith, 1995). A major portion of this work was carried out during the tenure of the first author (VY) at NIO as a Senior Research Fellow of the Council of Scientific and Industrial Research (CSIR), New Delhi. This is NIO contribution no. 4057.

References

Agrawal, P.K., Pandey, O.P., Negi, J.G., 1992. Madagascar: a continental fragment of the paleo-super Dharwar craton of India. Geology 20, 543–546.

Anil Kumar, Pande, K., Venkatesan, T.R., Bhaskar Rao, Y.J., 2001. The Karnataka Late Cretaceous dykes as products of the Marion hotspot at the Madagascar–India breakup event: evidence from $^{40}Ar/^{39}Ar$ geochronology and geochemistry. Geophysical Research Letters 28, 2715–2718.

Barron, E.J., 1987. Cretaceous plate tectonic reconstructions. Palaeogeography, Palaeoclimatology, Palaeoecology 59, 3–29

Bernard, A., Munschy, M., 2000. Le bassin des Mascareignes et le bassin de Laxmi (océan Indien occidental) se sont-ils formés à l'axe d'un même centre d'expansion? Comptes Rendus de l'Académie des Sciences. Series IIA. Earth and Planetary Science 330, 777–783.

Besse, J., Courtillot, V., 1988. Paleogeographic maps of the continents bordering the Indian Ocean since the Early Jurassic. Journal of Geophysical Research 93, 11791–11808.

Bhattacharya, G.C., Chaubey, A.K., 2001. Western Indian Ocean — a glimpse of the tectonic scenario. In: Sengupta, R., Desa, E. (Eds.), The Indian Ocean — a perspective. Oxford & IBH, New Delhi, pp. 691–729.

Biswas, S.K., 1982. Rift basins in western margin of India and their hydrocarbon prospects with special reference to Kutch Basin. American Association of Petroleum Geologists Bulletin 66, 1497–1513.

Biswas, S.K., 1987. Regional tectonic framework, structure and evolution of the western marginal basins of India. Tectonophysics 135, 307–327.

Cande, S.C., Kent, D.V., 1995. Revised calibration of the geomagnetic polarity time scale for the Late Cretaceous and Cenozoic. Journal of Geophysical Research 100, 6093–6095.

Chetty, T.R.K., Bhaskar Rao, Y.J., 2004. Structural framework of south India and the significance of major shear zones. Joint AOGS 1st Annual Meeting and 2nd APHW Conference, Asia Oceania Geosciences Society, Singapore, Abstracts, vol. 1, pp. 54–55.

Collier, J.S., Minshull, T.A., Kendall, J.M., Whitmarsh, R.B., Rümpker, G., Joseph, P., Samson, P., Lane, C.I., Sansom, V., Vermeesch, P.M., Hammond, J., Wookey, J., Teanby, N., Ryberg, T., Dean, S.M., 2004. Rapid continental breakup and microcontinent formation in the Western Indian Ocean. EOS, Transactions, American Geophysical Union 85, 481.

Crawford, A.R., 1978. Narmada–Son lineament of India traced into Madagascar. Journal of Geological Society of India 19, 144–153.

Dissanayake, C.B., Chandrajith, R., 1999. Sri Lanka–Madagascar Gondwana linkage: evidence for a Pan-African mineral belt. Journal of Geology 107, 223–235.

Dyment, J., 1991. Structure et évolution de la lithosphère océanique dans l'océan Indien: apport des données magnétiques. Doctorate Thesis, Université Louis Pasteur.

Goslin, J., Segoufin, J., Schlich, R., Fischer, R.L., 1980. Submarine topography and shallow structure of the Madagascar Ridge, Western Indian Ocean. Geological Society of America Bulletin 91, 741–753.

Intergovernmental Oceanographic Commission, International Hydrographic Organization, British Oceanographic Data Centre, 2003. General Bathymetric Chart of the Oceans (GEBCO) Digital Atlas (CD ROM). British Oceanographic Data Centre, Birkenhead.

Katz, M.B., Premoli, C., 1979. India and Madagascar in Gondwanaland based on matching Precambrian lincaments. Nature 279, 312–315.

Krishnan, M.S., 1968. Geology of India and Burma. Higgin-Bothams, Madras.

Lane, C.I., Minshull, T.A., Collier, J.S., Whitmarsh, R.B., Sansom, V., Evans, M.M., 2005. Extensive magmatism during the formation of the Laxmi Ridge rifted margin, NW Indian Ocean. Geophysical Research Abstracts 7, 04954.

Lapedes, D.N., 1978. McGraw-Hill Dictionary of Scientific and Technical Terms. McGraw-Hill Book Company, New York.

Lawver, L.A., Gahagan, L.M., Dalziel, I.W.D., 1999. A tight fit — Early Mesozoic Gondwana, a plate reconstruction perspective. Memoirs of National Institute of Polar Research. Special Issue 53, 214–229.

Meissner, B., Deters, P., Srikantappa, C., Kohler, H., 2002. Geochronological evolution of the Moyar, Bhavani and Palghat shear zones of southern India: implications for east Gondwana correlations. Precambrian Research 114, 149–175.

Menon, R.D., Santosh, M., 1995. A Pan-African gemstone province of East Gondwana. In: Yoshida, M., Santosh, M. (Eds.), India and Antarctica during the Precambrian. Geological Society of India Memoir, vol. 34, pp. 357–371.

Morgan, W.J., 1981. Hotspot tracks and the opening of the Atlantic and Indian Oceans. In: Emiliani (Ed.), The Sea. Wiley Interscience, New York, pp. 443–487.

Muller, R.D., Royer, J.Y., Lawver, L.A., 1993. Revised plate motions relative to the hotspot from combined Atlantic and Indian Ocean hotspot tracks. Geology 21, 275–278.

Naini, B.R., Talwani, M., 1982. Structural framework and the evolutionary history of the continental margin of Western India. In: Watkins, J.S., Drake, C.L. (Eds.), Studies in Continental Margin Geology. American Association of Petroleum Geologists Memoir, vol. 34, pp. 167–191.

National Geophysical Data Centre, 1998. GEODAS CD-ROM, Worldwide Marine Geophysical Data. National Oceanic and Atmospheric Administration, US Department of Commerce, Washington, DC.

Norton, I.O., Sclater, J.G., 1979. A model for the evolution of the Indian Ocean and the break-up of Gondwanaland. Journal of Geophysical Research 84, 6803–6830.

Pande, K., Sheth, H.C., Bhutani, R., 2001. ^{40}Ar–^{39}Ar age of the St. Mary's Islands volcanics, southern India: record of India–Madagascar break-up on the Indian subcontinent. Earth and Planetary Science Letters 193, 39–46.

Plummer, Ph.S., Belle, E.R., 1995. Mesozoic tectono-stratigraphic evolution of the Seychelles microcontinent. Sedimentary Geology 96, 73–91.

Pradeepkumar, A.P., Krishnanath, R., 2000. A Pan-African 'Humite Epoch' in East Gondwana: implications for Neoproterozoic Gondwana geometry. Journal of Geodynamics 29, 43–62.

Radhakrishna, T., Joseph, M., Mathai, J., 2004. Southern granulite terrain of India and constraints for the Precambrian continental assemblies. Joint AOGS 1st Annual Meeting and 2nd APHW Conference, Asia Oceania Geosciences Society, Singapore, Abstracts, vol. I, pp. 55–56.

Rao, T.C.S., Bhattacharya, G.C., 1975. Seismic profiler and magnetic studies off Quilon, south-west India. Indian Journal of Marine Sciences 4, 110–114.

Schlich, R., 1982. The Indian Ocean: aseimic ridges, spreading centres, and oceanic basins. In: Naim, A.E.M., Stehli, F.G. (Eds.), The Ocean Basins and Margins. Plenum Press, New York, pp. 51–147.

Storey, M., Mahoney, J.J., Saunders, A.D., Duncan, R.A., Kelley, S.P., Coffin, M.F., 1995. Timing of hotspot-related volcanism and the breakup of Madagascar and India. Science 267, 852–855.

Talwani, M., Reif, C., 1998. Laxmi Ridge — a continental sliver in the Arabian Sea. Marine Geophysical Researches 20, 259–271.

Todal, A., Eldhorn, O., 1998. Continental margin off western India and Deccan large igneous province. Marine Geophysical Researches 20, 273–291.

Torsvik, T.H., Tucker, R.D., Ashwal, L.D., Carter, L.M., Jamtveit, V., Vidyadharan, K.T., Venkataramana, P., 2000. Late Cretaceous India–Madagascar fit and timing of breakup related magmatism. Terra Nova 12, 220–224.

Wessel, P., Smith, W.H.F., 1995. New version of the Generic Mapping Tools released. EOS, Transactions, American Geophysical Union 76, 329.

Windley, B.F., Razafiniparany, A., Razakamanana, T., Ackermand, D., 1994. Tectonic framework of the Precambrian of Madagascar and its Gondwana connections. Geologische Rundschau 83, 642–659.

Yoshida, M., Rajesh, H.M., Santosh, M., 1999. Juxtaposition of India and Madagascar: a perspective. Gondwana Research 2, 449–462.